

Doctoral dissertation

Free radical reactions of sulfur-containing amino acids and peptides.

From reactive transients to stable products.

Wolnorodnikowe reakcje aminokwasów i peptydów zawierających atom siarki.

Od reaktywnych indywiduów przejściowych do produktów trwałych.

M.Sc. Eng. Katarzyna Nadzieja Grzyb

Supervision: prof. UAM dr hab. Tomasz Pędziński



The research was carried out in the Department of Chemical Physics and
Photochemistry/Faculty of Chemistry

Adam Mickiewicz University in Poznań

The doctoral dissertation is presented as a series of thematically coherent scientific
articles, published in peer-reviewed journals

Poznań 2025

The research presented in this dissertation was supported by the funds from „The Excellence Initiative – Research University” program grant no. 017/02/SNŚ/0008



ACKNOWLEDGEMENTS

First and foremost, I would like to express my sincere gratitude to my supervisor, **Professor Tomasz Pędziński**, for his invaluable guidance, unwavering support, and constant encouragement throughout the course of my PhD journey. His mentorship has not only advanced my scientific knowledge but also profoundly influenced my growth as an independent researcher. Working under his supervision has been a privilege, and I am genuinely thankful for the opportunity to learn from such a dedicated and inspiring scientist.

I would like to thank all the members of the **Department of Physical Chemistry and Photochemistry** for creating such a positive and intellectually stimulating environment. I feel incredibly fortunate to have had the opportunity to work with so many inspiring and encouraging people. I am especially thankful to **Dr Piotr Filipiak** and **Dr Kamil Jakub Frąckowiak** for their support in scientific struggles and endless conversations.

I would also like to extend my thanks to the **collaborators** and **co-authors** who I had the honor of working with throughout my PhD journey.

I gratefully acknowledge the financial support provided by the **Department of Chemistry, Adam Mickiewicz University** and **Initiative of Excellence - Research University**.

Thank you to my friends, **Dr Marta Kaczmarek** and **M.Sc. Eng. Agnieszka Przybylska** - sharing the highs and lows of academic life with those who truly understood its unique challenges was a constant reminder that I was not alone in this.

I am forever grateful to my family: to **Mom** and **Aunt** for their love, patience, and belief in me throughout this challenging journey; to **Chris Trzeźniewski** for being my constant source of support, encouragement, and joy; and finally, to **Franek** for being my ray of sunshine. On the toughest days, your laughter and smile gave me the strength to overcome every obstacle.

ABSTRACT

In recent decades, the oxidation reactions of amino acids, peptides, and proteins have been the focus of extensive research due to their biological significance. Because of the low oxidation potential, amino acids containing sulfur are particularly vulnerable to attacks by one-electron oxidants, such as short-lived excited states, free radicals, and reactive oxygen species. The oxidation of methionine and cysteine causes significant damage to proteins, and consequently, it is believed to contribute to neurodegenerative diseases like Alzheimer's disease, Parkinson's disease, biological aging, and type 2 diabetes. This has generated considerable interest in their studying. Despite the long history of one-electron oxidation of sulfide groups, certain aspects of this process remain unclear or controversial, such as the free radical reactions that lead to stable modifications of amino acids.

The aim of this doctoral dissertation was to thoroughly investigate and describe the mechanisms behind photosensitized and radiation-induced oxidation of biomimetic model amino acids that contain a sulfide group.

A series of five thematically coherent scientific articles (P1-P5) describes both transient and stable products of the oxidation reaction of model systems containing a sulfide group. The oxidation was sensitized by 3-carboxybenzophenone and also induced radiolytically, where the oxidizing agent was the hydroxyl radical. Short-lived transients (e.g., intermediates containing three-electron bonds, free radicals, and radical ions and reactive excited states) were investigated using time-resolved techniques (laser flash photolysis and pulse radiolysis), while stable products were identified using high-performance liquid chromatography coupled with tandem mass spectrometry (LC-MS/MS). Combining these complementary methods allowed us to address the impact of the substrate's structure (type of functional groups, length of the amino acid side chain) and the reaction conditions (pH) on the formation of transient and stable products. This helped to propose a fuller picture of the oxidation processes in selected biologically important compounds. Additionally, the aromatic ketones (benzophenone, 3-carboxybenzophenone, and 4-carboxybenzophenone), which are used as photosensitizers, were characterized in detail.

STRESZCZENIE

W ciągu ostatnich dekad reakcje utleniania aminokwasów, peptydów oraz białek były przedmiotem licznych badań ze względu na ich znaczenie biologiczne. Niski potencjał oksydacyjny sprawia, że na atak utleniaczy, takich jak krótko żyjące stany wzbudzone, wolne rodniki czy reaktywne formy tlenu, szczególnie narażone są aminokwasy zawierające atom siarki. Utlenianie metioniny oraz cysteiny prowadzi do poważnych uszkodzeń białek i w konsekwencji jest uważane za jedną z przyczyn schorzeń neurodegeneracyjnych takich jak: choroba Alzheimera, Parkinsona oraz biologiczne starzenie i cukrzyca typu 2. Jednak pomimo licznych badań poświęconych jednoelektronowemu utlenianiu grupy sulfidowej (tioeterowej), niektóre aspekty tego procesu nadal pozostają niejasne lub kontrowersyjne; na przykład reakcje wolnych rodników prowadzące do powstania trwałych modyfikacji w aminokwasach nadal wywołują wiele pytań.

W ramach pracy doktorskiej przeprowadzone zostały prace badawcze, których celem było dogłębne poznanie i uzupełnienie dotychczasowej wiedzy na temat mechanizmów jedno-elektronowego utleniania pochodnych metioniny - biomimetycznych układów modelowych aminokwasów zawierających grupę sulfidową. W serii pięciu tematycznie spójnych artykułów naukowych (P1-P5) zostały opisane zarówno produkty przejściowe, jak i trwałe, reakcji utleniania fotosensybilizowanego przez 3-karboksybenzofenon oraz utleniania indukowanego radiolitycznie, w którym utleniaczem jest rodnik hydroksylowy. Krótko żyjące produkty przejściowe (indywidua zawierające wiązanie trójelektronowe, rodniki, rodnikojony oraz reaktywne stany wzbudzone) zostały przebadane za pomocą technik czasowo-rozdzielczych (laserowej fotolizy błyskowej oraz radiolizy impulsowej), a produkty trwałe zostały zidentyfikowane z wykorzystaniem wysokosprawnej chromatografii cieczowej sprzężonej z tandemową spektrometrią mas (LC-MS/MS). Połączenie tych komplementarnych metod pozwoliło uzyskać odpowiedź na pytania o wpływ struktury substratu (rodzaju grup funkcyjnych, długości łańcucha bocznego), a także warunków reakcji (pH) na powstające produkty pośrednie oraz trwałe modyfikacje badanych związków. Dzięki temu otrzymano pełniejszy obraz procesów utleniania wybranych, biologicznie istotnych cząsteczek. Ponadto została przeprowadzona szczegółowa charakterystyka ketonów aromatycznych (benzofenonu, 3-karboksybenzofenonu oraz 4-karboksybenzofenonu), które stosowane są jako fotosensybilizatory.

TABLE OF CONTENTS

Abstract.....	4
Streszczenie	5
Abbreviations.....	8
1 Introduction.....	11
1.1 Sulfur-containing amino acids	11
1.2 Methionine	11
1.2.1 Methionine and Alzheimer's disease.....	13
1.3 Cysteine	14
1.4 Photosensitizers	15
1.5 Early events of photosensitized oxidation of methionine under anoxic conditions.....	19
1.6 Photosensitized oxidation of methyl-cysteine in an oxygen-free environment	23
1.7 Analysis of transients formed in anoxic radiation-induced oxidation of methionine	24
1.8 Stable products formation.....	26
1.8.1 Photosensitized oxidation	26
1.8.2 Radiation-induced oxidation.....	26
1.9 Literature review of photo- and radiation-induced oxidation of methionine derivatives in deoxygenated solutions	29
1.9.1 Photosensitized oxidation	29
1.9.2 Radiation-induced oxidation.....	30
1.10 Methodology.....	32
1.10.1 UV-Vis spectrophotometry	32
1.10.2 Laser flash photolysis	33
1.10.3 Pulse radiolysis	34
1.10.4 High-performance liquid chromatography	36

1.10.5	Mass spectrometry (MS).....	38
1.10.6	Tandem mass spectrometry (MS/MS)	39
2	Research objective	42
3	Discussion of the research	44
3.1	Sensitized photoreduction of selected benzophenones. Mass spectrometry studies of radical cross-coupling reactions (P1)	44
3.2	Early Events of Photosensitized Oxidation of Sulfur-Containing Amino Acids Studied by Laser Flash Photolysis and Mass Spectrometry (P2)	47
3.3	Radiation- and Photo-Induced Oxidation Pathways of Methionine in Model Peptide Backbone under Anoxic Conditions (P3)	50
3.4	The Fate of Sulfur Radical Cation of N-Acetyl-Methionine: Deprotonation vs. Decarboxylation (P4).....	53
3.5	Efficient decarboxylation of oxidized Cysteine unveils novel Free-Radical reaction pathways (P5).....	56
3.6	Summary and conclusions	59
4	References.....	61
5	List of Figures and Schemes	70
6	List of Tables.....	71
7	List of scientific achievements	73
8	Declarations of contribution	77
9	Reprints of publications	88

ABBREVIATIONS

$>\text{S}^{\bullet+}$	sulfur-centered radical cation
$^3(\text{BP})^*/^3(3\text{CB})^*/^3(4\text{CB})^*$	excited triplet state of benzophenone/3-carboxybenzophenone/4-carboxybenzophenone
3CB	3-carboxybenzophenone
4CB	4-carboxybenzophenone
Ac-Met	acetyl methionine
Ac-Met-NH ₂	acetyl methionine amide
Ac-Met-OCH ₃	acetyl methionine methyl ester
A β	β amyloid
BP	benzophenone
CB*	excited triplet state of 3-carboxybenzophenone/4-carboxybenzophenone
CB $^{\bullet-}$	3-carboxybenzophenone/4-carboxybenzophenone radical anion
CBH $^{\bullet}$	3-carboxybenzophenone/4-carboxybenzophenone ketyl radical
Cys	cysteine
CysS $^{\bullet}$	thiyl radical
CysSOH	sulfenic acid
DAD	Diode Array Detector
ET	electron transfer
HPLC	high-performance liquid chromatography
ISC	intersystem crossing
k_{bet}	back electron transfer rate constant
k_{bH}	back hydrogen atom transfer rate constant
k_{H}	deprotonation rate constant

k_{NH}	proton transfer from the protonated amino group rate constant
k_{sep}	charge separation rate constant
LC	liquid chromatography
LC-MS	liquid chromatography coupled with mass spectrometry
LC-MS/MS	liquid chromatography coupled with tandem mass spectrometry
LFP	laser flash photolysis
m/z	mass to charge ratio
MCRC	Methionine Centered Redox Cycle
MeCys	S-methyl-cysteine
Met	methionine
Met-NH ₂	methionine amide
Met-OCH ₃	methionine methyl ester
MetSO	methionine sulfoxide
MS	mass spectrometry
MS/MS	tandem mass spectrometry
Msr	methionine sulfoxide reductase
pKa	acid dissociation constant
PR	pulse radiolysis
QTOF	quadrupole time-of-flight
S \cdot :OH	hydroxysulfuranyl radicals
(S \cdot :N) ⁺	two-centered three-electron intramolecular bond between sulfur and nitrogen atoms
(S \cdot :O)	two centered three-electron intramolecular bond between sulfur and oxygen atoms

$(S:S)^+$	two centered three-electron intermolecular bond between two sulfur atoms
TOF	time-of-flight
VWD	variable wavelength detector
αC	radical centered on alpha-carbon
αN	α -aminoalkyl radical
$\alpha N_{\text{subs.}}$	α -amidoalkyl radical
αS	α -(alkylthio)alkyl radical
αS_1	α -(alkylthio)alkyl radical centered on terminal carbon atom
αS_2	α -(alkylthio)alkyl radical centered on γ (methylene) carbon atom
$\tau_{1/2}$	half lifetime
ϕ	quantum yield

1 INTRODUCTION

1.1 Sulfur-containing amino acids

Oxidation of amino acids, peptides, and proteins has been the subject of many studies due to its importance in medicine, biology, and basic chemistry [1,2]. Only two of twenty canonical amino acids incorporated into proteins contain sulfur. They are methionine (Met) and cysteine (Cys) [3]. **Figure 1** shows the structures of Met and Cys. Both those amino acids have antioxidant functions and play a key role in cellular metabolism regulation [4]. The sulfide group in methionine and the thiol group in cysteine are very susceptible to oxidation. Oxidative stress and redox homeostasis disruption lead to the irreversible modifications of methionine- and cysteine-containing peptides and proteins. Those non-reversible modifications to Met and Cys lead to pathological situations, considering their vital functions in organisms. Oxidized forms of methionine and cysteine are considered to be possible indicators of neurodegenerative conditions such as Parkinson's disease, Alzheimer's disease, biological aging, and type 2 diabetes [5].

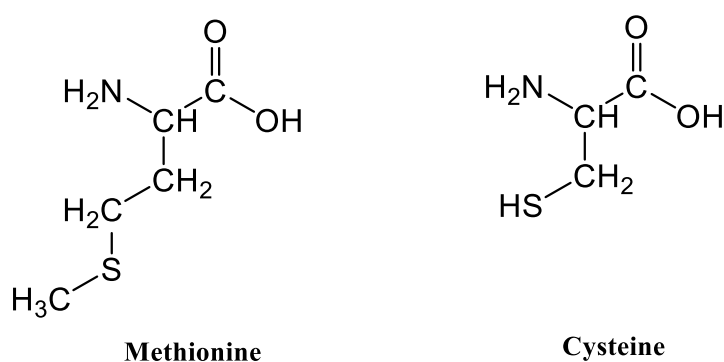


Figure 1 Structures of methionine (Met) and cysteine (Cys)

1.2 Methionine

The research on methionine started over 100 years ago, in 1922, when Mueller published a paper announcing the discovery of a new sulfur-containing amino acid [6,7]. It was isolated by acidic hydrolysis of casein. Mueller also proposed the correct empirical formula, C₅H₁₁NO₂S, but couldn't determine the structure of the new compound. Six years later, in 1928, Barger and Cayne succeeded in establishing the correct structure of this

new amino acid. They also proposed the name *methionine* as an abbreviation of γ -methylthiol- α -aminobutyric acid [8].

Met is one of the most hydrophobic amino acids. It is highly susceptible to oxidation by a variety of endogenous and exogenous sources, including oxidases, reactive oxygen species,

γ -radiation, metal-catalyzed oxidation, "leakage" from the electron transport chain, and "autooxidation" of flavins and xenobiotics [9]. Under aerobic conditions methionine oxidation frequently leads to the formation of methionine sulfoxide (MetSO) [10]. This modification converts the hydrophobic properties of methionine into hydrophilic properties, causing structural and conformational alterations and, ultimately, loss of biological activity [11]. Luckily, cells are equipped with a repair mechanism called the Met-centered redox cycle (MCRC) that involves two kinds of methionine sulfoxide reductases (Msr) to catalyze the reduction of MetSO back to Met (**Figure 2**) [10].

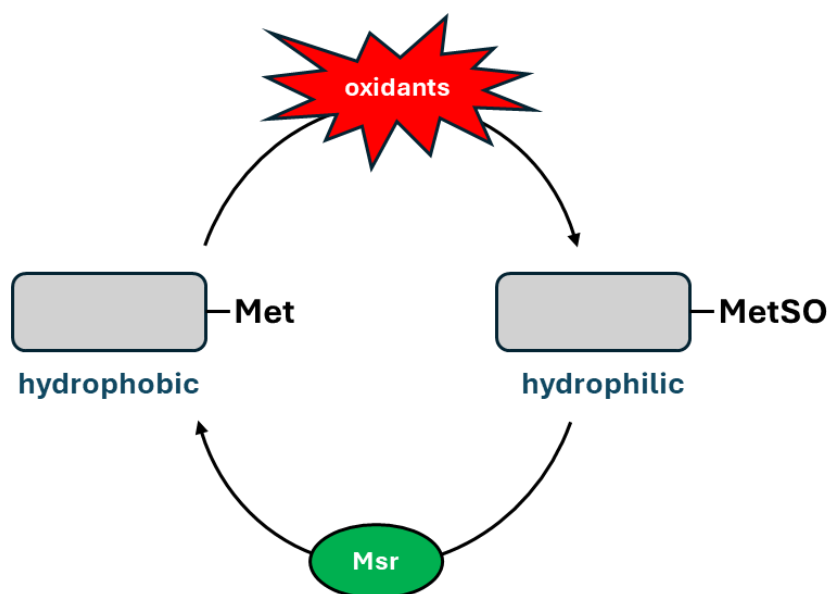


Figure 2 Met-centered redox cycle

Repeated oxidation cycle and subsequent reduction lead to the consumption of multiple forms of oxidants; thus, methionine residue is thought to act as an endogenous antioxidant defense system for proteins [9].

1.2.1 Methionine and Alzheimer's disease

Alzheimer's disease is one of the most common dementia-type disorders. It is a multifactorial disease whose specific etiology is complex and not yet definite. The amyloid theory is one popular (albeit controversial) hypothesis [12–14]. According to it, Alzheimer's disease is caused by oxidative stress and is characterized by "deposition of a special substance in the cortex," as described by Aloïs Alzheimer in 1907 [15]. This pathological protein deposition in and around the brain tissue is now called amyloid (senile) plaques. It is considered to be one of the pathological hallmarks of Alzheimer's disease (**Figure 3**). The primary component of senile plaque is a β -amyloid ($A\beta$) peptide generally composed of 40 or 42 amino acids and contains methionine residue in position 35 (Met₃₅) in its C-terminal domain.

In-vitro (EPR and NMR) and in-vivo studies have confirmed the critical role of methionine in aggregation, neurotoxicity of the $A\beta$, and radical generation [9,10,16]. The detection of methionine sulfoxide in senile plaques also confirms the significance of methionine in β -amyloid oxidation/reduction mechanisms [17].

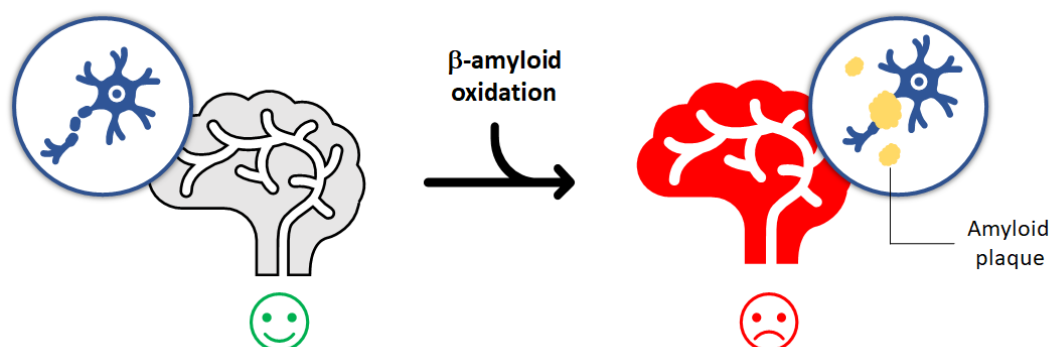


Figure 3 Oxidized β -amyloid peptide forms amyloid plaques that are hallmarks of Alzheimer's disease

In β -amyloid, methionine residue acts as an electron donor and reduces Cu (II) bound to the peptide. This redox reaction yields Cu (I) and methionine radical cation $>S^{\bullet+}$ that induces oxidative stress. It has been found to occur only with a full-length β -amyloid that contains both histidine that forms a complex with Cu(II), and methionine with reducing properties. The fragments of $A\beta$ that either lack N-terminal histidine or C-terminal methionine do not reduce Cu (II), and therefore, sulfur radical cation $>S^{\bullet+}$ is not formed [18,19]. No protein oxidation was also observed when Met₃₅ was replaced with cysteine [20]. This shows that oxidation of amino acid residue in $A\beta$ is highly site-specific. Besides Cu (II), many biologically relevant oxidants can readily oxidize methionine and yield

sulfur radical cation: hydroxyl radicals, peroxy radicals, singlet oxygen, and other excited states [21].

1.3 Cysteine

The indirect discovery of cysteine occurred in 1810 when William Hyde Wollstone isolated a crystalline substance, now identified as a cystine dimer, from urinary calculi. Numerous debates and incorrect structural assignments surrounded the research of cystine and cysteine in the 19th and early 20th centuries [7].

Cysteine is essential in protein structure due to its ability to form disulfide bonds with other cysteine residues [3]. It participates in tertiary and quaternary structures of proteins, forming intra- and intermolecular disulfide bonds. The S-S bonds stabilize the protein conformation and enhance resistance to extreme environments like highly acidic or alkaline pH and high temperature. They also shield the protein from enzyme breakdown [22].

Cysteine contains a thiol group, which is significantly more reactive than the sulfide group in methionine. The thiol group in cysteine can lose a proton to form thiolate with a negative charge, which increases its reactivity [23]. The pK_a of Cys side-chain is estimated to be 8.6 [24], but it is strongly dependent on the surrounding amino acids and can be as low as 2.5 [25] and as high as 10.5 [24].

A cysteine residue (especially as a thiolate) acts as a nucleophile; it can spontaneously react with electrophilic molecules and quickly oxidize in vivo by one- or two-electron oxidants [26,27]. The metastable products of those reactions are thiyl radical (CysS[•]) and sulfenic acid (CysSOH), respectively. Both of those species have biologically relevant functions. For example, CysS[•] takes part in the catalytic cycle of several enzymes, and CysSOH can react with thiols (e.g., cysteine to form cystine, and with S-glutathione) and form disulfide bonds that often result in changes in protein function [28–30]. **Figure 4** shows the oxidative modifications of cysteine in proteins and their biological consequence.

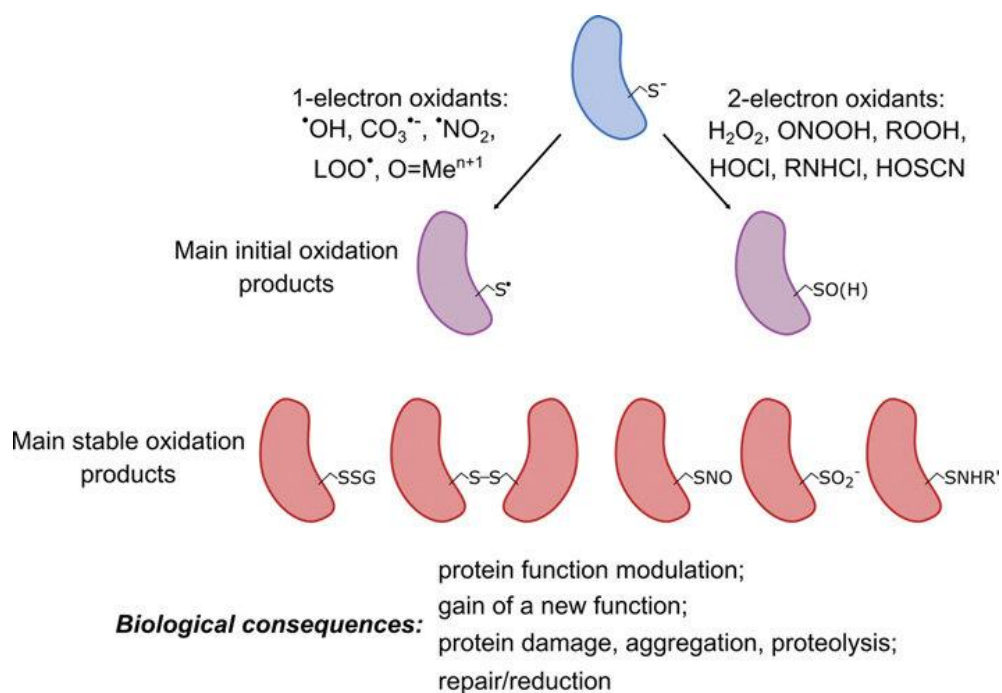


Figure 4 . Oxidative modifications of protein Cys and their biological consequence. The figure adapted from the paper [28] with publisher's permission. Copyright Portland Press Ltd 2019

S-methyl cysteine (MeCys) is a sulfide derivative of cysteine, characterized by substituting the hydrogen atom attached to the sulfur by a methyl group. This modification enhances the stability of MeCys and changes its reactivity, making it more similar to methionine. S-methyl cysteine exhibits potential antioxidant activity, which may help prevent or reduce oxidative stress, inflammation, and insulin resistance induced by high fructose [31].

1.4 Photosensitizers

Photosensitizers initiate photosensitized reactions by absorbing light, then act as donors and transfer the energy to the acceptor (target) molecules – quencher [32]. Photosensitized reactions are particularly useful when direct excitation of the target molecule is problematic, e.g. due to its absorption properties. Since methionine, cysteine, and their derivatives have their absorption maxima at about 200 nm, the sensitizer is crucial to their photooxidation.

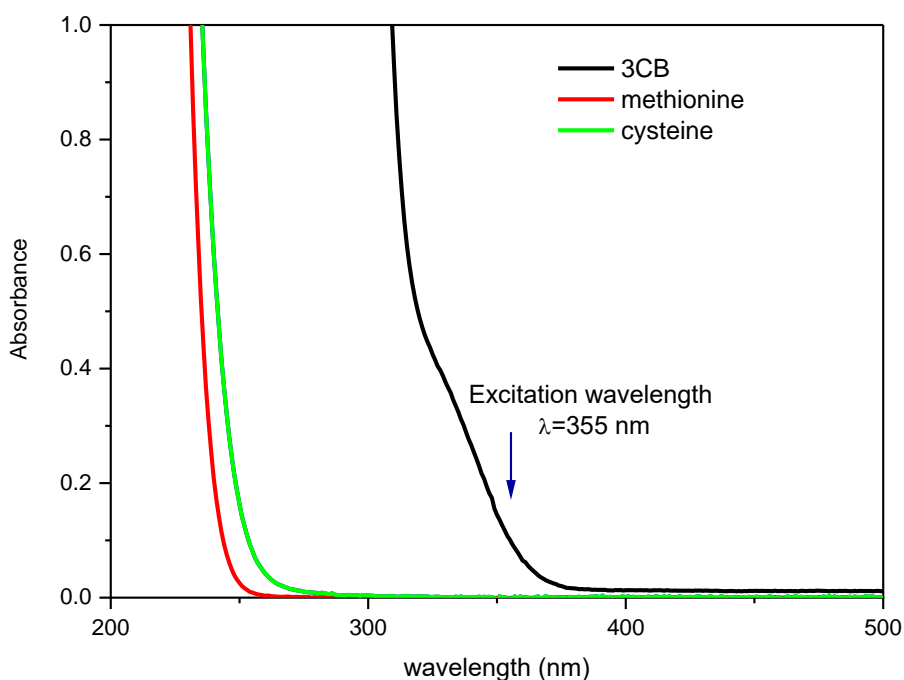


Figure 5 UV spectra of 3CB, Met, and Cys

As seen in the above spectra in **Figure 5**, in the 355 nm irradiation of solution containing 3- carboxybenzophenone (3CB) and quencher, the sensitizer is selectively excited, and the quencher stays in the ground state.

One of the most widely used triplet-state photosensitizers is benzophenone (BP). Research on the photochemistry of benzophenone dates back to the 19th century when Ciamciam and Stilber correctly recognized the product of photoreduction of BP in the alcoholic medium as photodimer – benzopinacol [33,34]. Since then, BP has been widely studied and has been successfully used in a variety of sensitized reactions involving organic and inorganic compounds, e.g., herbicides [35], aquatic contaminants [36,37], various sulfur-containing molecules [38–40], amino acids, peptides and proteins [41–50].

Unfortunately, benzophenone is hardly soluble in water; thus, its use in studying reactions in an aqueous environment is limited. Benzophenone derivatives that have carboxyl group in meta and para positions, respectively 3-carboxybenzophenone (3CB) and 4-carboxybenzophenone (4CB). They possess very similar photophysical properties – including the quantum yield of triplet formation of 1 – but are water-soluble therefore, are more helpful in studying biological systems. On the other hand, absorption spectra of 4CB-derived radicals partly overlap with the spectra of transients generated due to

methionine oxidation. This issue is resolved by using 3CB instead – 3CB-derived transients are hypsochromically-shifted and substantially less absorbing in the 370-400 nm region than the respective 4CB transients. **Figure 6** shows the transient absorption spectra of 3CB and 4CB.

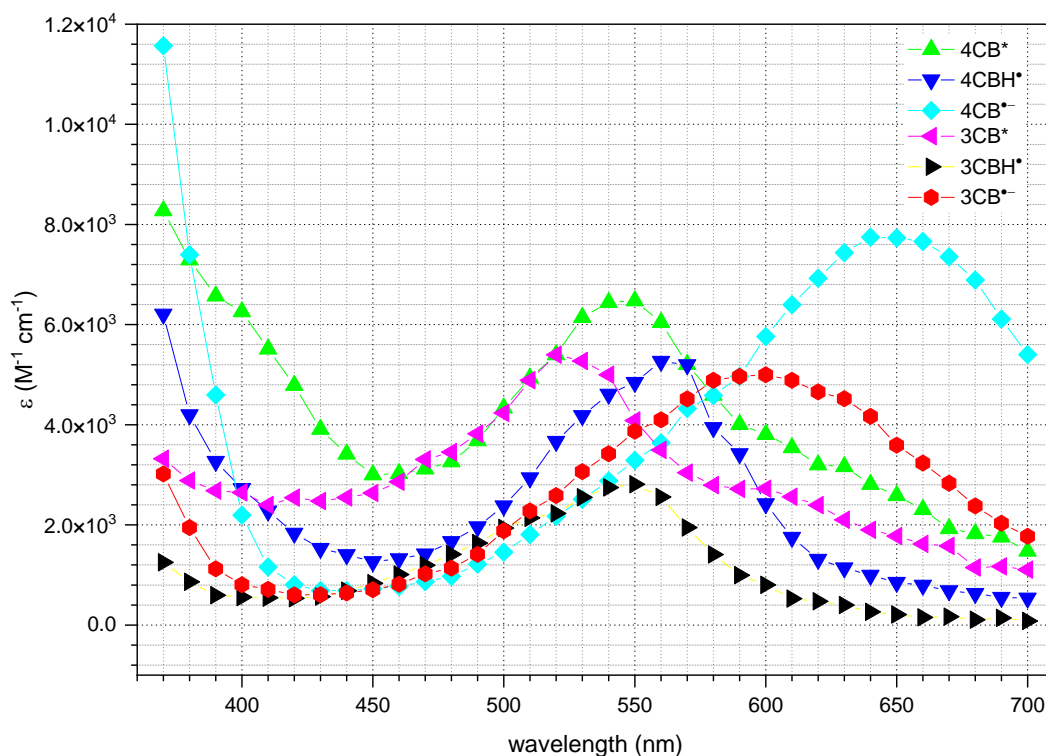


Figure 6 Transient absorption spectra of species derived from 4CB and 3CB excitation

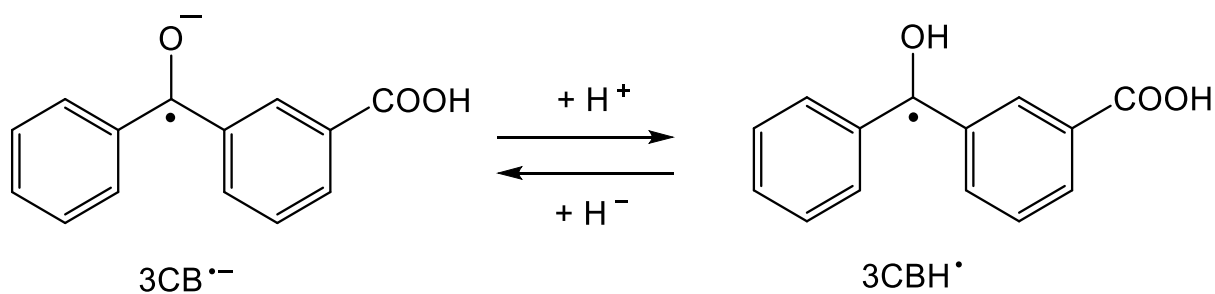
It is a significant advantage in the research of methionine-containing peptides – it allows a more accurate analysis of the kinetics of the absorption change in the abovementioned region.

A comparison of the photophysical properties of BP, 4CB, and 3CB is summarized in **Table 1**.

Table 1 Spectral characteristics of transients derived during reduction of BP, 4CB, and 3CB [51–53]

	BP		4CB		3CB	
	Absorption maximum (nm)	ϵ (molar absorption coefficient ($M^{-1} cm^{-1}$))	Maximum absorption (nm)	ϵ (molar absorption coefficient ($M^{-1} cm^{-1}$))	Maximum absorption (nm)	ϵ (molar absorption coefficient ($M^{-1} cm^{-1}$))
Excited triplet state	520	6500	535	6250	520	5400
Ketyl radical	550	3400	570	5900	550	2700
Radical anion	–	–	650	8800	600	5200

Another significant characteristic of 3-carboxybenzophenone and 4-carboxybenzophenone is their ability to undergo protonation (the acid-base equilibrium of $3CB^{\bullet-}$ and $3CBH^{\bullet}$ is shown in **Scheme 1**), a process that is dependent on the pH. This acid-base equilibrium can be described by the pK_a values of these compounds. Specifically, the pK_a of $3CBH^{\bullet}/3CB^{\bullet-}$ is 9.5 [51], while the pK_a of $4CBH^{\bullet}/4CB^{\bullet-}$ is 8.2 [40].



Scheme 1 Acid-base equilibrium of 3CB ketyl radical

The sensitizer plays a dual role in photosensitizer oxidation; it not only acts as an electron acceptor but also acts as a free radical scavenger, forming stable products that can be separated (HPLC) and identified (TOF-MS/MS).

1.5 Early events of photosensitized oxidation of methionine under anoxic conditions

Upon absorption of UV light, 3CB yields an excited singlet state, which undergoes efficient intersystem crossing to give the energetically lower excited triplet state ($^3\text{3CB}^*$). Generally, organic compounds can quench this excited triplet via electron- or hydrogen-transfer processes. The primary step of the photo-induced oxidation of methionine has been a topic of research since the 1970s [41].

The electron transfer (ET) from the quencher – electron-rich methionine residue – to $^3\text{3CB}^*$ results in the formation of an encounter complex: ($3\text{CB}^{\bullet-} \dots \text{S}^{\bullet+}$). It can decay via three different pathways [42,43,48,54,55]:

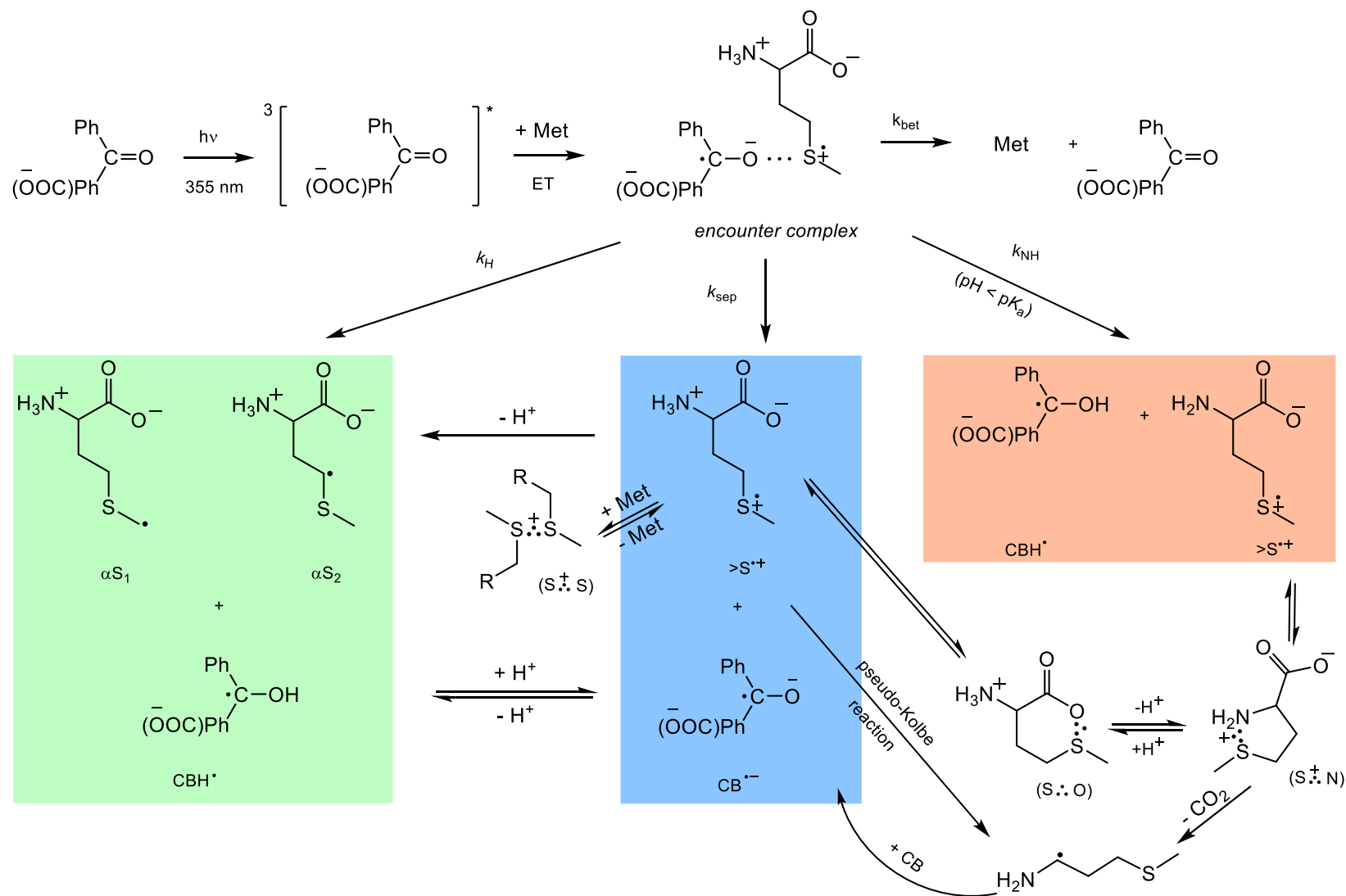
- 1) charge separation (k_{sep}) yielding 3CB radical anion ($3\text{CB}^{\bullet-}$) and sulfur radical cation ($\text{S}^{\bullet+}$),
- 2) proton transfer (k_{H}) yielding 3CB ketyl radical (3CBH^{\bullet}) and α -(alkylthio)alkyl radical (αS),
- 3) back electron transfer (k_{bet}), resulting in the regeneration of reagents in their ground state,
- 4) proton transfer within the encounter complex from the protonated amino group (possible when the amino group of the amino acid is not blocked) to $3\text{CB}^{\bullet-}$ (k_{NH}).

The main decay pathway at neutral and high pH is the diffusion apart of the encounter complex (k_{sep}). The initially formed sulfur radical cation ($>\text{S}^{\bullet+}$) can [52]:

- 1) be stabilized by the formation of a two-centered three-electron bond with any other neighboring atom having a lone electron pair (O, N, S) yielding ($\text{S}:\text{N}$) $^+$, ($\text{S}:\text{O}$), and/or ($\text{S}:\text{S}$) $^+$ transient species,
- 2) deprotonate yielding relatively stable α -(alkylthio)alkyl radical (αS),
- 3) decarboxylate and form α -aminoalkyl radicals (αN) via the pseudo-Kolbe mechanism.

Ultimately, the radicals that form stable products are αN , αS , and 3CBH^{\bullet} . Moreover, there are two possible structures of αS radicals – one in which the radical is located on the terminal carbon atom (αS_1) and the other (αS_2) in which the radical is located in the ε -position (see **Scheme 2** for the structures).

The presence of neighboring groups, such as the amide bond and the ester group, strongly affects the reaction pathways. The former rules out the possibility of proton transfer from the protonated amino group (excludes k_{NH}), and the latter eliminates decarboxylation.



Scheme 2 Mechanism of CB-sensitized photo-oxidation of methionine in aqueous solutions in the absence of oxygen

It is possible to follow the generation of the initial transients using time-resolved techniques, e.g., laser flash photolysis and radiolysis (more about laser flash photolysis and radiolysis setups in **Chapters 1.10.2 – Laser flash photolysis** and **1.10.3 – Pulse radiolysis**).

Using laser flash photolysis, allows to collect both transient absorption spectra at various delay times following the initial laser pulse and kinetic traces (absorption changes over time) at specific wavelengths. The obtained transient spectra comprise numerous overlapping spectra of several components (intermediates). They are decomposed into the individual spectra associated with the various transient species present via a multiple linear regression following the given **Equation 1** [56,57]:

$$\Delta A(\lambda_j) = \sum_j = \varepsilon_j(\lambda_i) a_j \quad (1)$$

where ε_j is the extinction coefficient of the j th species and the regression parameters, a_j , are equal to the concentration of the j th species times the optical path length of the monitoring light.

The procedure of resolving the transient spectra using the additive law of absorption, the reference spectra of transients, and the least squares method allows to follow the concentration changes of the transient species (short-lived excited triplet states, radicals, radical ions, other intramolecular and intermolecular three-electron transient species such as $(S\cdot\cdot S)^+$, $(S\cdot\cdot O)$ and/or $(S\cdot\cdot N)^+$ in time (the dependence of concentration as a function of time is called a concentration profile) and to observe the reaction kinetics [57]. **Figure 7** shows reference spectra of transient species: αS , αN_{subs} (αN radical that has substituted amino group), $(S\cdot\cdot N)^+$, $(S\cdot\cdot O)$, $(S\cdot\cdot S)^+$.

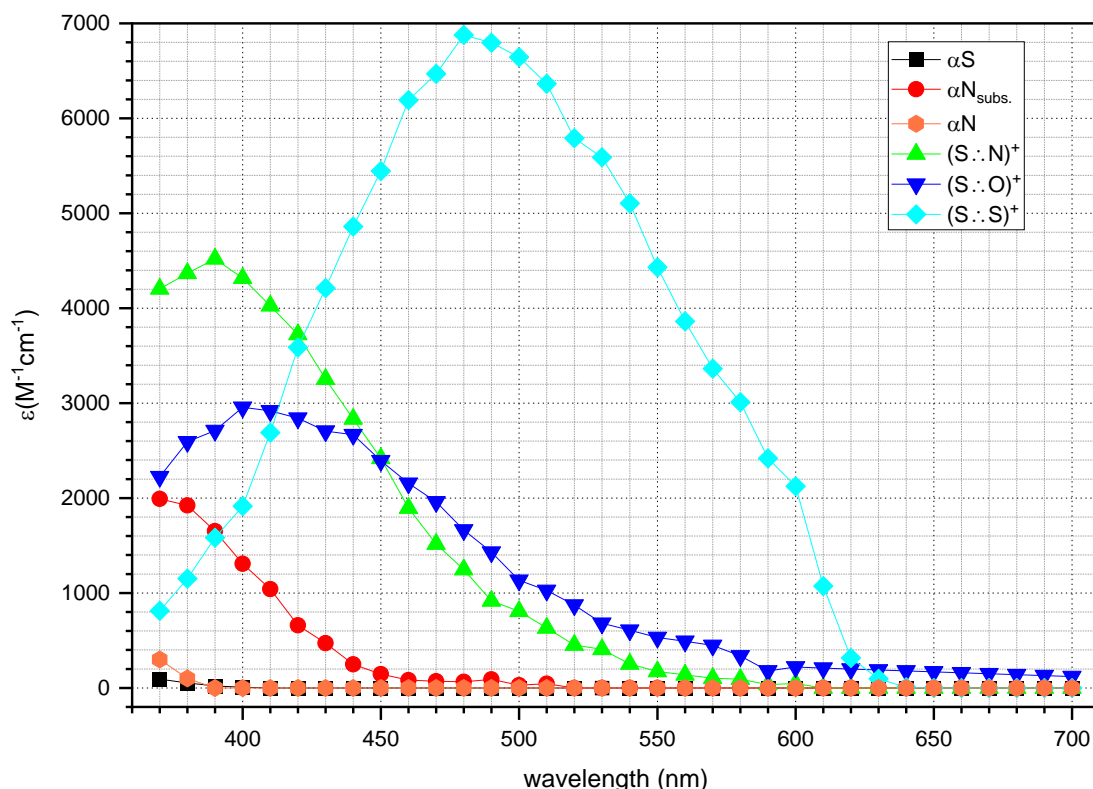


Figure 7 Reference spectra of transients

Unfortunately, the ground state absorption of the sensitizer – 3CB restricts the spectral range for nanosecond laser flash photolysis studies to wavelengths above 360 nm. Therefore, some transients, such as the α -(alkylthio)alkyl radical (α S) with its absorption maximum at $\lambda_{\text{max}} = 290$ nm and unsubstituted α -aminoalkyl radicals (α N) ($\lambda_{\text{max}} = 260$ nm), cannot be detected directly [58]. The sulfur radical cation ($>\text{S}^{\bullet+}$) is also not observable directly as it is unstable and quickly reacts with neighboring heteroatoms or is converted into $(\text{S}:\text{S})^+$ [59].

1.6 Photosensitized oxidation of methyl-cysteine in an oxygen-free environment

Research on the sensitized photooxidation of S-methyl cysteine is scarce and focused on comparing it with the oxidation mechanism of methionine.

It has been observed that MeCys does not form dimeric $(\text{S}:\text{S})^+$; instead, the structure of the amino acid favors the intramolecular electron transfer from the carboxylic group to the sulfur radical cation and subsequent decarboxylation reaction ($\phi_{\text{CO}_2} = 0.45$). The α -aminoalkyl radicals (α N) that are formed as a result of decarboxylation are good

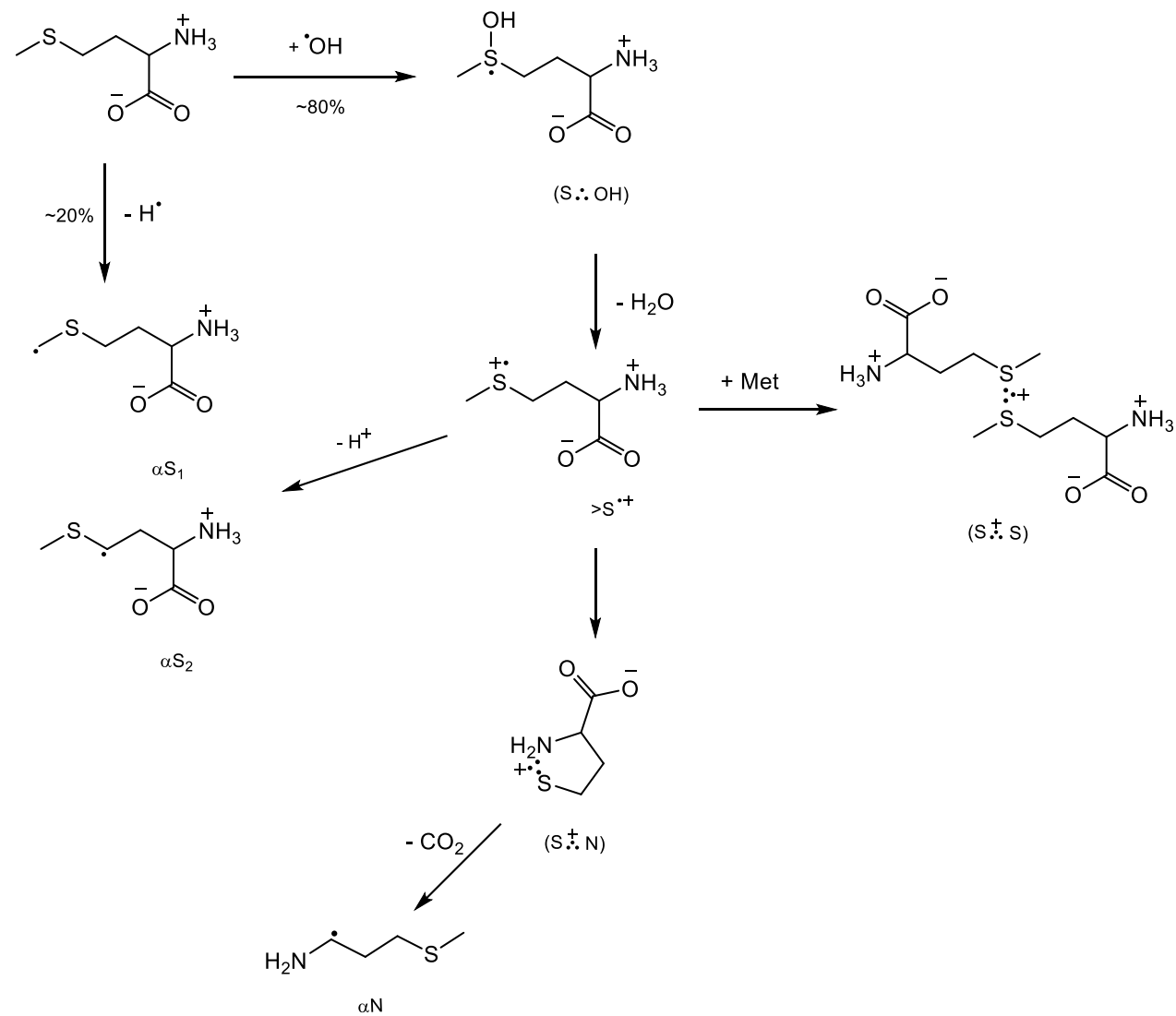
reductants. Their reaction with the sensitizer (CB) in the ground state is the source of the secondary radical anion ($\text{CB}^{\bullet-}$) [42,55].

1.7 Analysis of transients formed in anoxic radiation-induced oxidation of methionine

Klaus Dieter Asmus's group conducted extensive radiation chemical studies on methionine oxidation in the 1980s. Based on their research, the following mechanism and reaction rate constants are calculated [59–61].

The initial step of the radiation-induced oxidation of methionine is competition between the electrophilic addition of HO^\bullet radical (generated in the radiolysis of water) to the sulfur atom ($k = 1.8 \times 10^{10} \text{ M}^{-1} \text{ s}^{-1}$) and subsequent formation ($\text{S}:\text{OH}$) as an initial product and hydrogen atom abstraction ($k = 4.5 \times 10^9 \text{ M}^{-1} \text{ s}^{-1}$). The rate constants reveal a 1:4 ratio favoring HO^\bullet addition over hydrogen atom abstraction.

Further steps of the reaction and the formed products depend greatly on the pH. In strongly acidic solutions ($\text{pH} < 3$), ($\text{S}:\text{OH}$) undergoes dehydration, yielding sulfur radical cation $>\text{S}^{\bullet+}$ ($k = 10^5 \text{ s}^{-1}$). This reaction involves external protons from the solvent. The sulfur radical cation can either be deprotonated ($k = 2.4 \times 10^5 \text{ s}^{-1}$) to produce α -(alkylthio)alkyl radicals (αS) at low concentration or, at high concentration, it can be stabilized through intramolecular interaction with another unreacted molecule forming dimeric ($\text{S}:\text{S})^+$ complex ($k \approx 10^9 \text{ M}^{-1} \text{ s}^{-1}$). At higher pH (> 3), when the carboxyl group is deprotonated, the formation of $>\text{S}^{\bullet+}$ via dehydration involves a proton from the amino group ($-\text{NH}_3^+$). Subsequently, the sulfur radical cation can be stabilized via intramolecular interaction with the nitrogen atom and the formation of five-membered ($\text{S}:\text{N})^+$ ($k > 3.2 \times 10^6 \text{ s}^{-1}$). Opening the ring yields an N-centered radical cation, which then undergoes decarboxylation, forming the α -aminoalkyl radical (αN).



Scheme 3 Primary steps of methionine oxidation by $\cdot\text{OH}$ radicals in the deoxygenated aqueous solution. Source: [60]

1.8 Stable products formation

Despite the extensive studies on the photo- and radiation-induced oxidation of methionine and its derivatives, the analysis of the stable products of the reaction has only recently become the focus of the research. Furthermore, based on the structure of the post-oxidation stable products, it is also possible to deduce the structure of its radical precursor, which is essential when the transient cannot be directly observed (for example, α -(alkylthio)alkyl radical in laser flash photolysis). The quantitative analysis of stable products is often performed using high-performance liquid chromatography and mass spectrometry to acquire qualitative data (more about both techniques in **Chapters 1.10.4 – High-performance liquid chromatography** and **1.10.5 – Mass spectrometry**).

1.8.1 Photosensitized oxidation

The metastable intermediates generated in the sensitized anoxic oxidation can undergo radical cross-coupling, forming stable products. The mentioned intermediates are α S (two types: α S₁ and α S₂, see **Scheme 2** for the structures), α N, and CBH[•] radicals, which are generated respectively via deprotonation, decarboxylation, and reduction of the sensitizer (e.g., 3-carboxybenzophenone, 3CB or 4-carboxybenzophenone, 4CB). They can recombine differently depending on the reaction conditions, producing various adduct-type stable products. In sensitized oxidation, the intermediate with the highest concentration is ketyl radical (CBH[•]), which scavenges the other radicals. As a result, the possible stable products are α S-CBH, α N-CBH, α S- α S, α N- α N, α S- α N and CBH-CBH [62]. The dimeric products α S- α S, α N- α N, and α S- α N are less likely to be generated due to the small concentration of the precursor radicals; they are also more challenging to detect using high-performance liquid chromatography with a diode array detector (DAD) as they do not have a chromophore moiety (unlike adducts with CB that possess two aromatic rings).

1.8.2 Radiation-induced oxidation

Methionine sulfoxide is the main stable product of anoxic radiation-induced oxidation of methionine residue [63–66]. Nevertheless, there are still controversies concerning its formation. Two proposed mechanisms are direct HO[•] oxidation (one-electron oxidation) or a reaction with hydrogen peroxide generated *in situ* (two-electron oxidation). The one-electron oxidation observed in deoxygenated solutions involves the hydration of the sulfur in sulfur radical cation $>\text{S}^{\bullet+}$ [67]. On the other hand, it was proposed Met is

oxidized to MetSO by H_2O_2 generated from radiolysis of water (in oxygenated and deoxygenated solution), or H_2O_2 formed in the disproportionation of $\text{O}_2^{\bullet-}$ (in the presence of oxygen). HO^\bullet leads exclusively to the formation of aldehyde in the oxygenated solution, in the absence of oxygen, the amine is also generated. Besides oxidants HO^\bullet and H_2O_2 , water radiolysis also leads to other reactive reductive species, e^-_{aq} and H^\bullet (more about gamma radiolysis of water in **Chapter 1.10.3 – Pulse radiolysis**) [68]. The sulfur atom of methionine is selectively attacked by H^\bullet , yielding α -aminobutyric acid (Aba) in the absence of oxygen. When the oxygen is present, homoserine is formed instead [69–71].

Scheme 4 shows the reaction mechanism of the γ -irradiated solution of Met in the presence and absence of molecular oxygen [69].

1.9 Literature review of photo- and radiation-induced oxidation of methionine derivatives in deoxygenated solutions

Methionine comprises approximately 6% of proteins' total amino acid content [72]. Therefore, it is essential to investigate how neighboring groups and the positioning of methionine in the molecule influence its oxidation mechanism. Most studies in this area employ time-resolved techniques, such as laser flash photolysis and pulse radiolysis.

The N-terminal methionine residue in proteins can be mimicked by a methionine derivative in which the carboxylic group is blocked, for example, by an ester or amide group (e.g., Met-OCH₃, Met-NH₂). Conversely, when the amino group is modified to form an N-acetyl group, the amino acid resembles the amide bond found in C-terminal methionine (e.g., Ac-Met). Blocking amino and carboxylic groups imitates methionine as an internal amino acid residue (e.g., Ac-Met-OCH₃, Ac-Met-NH₂, Ac-Met-NH-CH₃).

1.9.1 Photosensitized oxidation

Depending on the structure of the Met-derivative and the experimental conditions (concentrations and pH), several reactions can occur following the formation of the encounter complex. Possible reactions include deprotonation, decarboxylation, interaction with nitrogen, cyclization to (S: $\dot{\text{N}}$)⁺ and forming an intermolecular (S: $\dot{\text{S}}$)⁺ radical cation. The intermediates observed in specific experiments depended on the pH and the structure of the terminal groups.

Table 2 summarizes the quantum yields of the primary intermediates of the photosensitized oxidation of methionine and its derivatives. From this data, it can be concluded that:

- 1) the (S: $\dot{\text{N}}$)⁺ is observed only when the amino group is unsubstituted; in Met-OCH₃ and Met-NH₂, it is the predominant transient species regardless pH (excluding CBH \bullet and CB \bullet^-) – it is formed via proton transfer from the protonated amino group to the CB \bullet^- radical anion within the encounter complex [CB \bullet^- ...>S \bullet^+] (k_{NH} pathway, see **Scheme 2**),
- 2) the decarboxylation reaction can be disregarded for all Met derivatives,
- 3) in case of Ac-Met oxidation, the primary intermediate is the dimeric sulfur radical cation ((S: $\dot{\text{S}}$)⁺),

- 4) at acidic pH, when both the amino and carboxylic groups are blocked (Ac-Met-OCH₃ and Ac-Met-NH₂), the quantum yields of (S.:N)⁺ and (S.:S)⁺ are low, with the ketyl radical (CBH•) as the primary intermediate.

Table 2 The quantum yields of the primary intermediates of the photosensitized oxidation of methionine and its derivatives

Met- derivative	pH	ϕCBH^\bullet	$\phi\text{CB}^{\bullet-}$	$\phi(\text{S}.: \text{N})^+$	$\phi(\text{S}.: \text{S})^+$	ϕCO_2	Ref.
Met	6	0.11	0.27	0	0.23	0.28	[42,48]
	11	0.05	0.66	0.38	0.10	0.55	
Met-OCH₃	6	0.39	0	0.20	0.04	0	[43,48]
	10	0	0.43	0.28	0.04	0	
Met-NH₂	5	0.39	0	0.28	0.10	0	[42,43,48]
	10	0	0.48	0.28	0.07	0	
Ac-Met	7	0.12	0.29	0	0.28	0.05	
	10	0.13	0.29	0	0.27	—	
Ac-Met-OCH₃	6	0.22	0.04	<0.05	0.07	0	[43,48]
	10	0.12	0.11	<0.05	—	—	[73]
Ac-Met-NH₂	6	0.19	0.07	0	0.09	0	[43,48]

1.9.2 Radiation-induced oxidation

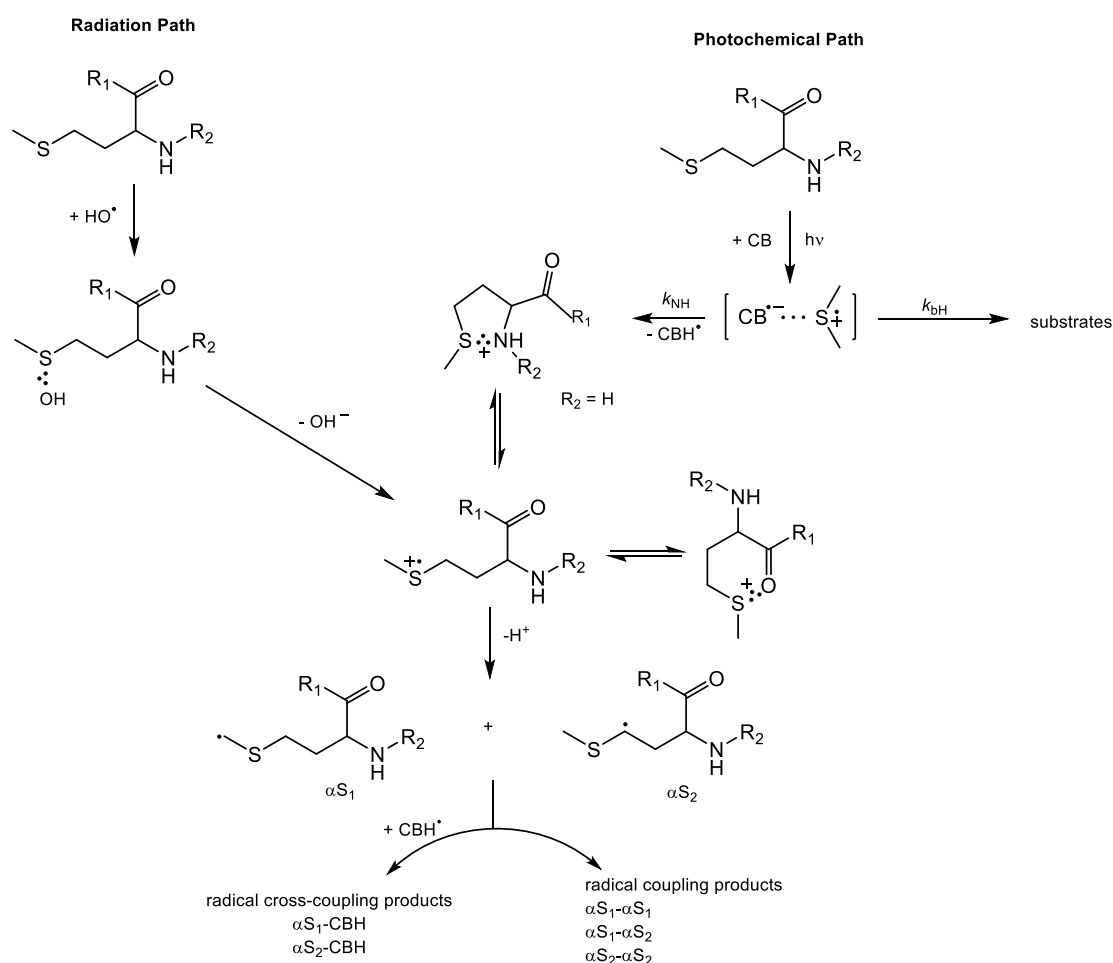
The initial steps of •OH-induced oxidation of methionine and its derivatives are similar: the formed transient species are (S.:OH), αS radicals, and (S.:S)⁺. Differences are observed in stabilizing the sulfur radical cation and forming three-electron bonds with heteroatoms, such as nitrogen and oxygen.

In acetylated methionine (Ac-Met), no interaction of sulfur with nitrogen was observed. However, decarboxylation is possible, albeit less effective than in methionine ($G(\text{CO}_2)_{\text{Ac-Met}}$ 0.27 vs $G(\text{CO}_2)_{\text{Met}}$ 0.52) [71]. Acetylation also extends the time of the adduct with OH (Ac-MetS.:OH) as there is not a -NH₃⁺ group that acts as an intramolecular proton donor in the decay of MetS.:OH [60,74,75].

On the other hand, substituting the carboxy group with the ester group eliminates the possibility of decarboxylation. It prolongs the half-time of (S.:N)⁺ to 1.1 ms, compared to the half-time of unsubstituted methionine: $\tau_{1/2} \text{Met}(\text{S}.: \text{N})^+ = 220 \text{ ns}$ [61].

Simultaneous blocking of the carboxyl and amino groups limits the possibilities of stabilizing the sulfur radical cation — the three-electron bonds could be formed only with oxygen or nitrogen in the acetyl, ester, or amide group. The research on the radiation-induced oxidation of Ac-Met-NH₂ and Ac-Met-OCH₃ shows that at pH 4.0 and 4.6, only kinetically favored (S:O)⁺ is formed whereas in higher pH, both (S:O)⁺ and (S:N)⁺ were observed [76]. For another dually blocked methionine derivative, Ac-Met-NH-CH₃ in neutral pH, only (S:N)⁺ species were detected. There are two possible structures of (S:N)⁺ as there is a nitrogen atom in the methylated amide moiety and an acetylated amino group. The *G*-value (*G* = 0.10 μmol J⁻¹) of both (S:N)⁺ structures reaches its maximum at 10 μs following the electron pulse and, at that time, accounts for 17% of the total present radicals [77].

Scheme 5 shows the photochemical and radiation paths of oxidation of methionine derivatives.



Scheme 5 The mechanism of CB-sensitized photo- and radiation-induced oxidation of methionine derivatives in aqueous solutions (*R*₁ represents -OCH₃, -NH₂ and -NHCH₃ groups, *R*₂ represents Ac- group or H-). Based on [48]

1.10 Methodology

1.10.1 UV-Vis spectrophotometry

UV-Vis absorption spectroscopy is a stationary spectroscopic method for analyzing substances containing chromophores (e.g., carbonyl groups and aromatic rings). A UV-Vis spectrophotometer measures the absorption (or transmission) of ultraviolet and visible light that passes through a sample, resulting in an absorption spectrum.

The principle for UV-Vis detection is Beer-Lambert law, which states that: "The absorbance (A) of a beam of collimated monochromatic radiation in a homogeneous isotropic medium is proportional to the absorption path length, l , and to the concentration, c , or — in the gas phase — to the pressure of the absorbing species, where the proportionality constant, ϵ , is called the molar (decadic) absorption coefficient" [78] – it is expressed by the following **Equation 2**:

$$A = \epsilon lc \quad (2)$$

In the multicomponent mixture, a principle of additivity of absorbance is applied. It says that the absorption of light by two or more compounds at the same wavelength is additive; in other words, the total absorbance of a mixture at a specific wavelength is the sum of the absorbance values of each compound in this mixture at that wavelength (**Equation 3**).

$$A_n = A_1 + A_2 + A_3 + \dots \quad (3)$$

The critical components of a spectrophotometer are a light source, sample area, and one or more detectors. **Figure 8** shows the schematic diagram of the spectrophotometer, including each component's role.

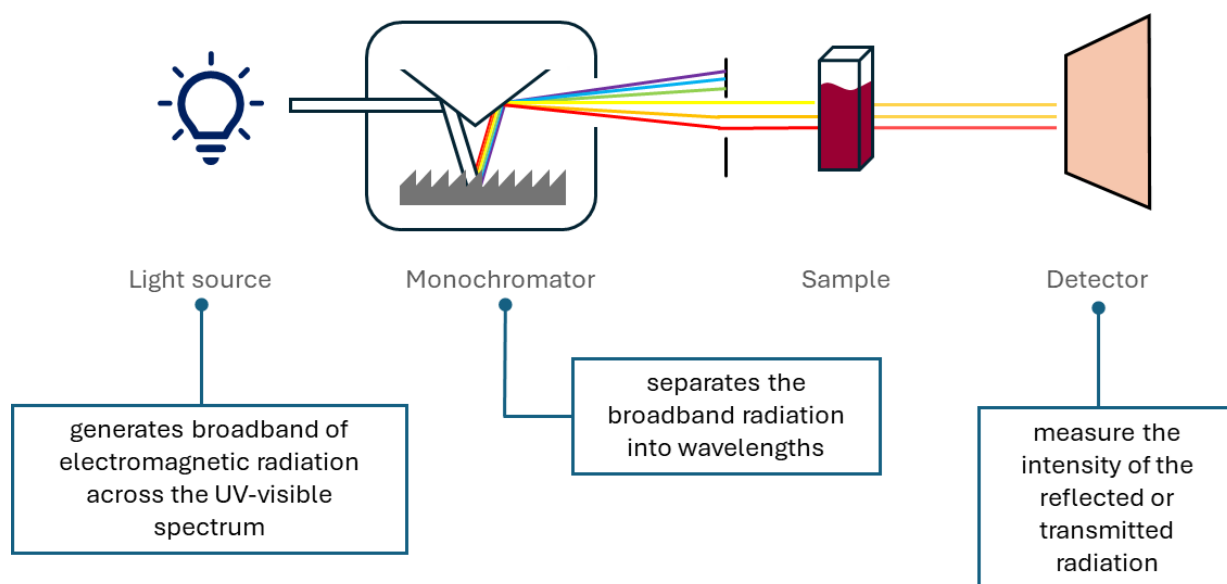


Figure 8 Scheme of the UV-Vis spectrophotometer

UV-Vis spectrophotometers are also commonly used as detectors in high-performance liquid chromatography (HPLC) systems due to their reliability, ease of use, and universal response to the chromophores. There are three common types of UV detectors. The fixed-wavelength detectors are not widely used today. They operate on one distinct wavelength, typically a 254 nm emission line from a low-pressure mercury lamp. Variable wavelength (VWD) and diode array detectors (DAD) determine the absorbance of the sample at a single wavelength or a wavelength range. In VWD, the polychromatic light spectrum generated by the deuterium lamp is directed onto a motorized diffraction grating, where it is dispersed into component wavelengths. Afterward, the grating is rotated to select a specific wavelength or a narrow range of wavelengths which passes through the slit to the flow cell and then to the photodetector. In DAD, the polychromatic light from the deuterium lamp first passes through the flow cell; the transmitted light is directed onto the diffraction grating and then onto the array of photodiodes. Spectra from individual photodiodes are generated simultaneously [79].

1.10.2 Laser flash photolysis

The laser flash photolysis (LFP) technique is a time-resolved method used to monitor fast photochemical processes. It provides information about the primary steps of the mechanism of the reactions happening during initial nano- and microseconds. LFP was used for the first time in 1950 by George Porter from Cambridge University [80]. It was such a pioneering invention that later, in 1967, he, together with Manfred Eigen and Ronald Norrish, were awarded the Nobel Prize in chemistry "for their studies of extremely

fast chemical reactions, effected by disturbing the equilibrium by means of very short pulses of energy" [81].

Laser flash photolysis is a "pump-probe" method, meaning first, a sample is excited using photons generated by a laser (pump). Then, a second pulse from a lamp (probe) monitors the change in the absorbance of the solution over time. The laser flash experiments were carried out at the Department of Physical Chemistry and Photochemistry at Adam Mickiewicz University, and the LFP setup used in this work is presented in **Figure 9**.

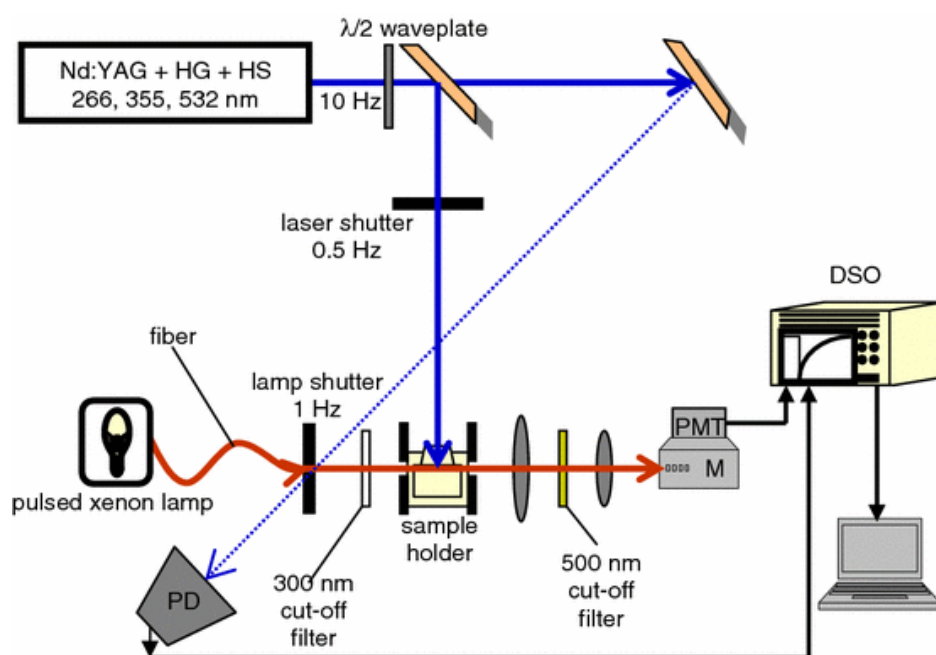


Figure 9 The experimental setup for nanosecond laser flash photolysis. Figure adapted from [73] with publisher's permission. Copyright Springer Nature 2009.

The crucial elements of this setup are Nd: YAG laser (a pump), which can generate 266, 355, and 532 nm excitation wavelengths at a 10 Hz repetition rate; pulsed xenon lamp (a probe); monochromator (M); photomultiplier (PMT); optics, mechanics, electronics (oscilloscope, photodiode, delay generator, shutters, filters); and computer [73].

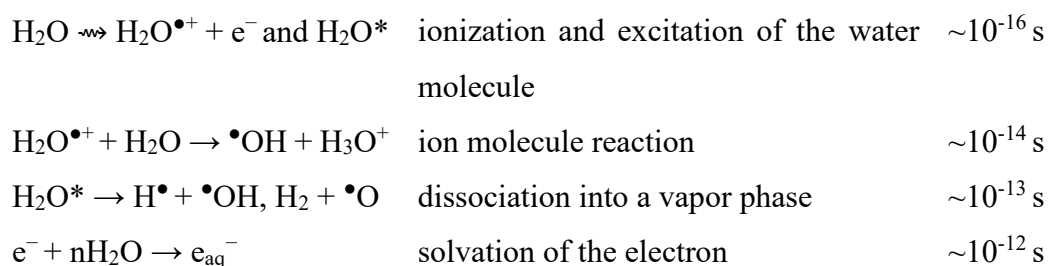
Apart from the concentration profiles mentioned in **Chapter 1.5 – Early events of photosensitized oxidation of methionine**, the laser flash photolysis also enables us to determine primary quantum yields using relative actinometry and an aqueous solution of 3-carboxybenzophenone as an actinometer since its spectral properties are known [51].

1.10.3 Pulse radiolysis

Pulse radiolysis (PR) and laser flash photolysis are used to generate and study transient species (radical ions, excited states, electrons, and free radicals). LFP and PR are pump-

probe methods, but in pulse radiolysis, the high-energy electrons generated in the accelerator act as a pump. Chromophoric groups are not required in the pulse radiolysis experiments because the ionization radiation is non-selective. Electrons interact with various molecules independently of their chemical nature and don't distinguish between solvent and solute. Consequently, because there are more molecules of solvent than the solute in the dilute solution ($[\text{solute}] \leq 0.1 \text{ mol dm}^{-3}$), the primary source of the radicals is the solvent. The solute-derived radicals are formed by interacting with solvent-derived radicals and the solute. The electron beam has low LET (linear energy transfer, which is the rate of energy loss per unit length of the particle); thus, the ionization events occur in small, well-separated regions called spurs [68,82].

In the aqueous solutions, the radiolysis of water is the source of the reactive species. The water radiolysis can be summarized by the following reactions (the indicated time is the time by which each event is completed):



By $\sim 10^{-12} \text{ s}$, all products from the above reactions are gathered in spurs. Next, these products begin to diffuse and react with other radicals and/or molecules of scavenger, forming secondary radicals or products. Within 10^{-7} s , these spur processes and diffusive-escape are complete, and radiolysis of water can be summed up in one reaction:



The numbers in brackets are the radiation chemical yields (G values) in $\mu\text{mol J}^{-1}$ [68].

The e_{aq}^- and H^\bullet are reducing agents, whereas HO^\bullet is an oxidant. To achieve a predominantly oxidizing environment, the aqueous solution is saturated with nitrous oxide (N_2O) to convert e_{aq}^- into HO^\bullet according to the following reaction:



Consequently, ~90% of radicals formed in water radiolysis are oxidants, and the remaining ~10% are H^\bullet which have reducing properties. The reaction of N_2O with H^\bullet is too slow ($k = 2.1 \times 10^6 \text{ dm}^3\text{mol}^{-1} \text{ s}^{-1}$) to be relevant [68,83].

The major components of the pulse radiolysis setup are similar to the laser flash photolysis setup described previously (**Chapter 1.10.2 - Laser flash photolysis**): pump (linear electron accelerator), digital oscilloscope, xenon lamps (probe), monochromator, photomultiplier, and computer. There are various detection systems available for pulse radiolysis, e.g., ultraviolet-visible-near infrared (UV-Vis-NIR) or infrared (IR) spectrophotometry, Raman spectroscopy, conductometry, electron paramagnetic resonance (EPR), nuclear magnetic resonance (NMR), light scattering (LS), chemically induced dynamic nuclear polarization (CIDNIP) [84].

The differences between laser flash photolysis and pulse radiolysis are summarized in **Table 3** below.

Table 3 Differences between LFP and PR

	Laser flash photolysis	Pulse radiolysis
Energy source	Laser pulses emitting photons	Accelerators generating high energy electrons
Mechanism	Photons interact with solute	In a dilute solution, electrons interact with the solvent
Chemical nature of the sample	Chromophore needed (with absorption matching to the wavelength of the laser)	No chromophore needed
Available spectral region	Fixed wavelength (depending on the type of the laser)	The whole spectral region is available

1.10.4 High-performance liquid chromatography

The classical column chromatography was invented in the early 1900s by Mikhail Tswett. He described the principle of the separation of plant pigments in 1903 in a lecture in Warsaw and first used the word "chromatography" in a paper published three years later. Chromatography is defined as: "a physical method of separation in which the components

to be separated are distributed between two phases, one of which is stationary (stationary phase) while the other (the mobile phase) moves in a definite direction" [78]. In liquid chromatography, the mobile phase is a liquid and "high-performance" ("or high-pressure") means that high pressure is applied to pass the mobile phase, contrary to "low pressure" (traditional) liquid chromatography which rely on gravity.

A lot of development in the area of liquid chromatography happened between the 1900s and nowadays: in the 1940s, paper chromatography was introduced (the technique used today as thin layer chromatography - TLC), and in the late 1950s, an amino-acid analyzer based on ion exchange chromatography was introduced, the early 1960s brought gel-penetration chromatography and finally in the late 1960s high-performance liquid chromatography was developed. Since then, the technique has been widely practiced, modified, and improved [79].

HPLC has become a powerful analytical tool used in both quantitative and qualitative studies of chemical reactions. After separation, the stable products can be identified, quantified, and purified. HPLC system consists of the pumping system, degassing unit, autosampler, column (and column oven), detector, and data processor. **Figure 10** below shows the HPLC system schematic, including each component's role.

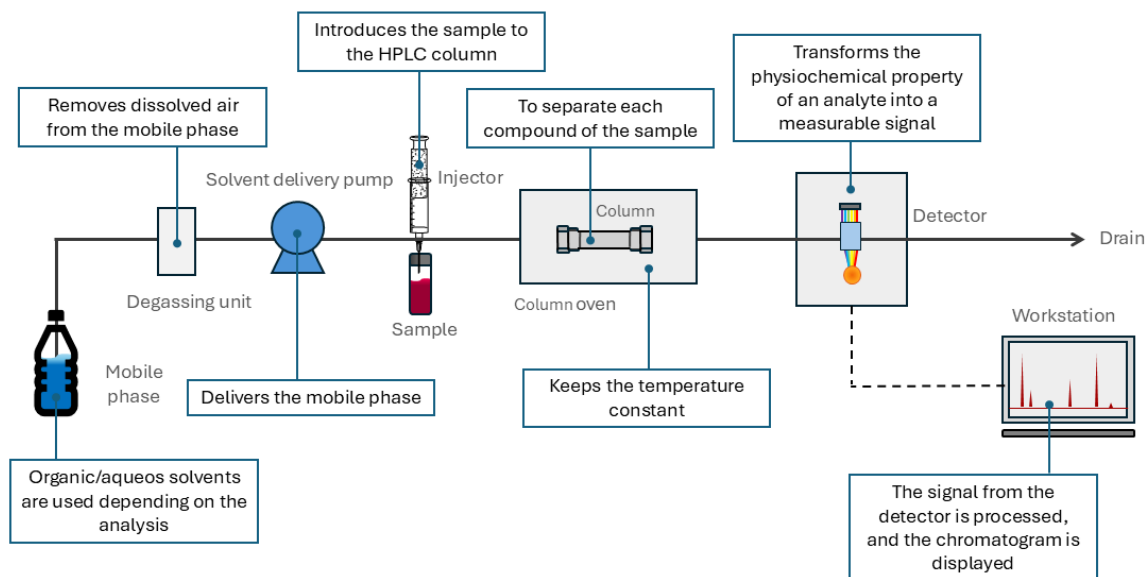


Figure 10 HPLC Flow Diagram

Two components that have the most significant influence on the successful separation of the mixture are the mobile phases (polar vs. non-polar) and the choice between gradient

vs. isocratic elution (meaning the solvent composition is changed throughout the separation or the solvent composition stays constant, respectively) and the choice of the HPLC column. The wide variety of commercially available columns and numerous HPLC-compatible solvents make HPLC a versatile experimental technique that can be customized and adjusted to the sample.

There are two primary HPLC separation modes. They are characterized by the choice of the column and mobile phase: reverse-phase (RPC) and normal phase chromatography (NPC). RPC features the non-polar stationary phase and the polar mobile phase (e.g., C18 column and a mixture of water and acetonitrile as the mobile phase). In contrast, a polar stationary phase (typically unbounded silica or silica bounded with cyano or amino groups) and a non-polar mobile phase (e.g. hexane) are used in NPC. Generally, the reverse-phase is used for water-soluble samples and the normal-phase for samples insoluble in water, preparative HPLC, and the separation of the isomers.

The final component in the HPLC system is the detector that transforms the physiochemical property of an analyte into a measurable signal. The choice of detector depends on the nature of the analytes and the required sensitivity. An example of a sample-specific detector is the UV-Vis detector described in **Chapter 1.10.1 – UV-Vis spectrophotometry**. The other popular detector – mass spectrometry – will be described below.

1.10.5 Mass spectrometry (MS)

The main purpose of the mass spectrometer is to produce ions and then separate and analyze them according to their mass-to-charge ratio (m/z). Mass spectra contain information about the elemental and isotopic composition of the analytes.

The mass spectrometer consists of three essential components: the ion source, the mass analyzer, and the detector. **Table 4** summarizes the role and examples of each element [85].

Table 4 *The components of the mass spectrometer*

Element	Role	Examples
the ion source	ionization of the sample	Chemical Ionization (CI), Atmospheric-Pressure Chemical Ionization (APCI), Electrospray Ionization (ESI), Matrix-Assisted Laser Desorption/Ionization (MALDI), Inductively Coupled Plasma (ICP)
the mass analyzer	separation of the ions according to m/z	Quadrupole, Ion Trap, Time-of-Flight (TOF), hybrids (e.g. Quadrupole Time-Of-Flight – QTOF)
the detector	converting a current of separated ions into a useable signal	Faraday Cup, Electron Multipliers, Electro-Optical Ion Detectors

Apart from being an independent analytical instrument, MS can be used as a detector in liquid chromatography, creating a powerful analytical technique (LC-MS) that combines the separation capabilities of liquid chromatography (LC) with the detection and identification capabilities of mass spectrometry (MS).

1.10.6 Tandem mass spectrometry (MS/MS)

Tandem mass spectrometry involves at least two stages of mass analysis. In the first stage, the precursor ions are primarily filtered according to their m/z and isolated in the first mass analyzer (MS^1). Then, the selected ions undergo fragmentation in the collision cell. The resulting fragment ions are again selected according to m/z and analyzed in the second mass analyzer (MS^2), finally reaching the detector. MS/MS instrumentation combines two or more identical types of mass analyzers in series, such as a triple quadrupole analyzer or a TOF/TOF analyzer. Alternatively, hybrid instruments for MS/MS can be developed by combining two or more mass analyzers; for example, a

quadrupole and TOF can be paired to create Q-TOF analyzers or a quadrupole and linear ion trap to form a Q-Trap instrument [86].

It is also possible to further extend the selection-fragmentation-detection sequence to produce the fragments of the product ions generated in the second mass analyzer (MS^2) and achieve even better sensitivity and specificity. This type of experiment is the MS^n experiment (where n represents the number of generations of ions being analyzed) [85].

MS/MS offers improved sensitivity and specificity compared to single-stage mass spectrometry. Tandem mass spectrometry and fragmentation experiments provide structural information on the photoproducts and, after detailed analysis, their metastable precursor radicals. It is even possible to determine which of the two carbon atoms the radical is localized.

High-resolution tandem mass spectrometry enables the identification of the unknown molecule based on the monoisotopic (exact) mass and the isotope distribution. Monoisotopic mass is the sum of the exact masses of the most abundant isotope of each element in the molecule. Meanwhile, the nominal mass is the molecular weight calculated using the integer of the atomic masses of the elements. Two molecules can have the same nominal mass but different empirical formulas and, therefore, different monoisotopic masses. For example, CH_4O and O_2 have the same nominal mass, 34 u, but their monoisotopic mass have detectable difference: $M_{CH_4O} = 32.02621$, $M_{O_2} = 31.98983$. The monoisotopic masses of more complex molecules differ on the fourth or fifth decimal place, and the high-resolution mass spectrometers can detect such subtle yet crucial differences. Mass accuracy shows the difference in parts per million (ppm) between the calculated exact mass of an ion and the mass measured by the mass spectrometer following **Equation 4**:

$$mass\ accuracy = \frac{measured\ mass - calculated\ exact\ mass * 10^6}{calculated\ exact\ mass} \quad (4)$$

In the high-resolution mass spectrum, one signal is presented as a series of peaks called isotope distribution. It shows the mass and the likelihood of the occurrence of different isotopic variants or isotopologues of a molecule [87]. Isotope abundances of the elements are compiled with and published by IUPAC [88]. **Table 5** shows the isotopes of sulfur and oxygen and their abundances.

Table 5 Isotopic abundance of sulfur and oxygen isotopes [88]

Element	Abundance [%]
sulfur	^{32}S 94.99
	^{33}S 0.75
	^{34}S 4.25
	^{36}S 0.01
oxygen	^{16}O 99.757
	^{17}O 0.038
	^{18}O 0.205

Isotopic distribution is a valuable tool for confirming the elemental composition of the molecule. For example, distinguishing between sulfone ($\text{R-SO}_2\text{-R'}$, $M_{\text{SO}_2} = 63.96190$) and disulfide (R-SS-R' , $M_{\text{SS}} = 63.94414$). The abundance of sulfur-34 is 4.25% (see **Table 5**), so when there are two sulfur atoms, the abundance of peak + 2 Da should be about 8.5%. The two isotope distributions in **Figure 11** show this difference based on the simple sulfone and disulfide.

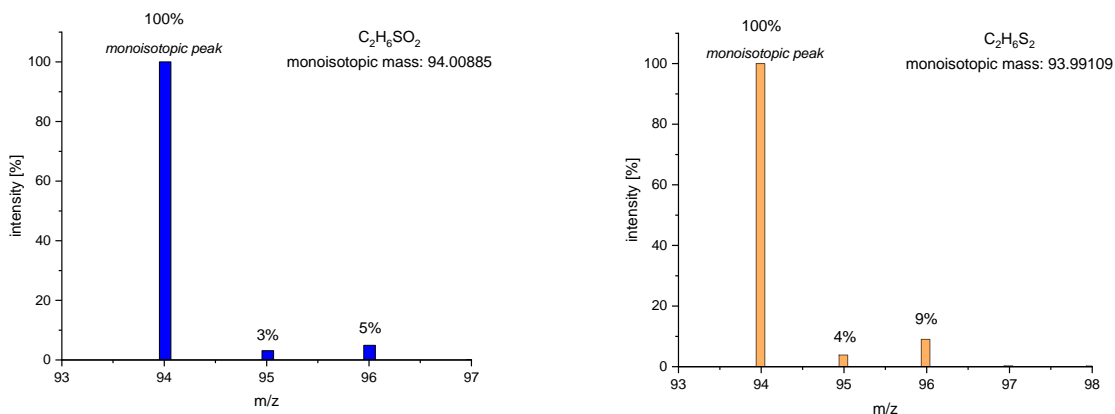


Figure 11 Isotope distribution of simple sulfone and disulfide [89]

2 RESEARCH OBJECTIVE

Previously, research primarily employed time-resolved techniques such as laser flash photolysis and pulse radiolysis to study the anoxic oxidation mechanisms of methionine, cysteine, and their derivatives. However, these methods alone do not adequately capture the complete dynamics between sulfur-containing amino acids, the excited triplet state of the sensitizer, or the reactive species generated from water radiolysis. A combination of steady-state and time-resolved approaches is necessary to comprehensively reveal the oxidation reaction's mechanism and follow the fate of the short-lived transients until they become stable products.

The main aim of this thesis was to **thoroughly investigate and describe the mechanisms behind photosensitized and radiation-induced oxidation of biomimetic model amino acids that contain a sulfide group**. Although these reactions have been studied for decades, their mechanisms remain only partially understood and require further exploration using modern and more sensitive techniques.

The specific objectives were to:

- (i) characterize in detail the photoreduction of the sensitizers – aromatic ketones;
- (ii) analyze quantitatively and qualitatively stable products and transient species (three-electron-bonded intermediates, free radicals, and radical ions) of the photosensitized and radiation-induced model compounds;
- (iii) describe the effect of the structure (neighboring functional groups, the length of the amino acid side chain) on the reactivity of studied compounds and the mechanism of their oxidation;
- (iv) explore the correlation between the three-electron bond and the structure of the stable product.

The presented doctoral dissertation is based on the following scientific papers:

P1 Grzyb, K.; Frański, R.; Pedzinski, T. Sensitized Photoreduction of Selected Benzophenones. Mass Spectrometry Studies of Radical Cross-Coupling Reactions. *Journal of Photochemistry and Photobiology B: Biology* 2022, 234, 112536. DOI: 10.1016/j.jphotobiol.2022.112536.

P2 Pedzinski, T.; Grzyb, K.; Kaźmierczak, F.; Frański, R.; Filipiak, P.; Marciniak, B. Early Events of Photosensitized Oxidation of Sulfur-Containing Amino Acids Studied by Laser Flash Photolysis and Mass Spectrometry. *Journal of Physical Chemistry B* 2020, 124 (35), 7564–7573.

DOI: 10.1021/acs.jpcb.0c06008.

P3 Pędzinski, T.; Grzyb, K.; Skotnicki, K.; Filipiak, P.; Bobrowski, K.; Chatgililoglu, C.; Marciniak, B. Radiation- and Photo-Induced Oxidation Pathways of Methionine in Model Peptide Backbone under Anoxic Conditions. *International Journal of Molecular Sciences* 2021, 22 (9), 4773.

DOI: 10.3390/ijms22094773.

P4 Grzyb, K.; Sehwat, V.; Pedzinski, T. The Fate of Sulfur Radical Cation of N-Acetyl-Methionine: Deprotonation vs. Decarboxylation. *Photochem* 2023, 3 (1), 98–108.

DOI: 10.3390/photochem3010007.

P5 Grzyb, K.; Kaźmierczak, F.; Pedzinski, T. Efficient Decarboxylation of Oxidized Cysteine Unveils Novel Free-Radical Reaction Pathways. *Journal of Photochemistry and Photobiology A: Chemistry* 2024, 451, 115530.

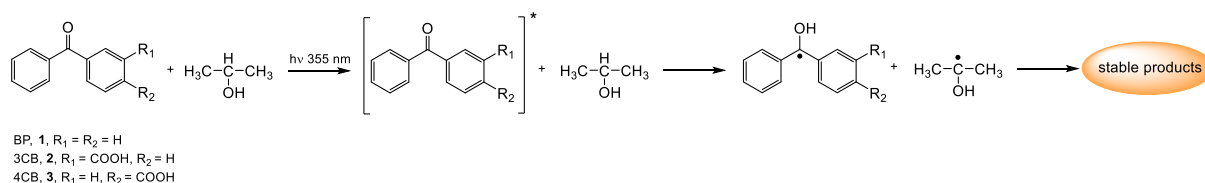
DOI: 10.1016/j.jphotochem.2024.115530.

3 DISCUSSION OF THE RESEARCH

3.1 Sensitized photoreduction of selected benzophenones. Mass spectrometry studies of radical cross-coupling reactions (P1)

The article (P1) describes the analysis of the stable and transient products yielded in the hydrogen atom transfer (HAT) reaction, sometimes referred to as electron transfer followed by proton transfer, between the selected sensitizer: benzophenone (BP, 1), 3-carboxybenzophenone (3CB, 2), 4-carboxybenzophenone (4CB, 3) and 2-propanol. This investigation complements the past research that mainly focused on time-resolved studies and treated the sensitizer only as a tool to study the reaction mechanism and products of the target molecule, e.g., amino acid.

As expected, the laser flash photolysis experiment showed that the transient products of the sensitizer's triplet state quenching by 2-propanol are the excited triplet state and ketyl radicals of the respective sensitizer. The stable reduction photoproducts were separated using high-performance liquid chromatography (HPLC) and identified by high-resolution tandem mass spectrometry (MS/MS). **Scheme 6** shows the general scheme of the reaction.



Scheme 6 Photoreduction of the excited triplet of benzophenones by 2-propanol

Three main types of stable photoproducts were:

- structural isomers of the radical cross-coupling of diphenyl ketyl and dimethyl ketyl radicals;
- benzopinacol and benzopinacol-like products;
- aldehyde.

There are two isomers of diphenyl ketyl-dimethyl ketyl adducts yielded from BP photoreduction, two from 3CB and one from 4CB. Those isomeric products have the same monoisotopic mass and, therefore, the same elemental composition, but the MS/MS

spectra showed substantial differences. By analyzing the diagnostic fragment ions, we determined the structures of the products. In one isomer, the dimethyl ketyl radical is attached to the phenyl ring of the sensitizer (type **A**), while the other has the dimethyl ketyl radical attached to the ketyl group of the diphenyl ketyl radical (type **B**) – both structures are shown in **Figure 12**.

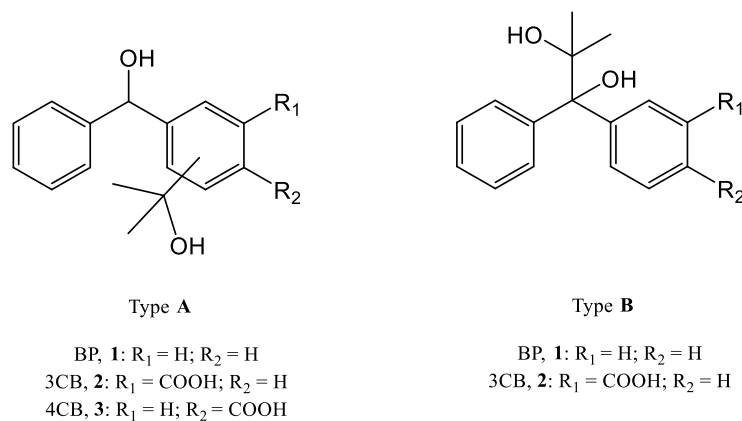


Figure 12 Type A and B of the photoproducts

The adduct with the substituted ring (type **A**) is formed more efficiently based on the area of the peak on the chromatogram. This isomer is the sole product of the 4CB reduction, likely due to the steric hindrance caused by the carboxylic group.

The diphenyl ketyl radical also undergoes dimerization, forming benzopinacol (one BP-BP dimer) and benzopinacol-like products (two 3CB-3CB dimers and two 4CB-4CB dimers). Dimerization of 3CBH[•] and 4CBH[•] produces dimers, each containing two stereocenters. One dimer adopts an SS or RR configuration, while the other is an RS isomer. As it is impossible to differentiate between the enantiomeric pair using the traditional achiral chromatographic column used in this study, it is presumed that one dimer has the SS or RR configuration, and the other the RS configuration.

Tandem mass spectrometry (MS/MS) analysis was conducted on all isomers of the dimers, revealing that the predominant fragmentation pattern involves the loss of a water molecule.

To examine the structures in more detail, the MS/MS analysis was performed not only for $[M+H]^+$ but also for $[M+H(-H_2O)]^+$ and $[M+H(-2H_2O)]^+$ ions. The structures of the ions are shown in **Figure 14**. The first water molecule is eliminated from the carboxylic group. This process is independent of the absolute configuration of the asymmetric carbon atom. Therefore, the product ion spectra of $[M+H]^+$ of 3CB-3CB and 4CB-4CB are identical.

The elimination of the second water molecule involves the hydroxyl group and is influenced by the carbon atom's absolute configuration. As a result, the product ion spectra of ions $[M+H(-H_2O)]^+$ are entirely different.

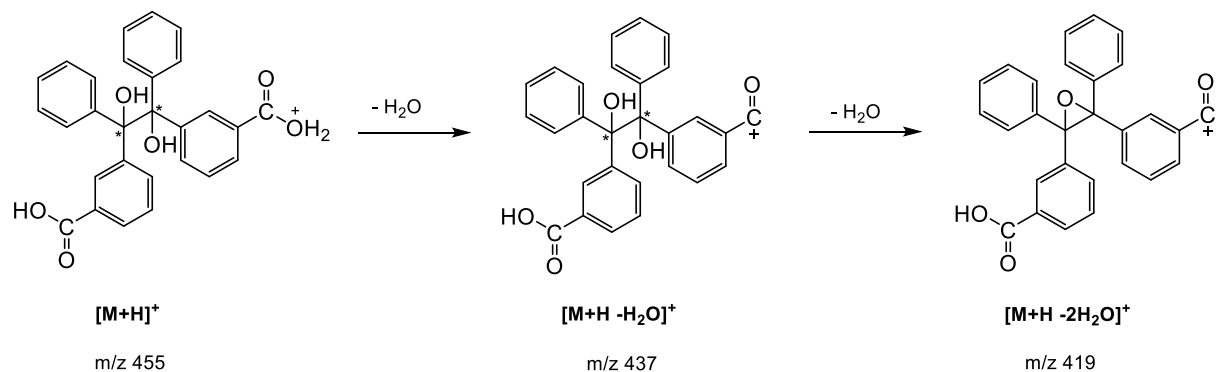


Figure 13 Water elimination from 3CBH-3CBH

The third type of stable product is the aldehyde formed in the reduction of the carboxylic group. It is one of the primary products of the reaction of 3CB and 4CB, while the aldehyde derived from BP – benzhydrol – appears only in trace amounts.

Article **P1** provides a comprehensive report describing the photoreduction of benzophenones using advanced, high-resolution techniques, specifically LC-QTOF-MS/MS. Although the reaction is typically viewed as straightforward and trivial, it has not been thoroughly explored regarding the formed isomeric stable products. High-resolution MS/MS spectrometry allows for monitoring the behavior of free radicals after their radical coupling reactions, resulting in stable products. This research completes the picture of the secondary reactions involving transients produced during the sensitized reduction of benzophenones. It offers foundational information for studies in which benzophenone and its derivatives are used as sensitizers, including the research described in this thesis.

3.2 Early Events of Photosensitized Oxidation of Sulfur-Containing Amino Acids Studied by Laser Flash Photolysis and Mass Spectrometry (P2)

Article **P2** is focused on the photooxidation of Ac-Met-NH-CH₃ and Ac-MeCys-NH-CH₃ sensitized by the triplet state of 3-carboxybenzophenone (³3CB*). Both these compounds mimic the behavior of internal methionine and methyl-cysteine in peptide as they have peptide-like bonds on both the C- and N-terminus and contain a sulfide (-C-S-CH₃) group, but the key difference is that the MeCys derivative has one less methylene group. Blocking amino and carboxyl groups also limits the number of possible photoreactions. This research aimed to unveil how the small structural change impacts the reaction mechanism. To accomplish this, a combination of time-resolved techniques (nanosecond laser flash photolysis, LFP) and steady-state methods (HPLC and HPLC-MS/MS) was employed to quantitatively and qualitatively characterize short-lived transients and stable products.

Two key differences in the initial reaction paths were observed. Firstly, for Ac-MeCys-NH-CH₃, the >S^{•+} is efficiently stabilized through the formation of a two-centered three-electron bond with either a nitrogen atom ((S:·N)⁺ intermediate) or an oxygen atom ((S:·O)⁺ intermediate). In contrast, neither (S:·N)⁺ nor (S:·O)⁺ was detected for Ac-Met-NH-CH₃. However, no intermolecular interaction and formation of dimeric (S:·S)⁺ were observed for either compound.

Secondly, even though all experiments were carried out in the same neutral pH, significantly lower than the pK_a of 3CBH[•]/3CB^{•-} (pK_a = 9.5 [51]), the quantum yield of the radical anion (3CB^{•-}) is considerably higher for methyl-cysteine analogue compared to methionine analogue. This observation suggests that for Ac-Met-NH-CH₃, proton transfer (*k_H*) dominates over charge separation (*k_{sep}*) (refer to **Scheme 2** in **Chapter 1.5 – Early events of photosensitizer oxidation of methionine** for context), whereas the contrary is observed for Ac-MeCys-NH-CH₃ where *k_{sep}* > *k_H*. This phenomenon can likely be attributed to structural factors. For proton transfer to occur, the proton must be accessible to the sensitizer. However, the steric effect restricts access to the proton of the methylene group in Ac-MeCys-NH-CH₃, making deprotonation of this group impossible. On the other hand, deprotonation of both the terminal methyl group and internal methylene group is possible for the Met derivative. The density functional theory (DFT) calculations additionally confirmed this explanation. As a result, for Ac-Met-NH-CH₃, two types of α-thioalkyl radicals (αS) are formed: terminal αS₁ and internal αS₂. In contrast, Ac-

MeCys-NH-CH₃ photooxidation produces only the terminal α S₁. Indeed, analysis of the stable products confirmed that the sole stable product of MeCys derivative photooxidation is the radical cross-coupling product of α S₁ and 3CBH[•] (α S₁-3CB), whereas for the methionine derivative, two adducts are formed: α S₁-3CBH and α S₂-3CBH. The structures of all stable products were confirmed by MS/MS analysis. **Figure 14** illustrates the factors and consequences of the photooxidation mechanism.

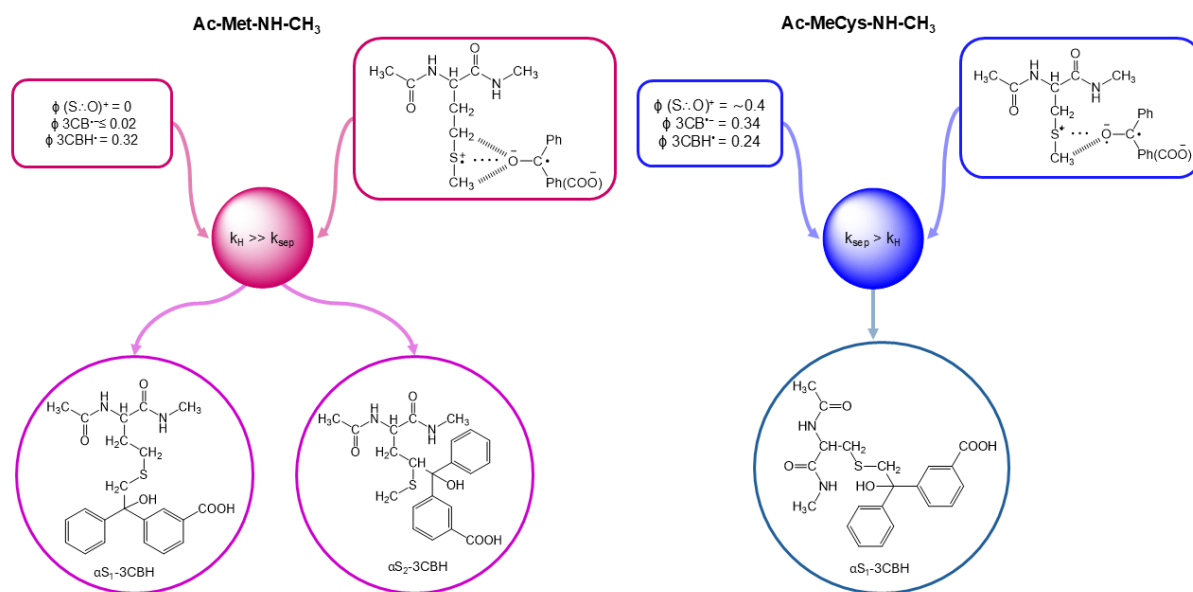


Figure 14 Differences in transient quantum yields, encounter complex geometry, and resulting stable products observed for Ac-Met-NH-CH₃ and Ac-MeCys-NH-CH₃

Based on the chromatograms acquired after various lengths of irradiation, it was possible to calculate the quantum yields of the amino acid disappearance. They were found to be 0.13 and 0.12 for the Met analogue and MeCys analogue, respectively. These values are significantly smaller than the quantum yields of the radicals generated in LFP, indicating that only a portion of the free radicals detected in laser flash photolysis lead to stable products; the rest regenerate to the initial reactants via a new proposed secondary reaction channel – back hydrogen atom transfer from ketyl radical to the carbon-centered α -thioalkyl radical (k_{bH}).

In conclusion, it was demonstrated that a minor structural change (one methylene group less in the methionine derivative compared to the methyl-cysteine derivative) significantly influences the primary and secondary steps of the reaction. Specifically, the Met derivative undergoes electron transfer followed by proton transfer within the

encounter complex (k_H), ultimately producing only neutral free radicals (αS and $3CBH^\bullet$). In contrast, in addition to the k_H pathway, electron transfer followed by charge separation (k_{sep}) was observed for the Cys derivative. This reaction pathway produces charged species: $>S^{\bullet+}$ and $3CB^{\bullet-}$. Regarding secondary reactions, Ac-Met-NH-CH₃ forms both αS_1 and αS_2 -type radicals, as indicated by the presence of radical-coupling products with $3CBH^\bullet$. On the other hand, methyl-cysteine only yields one type of radical-coupling product (αS_1 - $3CBH$). The geometry of the encounter complexes between 3CB and both compounds and the steric effects cause these mechanistic differences. Furthermore, the back hydrogen-atom transfer reaction from $3CBH^\bullet$ to αS was found to be a new competing process to radical coupling reaction.

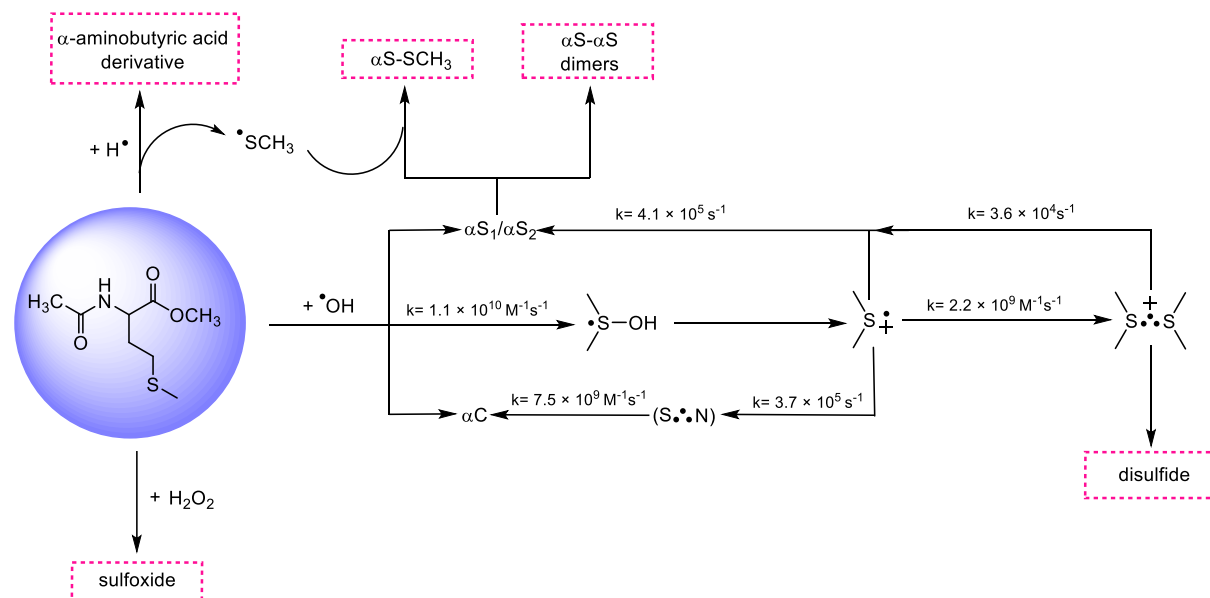
3.3 Radiation- and Photo-Induced Oxidation Pathways of Methionine in Model Peptide Backbone under Anoxic Conditions (P3)

Article **P3** examines the oxidation mechanism of acetyl methionine methyl ester (Ac-Met-OCH₃), which was investigated using complementary time-resolved radiation and photochemical techniques: pulse radiolysis and laser flash photolysis. The short-lived transient species generated by HO• and via electron transfer from the 3CB* were compared, and the formed stable products were separated using HPLC and characterized in detail using mass spectrometry.

The primary radiation-induced reaction pathway involved the addition of HO• to the sulfur atom of the methionine residue, forming the S:OH radical. S:OH radicals decayed into sulfur radical cations (>S^{•+}), which underwent further reactions to form (S:S)⁺, S:N, and αS radicals. In addition to the primary adduct formation, two minor reaction pathways were observed: deprotonation of the sulfide group, leading to αS radicals, and hydrogen abstraction from the αC-carbon (N-CH-CO group), resulting in αC radicals. Based on the obtained spectra and their resolution, it was possible to calculate the radiation chemical yield (*G*-value) and growth and decay rate constant for all detected transients. *G*-values show how the concentration of the transients changes over time. At 1.1 μs after the electron pulse, S:OH is the most abundant species, constituting 73.6% of all transients produced. At 3 μs, the yield of the (S:S)⁺, (S:N)⁺, and αS increases at the expense of S:OH. By 6 microseconds, αS radicals became the most abundant species, making up 45.6% of the total radicals, indicating its stability. After 1.1, 3, and 6 μs following the electron pulse, the total *G*-values were found to be 0.53, 0.56, and 0.57 μmol J⁻¹, respectively. These values align with the expected *G*-value of HO•, which is 0.56 μmol J⁻¹. The radiation-induced oxidation of Ac-Met-OCH₃ leads to the formation of ten stable products. Expectedly, one is formed via the reaction of the starting compound with H₂O₂. Reaction with H•, a minor product of water radiolysis, causes the loss of •SCH₃ and the formation of the derivative of α-aminobutyric acid. Disulfide is formed via fragmentation of (S:S)⁺. The αS radicals (terminal αS₁ and internal αS₂) are the precursors of two types of stable products. Firstly, they undergo radical cross-coupling forming dimers. Five isomeric αS-αS dimers with identical *m/z* were identified. The analysis of their MS/MS spectra revealed that there are three diastereoisomers of αS₂-αS₂ and two diastereoisomers of αS₂-αS₁. Secondly, αS radicals also react with •SCH₃ (generated during the reaction of

H[•] with Ac-Met-OCH₃), yielding two isomers: where •SCH₃ is attached to the terminal carbon (αS₁-SCH₃) and another which it is attached to the internal, γ-carbon (αS₂-SCH₃).

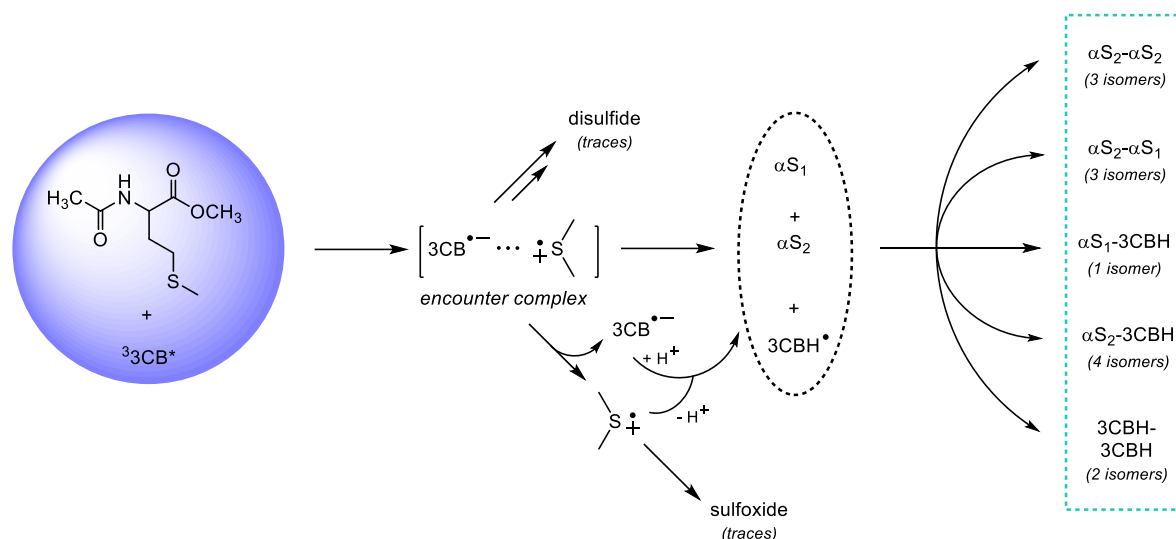
Scheme 7 shows the reaction pathways, including the rate constants of the formation of the radicals and the final stable products detected in LC-MS (in pink rectangles).



Scheme 7 The mechanism of the reaction of radicals generated by γ -irradiation with Ac-Met-OCH₃

Laser flash photolysis examined the reaction of Ac-Met-OCH₃ with the photosensitizer – 3- carboxybenzophenone. Upon 355 nm laser irradiation, the dominant transient species are the triplet state of 3CB (³3CB*) and ketyl radical (3CBH[•]) with only minor contribution of radical anion (3CB^{•-}). Because the absorption of these 3CB-derived species is so strong, the transient signals from the methionine derivative itself are masked.

LC-MS analysis of the irradiated samples revealed a complex mixture of products, including unreacted starting materials (Ac-Met-OCH₃ and 3CB) and several oxidized species that are formed via competing pathways: dimerization of the αS radicals (identical as in radiation-induced oxidation), dimerization of 3CBH[•], and cross-coupling of αS with 3CBH[•] radicals. Traces of disulfide and sulfoxide were also detected. Radical cross-termination yielded a total of five adducts: four assigned to αS₁-3CBH and one αS₂-3CBH as confirmed by MS/MS analysis. Dimerization of ketyl radical yielded two isomeric 3CBH-3CBH dimers. The mechanism of the reaction, including the formed stable products (in turquoise rectangles), is shown in **Scheme 8**.



Scheme 8 The mechanism of the photosensitized reaction of *Ac-Met-OCH₃*

The article **P3** highlights the differences and similarities between the radiation- and photo-induced oxidation of a methionine derivative, a simple biomimetic model amino acid. The difference in the initial step of the reaction – the addition of HO^\bullet versus an electron transfer and the formation of an encounter complex – naturally impacts the secondary reactions. Radiolytic oxidation leads to the formation of a wider variety of Met-derived transient species that are easier to detect, while the dominant transients observed in photolytic oxidation are derived from the sensitizer. Nevertheless, the main precursors of the final stable products under both conditions are α -(alkylthio)alkyl radicals (αS), although the mechanism of their formation and relative concentration differ ($\alpha\text{S}_2 : \alpha\text{S}_1$ ratio is 2:1 in radiolysis and 5:1 in photolysis).

3.4 The Fate of Sulfur Radical Cation of N-Acetyl-Methionine: Deprotonation vs. Decarboxylation (P4)

It is well known that the primary intermediate of methionine photooxidation is sulfur radical cation $>\text{S}^{\bullet+}$. Article **P4** describes the competition between the two reactions of $>\text{S}^{\bullet+}$ of acetyl methionine (Ac-Met): decarboxylation and deprotonation in neutral and basic pH. Acetyl methionine is the simplest model compound that mimics methionine in the C-terminal domain of proteins and peptides, and it should easily undergo decarboxylation as it has a free carboxylic group, ultimately leading to both αN -3CBH and αS -3CBH adducts.

The stable and transient products of the oxidation were characterized qualitatively and quantitatively. Additionally, a sensitive analytical method (LC-MS) for monitoring the decarboxylation of methionine-containing peptides based on a novel marker (αN -3CBH adduct) was developed.

At both pHs, the transient species identified using laser flash photolysis included 3CB radical anion ($3\text{CB}^{\bullet-}$), 3CB ketyl radical (3CBH^{\bullet}), and intramolecularly bonded ($\text{S}:\text{S})^+$. The acid-base equilibrium between $3\text{CB}^{\bullet-}$ and 3CBH^{\bullet} influenced the concentration of the 3CB-derived transient species both below and above $\text{p}K_{\text{a}}$ ($\text{p}K_{\text{a}} \approx 9.5$ [51]).

Irradiation of the solution containing Ac-Met and 3CB with a 355 nm laser resulted in the formation of nine stable post-oxidation products (the chromatogram is shown in **Figure 15**), identified as four stereoisomers of αS_2 -3CBH, one isomer of αS_1 -3CBH, two stereoisomers of αN -3CBH, and two stereoisomers of 3CBH-3CBH. Identical products were formed at neutral and basic pH.

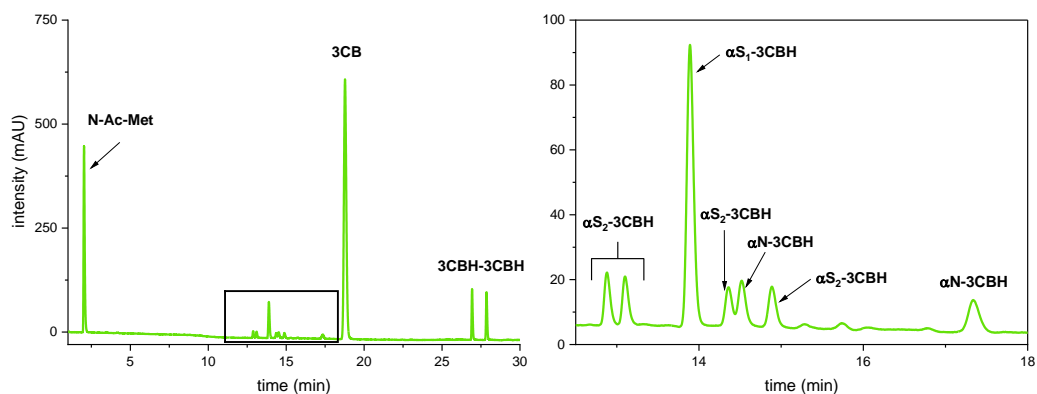
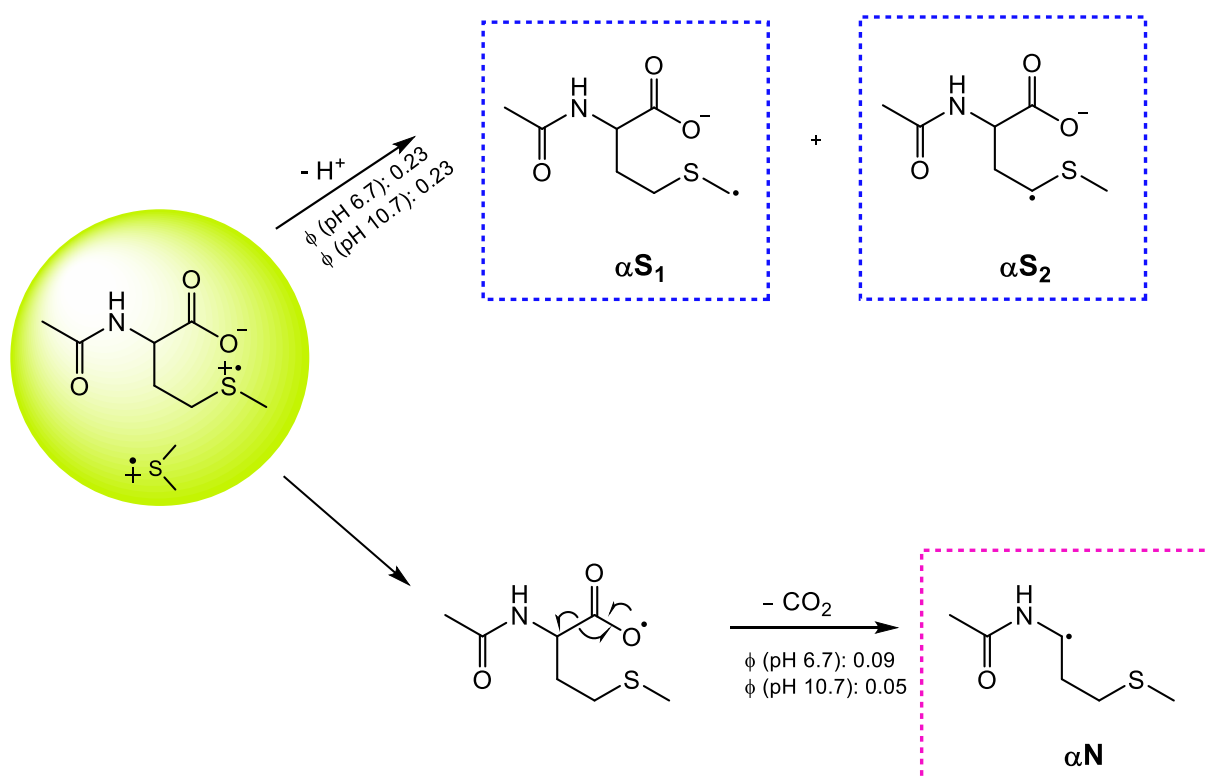


Figure 15 HPLC chromatogram of aqueous solutions containing N-Ac-Met and 3CB at pH 6.4 irradiation. The expansion of the chromatograms between 12 and 18 min is shown next to the chromatogram. Chromatograms were recorded at 220 nm

Because the αS cannot be detected using LFP due to its spectral overlap with the ground state absorption of the sensitizer, the evidence of the deprotonation is the detection of αS -3CBH adducts. On the other hand, covalently bonded αN -3CBH adduct can act as a probe for decarboxylation since αN are formed exclusively in decarboxylation reaction (via pseudo-Kolbe mechanism). The yields of the competing reactions, deprotonation and decarboxylation, were calculated based on the results from the photolysis experiment (quantum yield of the charge separation) and the chromatographic data (ratio of the area under the peaks of the formed photoproducts assuming that αS -3CBH and αN -3CBH adducts have the same molar absorption coefficient). The favored reaction pathway of $>S^{\bullet+}$ was shown to be deprotonation ($\phi = 0.23$ for both pH for deprotonation vs. $\phi = 0.09$ at pH 6.7 and $\phi = 0.05$ at pH 10.7 for decarboxylation). Thus, pH has essentially no impact on the competition between these two processes. The fate of the sulfur radical cation of Ac-Met is shown in **Scheme 9**.



Scheme 9 Two pathways of N-Ac-Met sulfur radical cation: deprotonation and decarboxylation

Utilizing LC-MS/MS for monitoring decarboxylation significantly enhanced the ability to determine the reaction with much higher sensitivity than previously reported. The combination of advanced time-resolved spectroscopy and high-resolution MS/MS spectrometry allowed to follow the fate of free radicals until they eventually yield stable

products through complex radical coupling reactions. Identifying these stable products and accurately assigning them structures offers undeniable evidence of the presence of free radicals, which is particularly beneficial when radicals are undetectable in time-resolved studies, as in the case of α S and α N.

3.5 Efficient decarboxylation of oxidized Cysteine unveils novel Free-Radical reaction pathways (P5)

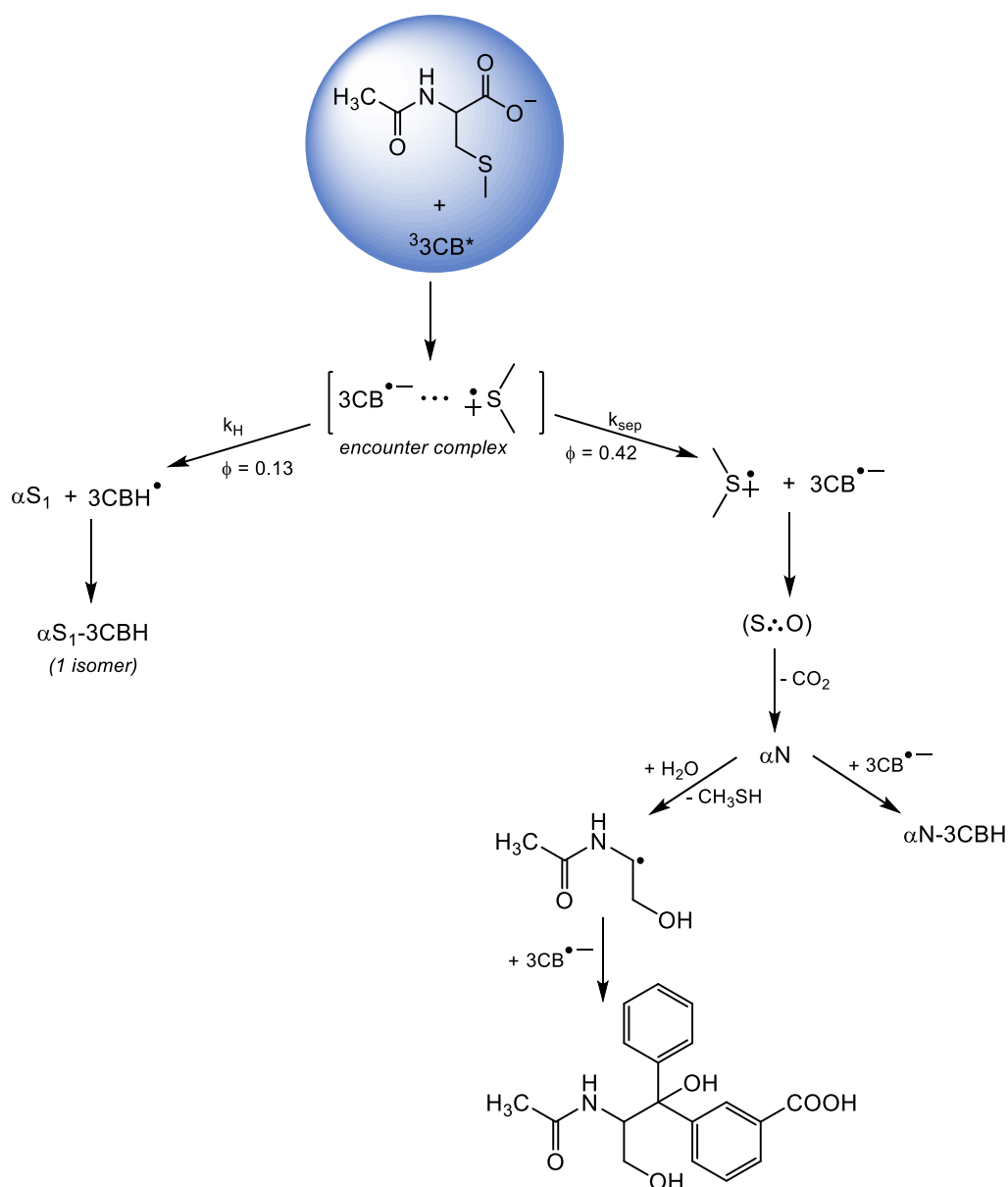
Acetyl methyl cysteine (Ac-MeCys) is an S-methylated derivative of cysteine with an acetylated amino group. The presence of the $-\text{SCH}_3$ group makes it similar to the previously studied Ac-Met (see **Chapter 3.4**). However, the key difference between those two compounds is the distance between the sulfide group and the peptide backbone. The effect of this seemingly minor structural difference (one less methylene group in Ac-MeCys) on the oxidation mechanism is studied using laser flash photolysis and LC-MS/MS and discussed in article **P5**.

The main finding of the research was the identification of α -amidoalkyl radicals (αN) as the primary products of oxidation formed through decarboxylation. αN was directly detected in the LFP experiment. Other observed transient species were 3CB^* , 3CBH^\bullet and $3\text{CB}^{\bullet-}$ and $(\text{S}:\text{O})$. The concentration of αN increases at the expense of $(\text{S}:\text{O})$, suggesting that αN was generated via the pseudo-Kolbe mechanism in which an electron transfer occurs from the carboxyl group to a sulfur-centered radical cation. Furthermore, the nearly identical quantum yields of αN and $3\text{CB}^{\bullet-}$ ($\phi_{\alpha\text{N}} = 0.39$ and $\phi_{3\text{CB}^{\bullet-}} = 0.42$) imply that the sole pathway of $>\text{S}^{\bullet+}$ is decarboxylation, and no deprotonation of $>\text{S}^{\bullet+}$ occurred. αS was formed as a result of the proton transfer within the encounter complex.

Once formed, αN radicals decay through two distinct pathways. The first involves their radical cross-coupling with ketyl radicals, resulting in the formation of two stereoisomers of αN - 3CBH adducts. The second pathway involves beta-scission followed by hydrolysis, which leads to the loss of CH_3SH and the subsequent formation of an alcohol derivative. These stable products were confirmed through LC-MS analysis, where the photoproducts were separated and identified based on the mass spectrum. Other characterized photoproducts were one isomer of αS - 3CBH adduct (whose precursor is terminal αS_1 radical) and two isomers of 3CBH - 3CBH .

The chromatographic data showed that the formation of αN radicals was more efficient than that of αS radicals, indicating a strong preference for decarboxylation over deprotonation. This was in stark contrast to Ac-Met, where the sulfur radical cation primarily undergoes deprotonation to form αS radicals, leading to a different set of reaction products. In Ac-MeCys, the preference for αN radical formation was attributed to the formation of a kinetically favorable five-membered $(\text{S}:\text{O})$ intermediate. In

contrast, Ac-Met, which contains one more methylene group, yields a six-membered intermediate that is less favorable. This difference results in a much higher quantum than expected yield of decarboxylation for Ac-MeCys ($\phi = 0.42$) compared to Ac-Met ($\phi = 0.09$), highlighting the importance of molecular geometry and kinetic stability of the intermediates in the trajectory of the reaction. The reaction mechanism is shown in **Scheme 10**.



Scheme 10 Mechanism of the photosensitized oxidation of Ac-MeCys

This study highlights the impact of molecular structure on free-radical reaction pathways. It demonstrates how rapid kinetics control these pathways, specifically showing that the formation of kinetically favored five-membered ($\text{S}\cdots\text{O}$) in Ac-MeCys significantly enhances the efficiency of decarboxylation. In addition, this work demonstrates how even

minor structural modifications of peptides influence their reactivity pathways and, consequently, the structures of stable modifications.

3.6 Summary and conclusions

This dissertation explores the anaerobic oxidation of sulfur-containing amino acids that have peptide-like bonds and mimic the behavior of the amino acids in complex protein structures: Ac-Met-NH-CH₃, Ac-MeCys-NH-CH₃, Ac-Met-OCH₃, Ac-Met, and Ac-MeCys. Additionally, photoreduction of the popular photosensitizers benzophenone, 3-carboxybenzophenone, and 4-carboxybenzophenone, which are essential to initiate photooxidation of the mentioned compounds, was studied. The mechanisms of the reactions were investigated using a combination of time-resolved and stationary methods, allowing for the observation of the transients from their generation to their conversion into stable products.

The results from the five peer-reviewed articles that comprise this doctoral dissertation helped accomplish the specific research objectives.

The main achievements presented in this doctoral dissertation are:

1. All stable products formed in the photoreduction of benzophenone, 3-carboxybenzophenone, and 4-carboxybenzophenone using liquid chromatography coupled with high-resolution tandem mass spectrometry were identified. These results clarify the mechanistic pathways involving benzophenone-based sensitizers (**P1**).
2. Small structural change between Met and MeCys derivatives (a difference of one methylene group) was shown to have a substantial effect on their reactivity:
 - Met derivative was shown to undergo mainly electron transfer followed by proton transfer, while charge separation was observed additionally for the MeCys derivative (**P2**);
 - Met derivative yielded multiple isomeric products, and oxidation of MeCys derivative led to one dominant photoproduct (**P2**);
 - Decarboxylation is the dominant decay pathway for MeCys derivative due to the formation of kinetically favored five-membered (S:O) ring (vs six-membered ring for Met derivative) (**P5**).
3. A new competing reaction pathway that leads to the regeneration of the sensitizer and the Met derivative in their ground state was also suggested (**P2**).
4. The mechanisms of photosensitized and radiation-induced oxidation were compared, revealing that the primary radicals involved in the formation of stable

products are α -(alkylthio)alkyl radicals (α S), although the underlying mechanisms of their formation differ (**P3**).

5. Decarboxylation of Ac-Met was observed, contradicting earlier beliefs that this process does not occur (**P4**). The yield of the decarboxylation was found to be independent of the pH of the solution.
6. A new decay mechanism of the radicals was described: it was proposed that α N undergoes hydrolysis and beta-scission resulting in respective alcohol formation (**P5**).

These conclusions were possible thanks to the excellent separation of the products using HPLC and the in-depth analysis of the MS/MS spectra. It is crucial to highlight the significant role that analyzing all stable products plays in elucidating the mechanisms of free radical reactions of sulfur-containing amino acids.

In summary, this dissertation offers insights into the photosensitized and radiation-induced oxidation of methionine and methyl-cysteine derivatives. These compounds act as models for internal Met and MeCys residues or mimic amino acids in the C-terminal domain of peptides.

4 REFERENCES

- [1] M.J. Davies, Oxidative Damage to Proteins, in: Encyclopedia of Radicals in Chemistry, Biology and Materials, John Wiley & Sons, Ltd, 2012. <https://doi.org/10.1002/9781119953678.rad045>.
- [2] D.I. Pattison, A.S. Rahmanto, M.J. Davies, Photo-oxidation of proteins, *Photochem. Photobiol. Sci.* 11 (2011) 38–53. <https://doi.org/10.1039/C1PP05164D>.
- [3] J.T. Brosnan, M.E. Brosnan, The Sulfur-Containing Amino Acids: An Overview, *The Journal of Nutrition* 136 (2006) 1636S-1640S. <https://doi.org/10.1093/jn/136.6.1636S>.
- [4] R.L. Levine, J. Moskowitz, E.R. Stadtman, Oxidation of Methionine in Proteins: Roles in Antioxidant Defense and Cellular Regulation, *IUBMB Life* 50 (2000) 301–307. <https://doi.org/10.1080/713803735>.
- [5] R. Kehm, T. Baldensperger, J. Raupbach, A. Höhn, Protein oxidation - Formation mechanisms, detection and relevance as biomarkers in human diseases, *Redox Biology* 42 (2021) 101901. <https://doi.org/10.1016/j.redox.2021.101901>.
- [6] J.H. Mueller, A new sulfur-containing amino-acid isolated from the hydrolytic products for casein, *Proc. Soc. Exp. Biol. Med.* 19 (n.d.) 161–163.
- [7] H. Bradford. Vickery, C.L.A. Schmidt, The History of the Discovery of the Amino Acids., *Chem. Rev.* 9 (1931) 169–318. <https://doi.org/10.1021/cr60033a001>.
- [8] G. Barger, F.P. Coyne, The amino-acid methionine; constitution and synthesis, *Biochem J* 22 (1928) 1417–1425.
- [9] R.L. Levine, L. Mosoni, B.S. Berlett, E.R. Stadtman, Methionine residues as endogenous antioxidants in proteins, *Proceedings of the National Academy of Sciences* 93 (1996) 15036–15040. <https://doi.org/10.1073/pnas.93.26.15036>.
- [10] N. Brot, H. Weissbach, Biochemistry and physiological role of methionine sulfoxide residues in proteins, *Archives of Biochemistry and Biophysics* 223 (1983) 271–281. [https://doi.org/10.1016/0003-9861\(83\)90592-1](https://doi.org/10.1016/0003-9861(83)90592-1).
- [11] E.R. Stadtman, J. Moskowitz, R.L. Levine, Oxidation of Methionine Residues of Proteins: Biological Consequences, *Antioxidants & Redox Signaling* 5 (2003) 577–582. <https://doi.org/10.1089/152308603770310239>.

- [12] G.B. Frisoni, D. Altomare, D.R. Thal, F. Ribaldi, R. van der Kant, R. Ossenkoppele, K. Blennow, J. Cummings, C. van Duijn, P.M. Nilsson, P.-Y. Dietrich, P. Scheltens, B. Dubois, The probabilistic model of Alzheimer disease: the amyloid hypothesis revised, *Nat Rev Neurosci* 23 (2022) 53–66. <https://doi.org/10.1038/s41583-021-00533-w>.
- [13] K.P. Kepp, N.K. Robakis, P.F. Høiland-Carlsen, S.L. Sensi, B. Vissel, The amyloid cascade hypothesis: an updated critical review, *Brain* 146 (2023) 3969–3990. <https://doi.org/10.1093/brain/awad159>.
- [14] D.J. Selkoe, J. Hardy, The amyloid hypothesis of Alzheimer’s disease at 25 years, *EMBO Molecular Medicine* 8 (2016) 595–608. <https://doi.org/10.15252/emmm.201606210>.
- [15] R.A. Stelzmann, H. Norman Schnitzlein, F. Reed Murtagh, An english translation of alzheimer’s 1907 paper, “über eine eigenartige erkankung der hirnrinde,” *Clinical Anatomy* 8 (1995) 429–431. <https://doi.org/10.1002/ca.980080612>.
- [16] P.K. Mandal, R.G. Roy, A. Samkaria, Oxidative Stress: Glutathione and Its Potential to Protect Methionine-35 of A β Peptide from Oxidation, *ACS Omega* 7 (2022) 27052–27061. <https://doi.org/10.1021/acsomega.2c02760>.
- [17] J. Dong, C.S. Atwood, V.E. Anderson, S.L. Siedlak, M.A. Smith, G. Perry, P.R. Carey, Metal Binding and Oxidation of Amyloid- β within Isolated Senile Plaque Cores: Raman Microscopic Evidence, *Biochemistry* 42 (2003) 2768–2773. <https://doi.org/10.1021/bi0272151>.
- [18] C.C. Curtain, F. Ali, I. Volitakis, R.A. Cherny, R.S. Norton, K. Beyreuther, C.J. Barrow, C.L. Masters, A.I. Bush, K.J. Barnham, Alzheimer’s disease amyloid-beta binds copper and zinc to generate an allosterically ordered membrane-penetrating structure containing superoxide dismutase-like subunits, *J Biol Chem* 276 (2001) 20466–20473. <https://doi.org/10.1074/jbc.M100175200>.
- [19] S. Varadarajan, J. Kanski, M. Aksenova, C. Lauderback, D.A. Butterfield, Different mechanisms of oxidative stress and neurotoxicity for Alzheimer’s A beta(1--42) and A beta(25--35), *J Am Chem Soc* 123 (2001) 5625–5631. <https://doi.org/10.1021/ja010452r>.

- [20] D.A. Butterfield, D. Boyd-Kimball, The critical role of methionine 35 in Alzheimer's amyloid β -peptide (1–42)-induced oxidative stress and neurotoxicity, *Biochimica et Biophysica Acta (BBA) - Proteins and Proteomics* 1703 (2005) 149–156. <https://doi.org/10.1016/j.bbapap.2004.10.014>.
- [21] W. Vogt, Oxidation of methionyl residues in proteins: Tools, targets, and reversal, *Free Radical Biology and Medicine* 18 (1995) 93–105. [https://doi.org/10.1016/0891-5849\(94\)00158-G](https://doi.org/10.1016/0891-5849(94)00158-G).
- [22] P. Giron, L. Dayon, J. Sanchez, Cysteine tagging for MS-based proteomics, *Mass Spectrometry Reviews* 30 (2011) 366–395. <https://doi.org/10.1002/mas.20285>.
- [24] J. Kyte, *Structure in protein chemistry*, 2nd ed, Garland Science, New York, 2007.
- [25] Z.R. Gan, W.W. Wells, Identification and reactivity of the catalytic site of pig liver thioltransferase., *Journal of Biological Chemistry* 262 (1987) 6704–6707. [https://doi.org/10.1016/S0021-9258\(18\)48299-3](https://doi.org/10.1016/S0021-9258(18)48299-3).
- [26] L. Gu, R.A.S. Robinson, Proteomic approaches to quantify cysteine reversible modifications in aging and neurodegenerative diseases, *PROTEOMICS – Clinical Applications* 10 (2016) 1159–1177. <https://doi.org/10.1002/prca.201600015>.
- [27] H.S. Chung, S.-B. Wang, V. Venkatraman, C.I. Murray, J.E. Van Eyk, Cysteine Oxidative Posttranslational Modifications, *Circulation Research* 112 (2013) 382–392. <https://doi.org/10.1161/CIRCRESAHA.112.268680>.
- [28] L. Turell, A. Zeida, M. Trujillo, Mechanisms and consequences of protein cysteine oxidation: The role of the initial short-lived intermediates, *Essays in Biochemistry* 64 (2020). <https://doi.org/10.1042/EBC20190053>.
- [29] M. Trujillo, B. Alvarez, R. Radi, One- and two-electron oxidation of thiols: mechanisms, kinetics and biological fates, *Free Radical Research* 50 (2016) 150–171. <https://doi.org/10.3109/10715762.2015.1089988>.
- [30] J.M. Held, B.W. Gibson, Regulatory Control or Oxidative Damage? Proteomic Approaches to Interrogate the Role of Cysteine Oxidation Status in Biological Processes*, *Molecular & Cellular Proteomics* 11 (2012) R111.013037. <https://doi.org/10.1074/mcp.R111.013037>.

- [31] G.P. Senthilkumar, Study the Effect of S-Methyl L-Cysteine on Lipid Metabolism in an Experimental Model of Diet Induced Obesity, JCDR (2013). <https://doi.org/10.7860/JCDR/2013/7304.3571>.
- [32] S.E. Braslavsky, Glossary of terms used in photochemistry, 3rd edition (IUPAC Recommendations 2006), Pure and Applied Chemistry 79 (2007) 293–465. <https://doi.org/10.1351/pac200779030293>.
- [33] N.D. Heindel, M.A. Pfau, A profitable partnership: Giacomo Ciamician and Paul Silber, J. Chem. Educ. 42 (1965) 383. <https://doi.org/10.1021/ed042p383>.
- [34] G. Ciamician, P. Silber, Chemische Lichtwirkungen, Ber. Dtsch. Chem. Ges. 33 (1900) 2911–2913. <https://doi.org/10.1002/cber.19000330326>.
- [35] N.B. Sul'timova, P.P. Levin, O.N. Chaikovskaya, Laser photolysis study of the transient products of 4-carboxybenzophenone-sensitized photolysis of chlorophenoxyacetic acid-based herbicides in aqueous micellar solutions, High Energy Chemistry 44 (2010) 393–398. <https://doi.org/10.1134/S0018143910050073>.
- [36] S. Canonica, H.-U. Laubscher, Inhibitory effect of dissolved organic matter on triplet-induced oxidation of aquatic contaminants, Photochem. Photobiol. Sci. 7 (2008) 547–551. <https://doi.org/10.1039/B719982A>.
- [37] J. Wenk, U. Von Gunten, S. Canonica, Effect of Dissolved Organic Matter on the Transformation of Contaminants Induced by Excited Triplet States and the Hydroxyl Radical, Environ. Sci. Technol. 45 (2011) 1334–1340. <https://doi.org/10.1021/es102212t>.
- [38] K. Bobrowski, B. Marciniak, G.L. Hug, A reinvestigation of the mechanism of photoreduction of benzophenones by alkyl sulfides, Journal of Photochemistry and Photobiology A: Chemistry 81 (1994) 159–168. [https://doi.org/10.1016/1010-6030\(94\)03787-6](https://doi.org/10.1016/1010-6030(94)03787-6).
- [39] J.B. Guttenplan, S.G. Cohen, Quenching and reduction of photoexcited benzophenone by thioethers and mercaptans, J. Org. Chem. 38 (1973) 2001–2007. <https://doi.org/10.1021/jo00951a007>.
- [40] S. Inbar, H. Linschitz, S.G. Cohen, Quenching and radical formation in the reaction of photoexcited benzophenone with thiols and thio ethers (sulfides). Nanosecond

flash studies, J. Am. Chem. Soc. 104 (1982) 1679–1682. <https://doi.org/10.1021/ja00370a038>.

[41] S.G. Cohen, S. Ojanpera, Photooxidation of methionine and related compounds, J. Am. Chem. Soc. 97 (1975) 5633–5634. <https://doi.org/10.1021/ja00852a079>.

[42] G.L. Hug, B. Marciniak, K. Bobrowski, Sensitized photo-oxidation of sulfur-containing amino acids and peptides in aqueous solution, Journal of Photochemistry and Photobiology A: Chemistry 95 (1996) 81–88. [https://doi.org/10.1016/1010-6030\(95\)04230-X](https://doi.org/10.1016/1010-6030(95)04230-X).

[43] G.L. Hug, K. Bobrowski, H. Kozubek, B. Marciniak, Photooxidation of Methionine Derivatives by the 4-Carboxybenzophenone Triplet State in Aqueous Solution. Intracomplex Proton Transfer Involving the Amino Group, Photochem Photobiol 68 (1998) 785–796. <https://doi.org/10.1111/j.1751-1097.1998.tb05285.x>.

[44] K. Bobrowski, C. Houée-Levin, B. Marciniak, Stabilization and Reactions of Sulfur Radical Cations: Relevance to One-Electron Oxidation of Methionine in Peptides and Proteins, Chimia 62 (2008) 728. <https://doi.org/10.2533/chimia.2008.728>.

[45] T. Pedzinski, K. Bobrowski, B. Marciniak, P. Filipiak, Unexpected Reaction Pathway of the Alpha-Aminoalkyl Radical Derived from One-Electron Oxidation of S-Alkylglutathiones, Molecules 25 (2020) 877. <https://doi.org/10.3390/molecules25040877>.

[46] A. Wojcik, A. Łukaszewicz, O. Brede, B. Marciniak, Competitive photosensitized oxidation of tyrosine and methionine residues in enkephalins and their model peptides, Journal of Photochemistry and Photobiology A: Chemistry 198 (2008) 111–118. <https://doi.org/10.1016/j.jphotochem.2008.02.027>.

[47] G.L. Hug, M. Bonifačić, K.-D. Asmus, D.A. Armstrong, Fast Decarboxylation of Aliphatic Amino Acids Induced by 4-Carboxybenzophenone Triplets in Aqueous Solutions. A Nanosecond Laser Flash Photolysis Study, J. Phys. Chem. B 104 (2000) 6674–6682. <https://doi.org/10.1021/jp001131p>.

[48] B. Marciniak, K. Bobrowski, Photo- and Radiation-Induced One-Electron Oxidation of Methionine in Various Structural Environments Studied by Time-Resolved Techniques, Molecules 27 (2022) 1028. <https://doi.org/10.3390/molecules27031028>.

- [49] K.J. Frąckowiak, T. Pędziński, K. Grzyb, M. Ignasiak-Kciuk, B. Marciniak, Influence of blocking groups on photo-oxidation of tyrosine and derivatives, *Journal of Photochemistry and Photobiology A: Chemistry* (2024) 115988. <https://doi.org/10.1016/j.jphotochem.2024.115988>.
- [50] M. Ignasiak-Kciuk, K. Nowicka-Bauer, M. Grzechowiak, T. Ravnsborg, K. Frąckowiak, O.N. Jensen, M. Jaskólski, B. Marciniak, Does the presence of ground state complex between a PR-10 protein and a sensitizer affect the mechanism of sensitized photo-oxidation?, *Free Radical Biology and Medicine* 198 (2023) 27–43. <https://doi.org/10.1016/j.freeradbiomed.2023.01.022>.
- [51] T. Pedzinski, K. Bobrowski, M. Ignasiak, G. Kciuk, G.L. Hug, A. Lewandowska-Andralojc, B. Marciniak, 3-Carboxybenzophenone (3-CB) as an efficient sensitizer in the photooxidation of methionyl-leucine in aqueous solutions: Spectral, kinetic and acid–base properties of 3-CB derived transients, *Journal of Photochemistry and Photobiology A: Chemistry* 287 (2014) 1–7. <https://doi.org/10.1016/j.jphotochem.2014.04.004>.
- [52] K. Bobrowski, G.L. Hug, B. Marciniak, H. Kozubek, The 4-carboxybenzophenone-sensitized photooxidation of sulfur-containing amino acids in alkaline aqueous solutions. Secondary photoreactions kinetics, *J. Phys. Chem.* 98 (1994) 537–544. <https://doi.org/10.1021/j100053a031>.
- [53] K. Bobrowski, B. Marciniak, The kinetics of the acid-base equilibrium of 4-carboxybenzophenone ketyl radical. A pulse radiolysis study, *Radiation Physics and Chemistry* 43 (1994) 361–364. [https://doi.org/10.1016/0969-806X\(94\)90028-0](https://doi.org/10.1016/0969-806X(94)90028-0).
- [54] G.L. Hug, K. Bobrowski, H. Kozubek, B. Marciniak, Photo-oxidation of Methionine-containing Peptides by the 4-Carboxybenzophenone Triplet State in Aqueous Solution. Competition Between Intramolecular Two-centered Three-electron Bonded ($S\cdots S$)⁺ and ($S\cdots N$)⁺ Formation, *Photochemistry and Photobiology* 72 (2000) 1–9. [https://doi.org/10.1562/0031-8655\(2000\)0720001POOMCP2.0.CO2](https://doi.org/10.1562/0031-8655(2000)0720001POOMCP2.0.CO2).
- [55] K. Bobrowski, B. Marciniak, G.L. Hug, 4-Carboxybenzophenone-sensitized photooxidation of sulfur-containing amino acids. Nanosecond laser flash photolysis and pulse radiolysis studies, *J. Am. Chem. Soc.* 114 (1992) 10279–10288. <https://doi.org/10.1021/ja00052a025>.

- [56] B. Marciniak, K. Bobrowski, G.L. Hug, Quenching of triplet states of aromatic ketones by sulfur-containing amino acids in solution. Evidence for electron transfer, *J. Phys. Chem.* 97 (1993) 11937–11943. <https://doi.org/10.1021/j100148a015>.
- [57] P. Filipiak, K. Bobrowski, G.L. Hug, D. Pogocki, C. Schöneich, B. Marciniak, New Insights into the Reaction Paths of 4-Carboxybenzophenone Triplet with Oligopeptides Containing N- and C-Terminal Methionine Residues, *J. Phys. Chem. B* 121 (2017) 5247–5258. <https://doi.org/10.1021/acs.jpcb.7b01119>.
- [58] P. Filipiak, K. Bobrowski, G.L. Hug, C. Schöneich, B. Marciniak, N-Terminal Decarboxylation as a Probe for Intramolecular Contact Formation in γ -Glu-(Pro)_n-Met Peptides, *J. Phys. Chem. B* 124 (2020) 8082–8098. <https://doi.org/10.1021/acs.jpcb.0c04371>.
- [59] K.D. Asmus, Stabilization of oxidized sulfur centers in organic sulfides. Radical cations and odd-electron sulfur-sulfur bonds, *Acc. Chem. Res.* 12 (1979) 436–442. <https://doi.org/10.1021/ar50144a003>.
- [60] K.O. Hiller, B. Masloch, M. Goebel, K.D. Asmus, Mechanism of the hydroxyl radical induced oxidation of methionine in aqueous solution, *J. Am. Chem. Soc.* 103 (1981) 2734–2743. <https://doi.org/10.1021/ja00400a042>.
- [61] K.-D. Asmus, M. Göbl, K.-O. Hiller, S. Mahling, J. Mönig, S \cdot :N and S \cdot :O three-electron-bonded radicals and radical cations in aqueous solutions, *J. Chem. Soc., Perkin Trans. 2* (1985) 641–646. <https://doi.org/10.1039/P29850000641>.
- [62] M.T. Ignasiak, T. Pedzinski, F. Rusconi, P. Filipiak, K. Bobrowski, C. Houée-Levin, B. Marciniak, Photosensitized Oxidation of Methionine-Containing Dipeptides. From the Transients to the Final Products, *J. Phys. Chem. B* 118 (2014) 8549–8558. <https://doi.org/10.1021/jp5039305>.
- [63] V. Kadicik, C. Sicard-Roselli, T.A. Mattioli, M. Kodicek, C. Houée-Levin, One-electron oxidation of β -amyloid peptide: sequence modulation of reactivity, *Free Radical Biology and Medicine* 37 (2004) 881–891. <https://doi.org/10.1016/j.freeradbiomed.2004.06.015>.
- [64] J.S. Sharp, K.B. Tomer, Analysis of the oxidative damage-induced conformational changes of apo- and holocalmodulin by dose-dependent protein oxidative

surface mapping, *Biophys J* 92 (2007) 1682–1692. <https://doi.org/10.1529/biophysj.106.099093>.

[65] O. Mozziconacci, K. Bobrowski, C. Ferreri, C. Chatgililoglu, Reactions of Hydrogen Atoms with Met-Enkephalin and Related Peptides, *Chemistry – A European Journal* 13 (2007) 2029–2033. <https://doi.org/10.1002/chem.200600828>.

[66] N. Gillard, S. Goffinont, C. Buré, M. Davidkova, J.-C. Maurizot, M. Cadene, M. Spothem-Maurizot, Radiation-induced oxidative damage to the DNA-binding domain of the lactose repressor, *Biochemical Journal* 403 (2007) 463–472. <https://doi.org/10.1042/BJ20061466>.

[67] M. Ignasiak, D. Scuderi, P. de Oliveira, T. Pedzinski, Y. Rayah, C. Houée Levin, Characterization by mass spectrometry and IRMPD spectroscopy of the sulfoxide group in oxidized methionine and related compounds, *Chemical Physics Letters* 502 (2011) 29–36. <https://doi.org/10.1016/j.cplett.2010.12.012>.

[68] G. Buxton, Chapter 1 An overview of the radiation chemistry of liquids, in: *Radiation Chemistry: From Basics to Applications in Material and Life Sciences*, EDP Sciences, 2008: pp. 3–16. <https://doi.org/10.1051/978-2-7598-0317-0.c004>.

[69] S. Barata-Vallejo, C. Ferreri, A. Postigo, C. Chatgililoglu, Radiation Chemical Studies of Methionine in Aqueous Solution: Understanding the Role of Molecular Oxygen, *Chem. Res. Toxicol.* 23 (2010) 258–263. <https://doi.org/10.1021/tx900427d>.

[70] A. Torreggiani, S. Barata-Vallejo, C. Chatgililoglu, Combined Raman and IR spectroscopic study on the radical-based modifications of methionine, *Anal Bioanal Chem* 401 (2011) 1231–1239. <https://doi.org/10.1007/s00216-011-5203-0>.

[71] C. Chatgililoglu, C. Ferreri, Reductive Stress of Sulfur-Containing Amino Acids within Proteins and Implication of Tandem Protein–Lipid Damage, *International Journal of Molecular Sciences* 22 (2021) 12863. <https://doi.org/10.3390/ijms222312863>.

[72] J.C. Aledo, Methionine in proteins: The Cinderella of the proteinogenic amino acids, *Protein Sci* 28 (2019) 1785–1796. <https://doi.org/10.1002/pro.3698>.

[73] T. Pedzinski, A. Markiewicz, B. Marciniak, Photosensitized oxidation of methionine derivatives. Laser flash photolysis studies, *Res Chem Intermed* 35 (2009) 497–506. <https://doi.org/10.1007/s11164-009-0046-4>.

- [74] K. Bobrowski, C. Schöneich, J. Holcman, K.-D. Asmus, 'OH radical induced decarboxylation of methionine-containing peptides. Influence of peptide sequence and net charge, *J. Chem. Soc., Perkin Trans. 2* (1991) 353–362. <https://doi.org/10.1039/P29910000353>.
- [75] B. Mishra, K.I. Priyadarsini, H. Mohan, Pulse radiolysis studies on reaction of 'OH radical with N-acetyl methionine in aqueous solution, *Res Chem Intermediat* 31 (2005) 625–632. <https://doi.org/10.1163/1568567054908961>.
- [76] C. Schöneich, D. Pogocki, G.L. Hug, K. Bobrowski, Free Radical Reactions of Methionine in Peptides: Mechanisms Relevant to β -Amyloid Oxidation and Alzheimer's Disease, *J. Am. Chem. Soc.* 125 (2003) 13700–13713. <https://doi.org/10.1021/ja036733b>.
- [77] C. Chatgililoglu, M. Grzelak, K. Skotnicki, P. Filipiak, F. Kazmierczak, G.L. Hug, K. Bobrowski, B. Marciniak, Evaluation of Hydroxyl Radical Reactivity by Thioether Group Proximity in Model Peptide Backbone: Methionine versus S-Methyl-Cysteine, *IJMS* 23 (2022) 6550. <https://doi.org/10.3390/ijms23126550>.
- [78] V. Gold, ed., *The IUPAC Compendium of Chemical Terminology: The Gold Book*, 4th ed., International Union of Pure and Applied Chemistry (IUPAC), Research Triangle Park, NC, 2019. <https://doi.org/10.1351/goldbook>.
- [79] L.R. Snyder, J.J. Kirkland, J.W. Dolan, *Introduction to modern liquid chromatography*, 3rd. ed, Wiley, Hoboken, NJ, 2010.
- [80] G. Porter, Flash photolysis and spectroscopy. A new method for the study of free radical reactions, *Proc. R. Soc. Lond. A* 200 (1950) 284–300. <https://doi.org/10.1098/rspa.1950.0018>.
- [81] The Nobel Prize in Chemistry 1967, (n.d.). <https://www.nobelprize.org/prizes/chemistry/1967/summary/>.
- [82] K. Bobrowski, Free radicals in chemistry, biology and medicine: Contribution of radiation chemistry., *Nukleonika* 50 (2005) S67–S76.
- [83] T.G. Truscott, Pulse Radiolysis and Flash Photolysis, in: E. Riklis (Ed.), *Photobiology: The Science and Its Applications*, Springer US, Boston, MA, 1991: pp. 237–247. https://doi.org/10.1007/978-1-4615-3732-8_28.

- [84] T. Szreder, Recent upgrading of the nanosecond pulse radiolysis setup and construction of laser flash photolysis setup at the Institute of Nuclear Chemistry and Technology in Warsaw, Poland, *Nukleonika* 67 (2022) 49–64. <https://doi.org/10.2478/nuka-2022-0005>.
- [85] E. De Hoffmann, V. Stroobant, E. De Hoffmann, *Mass spectrometry: principles and applications*, 3. ed., reprinted, Wiley, Chichester Weinheim, 2011.
- [86] S.N. Thomas, D. French, P.J. Jannetto, B.A. Rappold, W.A. Clarke, Liquid chromatography–tandem mass spectrometry for clinical diagnostics, *Nat Rev Methods Primers* 2 (2022) 1–14. <https://doi.org/10.1038/s43586-022-00175-x>.
- [87] J. Claesen, A. Rockwood, M. Gorshkov, D. Valkenburg, The isotope distribution: A rose with thorns, *Mass Spectrometry Reviews* 44 (2025) 22–42. <https://doi.org/10.1002/mas.21820>.
- [88] M. Berglund, M.E. Wieser, Isotopic compositions of the elements 2009 (IUPAC Technical Report), *Pure and Applied Chemistry* 83 (2011) 397–410. <https://doi.org/10.1351/PAC-REP-10-06-02>.
- [89] L. Patiny, A. Borel, ChemCalc: A Building Block for Tomorrow’s Chemical Infrastructure, *J. Chem. Inf. Model.* 53 (2013) 1223–1228. <https://doi.org/10.1021/ci300563h>.

5 LIST OF FIGURES AND SCHEMES

Figure 1 Structures of methionine (Met) and cysteine (Cys).....	11
Figure 2 Met-centered redox cycle	12
Figure 3 Oxidized β -amyloid peptide forms amyloid plaques that are hallmarks of Alzheimer's disease.....	13
Figure 4 . Oxidative modifications of protein Cys and their biological consequence. The figure adapted from the paper [28] with publisher’s permission. Copyright Portland Press Ltd 2019.....	15
Figure 5 UV spectra of 3CB, Met, and Cys	16
Figure 6 Transient absorption spectra of species derived from 4CB and 3CB excitation.....	17
Figure 7 Reference spectra of transients	23
Figure 8 Scheme of the UV-Vis spectrophotometer	33

Figure 9 The experimental setup for nanosecond laser flash photolysis. Figure adapted from [73] with publisher's permission. Copyright Springer Nature 2009.....	34
Figure 10 HPLC Flow Diagram.....	37
Figure 11 Isotope distribution of simple sulfone and disulfide [89].....	41
Figure 12 Type A and B of the photoproducts	45
Figure 13 Water elimination from 3CBH-3CBH.....	46
Figure 14 Differences in transient quantum yields, encounter complex geometry, and resulting stable products observed for Ac-Met-NH-CH ₃ and Ac-MeCys-NH-CH ₃	48
Figure 15 HPLC chromatogram of aqueous solutions containing N-Ac-Met and 3CB at pH 6.4 irradiation. The expansion of the chromatograms between 12 and 18 min is shown next to the chromatogram. Chromatograms were recorded at 220 nm.....	53
Scheme 1 Acid-base equilibrium of 3CB ketyl radical	18
Scheme 2 Mechanism of CB-sensitized photo-oxidation of methionine in aqueous solutions in the absence of oxygen	21
Scheme 3 Primary steps of methionine oxidation by •OH radicals in the deoxygenated aqueous solution. Source: [60].....	25
Scheme 4 Reactions of Met with H•, HO• and H ₂ O ₂ [69]	28
Scheme 5 The mechanism of CB-sensitized photo- and radiation-induced oxidation of methionine derivatives in aqueous solutions (R ₁ represents -OCH ₃ , -NH ₂ and -NHCH ₃ groups, R ₂ represents Ac- group or H-). Based on [48]	31
Scheme 6 Photoreduction of the excited triplet of benzophenones by 2-propanol	44
Scheme 7 The mechanism of the reaction of radicals generated by γ-irradiation with Ac-Met-OCH ₃	51
Scheme 8 The mechanism of the photosensitized reaction of Ac-Met-OCH ₃	52
Scheme 9 Two pathways of N-Ac-Met sulfur radical cation: deprotonation and decarboxylation.....	54
Scheme 10 Mechanism of the photosensitized oxidation of Ac-MeCys.....	57

6 LIST OF TABLES

Table 1 Spectral characteristics of transients derived during reduction of BP, 4CB, and 3CB [51–53]	18
--	----

Table 2 The quantum yields of the primary intermediates of the photosensitized oxidation of methionine and its derivatives	30
Table 3 Differences between LFP and PR.....	36
Table 4 The components of the mass spectrometer.....	39
Table 5 Isotopic abundance of sulfur and oxygen isotopes [88]	41

7 LIST OF SCIENTIFIC ACHIEVEMENTS

The list of published scientific articles:

- 1) Filipiak, P.; **Grzyb, K.**; Borkowska, M.; Pedzinski, T. *Unveiling the Triplet-State Interaction Mechanism Between 4-Carboxybenzophenone and 2-Naphthalene Sulfonate—A Laser Flash Photolysis Study*. *Photochem* **2025**, 5 (1), 4. DOI: 10.3390/photochem5010004.
IF: to be announced MNiSW: 5 Citations: 0
- 2) Frąckowiak, K. J.; Pędziński, T.; **Grzyb, K.**; Ignasiak-Kciuk, M.; Marciniak, B. *Influence of Blocking Groups on Photo-Oxidation of Tyrosine and Derivatives*. *Journal of Photochemistry and Photobiology A: Chemistry* **2025**, 458, 115988. DOI: 10.1016/j.jphotochem.2024.115988.
IF: 4.100 MNiSW: 70 Citations: 0
- 3) **Grzyb, K.**; Kaźmierczak, F.; Pedzinski, T. *Efficient Decarboxylation of Oxidized Cysteine Unveils Novel Free-Radical Reaction Pathways*. *Journal of Photochemistry and Photobiology A: Chemistry* **2024**, 451, 115530. DOI: 10.1016/j.jphotochem.2024.115530.
IF: 4.100 MNiSW: 70 Citations: 0
- 4) Gao, Q.; **Grzyb, K.**; Gamon, L. F.; Ogilby, P. R.; Pędziński, T.; Davies, M. J. *The Structure of Model and Peptide Disulfides Markedly Affects Their Reactivity and Products Formed with Singlet Oxygen*. *Free Radical Biology and Medicine* **2023**, 207, 320–329. DOI: 10.1016/j.freeradbiomed.2023.08.024
IF: 7.100 MNiSW: 200 Citations: 3
- 5) **Grzyb, K.**; Sehwat, V.; Pedzinski, T. *The Fate of Sulfur Radical Cation of N-Acetyl-Methionine: Deprotonation vs. Decarboxylation*. *Photochem* **2023**, 3 (1), 98–108. DOI: 10.3390/photochem3010007.
IF: to be announced MNiSW: 5 Citations: 1
- 6) **Grzyb, K.**; Frański, R.; Pedzinski, T. *Sensitized Photoreduction of Selected Benzophenones. Mass Spectrometry Studies of Radical Cross-Coupling Reactions*. *Journal of Photochemistry and Photobiology B: Biology* **2022**, 234, 112536. DOI: 10.1016/j.jphotobiol.2022.112536.
IF: 5.400 MNiSW: 100 Citations: 6

- 7) Lazewski, D.; Kucinska, M.; Potapkiy, E.; Kuzminska, J.; Tezyk, A.; Popenda, L.; Jurga, S.; Teubert, A.; Gdaniec, Z.; Kujawski, J.; **Grzyb, K.**; Pedzinski, T.; Murias, M.; Wierzchowski, M. *Novel Short PEG Chain-Substituted Porphyrins: Synthesis, Photochemistry, and In Vitro Photodynamic Activity against Cancer Cells*. International Journal of Molecular Sciences **2022**, *23* (17), 10029. DOI: 10.3390/ijms231710029.
IF: 5.600 MNiSW: 140 Citations: 8

- 8) Pędzinski, T.; **Grzyb, K.**; Skotnicki, K.; Filipiak, P.; Bobrowski, K.; Chatgililoglu, C.; Marciniak, B. *Radiation- and Photo-Induced Oxidation Pathways of Methionine in Model Peptide Backbone under Anoxic Conditions*. International Journal of Molecular Sciences **2021**, *22* (9), 4773. DOI: 10.3390/ijms22094773.
IF: 6.208 MNiSW: 140 Citations: 12

- 9) Pedzinski, T.; **Grzyb, K.**; Kaźmierczak, F.; Frański, R.; Filipiak, P.; Marciniak, B. *Early Events of Photosensitized Oxidation of Sulfur-Containing Amino Acids Studied by Laser Flash Photolysis and Mass Spectrometry*. Journal of Physical Chemistry B **2020**, *124* (35), 7564–7573. DOI: 10.1021/acs.jpcc.0c06008.
IF: 2.991 MNiSW: 140 Citations: 10

Impact factor (IF) from the year of publishing; source: Journal Citation Reports

MNiSW: Score based on the announcement of the Minister of Science and Higher Education dated January 5, 2024 on the list of scientific journals and peer-reviewed materials from international conferences

Scientific grants:

- 1) Principal Investigator in Minigrant for PhD students no. 017/02/SNŚ/0008

Oxidation of C-terminal domain methionine peptides. The fate of a sulfur radical cation: deprotonation vs. decarboxylation

Funding: The Excellence Initiative – Research University (IDUB)

Internships:

- 1) Radiation Laboratory, Notre Dame University (Indiana, USA); 22.09-13.10.2022;
Supervision: prof. Sylwia Ptasińska
- 2) Institute for Organic Synthesis and Photoreactivity (Bologna, Italy); 11-24.10.2021;
Supervision: dr Carla Ferreri

Scientific conferences

- 1) Grzyb K., Kaźmierczak F., Pedzinski T., *Efficient decarboxylation of oxidized Cysteine unveils novel free-Radical reaction pathways*, 29th IUPAC Symposium on Photochemistry, Valencia (Spain), 14-19.07 2024 (poster presentation)
- 2) Pedzinski T., Grzyb K., *The fate of sulfur radical cation of methionine and S-methyl-cysteine: deprotonation vs decarboxylation*, 32nd Miller Conference on Radiation Chemistry, Corsica (France), 3-9.06.2023 (oral presentation, co-authorship)
- 3) Grzyb K., Sehwat V., Pędziński T., *Oxidation of C-terminal domain methionine peptides. The fate of a sulfur radical cation in methionine-containing peptides oxidation: deprotonation vs. decarboxylation*, 28th IUPAC Symposium on Photochemistry, Amsterdam (The Netherlands), 17-22.07.2024 (poster presentation)
- 4) Grzyb K., Sehwat V., Marciniak B., Pędziński T., *Drogi reakcji kationorodnika siarkowego w utlenionej N-Acetylmetyoninie: deprotonacja i dekarboksylacja*, VII Łódź Symposium for PhD Students in Chemistry, Łódź (Poland), 24.09.2021 (oral presentation)
- 5) Grzyb K., Sehwat V., Marciniak B., Pędziński T., *Drogi reakcji kationorodnika siarkowego w utlenionej N-Acetylmetyoninie: deprotonacja i dekarboksylacja*, XIV Copernican Seminar of Doctoral Students, Toruń (Poland), 20-22.09.2021 (poster presentation)

Awards:

- 1) Laureate of 3 competitions organized within „The Excellence Initiative – Research University” program (2020-2024)
- 2) Distinction in the competition for the best poster in the field of chemistry during XIV Copernican Seminar of Doctoral Students 20-22.09.2021

8 DECLARATIONS OF CONTRIBUTION

mgr inż. Katarzyna Grzyb
Wydział Chemii UAM
Uniwersytetu Poznańskiego 8
61-614 Poznań
Email: katgrz3@amu.edu.pl

Poznań, 04.04.2025

OŚWIADCZENIE

Oświadczam, że:

1. w pracy: Grzyb, K.; Frański, R.; Pedzinski, T. Sensitized Photoreduction of Selected Benzophenones. Mass Spectrometry Studies of Radical Cross-Coupling Reactions. *Journal of Photochemistry and Photobiology B: Biology* **2022**, 234, 112536. mój udział polegał na: wykonaniu naświetlań stacjonarnych, czaso-rozdzielczych pomiarów spektroskopowych (nanosekundowa fotoliza błyskowa) oraz analizy wysokosprawnej chromatografii cieczowej, opracowaniu danych eksperymentalnych, interpretacji wyników eksperymentów, przygotowaniu rysunków, schematów, pierwszej wersji manuskryptu oraz odpowiedzi na pytania recenzentów;
2. w pracy: Pedzinski, T.; Grzyb, K.; Kaźmierczak, F.; Frański, R.; Filipiak, P.; Marciniak, B. Early Events of Photosensitized Oxidation of Sulfur-Containing Amino Acids Studied by Laser Flash Photolysis and Mass Spectrometry. *J. Phys. Chem. B* **2020**, 124 (35), 7564–7573. mój udział polegał na: wykonaniu naświetlań stacjonarnych, czaso-rozdzielczych pomiarów spektroskopowych (nanosekundowa fotoliza błyskowa) oraz analizy wysokosprawnej chromatografii cieczowej, opracowaniu danych eksperymentalnych, przygotowaniu schematów;
3. w pracy: Pedzinski, T.; Grzyb, K.; Skotnicki, K.; Filipiak, P.; Bobrowski, K.; Chatgililoglu, C.; Marciniak, B. Radiation- and Photo-Induced Oxidation Pathways of Methionine in Model Peptide Backbone under Anoxic Conditions. *IJMS* **2021**, 22 (9), 4773. mój udział polegał na: wykonaniu naświetlań stacjonarnych, czaso-rozdzielczych pomiarów spektroskopowych (nanosekundowa fotoliza błyskowa) oraz analizy wysokosprawnej chromatografii cieczowej, opracowaniu danych eksperymentalnych, interpretacji wyników badań, współudziale w eksperymentach γ -radiolizy, przygotowaniu schematów;
4. w pracy Grzyb, K.; Sehwat, V.; Pedzinski, T. The Fate of Sulfur Radical Cation of N-Acetyl-Methionine: Deprotonation vs. Decarboxylation. *Photochem* **2023**, 3 (1), 98–108. mój udział polegał na: wykonaniu naświetlań stacjonarnych, czasoworozdzielczych pomiarów spektroskopowych (nanosekundowa fotoliza błyskowa) oraz analizy wysokosprawnej chromatografii cieczowej, opracowaniu danych eksperymentalnych, interpretacji wyników eksperymentalnych, przygotowaniu rysunków, schematów, odpowiedzi na pytania recenzentów oraz pierwszej wersji manuskryptu oraz finansowaniu badań w ramach projektu IDUB
5. w pracy: Grzyb, K.; Kaźmierczak, F.; Pedzinski, T. Efficient Decarboxylation of Oxidized Cysteine Unveils Novel Free-Radical Reaction Pathways. *Journal of Photochemistry and Photobiology A: Chemistry* **2024**, 451, 115530. mój udział polegał na: wykonaniu naświetlań stacjonarnych, czasoworozdzielczych pomiarów spektroskopowych (nanosekundowa fotoliza błyskowa) oraz analizy wysokosprawnej chromatografii cieczowej, opracowaniu danych eksperymentalnych, interpretacji wyników badań, przygotowaniu rysunków, pierwszej wersji manuskryptu, odpowiedzi na pytania recenzentów oraz finansowaniu badań w ramach projektu IDUB.

Tomasz Pedzinski

Katarzyna Grzyb

Prof. UAM dr hab. Tomasz Pędziński
Wydział Chemii UAM
Uniwersytetu Poznańskiego 8
61-614 Poznań
Email: tomekp@amu.edu.pl

Poznań, 04.04.2025

OŚWIADCZENIE

Oświadczam, że:

1. w pracy: Grzyb, K.; Frański, R.; Pedzinski, T. Sensitized Photoreduction of Selected Benzophenones. Mass Spectrometry Studies of Radical Cross-Coupling Reactions. *Journal of Photochemistry and Photobiology B: Biology* **2022**, 234, 112536. mój udział polegał na: opracowaniu koncepcji pracy, zaplanowaniu i kierowaniu pracami eksperymentalnymi, interpretacji wyników eksperymentów, sprawdzeniu i wysłaniu manuskryptu, korespondencji z edytorem oraz dyskusji z recenzentami.
2. w pracy: Pedzinski, T.; Grzyb, K.; Kaźmierczak, F.; Frański, R.; Filipiak, P.; Marciniak, B. Early Events of Photosensitized Oxidation of Sulfur-Containing Amino Acids Studied by Laser Flash Photolysis and Mass Spectrometry. *J. Phys. Chem. B* **2020**, 124 (35), 7564–7573. mój udział polegał na: opracowaniu koncepcji pracy, zaplanowaniu i kierowaniu pracami eksperymentalnymi, interpretacji wyników eksperymentów, przygotowaniu manuskryptu, korespondencji z edytorem oraz dyskusji z recenzentami.
3. w pracy: Pędzinski, T.; Grzyb, K.; Skotnicki, K.; Filipiak, P.; Bobrowski, K.; Chatgililoglu, C.; Marciniak, B. Radiation- and Photo-Induced Oxidation Pathways of Methionine in Model Peptide Backbone under Anoxic Conditions. *IJMS* **2021**, 22 (9), 4773. mój udział polegał na: opracowaniu koncepcji pracy, zaplanowaniu i kierowaniu pracami eksperymentalnymi, interpretacji wyników eksperymentów oraz przygotowaniu manuskryptu.
4. w pracy Grzyb, K.; Sehwat, V.; Pedzinski, T. The Fate of Sulfur Radical Cation of N-Acetyl-Methionine: Deprotonation vs. Decarboxylation. *Photochem* **2023**, 3 (1), 98–108. mój udział polegał na: opracowaniu koncepcji pracy, zaplanowaniu i kierowaniu pracami eksperymentalnymi, interpretacji wyników badań, sprawdzeniu i wysłaniu manuskryptu, korespondencji z edytorem, dyskusji z recenzentami oraz finansowaniu badań w ramach projektu IDUB.
5. w pracy: Grzyb, K.; Kaźmierczak, F.; Pedzinski, T. Efficient Decarboxylation of Oxidized Cysteine Unveils Novel Free-Radical Reaction Pathways. *Journal of Photochemistry and Photobiology A: Chemistry* **2024**, 451, 115530. mój udział polegał na: opracowaniu koncepcji pracy, zaplanowaniu i kierowaniu pracami eksperymentalnymi, interpretacji wyników badań, sprawdzeniu i wysłaniu manuskryptu, korespondencji z edytorem oraz dyskusji z recenzentami oraz finansowaniu badań w ramach projektu IDUB.


.....

Prof. dr hab. Bronisław Marciniak
Centrum Zaawansowanych Technologii UAM
Ul. Uniwersytetu Poznańskiego 10
61-614 Poznań
Email: marcinia@amu.edu.pl

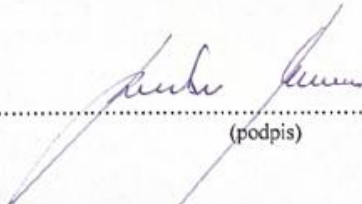
Poznań, 20 marca 2025

OŚWIADCZENIE

Oświadczam, że w pracach:

1. Pedzinski, T.; Grzyb, K.; Kaźmierczak, F.; Frański, R.; Filipiak, P.; Marciniak, B. Early Events of Photosensitized Oxidation of Sulfur-Containing Amino Acids Studied by Laser Flash Photolysis and Mass Spectrometry. *J. Phys. Chem. B* **2020**, *124* (35), 7564–7573.
2. Pędzinski, T.; Grzyb, K.; Skotnicki, K.; Filipiak, P.; Bobrowski, K.; Chatgililoglu, C.; Marciniak, B. Radiation- and Photo-Induced Oxidation Pathways of Methionine in Model Peptide Backbone under Anoxic Conditions. *LJMS* **2021**, *22* (9), 4773.

mój udział polegał na opracowaniu koncepcji badań, analizie i dyskusji wyników, sprawdzeniu manuskryptu oraz korespondencji z recenzentami i edytorem oraz finansowaniu badań w ramach NCN.


.....
(podpis)

Dr Piotr Filipiak
Wydział Chemii UAM
Uniwersytetu Poznańskiego 8
61-614 Poznań
Email: piotr@amu.edu.pl

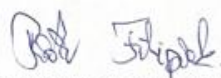
Poznań, 04.04.2025

OŚWIADCZENIE

Oświadczam, że w pracach:

1. Pedzinski, T.; Grzyb, K.; Kaźmierczak, F.; Frański, R.; Filipiak, P.; Marciniak, B. Early Events of Photosensitized Oxidation of Sulfur-Containing Amino Acids Studied by Laser Flash Photolysis and Mass Spectrometry. *J. Phys. Chem. B* **2020**, *124* (35), 7564–7573.
2. Pędzinski, T.; Grzyb, K.; Skotnicki, K.; Filipiak, P.; Bobrowski, K.; Chatgililoglu, C.; Marciniak, B. Radiation- and Photo-Induced Oxidation Pathways of Methionine in Model Peptide Backbone under Anoxic Conditions. *IJMS* **2021**, *22* (9), 4773.

mój udział polegał na pomocy przy pomocy w opracowaniu chromatograficznych metod rozdzielania oraz interpretacji wyników.



(podpis)

Prof. UAM dr hab. Rafał Frański
Wydział Chemii UAM
Uniwersytetu Poznańskiego 8
61-614 Poznań
Email: franski@amu.edu.pl

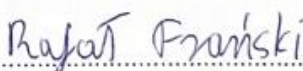
Poznań, 21.03.2025

OŚWIADCZENIE

Oświadczam, że w pracach:

1. Pedzinski, T.; Grzyb, K.; Kaźmierczak, F.; Frański, R.; Filipiak, P.; Marciniak, B. Early Events of Photosensitized Oxidation of Sulfur-Containing Amino Acids Studied by Laser Flash Photolysis and Mass Spectrometry. *J. Phys. Chem. B* **2020**, *124* (35), 7564–7573.
2. Grzyb, K.; Frański, R.; Pedzinski, T. Sensitized Photoreduction of Selected Benzophenones. Mass Spectrometry Studies of Radical Cross-Coupling Reactions. *Journal of Photochemistry and Photobiology B: Biology* **2022**, *234*, 112536.

mój udział polegał na pomocy w interpretacji widm masowych produktów badanych reakcji oraz sprawdzeniu części manuskryptu dotyczącej spektrometrii mas.


.....
(podpis)

Dr Franciszek Kaźmierczak
Wydział Chemii UAM
Uniwersytetu Poznańskiego 8
61-614 Poznań
E-mail: kazmak@amu.edu.pl

Poznań, 07.03.2025

OŚWIADCZENIE

Oświadczam, że w pracach:

1. Pedzinski, T.; Grzyb, K.; Kaźmierczak, F.; Frański, R.; Filipiak, P.; Marciniak, B. Early Events of Photosensitized Oxidation of Sulfur-Containing Amino Acids Studied by Laser Flash Photolysis and Mass Spectrometry. *J. Phys. Chem. B* **2020**, *124* (35), 7564–7573.
2. Grzyb, K.; Kaźmierczak, F.; Pedzinski, T. Efficient Decarboxylation of Oxidized Cysteine Unveils Novel Free-Radical Reaction Pathways. *Journal of Photochemistry and Photobiology A: Chemistry* **2024**, *451*, 115530.

mój udział polegał na syntezie badanych związków chemicznych.


.....
(podpis)

Prof. Chrysostomos Chatgililoglu
CNR – Istituto per la sintesi organica e la
fotoreattività (ISOF)
Via Piero Gobetti 101 • Bologna, Italy, 401294
Email:
chrysostomos.chatgililoglu@isof.cnr.it

date 20/03/2025

Declaration of contribution

Herein I declare my individual contribution to the following paper:

Pędzinski, T.; Grzyb, K.; Skotnicki, K.; Filipiak, P.; Bobrowski, K.; Chatgililoglu, C.; Marciniak, B. Radiation- and Photo-Induced Oxidation Pathways of Methionine in Model Peptide Backbone under Anoxic Conditions. *IJMS* **2021**, 22 (9), 4773.

My contribution to the above-mentioned paper included the development of the research concept, preparation of original draft review, and editing.


.....
(signature)

Prof. dr hab. Krzysztof Bobrowski
Instytut Chemii i Techniki Jądrowej
Ul. Dorodna 16
03-195 Warszawa
Email: kris@ichtj.waw.pl

Poznań, 14.02.2025 r.

OŚWIADCZENIE

Oświadczam, że w pracy:

Pędzinski, T.; Grzyb, K.; Skotnicki, K.; Filipiak, P.; Bobrowski, K.; Chatgililoglu, C.;
Marciniak, B. Radiation- and Photo-Induced Oxidation Pathways of Methionine in Model Peptide
Backbone under Anoxic Conditions. *LJMS* **2021**, 22 (9), 4773.

mój udział polegał na opracowaniu koncepcji badań, wykonaniu eksperymentów radiolizy impulsowej,
analizie i dyskusji wyników oraz korespondencji z recenzentami.

.....
(podpis)

Dr Konrad Skotnicki
Instytut Chemii i Techniki Jądrowej
Email: skotnicki.konrad@gmail.com

Warszawa, 27.11.2024

OŚWIADCZENIE

Oświadczam, że w pracy:

Pędzinski, T.; Grzyb, K.; Skotnicki, K.; Filipiak, P.; Bobrowski, K.; Chatgililoglu, C.; Marciniak, B. Radiation- and Photo-Induced Oxidation Pathways of Methionine in Model Peptide Backbone under Anoxic Conditions. *IJMS* **2021**, 22 (9), 4773.

mój udział polegał na wykonaniu radiolizy impulsowej oraz γ -radiolizy oraz analizie i dyskusji wyników.



.....
(podpis)

Vidhi Sehwat, M.Sc.
Dioscuri Centre for Modelling of
Posttranslational Modifications
Malopolska Centre of Biotechnology
Email: vidhi.sehwat@doctoral.uj.edu.pl

24th February 2025

Declaration of contribution

Herein, I declare my individual contribution to the following paper:

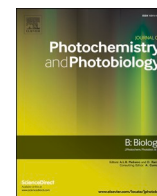
Grzyb, K.; Sehwat, V.; Pedzinski, T. The Fate of Sulfur Radical Cation of N-Acetyl-Methionine: Deprotonation vs. Decarboxylation. *Photochem* **2023**, 3 (1), 98–108.

My contribution to the abovementioned paper includes conducting experiments (stationary irradiation, laser flash photolysis, high-performance liquid chromatography), analyzing results from conducted experiments and tandem mass spectrometry data, preparing figures, and writing the original manuscript draft in the form of master's thesis for the completion of Erasmus Mundus Joint Master Degree SERP+.



(signature)

9 REPRINTS OF PUBLICATIONS



Sensitized photoreduction of selected benzophenones. Mass spectrometry studies of radical cross-coupling reactions

Katarzyna Grzyb^a, Rafał Frański^a, Tomasz Pedzinski^{a,b,*}

^a Faculty of Chemistry, Adam Mickiewicz University, Uniwersytetu Poznańskiego 8, 61-614 Poznań, Poland

^b Center for Advanced Technology, Adam Mickiewicz University, Uniwersytetu Poznańskiego 10, 61-614 Poznań, Poland

ARTICLE INFO

Keywords:

Photosensitizers
Photoreduction
Benzophenone
3-carboxybenzophenone
4-carboxybenzophenone
High resolution mass spectrometry

ABSTRACT

The hydrogen atom transfer reaction (HAT) between selected benzophenones (benzophenone BP, 3-carboxybenzophenone 3CB, and 4-carboxybenzophenone 4CB) and 2-propanol was reinvestigated focusing on stable product analysis. As expected, the primary species of these HAT's are the respective diphenyl and dimethyl ketyl radicals that eventually undergo several radical coupling reactions leading to stable photoproducts. However, the mechanisms of these free radical reactions remain unclear and open to question. In this report, we focus on the detailed analysis of the stable photoproducts of these reactions using liquid chromatography coupled with high-resolution mass spectrometry (LC-ESI-QTOF-MS/MS). Products of photopinacolization (benzpinacol and two diastereoisomers of 4CB and 3CB dimers) and isomeric radical cross-coupling adducts of respective diphenyl and dimethyl ketyl radicals were separated chromatographically, and their structures were determined by high-resolution MS/MS, and the mechanisms of the reactions are discussed.

1. Introduction

UVA and UVB light may interact with biomolecules directly or, more likely, through photosensitization by light-absorbing chromophores. Benzophenone (1) and its multiple derivatives, for example, 3-carboxybenzophenone (2) and 4-carboxybenzophenone (3) have been used as biochemical sensitizers due to their well-established photochemical properties under UVA irradiation: (i) typical photoactivation at 350–370 nm allows selective excitation without direct photoexposure of peptides, proteins, nucleosides or DNA; (ii) intersystem crossing yield $\phi_{isc} \approx 1$; (iii) relatively high yield of singlet oxygen generation through triplet-triplet energy transfer to molecular oxygen ($E_T \approx 290$ kJ/mol, $\phi_\Delta \approx 0.3$). These properties make benzophenone-derivatives excellent tools in fundamental biochemical studies of photosensitized damage processes that can take place through a variety of reactions: electron transfer, hydrogen atom transfer (HAT), energy transfer, or generation of reactive oxygen species [1,2].

The mechanisms of benzophenone- and carboxybenzophenone-sensitized reactions have been successfully studied in a variety of inorganic and organic compounds e.g., aquatic contaminants [3,4], 4-phenoxyphenol [5,6], herbicides [7], monuron [8], β 2-adrenoceptor agonists [9] and various sulfur-containing compounds e.g. sulfides and

thiols [10–12], amino acids and oligopeptides [13–26], carboxylic acids [27], sulfonamide antibiotics [28] and other model compounds [29–31]. These papers about sensitized photooxidation focus mostly on time-resolved analyses and investigate the nature and structure of transient species. The occasional stationary irradiation experiments focus primarily on the stable products derived from the quencher, and the final fate of the sensitizer is usually not considered.

The electron transfer quenching of the triplet state of the sensitizers leads to the formation of the radical anion ($BP^{\bullet-}$, $3CB^{\bullet-}$ or $4CB^{\bullet-}$) and/or ketyl radical (BPH^{\bullet} / $3CBH^{\bullet}$ / $4CBH^{\bullet}$). The equilibrium between those two transients depends strongly on the pH of the solution [16,23,29].

The physical and chemical properties of benzophenone, 3-carboxybenzophenone, and 4-carboxybenzophenone as well as the kinetic and spectral characteristics of transients derived from them vary. Benzophenone is insoluble in water thus its applicability in studies on biological systems that require an aqueous environment is limited. On the other hand, 3-carboxybenzophenone and 4-carboxybenzophenone are water-soluble, and therefore they are often more useful. Using 3CB instead of 4CB as a sensitizer expands the available spectral region up to the visible and near UV region (370–400 nm) since 3CB-derived transients are considerably less absorbing in that spectral range than the

* Corresponding author at: Faculty of Chemistry, Adam Mickiewicz University, Uniwersytetu Poznańskiego 8, 61-614 Poznań, Poland.

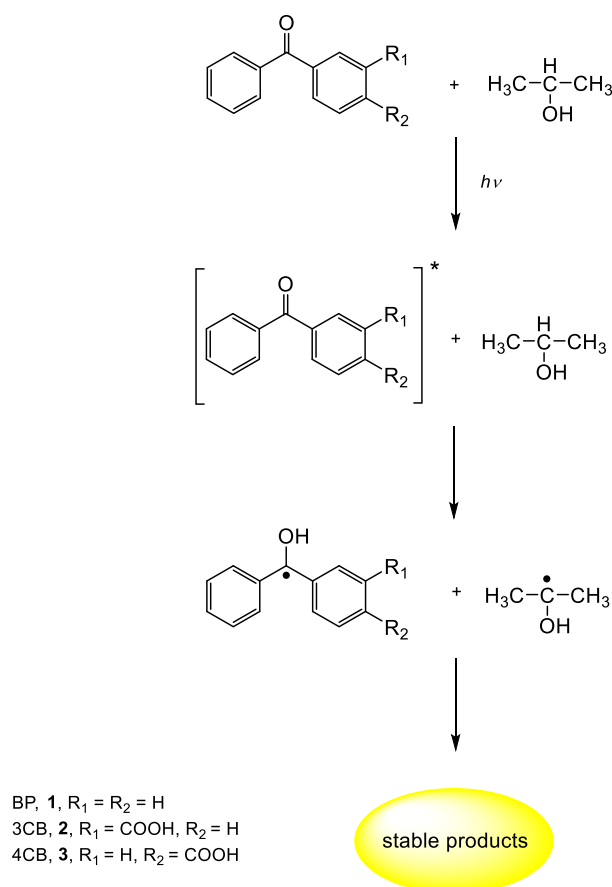
E-mail address: tomekp@amu.edu.pl (T. Pedzinski).

<https://doi.org/10.1016/j.jphotobiol.2022.112536>

Received 26 April 2022; Received in revised form 11 July 2022; Accepted 27 July 2022

Available online 1 August 2022

1011-1344/© 2022 The Authors. Published by Elsevier B.V. This is an open access article under the CC BY license (<http://creativecommons.org/licenses/by/4.0/>).



Scheme 1. General scheme for the photoreduction of the excited triplet of benzophenones by 2-propanol

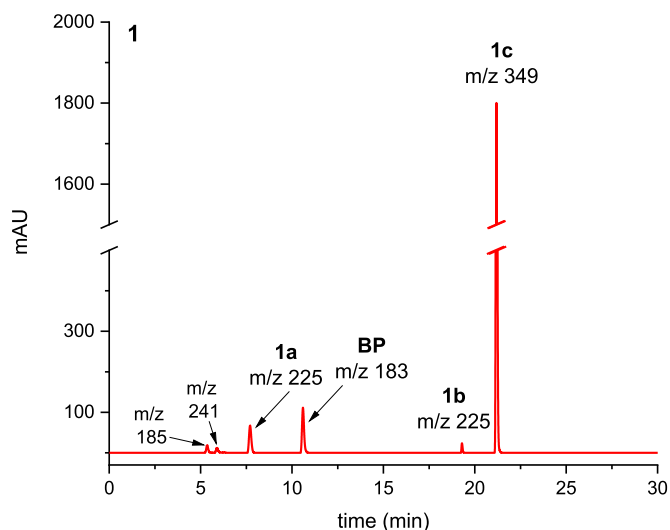


Fig. 1. LC-MS chromatogram of 355 nm irradiated samples of benzophenone (BP) containing 2-propanol. Peaks are labeled with m/z of the most intense peak of the acquired MS spectrum.

respective 4CB transients.

The first report on the formation of benzopinacol by irradiation of a solution of benzophenone in aliphatic alcohols dates back to the 19th century when Ciamician and Silber correctly interpreted the structure of the photodimer [32]. Since then this photochemical reaction has been extensively explored in various conditions and using a wide range of

techniques [33–43]. The nature of the formed transient species and the mechanism of the reaction have especially been the subject of numerous detailed studies. On the other hand, very few reports focus on a thorough analysis of stable products [40].

The photochemical reaction of benzophenone with a suitable reductant, e.g. 2-propanol, yields a diphenyl ketyl radical and a radical derived from the reductant (e.g. a dimethyl ketyl radical in the case of 2-propanol). Subsequently, those radicals can undergo various dimerization and coupling reactions that lead to the formation of several products: acetone, pinacol, benzhydrol, benzopinacol, unsymmetrical pinacol, and para-substituted benzophenone [40,42,44].

It has also been observed that the coupling reaction yields the intermediate, generally called “light-absorbing transient” (LAT), that exhibits an absorption maximum at 358 nm [42]. The structure of LAT was a controversial subject, and two possible structures of this photoproduct have been discussed throughout the years: one being the product of dimerization of a diphenyl ketyl radical called “isobenzopinacol” [38,39] and the other - a cross-coupling product of diphenyl ketyl and hydroxyalkyl radicals [37,42,45]. Ultimately the experimental evidence indicated the latter to be correct. The ability of the excited triplet state of benzophenone to efficiently abstract a hydrogen atom from an H-donor and its relatively low reduction potential are the main reasons why benzophenone is an excellent one-electron triplet-state oxidant [46].

There is a need for a comprehensive report on the photophysical properties of benzophenones studied with modern, currently used techniques such as liquid chromatography with tandem mass spectrometry (LC-MS/MS). High-resolution mass spectrometry is a powerful technique for characterization and structural analysis of the stable photoproducts. It can provide the molecular composition of the products based on the measured exact masses (or more precisely m/z values). Additionally, MSMS fragmentation experiments provide the structural information of the photoproducts and, after detailed analysis, their precursor radicals. In the present study, we investigated both transient species and, often considered, trivial stable products of the photoreduction of commonly used photosensitizers: benzophenone (BP),

3-carboxybenzophenone (3CB), and 4-carboxybenzophenone (4CB).

The exact structures of the benzopinacol-like products were described based on the MS/MS fragmentation experiments.

2. Experimental

Benzophenone (BP, 1), 3-carboxybenzophenone (3CB, 2), and 4-carboxybenzophenone (4CB, 3) were obtained commercially from Sigma-Aldrich as the best available grade and was used as received. The deionized water for the experiments was purified using a commercial system from Millipore, model Simplicity (Billerica, MA, USA).

Absorption spectra were measured using a Cary 5000 UV/vis spectrophotometer. A benzophenone-benzhydrol actinometer was used for the determination of the quantum yields of sensitizer disappearance [47].

The laser flash photolysis (LFP) setup used in this work has been described in detail elsewhere [29]. Briefly, this setup employs an Nd:YAG laser (Spectra Physics, Mountain View, CA, USA, model INDI 40–10) with a 355 nm excitation wavelength as the light pump and a pulsed xenon lamp (Applied Photophysics, Surrey, UK) to probe the excited sample. Kinetic traces were recorded between 370 and 750 nm at 10 nm intervals. The sample contained the sensitizer (BP, 3CB or 4CB, 4 mM) and 2-propanol (10% v/v).

Steady-state photochemical irradiation experiments were performed in a 1 cm × 1 cm rectangular cell on an optical bench irradiation system using a Genesis CX355 STM OPPL laser (Coherent), with a 355 nm emission wavelength (the output power used was set at 50 mW). After steady-state irradiations, samples (BP, 6 mM, 3CB, 3.6 mM and 4CB, 3.7 mM each containing 10% v/v of 2-propanol) were subjected to LC-MS and MS/MS analyses.

The LC-MS measurements were carried out using a liquid

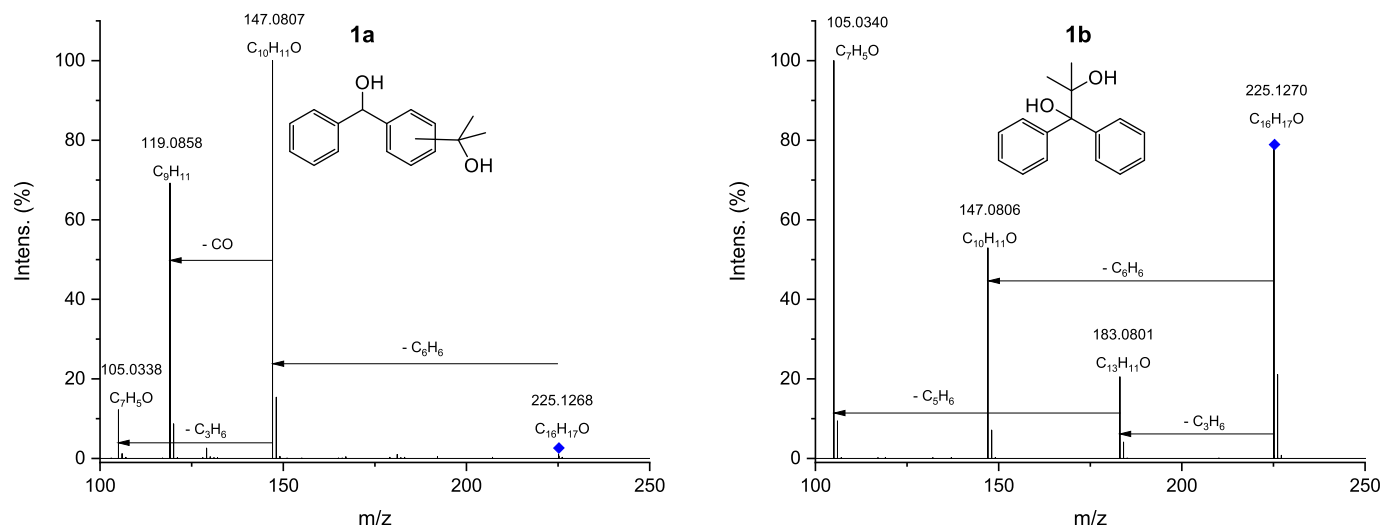


Fig. 2. High-resolution MS/MS spectra of the product ions $[M + H_2O]^+$ of **1a** (m/z 225.1268) and **1b** (m/z 225.1270).

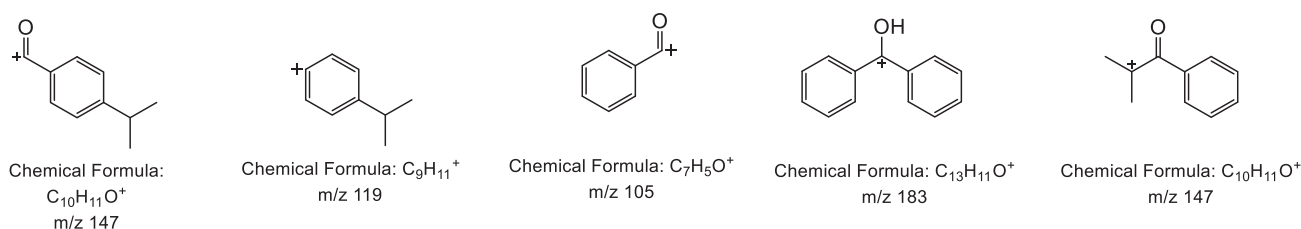


Fig. 3. Plausible structures of the product ions at m/z 147, 119, 105, and 183 (from MS/MS fragmentations of **1a** and **1b**).

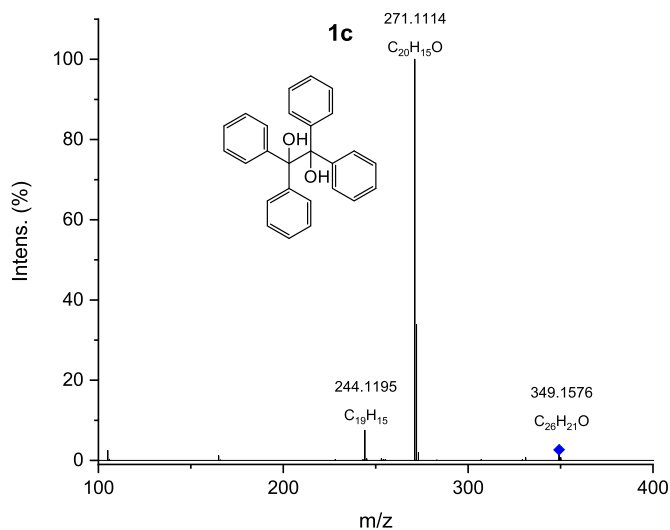


Fig. 4. High-resolution MS/MS spectrum of the product ion $[M + H_2O]^+$ of **1c** (m/z 349.1576).

chromatography Thermo Scientific/ Dionex Ultimate 3000 system equipped with a C18 reversed-phase analytical column (2.6 μ m, 2.1 mm \times 100 mm, Thermo-Scientific, Sunnyvale, CA, USA). The column temperature was set to 45 $^{\circ}$ C. Two eluents were used: water and acetonitrile with 0.1% (v/v) formic acid. The separation of 3CB and 4CB reduction photoproducts was achieved using a gradient elution: from 7 to 60% of acetonitrile at a flow rate of 0.3 ml/min for 42 min, and the separation of photoproducts of BP reduction with the gradient of 30–60% in 30 min.

This UHPLC system was coupled to a hybrid QTOF mass spectrometer (Impact HD, Bruker Daltonik, Bremen, Germany). The ions were generated by electrospray ionization (ESI) in positive mode. MS/MS fragmentation mass spectra were produced by collisions (CID, collision-induced dissociation) with nitrogen gas in the Q2 section of the spectrometer.

All of the LFP and stationary irradiation experiments were performed in oxygen-free solutions at neutral pH.

3. Results and discussion

3.1. Laser flash photolysis

As can be seen in Scheme 1, upon 355 nm excitation, the triplet of the sensitizer was generated. Then the hydrogen-transfer (sometimes referred to as electron transfer followed by proton transfer) reaction

Table 1

Obtained mass accuracies (errors) for products yielded in photoreduction of benzophenone (**1**).

Compound	Retention time (min)	Accurate mass (measured)	Exact mass (calculated)	Mass accuracy (ppm)	Composition
1a	7.9	225.1268	225.1279	−5.06	$C_{16}H_{17}O$
1, BP	10.8	183.0805	183.0810	−4.18	$C_{13}H_{11}O$
1b	19.5	225.1270	225.1279	−1.96	$C_{16}H_{17}O$
1c	20.8	349.1576	349.1592	−4.70	$C_{26}H_{21}O$

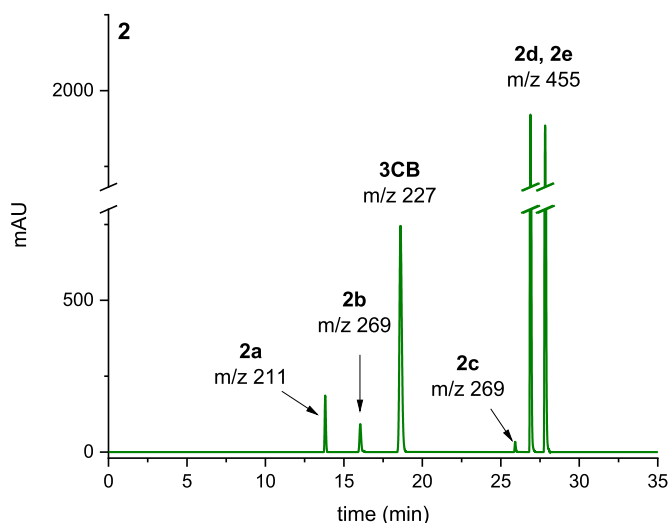


Fig. 5. LC-MS chromatogram of 355 nm irradiated samples of 3-carboxybenzophenone (3CB) containing 2-propanol. Peaks are labeled with m/z of the most intense peak of the acquired MS spectrum.

leads to the formation of the respective ketyl radical (BPH^\bullet , 3CBH^\bullet , 4CBH^\bullet). If the pH of the aqueous solution was higher than pK_a ($\text{pK}_a(3\text{CBH}^\bullet) = 9.5$, $\text{pK}_a(4\text{CBH}^\bullet) = 8.2$), the ketyl radical deprotonated yielding the corresponding radical anion ($3\text{CB}^{\bullet-}$, $4\text{CB}^{\bullet-}$) [23,48,49].

The transient spectra recorded for all of the investigated compounds at a short time after the laser flash (30–700 ns) showed a characteristic band in the visible part of the spectrum

($\lambda_{\text{max BP}} = 520 \text{ nm}$, $\lambda_{\text{max 3CB}} = 530 \text{ nm}$, $\lambda_{\text{max 4CB}} = 535 \text{ nm}$) that can be assigned to the triplet state of the sensitizer. Within several microseconds, the maximum shifted to the longer wavelengths ($\lambda_{\text{max BP, 3CB}} =$

550 nm, $\lambda_{\text{max 4CB}} = 570 \text{ nm}$) indicating the formation of the respective ketyl radical [23,48–50]. For the transient absorption spectra refer to Fig. S1.

3.2. Stable products analysis

3.2.1. Benzophenone (BP, 1)

As shown in Fig. 1 three main photoproducts, formed in the photo-reduction of benzophenone, eluted with the retention times of approximately 8 min (product 1a),

19.5 min (product 1b), and 21 min (product 1c).

Although the retention time of product 1a and product 1b differ substantially, they exhibited the same mass to charge ratio m/z 225 which suggests their isomeric nature, confirmed by the monoisotopic mass of both products: m/z 225.1268 and m/z 225.1270 and the same elemental composition: $\text{C}_{16}\text{H}_{17}\text{O}$. Those peaks are assigned to the adduct of benzophenone and 2-propanol after a dehydration reaction (typical reaction occurring in MS ion source, m/z of the parent ion MH^+ is 243) [51–56].

The MS/MS fragmentation of those compounds presented in Fig. 2 revealed significant structural differences between these two isomeric photoproducts. (See Fig. 3.)

The exact mass of the product ion detected for only 1a with m/z 119.0858 corresponds to the molecular formula of C_9H_{11} . The existence of a fragment ion with such a composition is possible only when the dimethyl ketyl radical is attached to the phenyl ring of benzophenone. Such a product of photoreduction of benzophenone by 2-propanol was previously reported by Rubin et al. [40]. Further confirmation of the formation of this type of product was the loss of carbon monoxide from the ion at m/z 147 which involves a ketyl carbon atom shown in Fig. 2.

The diagnostic product ion at m/z 183 detected for photoproduct 1b was formed after the neutral loss of C_3H_6 , and it corresponds to the benzhydryl cation. This suggests that the dimethyl ketyl radical was

Table 2

Obtained mass accuracies (errors) for products yielded in photoreduction of 3-carboxybenzophenone (2).

Compound	Retention time (min)	Accurate mass (measured)	Exact mass (calculated)	Mass accuracy (ppm)	Composition
2a	13.7	211.0751	211.0759	−3.81	$\text{C}_{14}\text{H}_{11}\text{O}_2$
2b	15.9	269.1174	269.1178	−1.37	$\text{C}_{17}\text{H}_{17}\text{O}_3$
2, 3CB	18.5	227.0705	227.0708	−1.41	$\text{C}_{14}\text{H}_{11}\text{O}_3$
2c	26.0	269.1173	269.1178	−1.74	$\text{C}_{17}\text{H}_{17}\text{O}_3$
2d	26.9	455.1489	455.1495	−1.24	$\text{C}_{28}\text{H}_{23}\text{O}_6$
2e	27.8	455.1494	455.1495	−0.14	$\text{C}_{28}\text{H}_{23}\text{O}_6$

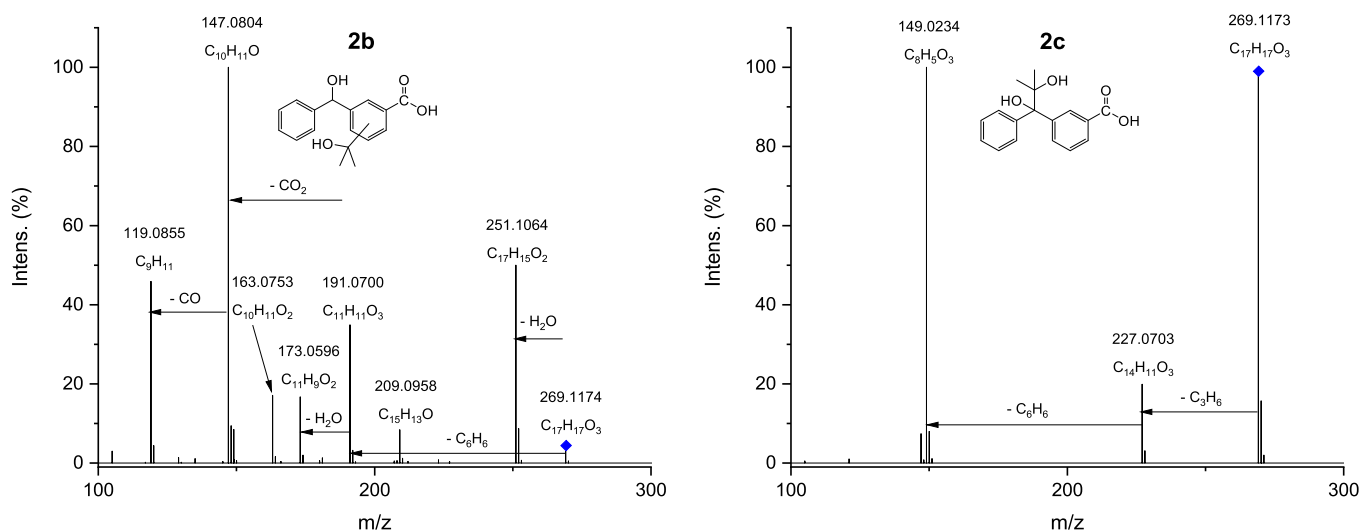
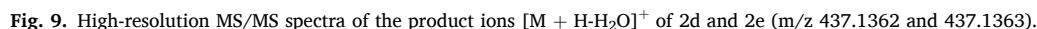
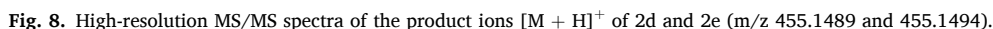
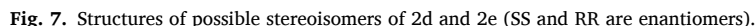


Fig. 6. High-resolution MS/MS spectra of the product ions $[\text{M} + \text{H}_2\text{O}]^+$ of 2b and 2c (m/z 269.1174 and 269.1173).



The product 1c at m/z 349.1576 corresponds to benzopinacol after the elimination of one water molecule. The loss of the water molecule is a common fragmentation pathway of ions $[M + H]^+$ observed for the compounds bearing the hydroxyl group [51–56]. The MS/MS analysis of the $[M + H - H_2O]^+$ ion of 1c is presented in Fig. 4.

times of 5.5–6 min, see Fig. 1. One with m/z 185.0957 is assigned to benzhydrol and the other product with m/z 241.1226 is possibly a secondary product derived from product 1a. The exact masses of the diagnostic ions from MS/MS experiments allowed us to suggest the structures of the photoproducts that are collected in Table 1.

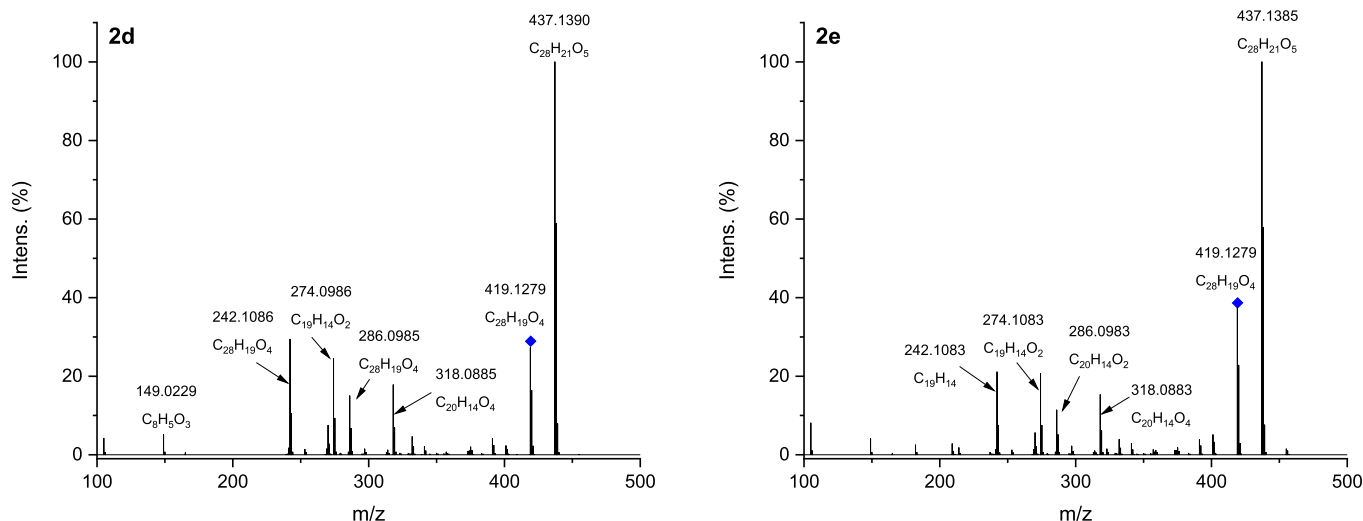


Fig. 10. High-resolution MS/MS spectra of the product ions $[M + H-2H_2O]^+$ of 2d and 2e (m/z 419.1279 and 419.1279).

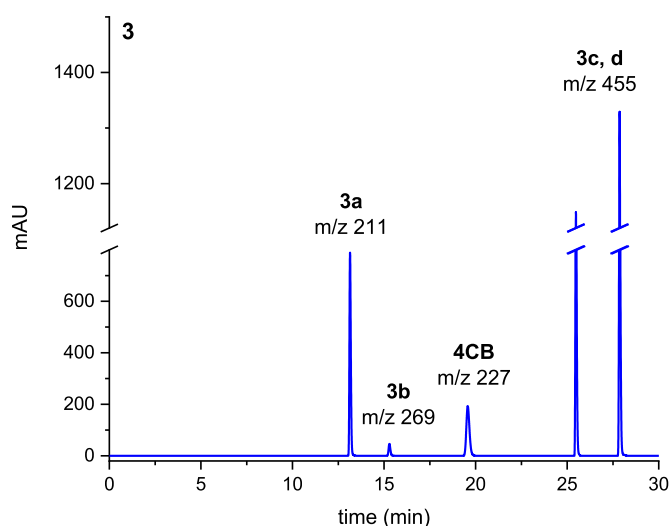


Fig. 11. LC-MS chromatogram of 355 nm irradiated samples of 4-carboxybenzophenone (4CB) containing 2-propanol. Peaks are labeled with m/z of the most intense peak of the acquired MS spectrum.

3.2.2. 3-carboxybenzophenone (3CB, 2)

As presented in Fig. 5, the photoreduction of 3-carboxybenzophenone yielded five photoproducts: 2a (m/z 211.0754, retention time 14 min), 2b (m/z 269.1174, retention time 16 min), 2c (m/z 269.1173, retention time 26 min), 2d (m/z 455.1652, retention time 27 min) and photoproduct 2e (m/z 455.1650, retention time 28 min). For high resolution m/z values see Table 2.

The peak with m/z 211 (photoproduct 2a) was assigned to the aldehyde derived from the reduction of the carboxylic group of 3-carboxybenzophenone (for MS/MS spectrum see Fig. S3).

Table 3

Obtained mass accuracies (errors) for products yielded in photoreduction of 4-carboxybenzophenone (3).

Compound	Retention time (min)	Accurate mass (measured)	Exact mass (calculated)	Mass accuracy (ppm)	Composition
3a	13.0	211.0754	211.0759	-2.39	$C_{14}H_{11}O_2$
3b	15.2	269.1175	269.1178	-1.00	$C_{17}H_{17}O_3$
3, 4CB	19.4	227.0700	227.0708	-3.61	$C_{14}H_{11}O_3$
3c	25.6	455.1563	455.1495	15.02	$C_{28}H_{23}O_6$
3d	27.8	455.1562	455.1495	14.80	$C_{28}H_{23}O_6$

Two products with m/z 269 (2b and 2c) were detected (they correspond to $[M + H-2H_2O]^+$ ion - product of the dehydration of the parent ion, the molecular ion $[MH]^+$ m/z 287 was not detected).

They have the same molecular composition, but possess different MS/MS spectra (Fig. 6) suggesting that they are isomers. The fragmentation pathways of 2b and 2c are similar to 1a and 1b.

The MS/MS fragmentation of 2b corresponded to the loss of neutral molecules of water, carbon monoxide, carbon dioxide and aromatic ring and showed a fragmentation peak with m/z 119.0855, identical to the fragment from the photoproduct 1a, therefore suggesting that the dimethyl ketyl is attached to a phenyl ring. On the other hand, the first step in the fragmentation pattern of 2c corresponds to the loss of the neutral species of C_3H_6 yielding a product ion at m/z 227.0703 indicating that the dimethyl ketyl radical is attached to the ketyl carbon of the 3CB.

Photoproducts 2d and 2e showed the same molecular composition ($C_{28}H_{23}O_6$) suggesting their isomeric nature. One of the peaks corresponds to the SS or RR isomer, whereas the second peak corresponds to the RS isomer (see Fig. 7), however, it is difficult to assign the peaks to the particular isomers. Separation of enantiomers (SS, RR) by liquid chromatography can be performed only with the achiral stationary phase, whereas the standard C18 column was used in this study.

Fig. 8 shows the product ion spectra of ions $[M + H]^+$ for 2d and 2e. The fragmentations of both ions are similar. The differences lie in the different relative abundances of the product ions formed by the loss of H_2O molecules (m/z 437 and 419, their plausible structures are shown in Fig. S5). Loss of the H_2O molecule ($-m/z$ 18) is a common fragmentation pathway of ions observed for the compounds bearing carboxylic or hydroxylic groups [51–56]. The first elimination of the H_2O molecule involves the carboxylic group, and it is not affected by the configuration of asymmetric carbon atoms. On the other hand, the second elimination of the H_2O molecule involves hydroxyl group, thus the configuration of asymmetric carbon atoms can affect the loss of the second H_2O molecule which is reflected by the relative abundances of ions $[M + H]^+$, $[M + H-2H_2O]^+$, and $[M + H-2H_2O]^+$ in Fig. 8 (MS/MS of 2d and 2e).

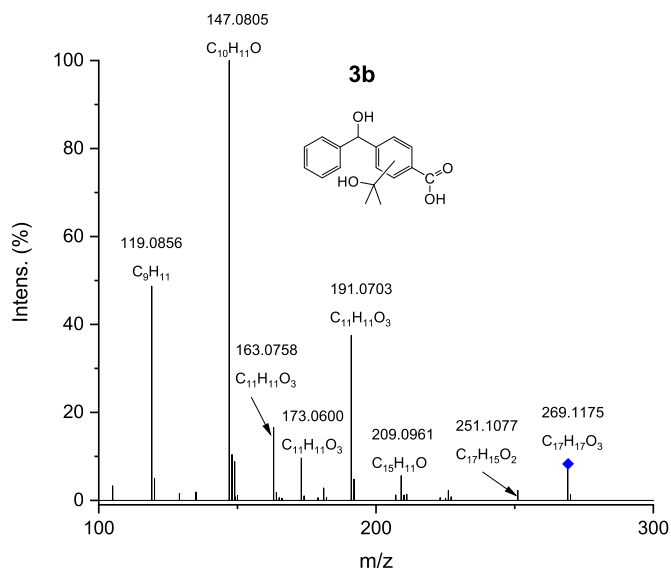


Fig. 12. High-resolution MS/MS spectrum of the product ion $[M + H-H_2O]^+$ of **3b** (m/z 269.1175) – m/z of the parent ion MH^+ is 287.

The product ions at m/z 182, 211, and 227 were formed as a result of the breaking of the bond between the asymmetric carbon atoms of $[M + H]^+$ ions (the plausible structures are shown in Fig. S6). Their formation was not affected by the configuration of the asymmetric carbon atoms since they have identical relative abundances for **2d** and **2e** (Fig. 8). It is worth noting that the formation of the product ion at m/z 182 is an example of the violation of the ‘even-electron rule’ [57–60].

Fig. 9 shows the product ion spectra of ions $[M + H-H_2O]^+$ for **2d** and **2e**. The spectra are noticeably different, indicating that their fragmentation is affected by the configuration of the asymmetric carbon atoms. Based on the obtained accurate masses we have deduced the elemental composition of the product ions. However, it is very difficult to propose even their tentative structures. For example, how can one rationalize the formation of the product ion at m/z 318 which is formed after the loss of H_2O , C_6H_5 (phenyl moiety), and two carbon atoms from **2c** $[M + H-H_2O]^+$? It is also possible that we are dealing with a very rare example of the attachment of background gases to the product ions, namely O_2 or CO_2 [61,62]. For example, the product ion at m/z 214 may be formed by the O_2 attachment to the product ion at m/z 182 (Fig. S6).

Fig. 10 shows the product ion spectra of ions $[M + H-2H_2O]^+$ for **2d** and **2e**. Both spectra are similar regarding the most abundant product ions, but the differences concern the relative ion abundances. Thus, the ions $[M + H-2H_2O]^+$ for **2d** and **2e**, most probably have the same

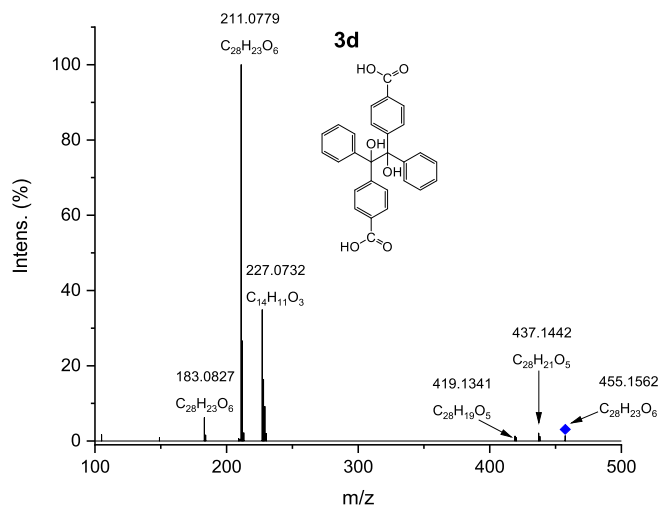
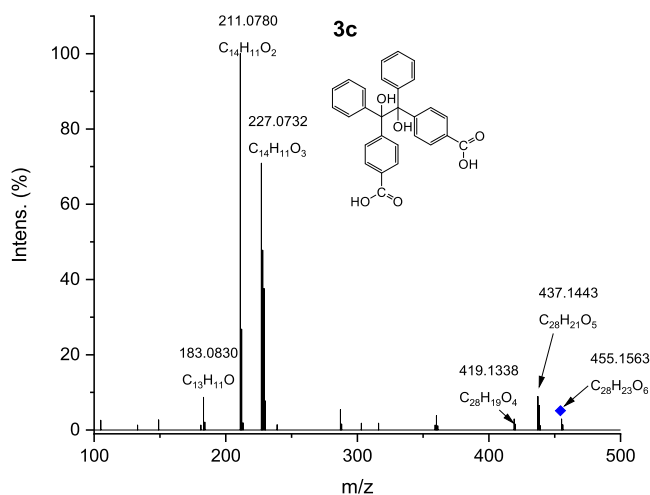


Fig. 13. High-resolution MS/MS spectra of the product ions $[M + H]^+$ of **3c** and **3d** (m/z 455.1563 and 455.1562).

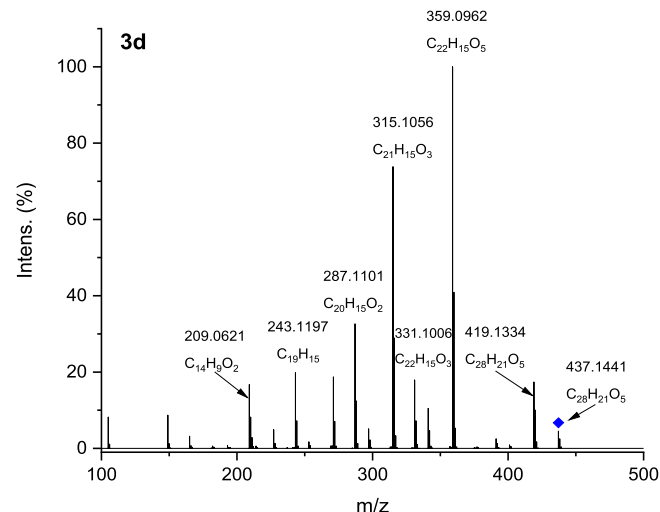
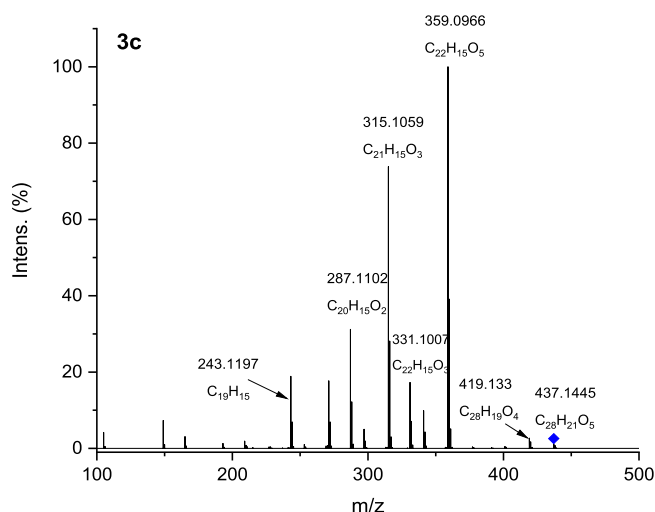


Fig. 14. High-resolution MS/MS spectra of the product ions $[M + H-H_2O]^+$ of **3c** and **3d** (m/z 437.1445 and 437.1441).

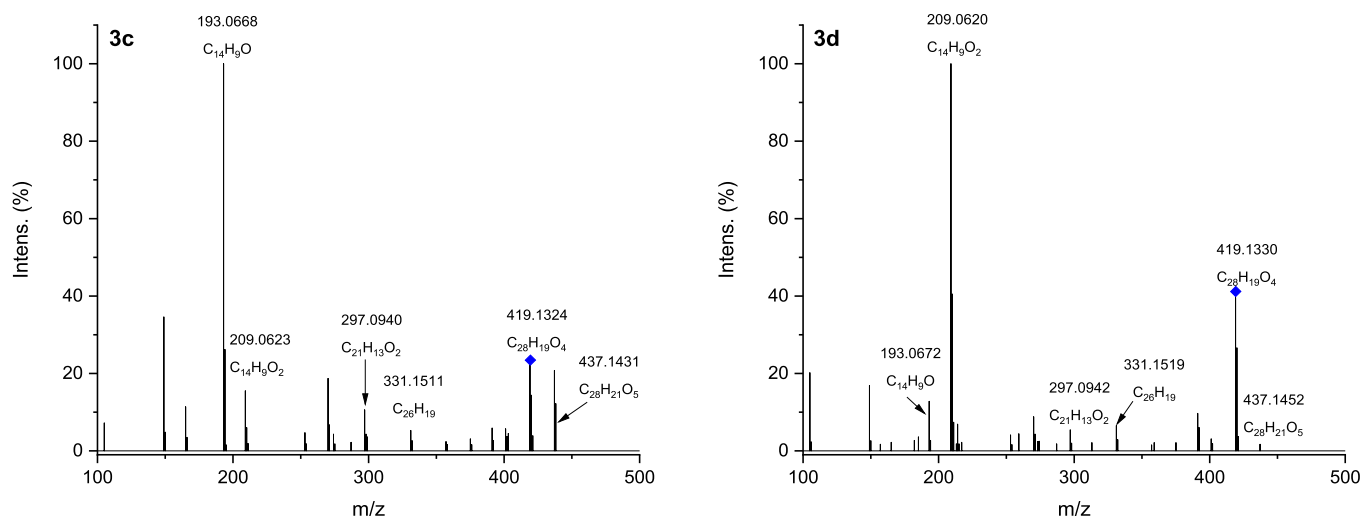


Fig. 15. High-resolution MS/MS spectra of the product ions $[M + H-2H_2O]^+$ of 3c and 3d (m/z 419.1324 and 419.1330).

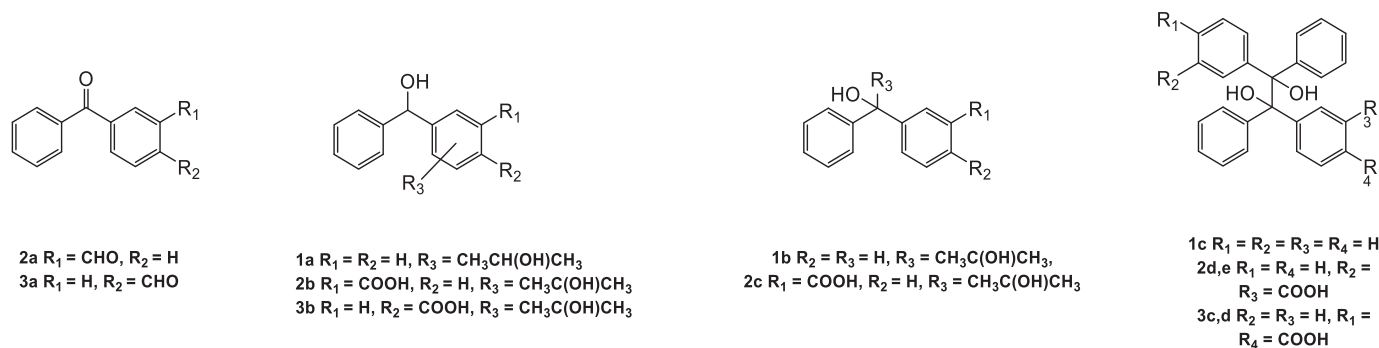


Fig. 16. Structures of main stable products of photoreduction of benzophenone (1a, 1b, 1c), 3-carboxybenzophenone (2a, 2b, 2c, 2d, 2e) and 4-carboxybenzophenone (3a, 3b, 3c, 3d).

structures but different internal energy. The observed most abundant product ions are the same as those observed for 2d $[M + H-2H_2O]^+$ (Fig. 9), and it is very difficult to propose even their tentative structures.

3.2.3. 4-carboxybenzophenone (4CB, 3)

The LC-MS chromatogram of the irradiated sample of 3 is shown in Fig. 11. Four photoproducts were detected in the chromatographic analysis: photoproduct 3a (m/z 211.0771, retention time 13 min), photoproduct 3b (m/z 269.1199, retention time 15 min), photoproduct 3c (m/z 455.1563, retention time 26 min) and photoproduct 3d (m/z 455.1562, retention time 28 min). High-resolution m/z data can be found in Table 3.

The product 3a with m/z 211 was identified as the aldehyde formed in the reduction carboxylic group of 4-carboxybenzophenone (for MS/MS spectrum see Fig. S8).

Interestingly, only one photoproduct with m/z 269 (3b) was detected after irradiation of 4CB, its fragmentation spectrum is presented in Fig. 12. It is identical to the MS/MS spectrum of 2b (Fig. 6). Thus dimethyl ketyl must be attached to the phenyl ring. We suggest that only one photoproduct with m/z 269 was formed due to a steric effect. The carboxylic group in the para position in 4CB might hinder the radical cross-coupling of the dimethyl ketyl radical and the diphenyl ketyl radical.

Both fragmentation patterns of $[M + H]^+$ of 3c and 3d (Fig. 13) show the same most abundant product ions, but the differences lie in their relative intensities. The product ions observed for the $[M + H]^+$ ions of 3c and 3d are almost identical to those of 2d and 2e (Fig. 8) – the

position of the carboxylic group does not affect the fragmentation pathway.

As shown in Fig. 14, fragmentation patterns of $[M + H-2H_2O]^+$ product ions of 3c and 3d are slightly different. Interestingly, the fragmentation patterns observed for the $[M + H-2H_2O]^+$ product ions of 3c and 3d differ evidently from the ones of 2d and 2e (Fig. 9).

Fig. 15 shows the product ion spectra of $[M + H-2H_2O]^+$ of 3c and 3d: the same fragment ions are present in both spectra but their relative abundances differ noticeably.

4. Conclusions

The stable products formed in the sensitized photoreduction of benzophenone (BP, 1), 3-carboxybenzophenone (3CB, 2), and 4-carboxybenzophenone (4CB, 3) were characterized in detail. The quenching of the triplet state of the sensitizers by 2-propanol yields three main types of photoproducts (their structures are shown in Fig. 16):

- structural isomers of radical cross-coupling products of diphenyl ketyl and dimethyl ketyl radicals: one, in which radical derived from the quencher is attached to the phenyl ring (1a, 2b, 3b) and the other, in which it is attached to the carbon atom (1b, 2c);
- benzpinacol (1c) and diastereoisomers of benzpinacol-like products (2d, 2e, 3c, 3d);
- aldehydes formed as the result of the reduction of the carboxylic group of the sensitizer (2a, 3a).

High-resolution mass spectrometry allowed us to determine the structures of those photoproducts and distinguish between isomers.

A detailed study of sensitized photoreduction of selected benzophenone-based sensitizers described here offers a valuable contribution to the research on the photochemical reactions employing benzophenone, 3-carboxybenzophenone, and 4-carboxybenzophenone as photosensitizers. This study shows the potential for the investigation of the stable products of the free radical reactions of molecules of biological significance. The insight into the role of benzophenone (and particularly its water-soluble derivatives) into the mechanistic pathways of biologically relevant processes is presented.

Author agreement

Hereby, I certify that all authors have seen and approved the final version of the revised manuscript being submitted. I warrant that the article is the authors' original work, hasn't received prior publication and isn't under consideration for publication elsewhere.

Declaration of Competing Interest

The authors declare that they have no known competing financial interests or personal relationships that could have appeared to influence the work reported in this paper.

Acknowledgments

K.G. gratefully acknowledges the ISOF - Istituto per la Sintesi Organica e la Fotoreattività (Italy) staff and personally Dr. Carla Ferreri and Dr. Anna Sansone for the hospitality during her stay in the ISOF. The authors would like to thank Dr. Gordon L. Hug from the Notre Dame Radiation Laboratory (USA) and Prof. Chrystostomos Chatgililoglu from ISOF (Italy) for their valuable comments on the manuscript. This research was funded by the Initiative of Excellence – Research University, project no. 003/13/UAM/0023.

Appendix A. Supplementary data

Supplementary data to this article can be found online at <https://doi.org/10.1016/j.jphotobiol.2022.112536>.

References

- [1] M.C. Cuquerella, V. Lhiaubet-Vallet, J. Cadet, M.A. Miranda, Benzophenone photosensitized DNA damage, *Acc. Chem. Res.* 45 (2012) 1558–1570.
- [2] G. Dorman, G.D. Prestwich, Benzophenone Photophores in biochemistry, *Biochemistry* 33 (1994) 5661–5673.
- [3] S. Canonica, H.U. Laubscher, Inhibitory effect of dissolved organic matter on triplet-induced oxidation of aquatic contaminants, *Photochem. Photobiol. Sci.* 7 (2008) 547–551.
- [4] J. Wenk, U. von Gunten, S. Canonica, Effect of dissolved organic matter on the transformation of contaminants induced by excited triplet states and the hydroxyl radical, *Environ. Sci. Technol.* 45 (2011) 1334–1340.
- [5] S. Net, L. Nieto-Gligorovski, S. Gligorovski, H. Wortham, Heterogeneous ozonation kinetics of 4-phenoxyphenol in the presence of photosensitizer, *Atmos. Chem. Phys.* 10 (2010) 1545–1554.
- [6] S. Net, L. Nieto-Gligorovski, S. Gligorovski, B. Temime-Roussel, S. Barbat, Y. G. Lazarou, H. Wortham, Heterogeneous light-induced ozone processing on the organic coatings in the atmosphere, *Atmos. Environ.* 43 (2009) 1683–1692.
- [7] N.B. Sul'timova, P.P. Levin, O.N. Chaikovskaya, Laser photolysis study of the transient products of 4-carboxybenzophenone-sensitized photolysis of chlorophenoxyacetic acid-based herbicides in aqueous micellar solutions, *High Ener. Chem.* 44 (2010) 393–398.
- [8] Q. Wu, X. Zheng, K. Pei, Phototransformation mechanism of monuron induced by the triplet benzophenone in aqueous solution, *J. Phys. Org. Chem.* 28 (2015) 428–430.
- [9] L. Zhou, M. Sleiman, L. Fine, C. Ferronato, P. de Sainte Claire, E. Vulliet, J.-M. Chovelon, G. Xiu, C. Richard, Contrasting photoreactivity of β 2-adrenoceptor agonists salbutamol and terbutaline in the presence of humic substances, *Chemosphere* 228 (2019) 9–16.
- [10] S. Inbar, H. Linschitz, S.G. Cohen, Quenching and radical formation in the reaction of photoexcited benzophenone with thiols and thio ethers (sulfides). Nanosecond flash studies, *J. Am. Chem. Soc.* 104 (1982) 1679–1682.
- [11] J.B.C. Guttenplan, G. Saul, Quenching and reduction of Photoexcited benzophenone by Thioethers and Mercaptans, *J. Organomet. Chem.* 38 (1973) 2001–2007.
- [12] K. Bobrowski, B. Marciniak, G.L. Hug, A reinvestigation of the mechanism of photoreduction of benzophenones by alkyl sulfides, *J. Photochem. Photobiol. A Chem.* 81 (1994) 159–168.
- [13] S.G. Cohen, S. Ojanpera, Photooxidation of methionine and related compounds, *J. Am. Chem. Soc.* 97 (1975) 5633–5634.
- [14] K. Bobrowski, B. Marciniak, G.L. Hug, 4-Carboxybenzophenone-sensitized photooxidation of sulfur-containing amino acids. Nanosecond laser flash photolysis and pulse radiolysis studies, *J. Am. Chem. Soc.* 114 (1992) 10279–10288.
- [15] B. Marciniak, K. Bobrowski, G.L. Hug, Quenching of triplet states of aromatic ketones by sulfur-containing amino acids in solution. Evidence for electron transfer, *J. Phys. Chem.* 97 (1993) 11937–11943.
- [16] K. Bobrowski, G.L. Hug, B. Marciniak, H. Kozubek, The 4-carboxybenzophenone-sensitized photooxidation of sulfur-containing amino acids in alkaline aqueous solutions. Secondary photoreactions kinetics, *J. Phys. Chem.* 98 (1994) 537–544.
- [17] B. Marciniak, G.L. Hug, K. Bobrowski, H. Kozubek, Mechanism of 4-carboxybenzophenone-sensitized photooxidation of methionine-containing dipeptides and tripeptides in aqueous solution, *J. Phys. Chem.* 99 (1995) 13560–13568.
- [18] G.L. Hug, B. Marciniak, K. Bobrowski, Sensitized photo-oxidation of sulfur-containing amino acids and peptides in aqueous solution, *J. Photochem. Photobiol. A Chem.* 95 (1996) 81–88.
- [19] G.L. Hug, K. Bobrowski, H. Kozubek, B. Marciniak, Photooxidation of Methionine Derivatives by the 4-Carboxybenzophenone Triplet State in Aqueous Solution. Intracomplex Proton Transfer Involving the Amino Group, *Photochem. Photobiol.* 68 (1998) 785–796.
- [20] K. Bobrowski, C. Houée-Levin, B. Marciniak, Stabilization and reactions of sulfur radical cations: relevance to one-Electron oxidation of methionine in peptides and proteins, *CHIMIA Internat. J. Chem.* 62 (2008) 728–734.
- [21] M.T. Ignasiak, T. Pedzinski, F. Rusconi, P. Filipiak, K. Bobrowski, C. Houée-Levin, B. Marciniak, Photosensitized Oxidation of Methionine-Containing Dipeptides. From the transients to the final products, *J. Phys. Chem. B* 118 (2014) 8549–8558.
- [22] T. Pedzinski, K. Bobrowski, B. Marciniak, P. Filipiak, Unexpected reaction pathway of the alpha-Aminoalkyl radical derived from one-Electron oxidation of S-Alkylglutathiones, *Molecules* 25 (2020).
- [23] T. Pedzinski, K. Bobrowski, M. Ignasiak, G. Kciuk, G.L. Hug, A. Lewandowska-Andralojc, B. Marciniak, 3-Carboxybenzophenone (3-CB) as an efficient sensitizer in the photooxidation of methionyl-leucine in aqueous solutions: spectral, kinetic and acid-base properties of 3-CB derived transients, *J. Photochem. Photobiol. A Chem.* 287 (2014) 1–7.
- [24] A. Wojcik, A. Lukaszewicz, O. Brede, B. Marciniak, Competitive photosensitized oxidation of tyrosine and methionine residues in enkephalins and their model peptides, *J. Photochem. Photobiol. A Chem.* 198 (2008) 111–118.
- [25] G.L. Hug, M. Bonifacic, K.-D. Asmus, D.A. Armstrong, Fast Decarboxylation of Aliphatic Amino Acids Induced by 4-Carboxybenzophenone Triplets in Aqueous solutions. A nanosecond laser flash photolysis study, *J. Phys. Chem. B* 104 (2000) 6674–6682.
- [26] B. Marciniak, K. Bobrowski, Photo- and radiation-induced one-Electron oxidation of methionine in various structural environments studied by time-resolved techniques, *Molecules* 27 (2022) 1028.
- [27] B. Marciniak, K. Bobrowski, G.L. Hug, J. Rozwadowski, Photoinduced Electron transfer between sulfur-containing carboxylic acids and the 4-Carboxybenzophenone triplet state in aqueous solution, *J. Phys. Chem.* 98 (1994) 4854–4860.
- [28] J. Wenk, M. Aeschbacher, M. Sander, U.v. Gunten, S. Canonica, Photosensitizing and inhibitory effects of Ozonated dissolved organic matter on triplet-induced contaminant transformation, *Environ. Sci. Technol.* 49 (2015) 8541–8549.
- [29] T. Pedzinski, A. Markiewicz, B. Marciniak, Photosensitized oxidation of methionine derivatives. Laser flash photolysis studies, *Res. Chem. Intermed.* 35 (2009) 497–506.
- [30] T. Pedzinski, K. Grzyb, F. Kaźmierczak, R. Frański, P. Filipiak, B. Marciniak, Early events of photosensitized oxidation of sulfur-containing amino acids studied by laser flash photolysis and mass spectrometry, *J. Phys. Chem. B* 124 (2020) 7564–7573.
- [31] T. Pedzinski, K. Grzyb, K. Skotnicki, P. Filipiak, K. Bobrowski, C. Chatgililoglu, B. Marciniak, Radiation- and photo-induced oxidation pathways of methionine in model peptide backbone under anoxic conditions, *Int. J. Mol. Sci.* 22 (2021).
- [32] G. Ciamician, P. Silber, Chemische Lichtwirkungen, *Ber. Dtsch. Chem. Ges.* 33 (1900) 2911–2913.
- [33] J.N. Pitts, R.L. Letsinger, R.P. Taylor, J.M. Patterson, G. Recktenwald, R.B. Martin, Photochemical reactions of benzophenone in Alcohols, *J. Am. Chem. Soc.* 81 (1959) 1068–1077.
- [34] S.G. Cohen, H.M. Chao, Photoreduction of aromatic ketones by amines. Studies of quantum yields and mechanism, *J. Am. Chem. Soc.* 90 (1968) 165–173.
- [35] S.G. Cohen, J.I. Cohen, Effect of medium on transients and on observed quantum yields in Photoreduction of benzophenone by 2-propanol, *Israel J. Chem.* 6 (1968) 757–767.
- [36] S.G. Cohen, J.I. Cohen, Effects of solvent on transients and on quantum yields in photoreduction of ketones, *Tetrahedron Lett.* 9 (1968) 4823–4826.
- [37] N. Filipescu, F.L. Minn, Photoreduction of benzophenone in isopropyl alcohol, *J. Am. Chem. Soc.* 90 (1968) 1544–1547.
- [38] J. Chilton, L. Giering, C. Steel, The effect of transient photoproducts in benzophenone-hydrogen donor systems, *J. Am. Chem. Soc.* 98 (1976) 1865–1870.
- [39] P. Colman, A. Dunne, M.F. Quinn, Flash photolysis studies of benzophenone in ethanol, *J. Chem. Soc. Faraday Trans. 1: Phys. Chem. Condensed Phases* 72 (1976) 2605–2609.

- [40] M.B. Rubin, New observations on the photopinacolization of benzophenone in aliphatic alcohols, *Tetrahedron Lett.* 23 (1982) 4615–4618.
- [41] J.C.A. Scaiano, E. B., L.C. Stewart, Photochemistry of benzophenone in micelles. Formation and decay of radical pairs, *J. Am. Chem. Soc.* 104 (1982) 5673–5679.
- [42] A. Demeter, T. Bérces, Study of the long-lived intermediate formed in the photoreduction of benzophenone by isopropyl alcohol, *J. Photochem. Photobiol. A Chem.* 46 (1989) 27–40.
- [43] A.D. Scully, M.A. Horsham, P. Aguas, J.K.G. Murphy, Transient products in the photoreduction of benzophenone derivatives in poly(ethylene-vinyl alcohol) film, *J. Photochem. Photobiol. A Chem.* 197 (2008) 132–140.
- [44] A. Demeter, B. László, T. Bérces, Kinetics of Ketyl radical reactions occurring in the Photoreduction of benzophenone by isopropyl alcohol, *Berichte der Bunsengesellschaft für physikalische Chemie* 92 (1988) 1478–1485.
- [45] C. Viltres Costa, M.A. Grela, M.S. Churio, On the yield of intermediates formed in the photoreduction of benzophenone, *J. Photochem. Photobiol. A Chem.* 99 (1996) 51–56.
- [46] C. Walling, M.J. Gibian, Hydrogen abstraction reactions by the triplet states of Ketones, *J. Am. Chem. Soc.* 87 (1965) 3361–3364.
- [47] S.L. Murov, I. Carmichael, G.L. Hug, *Handbook of Photochemistry*, CRC Press, 1993.
- [48] K. Bobrowski, B. Marciniak, The kinetics of the acid-base equilibrium of 4-carboxybenzophenone ketyl radical. A pulse radiolysis study, *Radiat. Phys. Chem. - Radiat Phys Chem* 43 (1994) 361–364.
- [49] S. Inbar, H. Linschitz, S.G. Cohen, Quenching, radical formation, and disproportionation in the photoreduction of 4-carboxybenzophenone by 4-carboxybenzhydrol, hydrazine, and hydrazinium ion, *J. Am. Chem. Soc.* 103 (1981) 7323–7328.
- [50] R.V. Bensasson, J.-C. Gramain, Benzophenone triplet properties in acetonitrile and water. Reduction by lactams, *J. Chem. Soc., Faraday Trans. 1: Physical Chem. Condensed Phases* 76 (1980) 1801–1810.
- [51] S. Xu, J. Pavlov, A.B. Attygalle, Collision-induced dissociation processes of protonated benzoic acid and related compounds: competitive generation of protonated carbon dioxide or protonated benzene, *J. Mass Spectrom.* 52 (2017) 230–238.
- [52] R. Frański, M. Zalas, B. Gierczyk, G. Schroeder, Electro-oxidation of diclofenac in methanol as studied by high-performance liquid chromatography/electrospray ionization mass spectrometry, *Rapid Commun. Mass Spectrom.* 30 (2016) 1662–1666.
- [53] B. Balta, V. Aviyyente, C. Lifshitz, Elimination of water from the carboxyl group of GlyGlyH⁺, *J. Am. Soc. Mass Spectrom.* 14 (2003) 1192–1203.
- [54] P.A. D'Agostino, L.R. Provost, J.R. Hancock, Analysis of mustard hydrolysis products by packed capillary liquid chromatography–electrospray mass spectrometry, *J. Chromatogr. A* 808 (1998) 177–184.
- [55] L.A.L. da Silva, L.P. Sandjo, A. Misturini, G.F. Caramori, M.W. Biavatti, ESI-QToF-MS characterization of hirsutinolide and glaucolide sesquiterpene lactones: fragmentation mechanisms and differentiation based on Na⁺/H⁺ adducts interactions in complex mixture, *J. Mass Spectrom.* 54 (2019) 915–932.
- [56] Y.-C. Ma, H.-Y. Kim, Determination of steroids by liquid chromatography/mass spectrometry, *J. Am. Soc. Mass Spectrom.* 8 (1997) 1010–1020.
- [57] M. Holčapek, R. Jirásko, M. Lísa, Basic rules for the interpretation of atmospheric pressure ionization mass spectra of small molecules, *J. Chromatogr. A* 1217 (2010) 3908–3921.
- [58] Y. Cai, Z. Mo, N.S. Rannulu, B. Guan, S. Kannupal, B.C. Gibb, R.B. Cole, Characterization of an exception to the ‘even-electron rule’ upon low-energy collision induced decomposition in negative ion electrospray tandem mass spectrometry, *J. Mass Spectrom.* 45 (2010) 235–240.
- [59] R. Frański, B. Gierczyk, T. Kozik, Ł. Popenda, M. Beszterda, Signals of diagnostic ions in the product ion spectra of [M – H] – ions of methoxylated flavonoids, *Rapid Commun. Mass Spectrom.* 33 (2019) 125–132.
- [60] M. Karni, A. Mandelbaum, The ‘even-electron rule’, *Org. Mass Spectrom.* 15 (1980) 53–64.
- [61] Y. Chai, H. Chen, C. Lu, An intriguing “reversible reaction” in the fragmentation of deprotonated dicamba and benzoic acid in a Q-orbitrap mass spectrometer: loss and addition of carbon dioxide, *Rapid Commun. Mass Spectrom.* 34 (2020), e8893.
- [62] Y. Chai, L. Wang, C. Lu, Formation of molecular oxygen- and water-attached fragment ions in the fragmentation of protonated 3-(phenylthio)chromones, *Rapid Commun. Mass Spectrom.* 34 (2020), e8567.

Supporting Information

Sensitized photoreduction of selected benzophenones. Mass spectrometry studies of radical cross-coupling reactions

¹ Katarzyna Grzyb, ¹ Rafał Frański, ^{1,2} Tomasz Pedzinski*

¹ *Faculty of Chemistry, Adam Mickiewicz University, Uniwersytetu Poznańskiego 8, 61-614*

Poznań, Poland

² *Center for Advanced Technology, Adam Mickiewicz University, Uniwersytetu Poznańskiego*

10, 61-614 Poznań, Poland

** corresponding author: tomekp@amu.edu.pl*

Content:

Figure S1	S2
Figure S2	S2
Figure S3	S3
Figure S4	S3
Figure S5	S4
Figure S6	S4
Figure S7	S4
Figure S8	S5
Table 1	S5

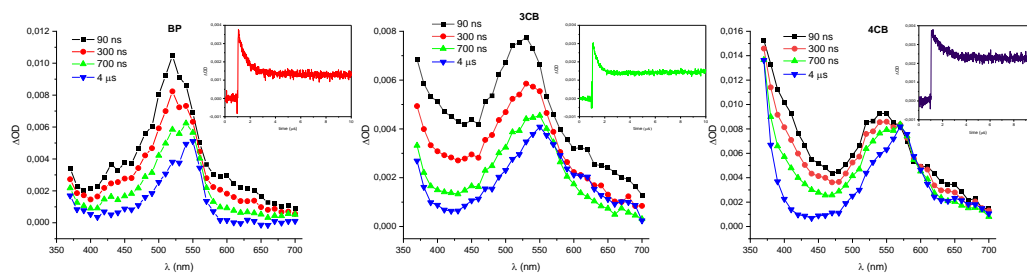


Figure S1. Transient absorption spectra of BP, 3CB and 4CB samples containing 2-propanol recorded after 355 nm laser pulse at 90, 300, 700 ns and 4 μ s delays; insets: kinetics of decays of excited triplet state of each sensitizer, recorded at 530 nm for BP, 520 nm for 3CB and 540 nm for 4CB.

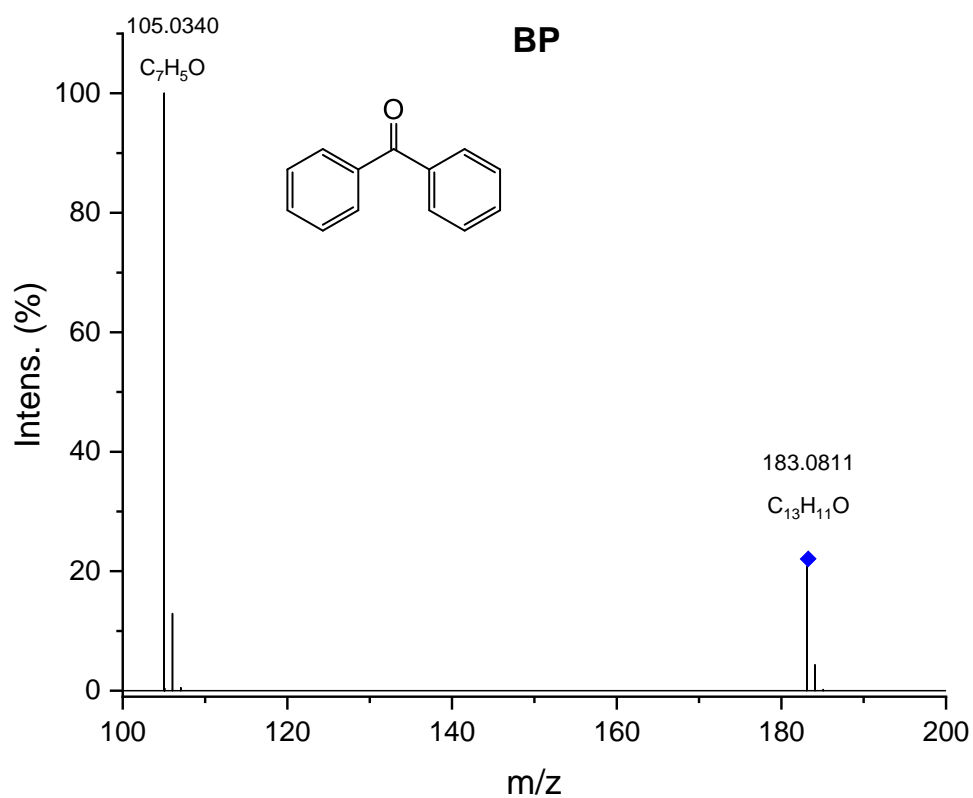


Figure S2. High-resolution MS/MS spectrum of the product ion $[M+H]^+$ of (BP, **1**) (m/z 183.0811)

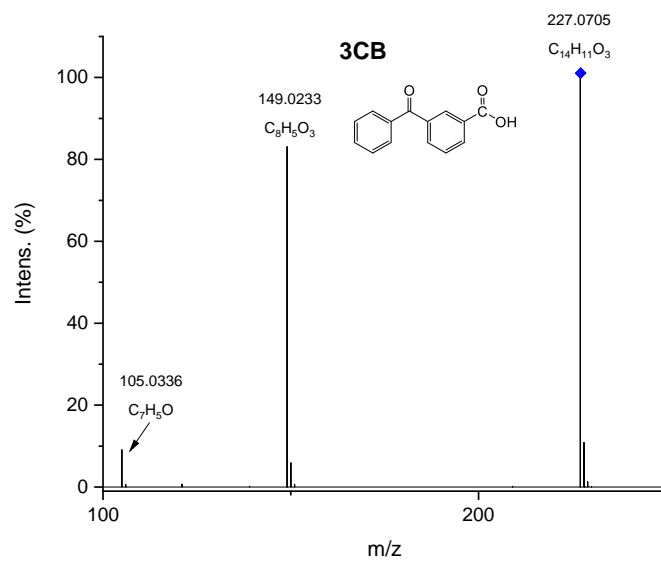


Figure S3. High-resolution MS/MS spectrum of the product ion $[M+H]^+$ of 3-carboxybenzophenone (3CB, **2**) (m/z 227.0705)

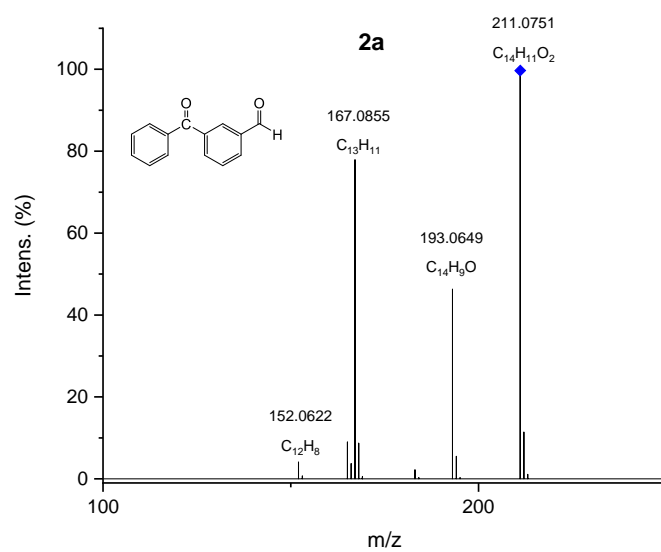


Figure S4. High-resolution MS/MS spectrum of the product ion $[M+H]^+$ of photoproduct **2a** (m/z 211.0751)

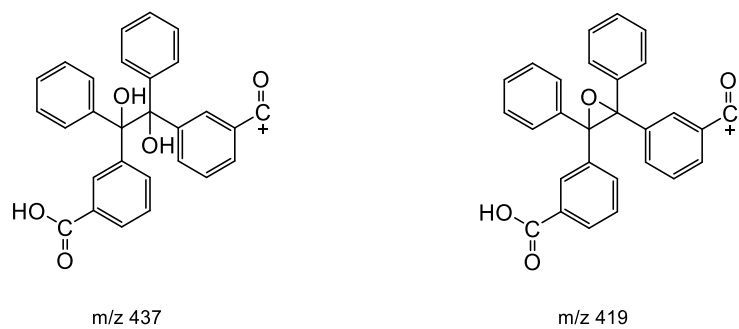


Figure S5. Plausible structures of the product ions at m/z 437 and 419.

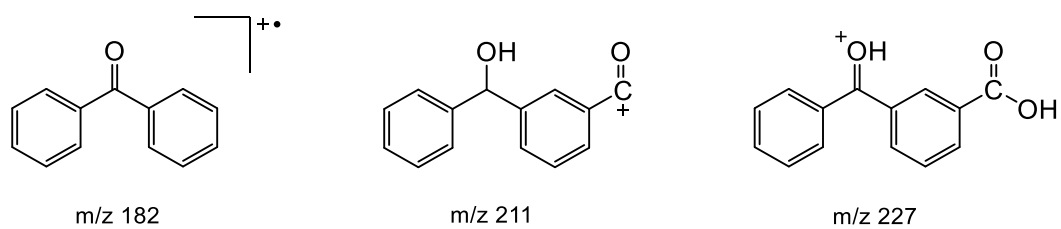


Figure S6. Plausible structures of the product ions at m/z 182, 211, and 227 (from MSMS fragmentations of **2d** and **2e**)

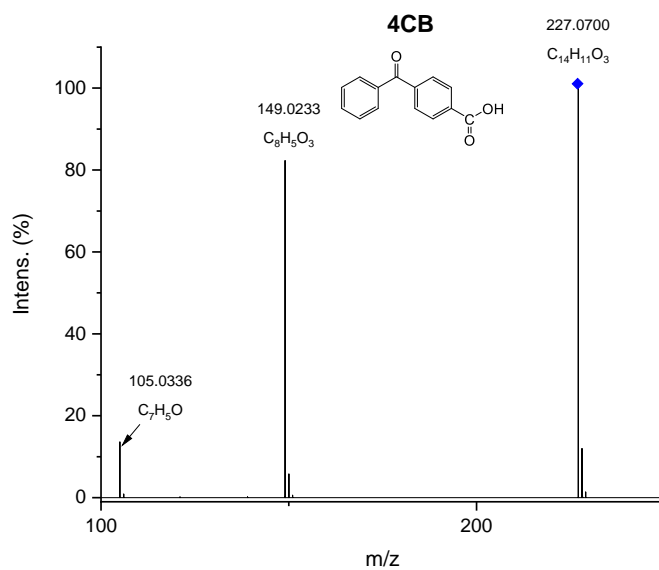


Figure S7. High-resolution MS/MS spectrum of the product ion $[\text{M}+\text{H}]^+$ of 4-carboxybenzophenone (4CB, **3**) (m/z 227.0700)

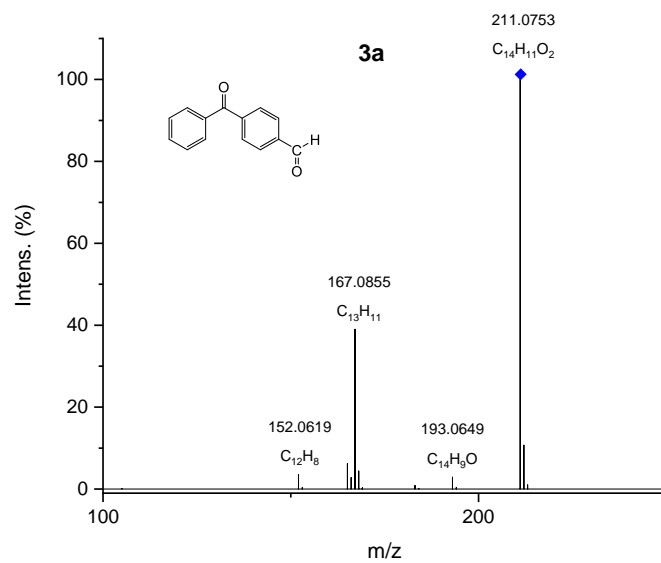


Figure S8. High-resolution MS/MS spectrum of the product ion $[M+H]^+$ of photoproduct **3a** (m/z 211.0753)

Table 1 Quantum Yields of Substrate Disappearance from 355 nm Laser Irradiations^a

	BP	3CB	4CB
Φ	0.26	0.34	0.24

^a± 20% experimental error

Early Events of Photosensitized Oxidation of Sulfur-Containing Amino Acids Studied by Laser Flash Photolysis and Mass Spectrometry

Tomasz Pedzinski, Katarzyna Grzyb, Franciszek Kaźmierczak, Rafał Frański, Piotr Filipiak, and Bronisław Marciniak*

Cite This: *J. Phys. Chem. B* 2020, 124, 7564–7573

Read Online

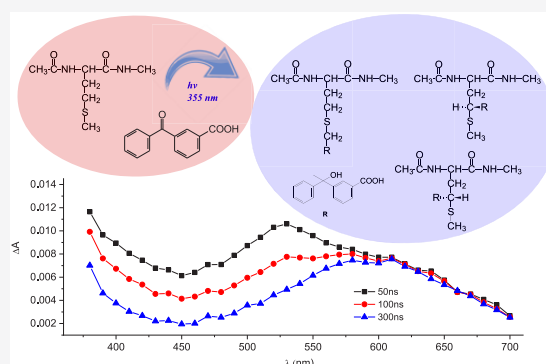
ACCESS |

Metrics & More

Article Recommendations

Supporting Information

ABSTRACT: The mechanism of photooxidation of methionine (N-Ac-Met-NH-CH₃, **1**) and methyl-cysteine (N-Ac-MeCys-NH-CH₃, **2**) analogues by 3-carboxybenzophenone triplet (3CB*) in neutral aqueous solution was studied using techniques of nanosecond laser flash photolysis and steady-state photolysis. The short-lived transients derived from 3CB and sulfur-containing amino acids were identified, and their quantum yields and kinetics of formation and decay were determined. The stable photoproducts were analyzed using liquid chromatography coupled with high-resolution mass spectrometry. Substantial differences in the mechanisms were found for methionine and S-methyl-cysteine analogues for both primary and secondary photoreactions. A new secondary reaction channel (back hydrogen atom transfer from the ketyl radical to the carbon-centered α -thioalkyl radical yielding reactants in the ground states) was suggested. The detailed mechanisms of 3CB* sensitized photooxidation of **1** and **2** are proposed and discussed.



INTRODUCTION

The mechanisms of photosensitized and radiation-induced oxidation of amino acids and peptides have been investigated mainly due to the biological significance of such processes.^{1–8} One of the sites primarily attacked by oxidative agents such as short-lived excited states, free radicals, or reactive oxygen species is the thioether moiety of methionine (Met) residues. Met oxidation can cause serious consequences during oxidative stress;¹ however, despite the numerous studies focused on the one-electron oxidation processes of the methionine residue, some aspects of the process still remain unclear or controversial (e.g., the fate of free radicals leading to stable modifications of the amino acids^{9,10}). One-electron oxidation of Met-containing peptides and proteins in solution occurs easily, e.g., by using strongly oxidizing hydroxyl radicals (\bullet OH) from water radiolysis or through photosensitization using carboxybenzophenone (CB) excited triplets as electron acceptors.^{3,6,11} The transients formed in the oxidation of Met-containing peptides by various one-electron oxidants have been well-characterized.^{3,6,11–15} The initially formed sulfur radical cation can interact with electron-rich atoms (O, N, or S), yielding two-centered three-electron bonds. It can also irreversibly deprotonate, yielding a carbon-centered, α -(alkylthio)alkylmet-containing radical (α S) as presented in Scheme 1.

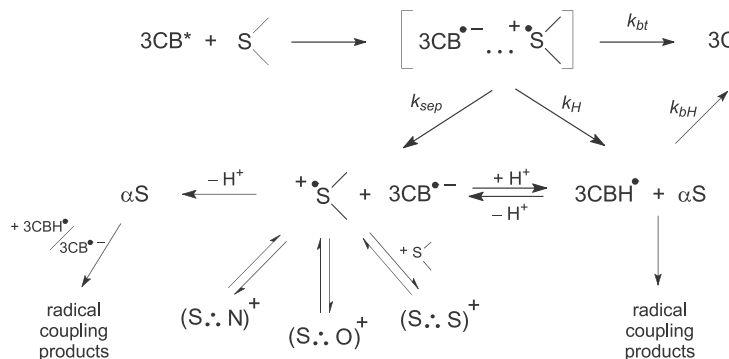
Similar to the Met-containing peptides, the mechanisms of photoinduced and radiation-induced oxidation of peptides

containing S-alkyl-cysteine residues (i.e., S-alkylglutathiones) were also studied due to their significant biological role in living organisms (e.g., see refs 14 and 26). Despite many reports devoted to the detailed mechanisms of radical reactions and their transformations in the sensitized photooxidation of Met- and S-Me-Cys peptides, some doubts remain as to their final fates (i.e., the stable oxidation products). Surprisingly, there are only a few reports that combine complementary time-resolved and steady-state techniques in the photoinduced and radiation-induced oxidation of Met-containing peptides.^{9,10,16} It is, therefore, rational to use relatively simple model structures, such as the compounds investigated in this paper (see Figure 1), to carry out these complementary time-resolved laser flash photolysis and stationary photochemical irradiations experiments.

In this work, we investigated the mechanism of one-electron, photosensitized oxidation of two synthetic amino acids containing a thioether moiety N-Ac-Met-NH-CH₃, **1**, and N-Ac-MeCys-NH-CH₃, **2** (see Figure 1 for structures) in aqueous

Received: July 1, 2020
Revised: August 6, 2020
Published: August 6, 2020



Scheme 1. General Scheme for 3CB Triplet Photosensitized Oxidation of S-Containing Compounds^a

^a3CB denotes 3-carboxybenzophenone; 3CBH•, ketyl radical; 3CB*•-, radical anion; S<, sulfur-containing compound; αS, carbon-centered α-thioalkyl radical; (S...N)⁺, intramolecular two-centered three-electron bonded species; (S...S)⁺, intermolecular two-centered three-electron bonded species; (S...O)⁺, intramolecular two-centered three-electron bonded species.

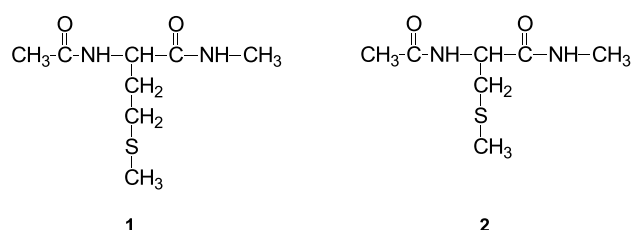


Figure 1. Structures of peptide model compounds used in this work: N-Ac-Met-NH-CH₃ (1) and N-Ac-MeCys-NH-CH₃ (2).

solutions. The compounds studied in this paper are better models for internal Met and S-MeCys residues in peptides and proteins than previously investigated 3-(methylthio)-propylamine (3-MTPA) and *N*-acetyl-3-(methylthio)-propylamine (3-AcMTPA)^{17,18} since they possess the peptide-like bonds on both C and N terminals, ruling out the possibility for decarboxylation and the possibility of proton transfer from the protonated N-terminal group.^{4,18,19} Both short-lived transients and the stable products from photosensitized irradiations of aqueous solutions of the studied compounds were identified in the current work showing significant differences between Met and S-MeCys analogues. Time-resolved and steady-state experimental approaches allowed us, based on the model compounds, to suggest the mechanism of one-electron oxidation which is important for unraveling the redox chemistry in sulfur-containing amino acids, peptides, and proteins.

EXPERIMENTAL SECTION

The synthetic procedure, as well as spectral characterization, of S-MeCys and Met-analogues is described in the [Supporting Information](#).

3-Carboxybenzophenone (3CB) was obtained commercially from Sigma-Aldrich as the best available grade and was used as received. The deionized water for the experiments was purified using a commercial system from Millipore, model Simplicity (Billerica, MA, USA).

The laser flash photolysis (LFP) setup used in this work has been described in detail elsewhere.¹³ Samples for LFP experiments were excited using 355 nm, the third harmonic of a Nd:YAG laser (Spectra Physics Mountain View, CA, USA, model INDI 40-10) with pulses of 6–8 ns duration. The monitoring system consisted of a 150 W pulsed Xe lamp with a

lamp pulser (Applied Photophysics, Surrey, U.K.), a monochromator (Princeton Instruments, model Spectra Pro SP-2357, Acton, MA, USA), and a R955 model photomultiplier (Hamamatsu, Japan), powered by a PS-310 power supply (Stanford Research System, Sunnyvale, CA, USA). The data processing system consisted of real time acquisition using a digital oscilloscope (WaveRunner 6100A, LeCroy, Chestnut Ridge, NY, USA) which was triggered by a fast photodiode (Thorlabs, DET10M, ~1 ns rise time). The data from the oscilloscope were transferred to a computer equipped with software based on LabView 8.0 (National Instruments, Austin, TX, USA) which controls the timing and acquisition functions of the system. Data acquired on the nanosecond laser setup were analyzed using Origin 8.0 fitting functions. For the determination of the quantum yields of the transients, relative actinometry was used according to the procedure described in ref 20, taking 3CB in aqueous solution as the actinometer and $\epsilon_{520} = 5400 \text{ M}^{-1} \text{ cm}^{-1}$ for the T–T absorption of 3CB.¹¹

Steady-state photochemical irradiation experiments were performed in a 1 cm × 1 cm rectangular cell on an optical bench irradiation system using a Genesis CX355 STM OPPL laser (Coherent), with a 355 nm emission wavelength (the output power used was set at 20 mW). Absorption spectra were measured using a Cary 5000 UV/vis spectrophotometer. A benzophenone-benzhydrol actinometer was used for the determination of the quantum yields of amino acid disappearance.²¹ The MS experiments were carried out using a hybrid QTOF instrument (Impact HD, Bruker). Ions were generated by electrospray ionization (ESI). MS/MS fragmentation mass spectra were produced by collisions (CID, collision-induced dissociation) with nitrogen gas in the Q2 section of the spectrometer. The MS instrument was coupled with an HPLC chromatographic system (Ultimate 3000, Thermo/Dionex) equipped with an autosampler, a vacuum degasser, and a diode-array detector. Separation was achieved using a C18 reversed-phase analytical column (2.6 μm, 2.1 mm × 100 mm, Thermo-Scientific) eluted with a gradient from 3% to 60% of acetonitrile and water (with 0.1% formic acid) at a flow rate of 0.3 mL/min for 30 min.

All LFP and stationary irradiation experiments were performed in oxygen-free aqueous solutions at neutral pH.

RESULTS AND DISCUSSION

The general mechanism of primary reactions in the one-electron oxidation of methionine and S-methylcysteine

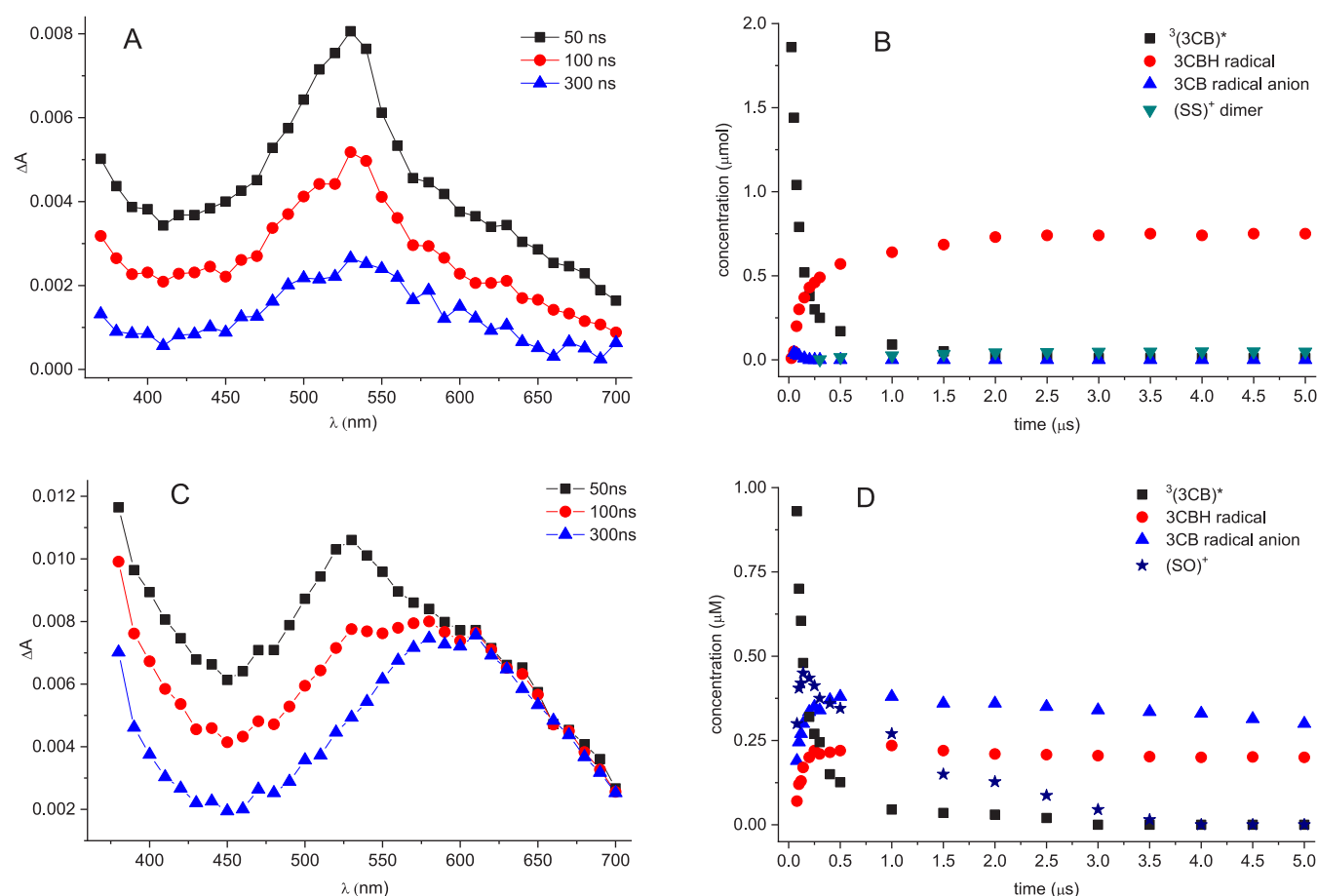


Figure 2. (A) Optical transient absorption spectra of N-Ac-Met-NH-CH₃ (5 mM, pH = 6.8) recorded after the 355 nm laser pulse at 50, 100, and 300 ns delays; (B) concentration profiles calculated at different delay times with respect to the laser pulse for the reaction of 3CB excited triplet quenched by N-Ac-Met-NH-CH₃ (5 mM) in aqueous solution at pH = 6.8; (C) optical transient absorption spectra of N-Ac-Me-Cys-NH-CH₃ (5 mM, pH = 6.8) recorded after the 355 nm laser pulse at 50, 100, and 300 ns delays; (D) Concentration profiles calculated at different delay times with respect to the laser pulse for the reaction of 3CB excited triplet quenched by Ac-MeCys-NH-CH₃ (5 mM) in aqueous solution at pH = 6.8 (see text for details).

Table 1. Quantum Yields of Radical Species Generation from LFP Experiments and Quantum Yields of Amino Acids Disappearance from Stationary Irradiations^a

	$\Phi(3CB^{\bullet-})$	$\Phi(3CBH^{\bullet})$	$\Phi(\text{total})$	$\Phi(S^{\bullet+}O)^+$	Φ_{dis}
N-Ac-Met-NH-CH ₃	≤ 0.02	0.32	0.34	0	0.13
Ac-MeCys-NH-CH ₃	0.34	0.24	0.58	~ 0.40	0.12

^a $\pm 15\%$ experimental error.

analogues seems to be well-known^{3,4} and is presented in Scheme 1. As can be seen in Scheme 1, the free radicals are generated in three primary processes: (i) electron transfer followed by charge separation (k_{sep}) yielding $3CB^{\bullet-}$ radical anions (which are then involved in a water-assisted protonation reaction) and an $>S^{\bullet+}$ radical cation; (ii) electron transfer followed by proton transfer within the encounter complex (k_H) yielding a $3CBH^{\bullet}$ radical and an αS radical; (iii) back electron transfer (k_{bt}) to regenerate the reactants in their ground states. It should be pointed out that the k_{sep} reaction path gives charged species while the k_H reaction path eventually yields neutral free radicals. The k_{bH} reaction of $3CBH^{\bullet}$ with αS radicals leads to the formation of the reactants in their ground states (the exothermicity of this reaction (ΔH) is estimated to be approximately -60 kcal/mol). This value is in a good agreement with the exothermicity of cross-disproportionation of the alkyl radicals leading to double

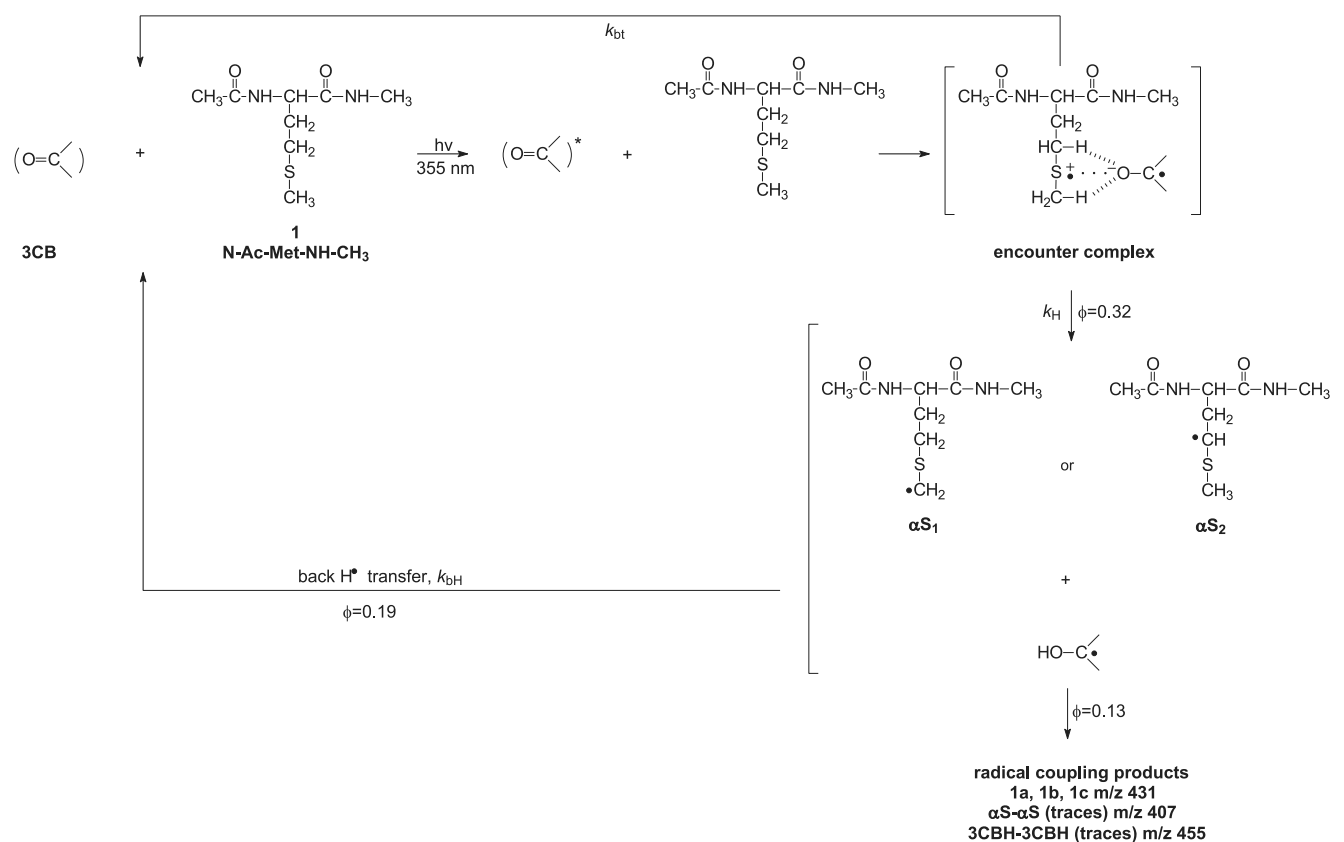
bond formation calculated by Benson²² showing that this process (k_{bH}) remains in competition with radical coupling reaction.

The photosensitized oxidation of sulfur-containing compounds leads to a sulfur-centered radical cation ($>S^{\bullet+}$) as a primary intermediate. This radical cation can be reversibly stabilized by the formation of three-electron bonds with electron-rich nucleophilic centers (S, N, or O atom) or irreversibly deprotonate yielding a relatively stable carbon-centered radical (αS); see Scheme 1.

The spectra obtained from photosensitized oxidation (see Figure 2) of both amino acids were deconvoluted into individual components by using a linear regression technique:

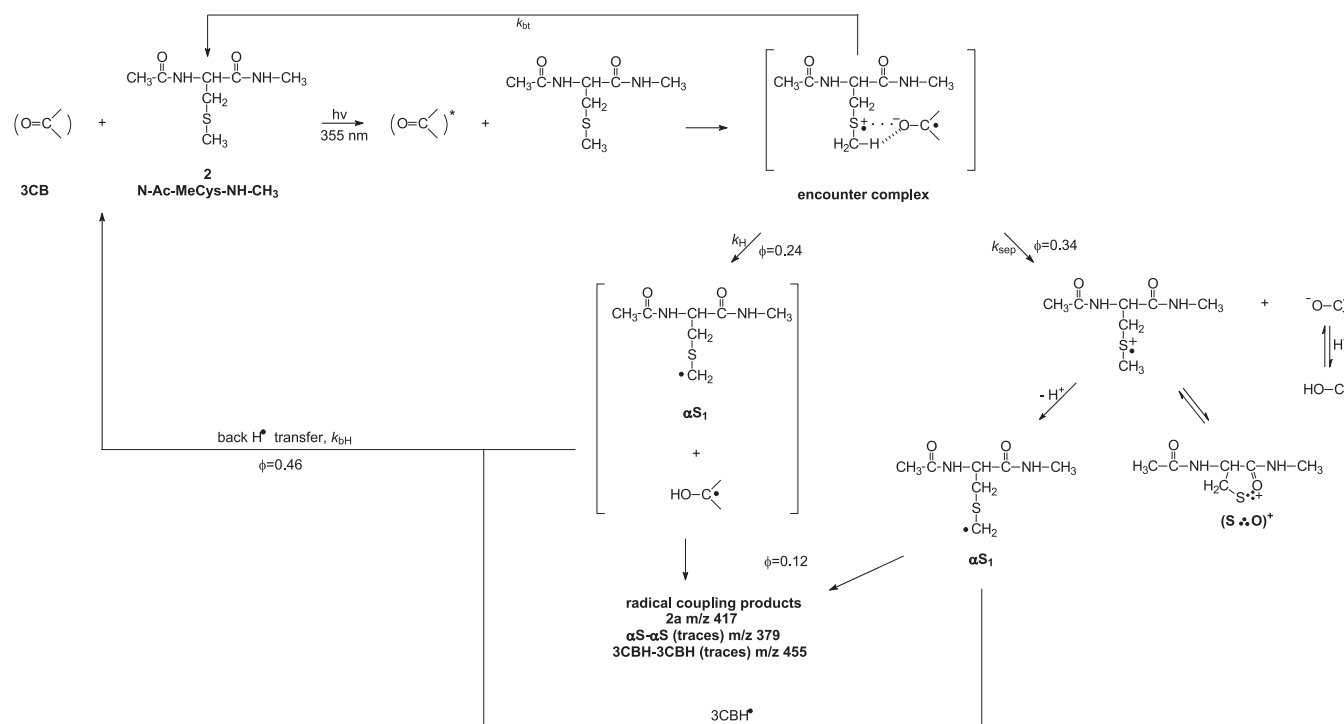
$$\Delta A(\lambda_j) = \sum_n^{i=1} \epsilon_i(\lambda_j) a_i$$

Scheme 2. Mechanism of 3CB* Photosensitized Oxidation of N-Ac-Met-NH-CH₃, Ultimately Leading to Radical-Coupling Reactions between α S and 3CB Ketyl Radicals Yielding Isomeric Photoproducts 1a, 1b, and 1c^a



^aSee Figure 4 for final products structures. Square brackets denote the geminate radical species.

Scheme 3. Mechanism of 3CB* Photosensitized Oxidation of Ac-MeCys-NH-CH₃, Ultimately Leading to Radical-Coupling Reactions between α S and 3CB Ketyl Radicals Yielding Isomeric Photoproduct 2a^a



^aSee Figure 4 for final products structures. Square brackets denote the geminate radical species.

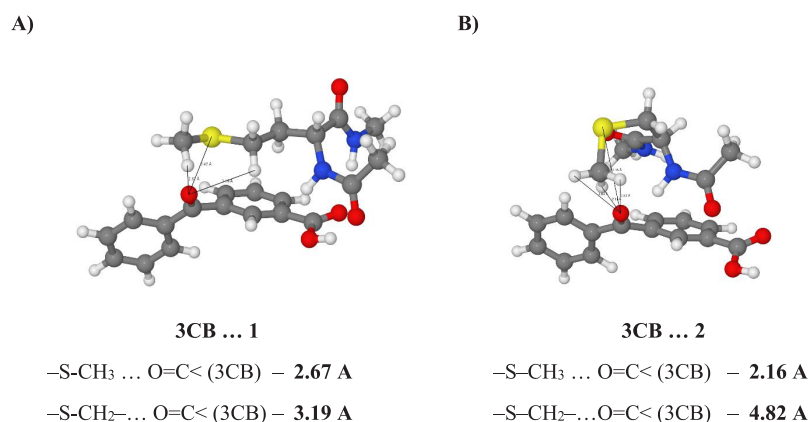


Figure 3. Calculated (DFT) O–H distances for the most stable conformations for encounter complexes, [3CB...⁺S<]: (A) N-Ac-Met-NH-CH₃ (1); (B) Ac-MeCys-NH-CH₃ (2).

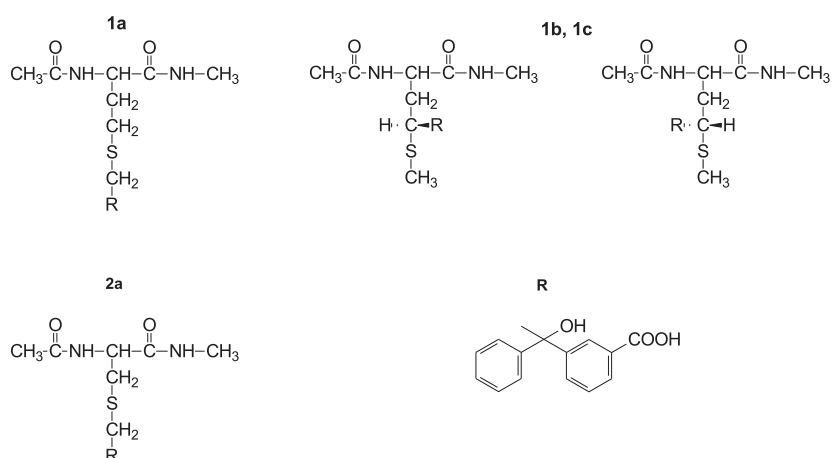


Figure 4. Structures of main stable products of 3CB* photosensitized reaction with N-Ac-Met-NH-CH₃ (products 1a, 1b, 1c) and Ac-MeCys-NH-CH₃ (2a).

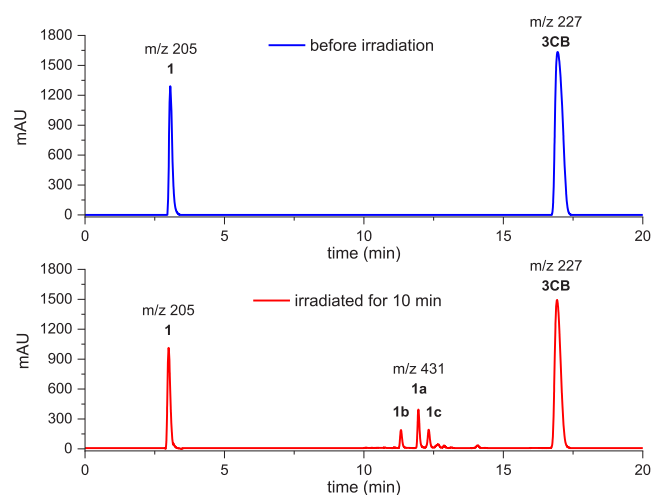


Figure 5. LC–MS chromatogram of 355 nm irradiated (lower panel) and nonirradiated (upper panel) aqueous solution containing 3CB (2 mM) and N-Ac-Met-NH-CH₃ (5 mM) at pH = 6.8. The numbers above the peaks indicate the *m/z* values of the parent MH⁺ ion (for exact masses, refer to the text).

The details of this deconvolution procedure has been described earlier in refs 20 and 23, together with the reference spectra of all of the expected transients. The optical spectra of

both (S:N)⁺ and (S:O)⁺ are very similar and exhibit their absorption maxima around $\lambda_{\max} = 390$ nm.^{14,24–26} Hence, the analysis of the obtained transient absorption spectra for compound 2 was based on the approximation that the transients at $\lambda_{\max} = 390$ nm were attributed to the (S:O)⁺ species (vide infra).

An important observation from the nanosecond laser flash photolysis experiments (see the concentration profiles in Figure 2) is that there was an efficient stabilization of [>]S^{•+} through the formation of two-centered three-electron bonded cyclic intermediates observed for N-Ac-MeCys-NH-CH₃ (compound 2). The most rational explanation for the formation of the 390 nm absorbing transient is that the sulfur-centered radical cation was intramolecularly stabilized by the formation of a three-electron bond with a nitrogen atom (five-membered ring intermediate, (S:N)⁺) or with an oxygen (six- or five-membered ring, (S:O)⁺). This stabilization remains in competition with the deprotonation of the [>]S^{•+}, the primarily formed intermediate, eventually leading to the formation of a much more stable, carbon-centered α -thioalkyl radical (α S). Interestingly, no intermolecular stabilization by the formation of (S:S)⁺ was observed in these studies. This is due to the negligibly small yield of [>]S^{•+} formation for 1 and competing processes of [>]S^{•+} reactions for 2 (see Scheme 3), resulting in relatively low transient concentrations.

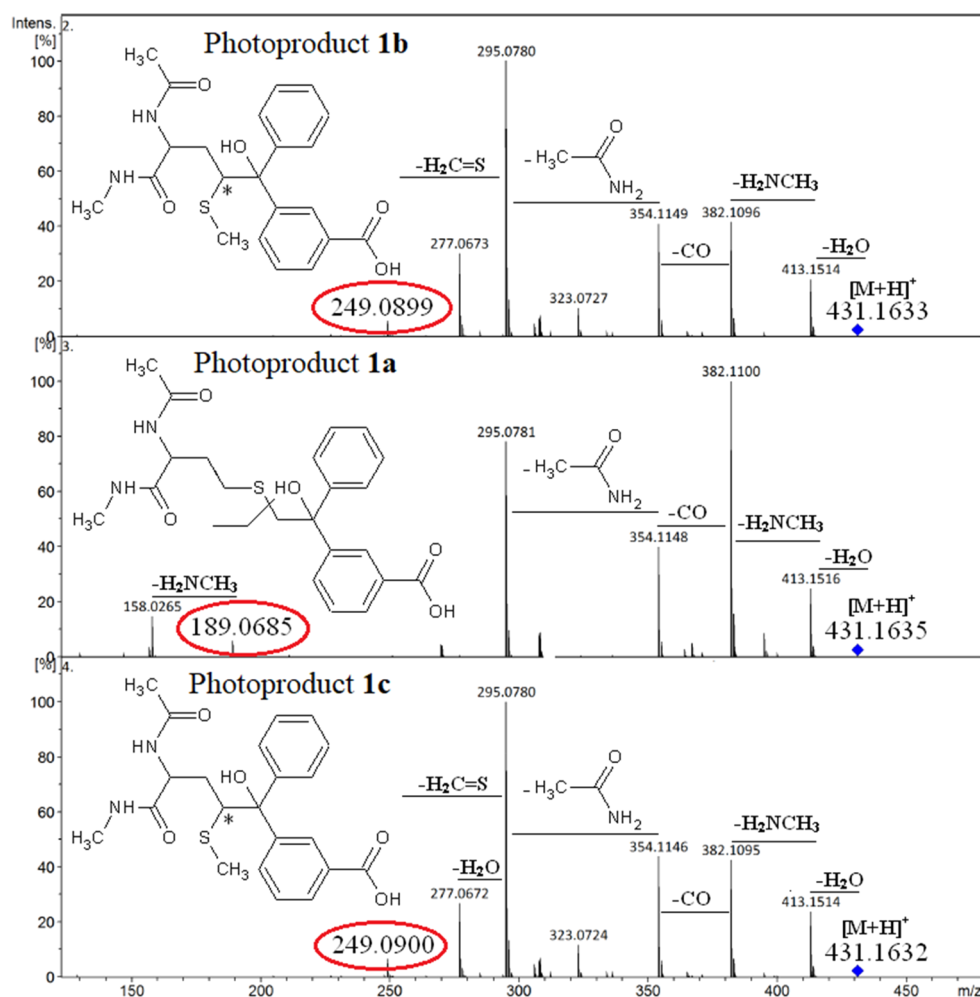


Figure 6. Product ion spectra of $[M + H]^+$ ($m/z = 431$) ions of the photoproduct **1a** (middle) and the diastereomeric photoproducts **1b** and **1c** (top and bottom) of N-Ac-Met-NH-CH₃ oxidation at pH = 6.8. Red circles indicate the diagnostic product ions for each isomer (see Table 2 for details).

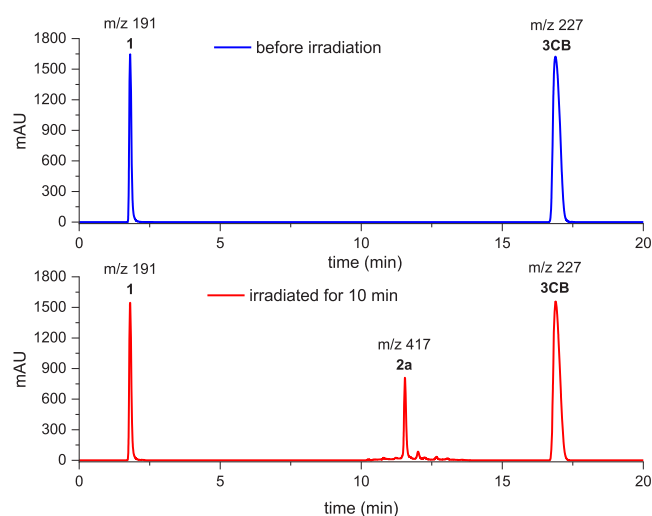


Figure 7. LC–MS chromatogram of 355 nm irradiated (lower panel) and nonirradiated (upper panel) aqueous solution containing 3CB (2 mM) and Ac-MeCys-NH-CH₃ (5 mM) at pH = 6.8. The numbers above the peaks indicate the m/z values of the parent MH^+ ion (for exact masses please refer to the text).

The sulfur-centered radical cation $>S^{\bullet+}$ can be, in fact, a precursor of the $(S:N)^+$ or $(S:O)^+$ intermediate. The formation of six-membered $(S:O)^+$ intermediates was postulated earlier by Schoeneich et al.^{27,28} for radiation-induced oxidation of the methionine amide N-Ac-Met-NH₂, a compound similar in structure to N-Ac-Met-NH-CH₃ studied here. However, as it was shown in this work for compound **1** and in the sensitized photooxidation of N-Ac-Met-OCH₃ by Pedzinski et al.,¹³ the $(S:N)^+$ and $(S:O)^+$ intermediates were not detected in neutral aqueous solutions. However, in the case of Ac-MeCys-NH-CH₃ (compound **2**) the formation of five-membered ring, $(S:O)^+$, intermediates was postulated by the analogy to the transient observed for the oxidation of S-Me-glutathione, analogue of compound **2**.²⁶ Moreover, it is difficult to directly compare the experimental results from LFP (present work) and pulse radiolysis^{27,28} since the initial steps in the mechanism of the photolysis and radiolysis are different (electron transfer quenching vs OH radical addition), and this difference affects the secondary reactions.

The significant difference in the initial reaction paths of compounds **1** and **2** can also be explained by the structure of the encounter complex formed as a result of collisional quenching of 3CB* by **1** or **2**. The transient absorption spectra and the concentration profiles of intermediates obtained from LFP experiments are presented in Figure 2. Although the pH

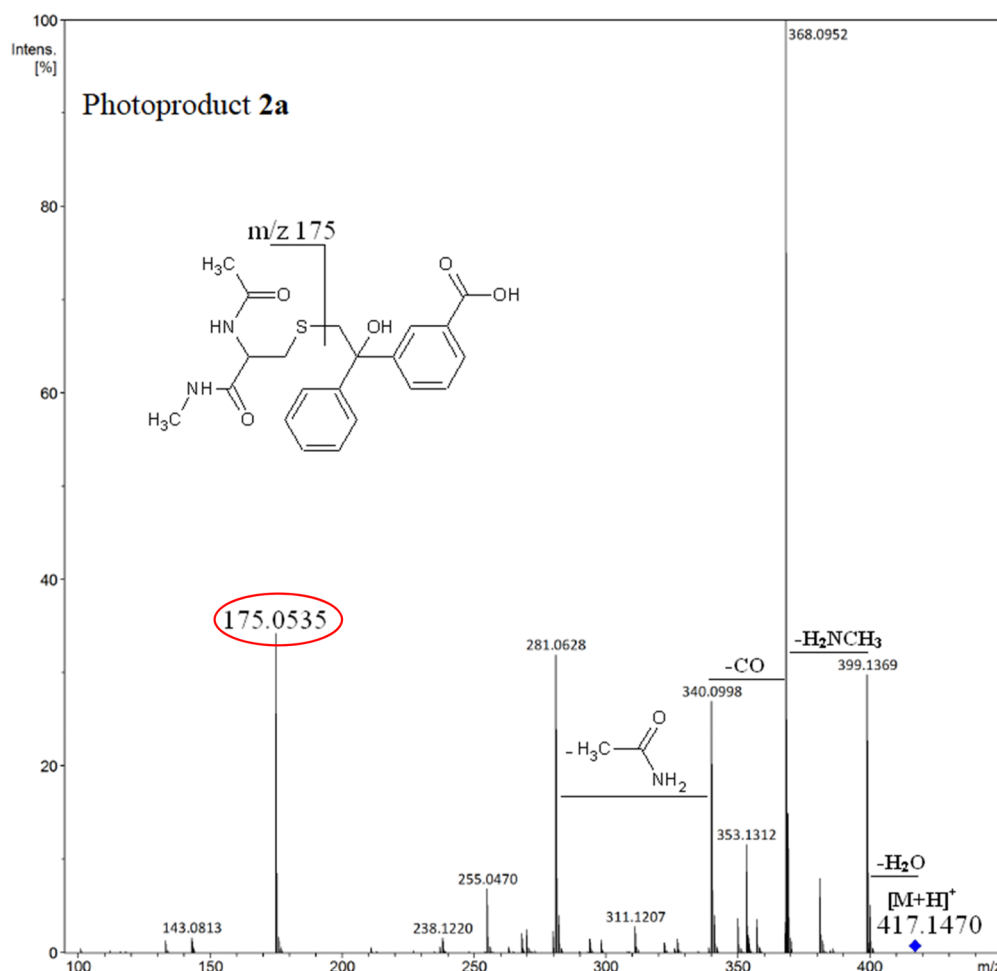


Figure 8. Product ion spectrum of $[M + H]^+$ (m/z 417) ion of photoproduct 2a of Ac-MeCys-NH-CH₃ oxidation at pH = 6.8.

Table 2. Obtained Mass Accuracies (Errors) for Diagnostic Product Ions for Fragmentation of 1 (m/z 431) and 2 (m/z 417)

diagnostic product	measured mass	exact mass	mass accuracy	composition
1a (-CH ₂ R)	189.0685	189.0698	−6.9 ppm	C ₇ H ₁₃ N ₂ O ₂ S
1b	249.0899	249.0916	−6.8 ppm	C ₁₇ H ₁₃ O ₂
1c	249.0900	249.0916	−6.4 ppm	C ₁₇ H ₁₃ O ₂
2a (-CH ₂ R)	175.0535	175.0541	−3.4 ppm	C ₆ H ₁₁ N ₂ O ₂ S

of the experiments is the same (neutral) and is well below the pK_a of 3CBH[•]/3CB^{•−} ($pK_a = 9.5$ ¹¹), there were noticeably more radical anions generated for Ac-MeCys-NH-CH₃ (compound 2) as compared to the methionine analogue (compound 1). The quantum yields for generating the ketyl radicals 3CBH[•] and ketyl radical anions 3CB^{•−} reflecting the efficiencies of the primary photochemical reactions k_{sep} and k_H are summarized in Table 1. The quantitative results in Table 1 remain in excellent agreement with earlier studies on the compounds of similar structure.^{4,7,13}

It can be assumed that at pH = 6.8 the protonation of initially formed 3CB radical anions (primary electron transfer product) will be relatively slow. In the time window of the LFP experiment (up to 5 μ s), the equilibrium between the two forms of the ketyl radical (3CB^{•−} and 3CBH[•]) was still not established. This equilibration occurred on a longer time scale due to the low concentration of protons at neutral pH and a

low value for the water-assisted protonation rate constant (the protonation rate constants by H⁺, $k_{H^+} = 6.4 \times 10^{10} \text{ M}^{-1} \text{ s}^{-1}$, and water, $k_{H_2O} = 5.1 \times 10^2 \text{ M}^{-1} \text{ s}^{-1}$, are known and can be found in ref 11). Moreover, both radicals were involved in reactions with α S (radical-coupling) as shown in the reaction, Scheme 1. In other words, the ketyl radicals decayed due to the coupling reactions as well as due to slow equilibration between 3CB^{•−} and 3CBH[•].

The concentration profiles of transients from LFP experiments (see Figure 2) clearly suggest that since very little 3CB^{•−} was observed for N-Ac-Met-NH-CH₃, the k_H reaction path dominated over k_{sep} for compound 1 (only negligible amounts of charge-separation products were observed). This means that the k_H pathway was the main primary photochemical reaction leading to the disappearance of the Met analogue ($k_H \gg k_{sep}$, see Scheme 2). On the other hand, for Ac-MeCys-NH-CH₃, higher yields of 3CB^{•−} generation in comparison with 3CBH[•] were observed even at neutral pH showing that $k_{sep} > k_H$. A possible explanation of this behavior may be the difference in the primary photochemical reaction reactivity of both compounds (N-Ac-Met-NH-CH₃ (1) and Ac-MeCys-NH-CH₃ (2)) in the initial stages of the process, right after electron transfer in the solvent cage, within the encounter complex (vide infra). This argument is further supported by the observation of an intramolecular three-electron-bonded (S:O)⁺ species for Ac-MeCys-NH-CH₃ (from which charged radical species were produced: 3CB^{•−}

and $>S^{++}$ as presented in Scheme 3). No such stabilization was observed for N-Ac-Met-NH-CH₃, where the radicals observed to be formed from the separating encounter complex were the neutral radicals 3CBH \cdot and αS . This striking difference in reactivity between these two compounds, of such similar structure, can be reasonably explained by structural (steric) factors. One should notice that after electron transfer in the encounter complex, the hydrogen atoms attached to the carbon adjacent to the sulfur atom become acidic and therefore can possibly form hydrogen bonds, e.g., with the neighboring carbonyl oxygen of the sensitizer (as shown in Scheme 3). Due to the steric effect, such bonding would make the proton from the methylene group inaccessible for the k_H path of the reaction for the compound 2, and consequently, no deprotonation at this carbon atom can occur. This steric effect of the sensitizer approaching the reaction center was additionally supported by the DFT calculation (Prof. Jacek Koput, private communication; see Figure 3) describing the structures of encounter complexes $[3CB\cdots^+S<]$ in the most stable conformations for Ac-MeCys-NH-CH₃ (2) and N-Ac-Met-NH-CH₃ (1). The distances between the oxygen atom of 3CB and the hydrogen atoms of the methyl and methylene groups neighboring the sulfur atom of 1 were both small and equal to 2.67 and 3.19 Å, whereas for compound 2 they were 2.16 and 4.82 Å for methyl and methylene groups, respectively.

The results discussed above show that the k_H reaction path in the oxidation of 1 involves proton transfer from both carbon atoms neighboring the sulfur atom, resulting in two αS -type radicals (αS_1 and αS_2 as shown in Scheme 2). The access to this "internal" proton in the encounter complex with Ac-MeCys-NH-CH₃ (see Scheme 3) is sterically more difficult, making the k_{sep} path more efficient in the case of 2 (Ac-MeCys-NH-CH₃). Consequently, only one type of αS radical (localized on the terminal carbon atom and depicted as αS_1) is being formed in this case (see stable product analysis).

The steady-state irradiations of the 3CB-amino acid systems (with 1 or 2) led to the decomposition of the reactants and the generation of various stable products. The quantum yields of disappearance of the amino acids (Φ_{dis}) were found to be 0.13 and 0.12 (± 0.02) for 1 and 2, respectively. These values are significantly smaller than the quantum yields of the radicals obtained from LFP (see Table 1), indicating that only a fraction of the radical-coupling reactions in the radical pairs (as presented in Schemes 2 and 3) is involved in the formation of stable products. The remaining quantities of free radicals undergo back H atom transfer process (k_{bH}). In other words, only the fraction of the free radicals generated (and observed in LFP as shown in Table 1) generates stable products and the remaining radicals undergo the radical disproportionation reaction (k_{bH}) regenerating the initial reactants.

It is noteworthy that small amounts of the sulfoxide ($>S=O$) were detected after steady-state irradiation and LC-MS stable product analysis of 1, while no sulfoxide was formed in the oxidation of 2. Since the solutions were purged with high purity argon prior reaction, $>S=O$ could not be produced in a reaction with molecular oxygen. The mechanism of sulfoxide formation from bimolecular αS radical disproportionation has been proposed earlier,^{9,18} and it involves the γ -carbon-centered radical. This type of radical (αS_2) is present exclusively in the oxidation of 1, while the photosensitized oxidation of compound 2 yields only one type of αS radical (αS_1 , localized on the terminal C atom) and cannot be a precursor for any sulfoxide formation.

As explained above, the photosensitized oxidation reaction led to two major types of relatively stable, carbon-centered radicals: ketyl radicals from 3CB reduction and two types of αS radicals derived from amino-acid oxidation and/or subsequent $>S^{++}$ deprotonation (as presented in Scheme 1). These two radicals (αS and 3CBH \cdot) are known to undergo radical-coupling reactions yielding the adduct-type photoproducts¹⁰ of different structures depending on the exact structure of their precursors. Moreover, once the αS radicals are produced (either from the deprotonation of $>S^{++}$ or from the k_H reaction pathway as described above), the question arises on which of the two carbon atoms is the radical localized? To answer this question, the samples containing 3CB and the quencher were irradiated and subsequently analyzed using HPLC with a standard spectrophotometric detection and coupled with high-resolution MS and MS/MS detection. This stable product analysis is therefore very helpful in collecting information on the nature and structure of the free-radical species taking part in such photooxidation processes. High-resolution MS is a very powerful technique for analysis of the stable photoproducts since, from the measured exact masses (or more precisely m/z values) of the products, one can prove the molecular composition of the products. However, there is no structural information from such experiments. MSMS fragmentation experiment, on the other hand, may provide the structural information on the photoproducts and, after detailed analysis, their precursor radicals.

The αS -type radicals produced in the oxidation of both compounds (αS_1 and αS_2 for 1 and only αS_1 for 2) ultimately led to radical-coupling products with the 3CB ketyl radical (3CBH \cdot) and traces of αS - αS dimeric products (as shown in the Supporting Information). As expected, only one main stable product was detected for 2 with m/z 417, while three isomers (one structural 1a and two optical 1b and 1c) with m/z 431 were observed for 1 (see Figures 4–6).

Stable Product Analysis: N-Ac-Met-NH-CH₃ Oxidation. As can be seen on the chromatograms in Figure 5, three main photoproducts eluted with retention times of approximately 11–12.5 min were detected after 10 min, 355 nm irradiation. All products showed the same molecular composition at m/z 431.1633, suggesting their isomeric nature (photoproducts 1a, 1b, and 1c; see Figure 4 for suggested structures).

The MSMS fragmentation was performed for the $[M + H]^+$ product ion at m/z 431, and as can be seen in Figure 6, the fragmentation revealed significant structural differences between the photoproducts. The main fragmentation pathways of 1a, 1b, and 1c correspond to the decomposition of the methionine moiety. However, the diagnostic product ion at m/z 189 detected for photoproduct 1a clearly indicates that the benzophenone moiety (depicted as R) was attached to the S-methyl group. Furthermore, the diagnostic product ions at m/z 249 detected for diastereomeric photoproducts 1b and 1c indicate that these two compounds possess the -S-CH₃ moiety; thus -R must be attached to the S-methylene group. It is therefore clear, that the photoproducts 1a, 1b, and 1c were generated in a radical-coupling reaction between two types of radical species as described above (αS and the 3CBH \cdot ketyl radical). It is noteworthy that, as expected, traces of αS - αS radical-coupling products (m/z 405) were also detected (see small peaks at retention times 12–14 min in Figure 5), but these photoproducts were not analyzed in this work due to their small yields. Following the same line of reasoning, also

the traces of benzpinacol-like products (3CBH–3CBH) were detected in the LC–MS analysis. The mechanism of 3CB* photosensitized oxidation of N-Ac-Met-NH-CH₃ is summarized in Scheme 2.

Stable Product Analysis: N-Ac-MeCys-NH-CH₃ Oxidation. As presented in Figure 7, only one main photoproduct eluting with a retention time of approximately 11.5 min was detected after irradiation. This photoproduct (2a) shows its MS spectrum with one clear peak at *m/z* 417, and the difference of 14 Da (CH₂ group) suggests that the structure of this product is very similar to the Met analogue discussed above. The MSMS fragmentation (Figure 8) of [M + H]⁺ at *m/z* 417, analogically as for [M + H]⁺ ion of photoproduct 1a, corresponds to the decomposition of the cysteine moiety (loss of neutral molecules of water, methylamine, carbon monoxide, and acetamide). The diagnostic product ion at *m/z* 175, however, clearly indicates that R is attached to the S-methyl group. Therefore, the photoproduct 2a is similar in structure to photoproduct 1a (see Figure 4). As in the case of N-Ac-Met-NH-CH₃ oxidation, traces of αS–αS radical-coupling products (*m/z* 379) and benzpinacol-type products (*m/z* 455) were also detected for Ac-MeCys-NH-CH₃ (Scheme 3).

The exact masses of diagnostic ions from MSMS experiments that allowed us to suggest the structures of photoproducts are collected in Table 2.

On the basis of the data obtained in the flash photolysis and stationary irradiation followed by the LC–MS analysis of the stable photoproducts, the mechanism of 3CB* photosensitized oxidation of Ac-MeCys-NH-CH₃ is presented in Scheme 3.

CONCLUSIONS

The mechanisms for photosensitized oxidation of methionine (N-Ac-Met-NH-CH₃, 1) and methyl-cysteine (Ac-MeCys-NH-CH₃, 2) analogues by 3-carboxybenzophenone excited triplet (3CB*) in neutral aqueous solutions were shown to differ significantly. The differences observed for primary and secondary photoreactions are summarized below.

For primary photochemical reactions (Scheme 1), the following were observed.

- For compound 1 only one primary photoreaction, namely, electron transfer followed by proton transfer within the encounter complex, *k*_H leading to the formation of ketyl radical 3CBH* and α-thioalkyl radical (αS) was observed with the quantum yield Φ(3CBH*) = 0.32.
- For compound 2 both *k*_H and *k*_{sep} (electron transfer followed by charge separation) primary photoreactions were observed with the quantum yields Φ(3CBH*) = 0.24 and Φ(3CB*[−]) = 0.34, respectively.

For secondary reactions leading to stable products (Schemes 2 and 3), the following were observed.

- For compound 1 both αS₁ and αS₂-type radicals were formed as proven by the detection of radical-coupling products with 3CB ketyl radicals (αS₁-3CBH and two diastereoisomers of αS₂-3CBH). This indicates that hydrogen atoms from the methyl and methylene groups attached to the sulfur atom in the amino acid side chain CH₃-S-CH₂- participate in the reaction mechanism,
- For compound 2 only one type of radical-coupling product (αS₁-3CBH) was found and only a hydrogen atom from the methyl group (CH₃-S-) was involved,

- The back H-atom transfer reaction of 3CBH* with αS radicals (*k*_{bH}) leading to regeneration of reactants in the ground states was shown to compete with the radical-coupling reactions.

The differences in the photoreaction mechanisms were rationalized by the differences in geometry of the encounter complexes of 3CB with both amino acids (a steric effect for compound 2).

In summary, it was demonstrated that a small change in the structure of the sulfur-containing amino acid (one methylene group less for S-methyl-cysteine analogue in comparison to methionine) led to significant changes in the mechanisms of the photosensitized oxidation of N-Ac-Met-NH-CH₃ (1) and Ac-MeCys-NH-CH₃ (2) by the 3-carboxybenzophenone excited triplet in neutral aqueous solutions.

ASSOCIATED CONTENT

Supporting Information

The Supporting Information is available free of charge at <https://pubs.acs.org/doi/10.1021/acs.jpcb.0c06008>.

Comment S1 on the synthesis procedure; Figure S1 showing extracted ion chromatogram and MS spectrum of the >S=O photoproduct; Figure S2 showing αS–αS traces (MS spectra) detected for 1 and 2 (PDF)

AUTHOR INFORMATION

Corresponding Author

Bronisław Marciniak – Center for Advanced Technology and Faculty of Chemistry, Adam Mickiewicz University, 61-614 Poznań, Poland; orcid.org/0000-0001-8396-0354; Email: marcinia@amu.edu.pl

Authors

Tomasz Pedzinski – Center for Advanced Technology and Faculty of Chemistry, Adam Mickiewicz University, 61-614 Poznań, Poland; orcid.org/0000-0002-4765-6264

Katarzyna Grzyb – Faculty of Chemistry, Adam Mickiewicz University, 61-614 Poznań, Poland; orcid.org/0000-0002-7035-3456

Franciszek Kaźmierczak – Faculty of Chemistry, Adam Mickiewicz University, 61-614 Poznań, Poland

Rafał Frański – Faculty of Chemistry, Adam Mickiewicz University, 61-614 Poznań, Poland; orcid.org/0000-0002-1080-9968

Piotr Filipiak – Center for Advanced Technology and Faculty of Chemistry, Adam Mickiewicz University, 61-614 Poznań, Poland; orcid.org/0000-0001-9141-2163

Complete contact information is available at: <https://pubs.acs.org/doi/10.1021/acs.jpcb.0c06008>

Author Contributions

Conceptualization was by B.M., T.P., and P.F. Formal analysis was by B.M., T.P., P.F., and R.F. Funding acquisition was by B.M. Synthesis was by F.K. Investigation was by K.G., T.P., and P.F. Methodology was by T.P. and B.M. Validation was by T.P., R.F., and B.M. For writing of the manuscript, the original draft preparation was by K.G. and T.P. and the review and editing were by T.P. and B.M.

Funding

This research was funded by the National Science Centre Poland, Grant UMO-2017/27/B/ST4/00375 (B.M.).

Notes

The authors declare no competing financial interest.

ACKNOWLEDGMENTS

The authors thank Prof. Jacek Koput from the Faculty of Chemistry (AMU, Poznan, Poland) for DFT calculations and Dr. Gordon Hug from the Notre Dame Radiation Laboratory (USA) for valuable comments on the manuscript.

REFERENCES

- (1) Davies, M. J. Oxidative Damage to Proteins. In *Encyclopedia of Radicals in Chemistry, Biology and Materials*; John Wiley & Sons, Ltd., 2012.
- (2) Davies, M. J. The oxidative environment and protein damage. *Biochim. Biophys. Acta, Proteins Proteomics* **2005**, 1703 (2), 93–109.
- (3) Bobrowski, K.; Marciniak, B.; Hug, G. L. 4-Carboxybenzophenone-Sensitized Photooxidation of Sulfur-Containing Amino-Acids - Nanosecond Laser Flash-Photolysis and Pulse-Radiolysis Studies. *J. Am. Chem. Soc.* **1992**, 114 (26), 10279–10288.
- (4) Hug, G. L.; Bobrowski, K.; Kozubek, H.; Marciniak, B. Photooxidation of methionine derivatives by the 4-carboxybenzophenone triplet state in aqueous solution. Intracomplex proton transfer involving the amino group. *Photochem. Photobiol.* **1998**, 68 (6), 785–796.
- (5) Hug, G. L.; Bobrowski, K.; Kozubek, H.; Marciniak, B. Photooxidation of methionine-containing peptides by the 4-carboxybenzophenone triplet state in aqueous solution. Competition between intramolecular two-centered three-electron bonded (SS)+ and (SN)+ formation. *Photochem. Photobiol.* **2000**, 72 (1), 1–9.
- (6) Bobrowski, K.; Houée-Levin, C.; Marciniak, B. Stabilization and Reactions of Sulfur Radical Cations: Relevance to One-Electron Oxidation of Methionine in Peptides and Proteins. *Chimia* **2008**, 62 (9), 728–734.
- (7) Marciniak, B.; Hug, G. L.; Kozubek, H.; Bobrowski, K. Mechanism of 4-carboxybenzophenone-sensitized photooxidation of methionine-containing dipeptides and tripeptides in aqueous solution. *J. Phys. Chem.* **1995**, 99 (36), 13560–13568.
- (8) Hug, G. L.; Marciniak, B.; Bobrowski, K. Sensitized photooxidation of sulfur-containing amino acids and peptides in aqueous solution. *J. Photochem. Photobiol., A* **1996**, 95 (1), 81–88.
- (9) Ignasiak, M.; Scuderi, D.; de Oliveira, P.; Pedzinski, T.; Rayah, Y.; Levin, C. H. Characterization by mass spectrometry and IRMPD spectroscopy of the sulfoxide group in oxidized methionine and related compounds. *Chem. Phys. Lett.* **2011**, 502 (1–3), 29–36.
- (10) Ignasiak, M. T.; Pedzinski, T.; Rusconi, F.; Filipiak, P.; Bobrowski, K.; Houée-Levin, C.; Marciniak, B. Photosensitized Oxidation of Methionine-Containing Dipeptides. From the Transients to the Final Products. *J. Phys. Chem. B* **2014**, 118 (29), 8549–8558.
- (11) Pedzinski, T.; Bobrowski, K.; Ignasiak, M.; Kciuk, G.; Hug, G. L.; Lewandowska-Andralojc, A.; Marciniak, B. 3-Carboxybenzophenone (3-CB) as an efficient sensitizer in the photooxidation of methionyl-leucine in aqueous solutions: Spectral, kinetic and acid-base properties of 3-CB derived transients. *J. Photochem. Photobiol., A* **2014**, 287, 1–7.
- (12) Bobrowski, K.; Hug, G. L.; Pogocki, D.; Marciniak, B.; Schöneich, C. Stabilization of sulfide radical cations through complexation with the peptide bond: Mechanisms relevant to oxidation of proteins containing multiple methionine residues. *J. Phys. Chem. B* **2007**, 111 (32), 9608–9620.
- (13) Pedzinski, T.; Markiewicz, A.; Marciniak, B. Photosensitized oxidation of methionine derivatives. Laser flash photolysis studies. *Res. Chem. Intermed.* **2009**, 35 (4), 497–506.
- (14) Bobrowski, K.; Hug, G. L.; Pogocki, D.; Marciniak, B.; Schöneich, C. Sulfur Radical Cation–Peptide Bond Complex in the One-Electron Oxidation of S-Methylglutathione. *J. Am. Chem. Soc.* **2007**, 129 (29), 9236–9245.
- (15) Goez, M.; Rozwadowski, J.; Marciniak, B. CIDNP Spectroscopic Observation of (S:+N) Radical Cations with a Two-Center Three-Electron Bond During the Photooxidation of Methionine. *Angew. Chem., Int. Ed.* **1998**, 37 (5), 628–630.
- (16) Barata-Vallejo, S.; Ferreri, C.; Zhang, T.; Permentier, H.; Bischoff, R.; Bobrowski, K.; Chatgililoglu, C. Radiation chemical studies of Gly-Met-Gly in aqueous solution. *Free Radical Res.* **2016**, 50 (sup1), S24–S39.
- (17) Tripathi, G. N. R.; Tobien, T. The intramolecular sulfur–nitrogen bond in aqueous 3-(methylthio)propylamine radical cation. *J. Phys. Chem. A* **2001**, 105 (14), 3498–3504.
- (18) Pedzinski, T.; Kazmierczak, F.; Filipiak, P.; Marciniak, B. Oxidation studies of a novel peptide model N-acetyl-3-(methylthio)propylamine. *J. Photochem. Photobiol., A* **2017**, 336, 98–104.
- (19) Hashimoto, M.; Eda, Y.; Osanai, Y.; Iwai, T.; Aoki, S. A novel decarboxylation of alpha-amino acids. A facile method of decarboxylation by the use of 2-cyclohexen-1-one as a catalyst. *Chem. Lett.* **1986**, 15 (6), 893–896.
- (20) Filipiak, P.; Bobrowski, K.; Hug, G. L.; Pogocki, D.; Schöneich, C.; Marciniak, B. New Insights into the Reaction Paths of 4-Carboxybenzophenone Triplet with Oligopeptides Containing N- and C-Terminal Methionine Residues. *J. Phys. Chem. B* **2017**, 121 (20), 5247–5258.
- (21) Murov, S. L.; Carmichael, I.; Hug, G. L. *Handbook of Photochemistry*, 2nd ed.; Taylor & Francis, 1993.
- (22) Benson, S. W. Disproportionation of free radicals. *J. Phys. Chem.* **1985**, 89 (20), 4366–4369.
- (23) Bobrowski, K.; Hug, G. L.; Marciniak, B.; Kozubek, H. 4-Carboxybenzophenone-sensitized photooxidation of sulfur-containing amino acids in alkaline aqueous solutions. Secondary photoreactions kinetics. *J. Phys. Chem.* **1994**, 98 (2), 537–544.
- (24) Asmus, K. D.; Gobl, M.; Hiller, K. O.; Mahling, S.; Monig, J. S-N and S-O 3-Electron-Bonded Radicals and Radical Cations in Aqueous-Solutions. *J. Chem. Soc., Perkin Trans. 2* **1985**, No. 5, 641–646.
- (25) Glass, R. S. *Sulfur-Centered Reactive Intermediates in Chemistry and Biology*; Plenum Press: New York, 1990; Vol. 97, pp 213–226.
- (26) Filipiak, P.; Hug, G. L.; Bobrowski, K.; Pedzinski, T.; Kozubek, H.; Marciniak, B. Sensitized Photooxidation of S-Methylglutathione in Aqueous Solution: Intramolecular (SO) and (SN) Bonded Species. *J. Phys. Chem. B* **2013**, 117 (8), 2359–2368.
- (27) Schöneich, C.; Pogocki, D.; Bobrowski, K.; Hug, G. L. Free Radical Reactions of Methionine in Peptides: Mechanisms Relevant to β -Amyloid Oxidation and Alzheimer's Disease. *J. Am. Chem. Soc.* **2003**, 125 (45), 13700–13713.
- (28) Schöneich, C.; Pogocki, D.; Wisniowski, P.; Hug, G. L.; Bobrowski, K. Intramolecular Sulfur–Oxygen Bond Formation in Radical Cations of N-Acetylmethionine Amide. *J. Am. Chem. Soc.* **2000**, 122 (41), 10224–10225.

Supporting Information for

The Early Events of Photosensitized Oxidation of Sulfur-Containing Amino Acids Studied by Laser Flash Photolysis and Mass Spectrometry

Tomasz Pedzinski^{1,2}, Katarzyna Grzyb², Franciszek Kaźmierczak², Rafał Frański², Piotr

Filipiak^{1,2}, Bronisław Marciniak^{1,2}*

¹Center for Advanced Technology, Adam Mickiewicz University, 10 Uniwersytetu Poznańskiego Str., 61-614 Poznań, Poland

²Faculty of Chemistry, Adam Mickiewicz University, 8 Uniwersytetu Poznańskiego Str., 61-614 Poznań, Poland

Contents:

Comment S1. The synthesis procedure

P.S2

Figure S1. Sulfoxide detected for N-Ac-Met-NH-CH₃ (compound **1**): extracted ion chromatogram (after 10 min irradiation) and MS spectrum of the >S=O photoproduct (m/z for unoxidized compd. **1** is 205.1011). Sulfoxide was not detected for N-Ac-MeCys-NH-CH₃ (compound **2**).

P.S2

Figure S2. alphaS-alphaS traces (MS spectra) detected for **1** and **2**.

P.S3

Comment S1. The synthesis procedure:

The compounds *N*-Ac-Met-NH-CH₃ (**1**) and *N*-Ac-MeCys-NH-CH₃ (**2**) studied in this work were synthesized in the following reaction sequence: both the starting Met and Cys were transformed into the respective methyl esters hydrochlorides first, then the amino groups were acetylated and finally the ester functionality transformed into methylamides.

The desired products of the above reaction sequence were purified by column chromatography using as an eluent a gradient of mixture of methylene chloride-methanol.

The reaction products were characterized by spectral methods and they displayed the expected properties.

1. N-Ac-Met-NH-CH₃ sulfoxide detection:

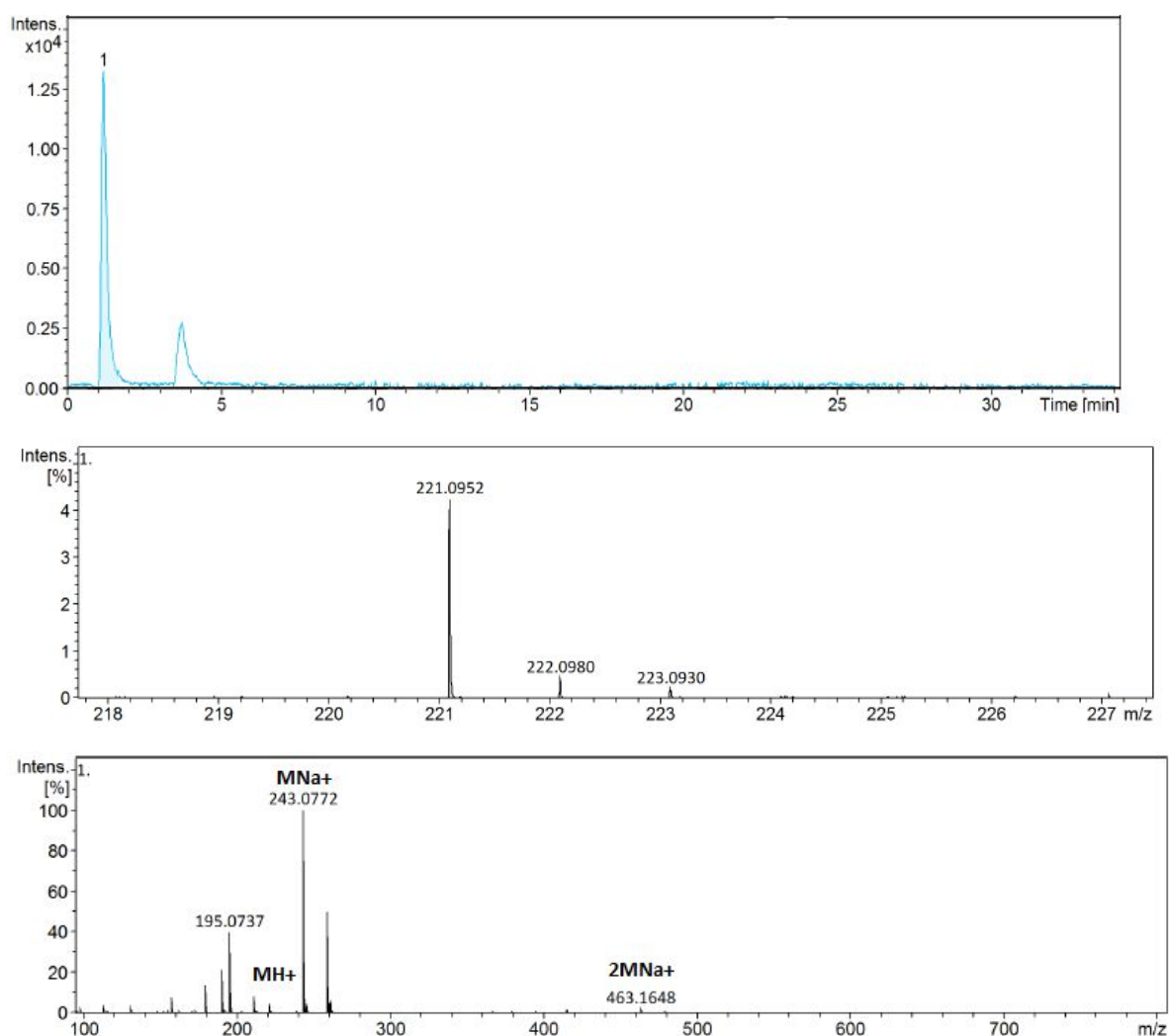
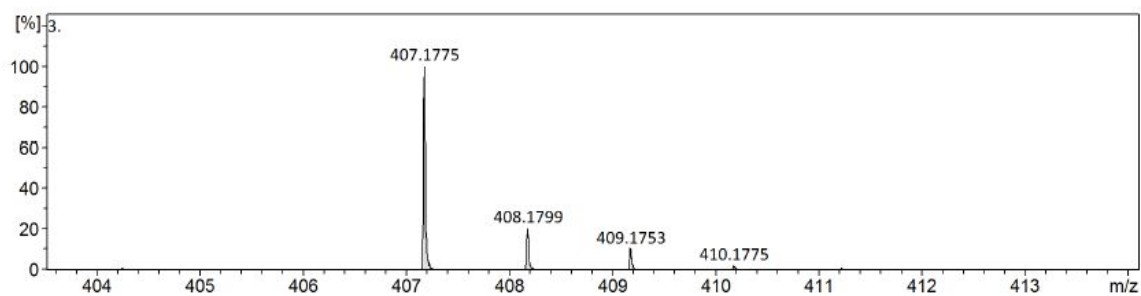


Fig. S1 Sulfoxide detected for *N*-Ac-Met-NH-CH₃ (compound **1**): extracted ion chromatogram (after 10 min irradiation) and MS spectrum of the >S=O photoproduct (m/z for unoxidized compd. **1** is 205.1011). Sulfoxide was not detected for *N*-Ac-MeCys-NH-CH₃ (compound **2**).

2. α S- α S detection:

N-Ac-Met-NH-CH₃ α S dimer (expected m/z = 407.1787)



N-Ac-MeCys-NH-CH₃ α S dimer (expected m/z = 379.1474)

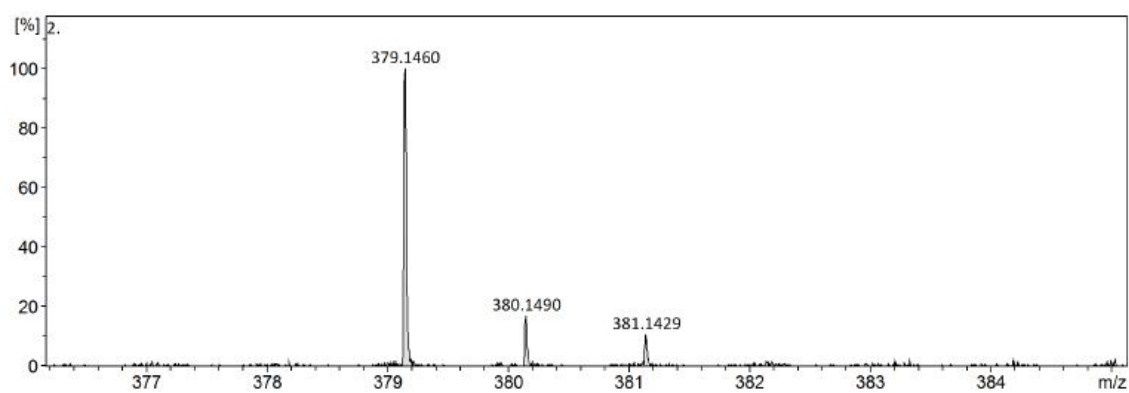


Fig. S2 α S- α S traces (MS spectra) detected for **1** and **2**.



Article

Radiation- and Photo-Induced Oxidation Pathways of Methionine in Model Peptide Backbone under Anoxic Conditions

Tomasz Pędzinski ^{1,2} , Katarzyna Grzyb ² , Konrad Skotnicki ³, Piotr Filipiak ^{1,2} , Krzysztof Bobrowski ^{3,*} , Chrysostomos Chatgililoglu ^{1,4,*} and Bronisław Marciniak ^{1,2,*}

¹ Center for Advanced Technology, Adam Mickiewicz University, Uniwersytetu Poznańskiego 10, 61-614 Poznań, Poland; tomekp@amu.edu.pl (T.P.); piotrf@amu.edu.pl (P.F.)

² Faculty of Chemistry, Adam Mickiewicz University, Uniwersytetu Poznańskiego 8, 61-614 Poznań, Poland; katgrz3@amu.edu.pl

³ Institute of Nuclear Chemistry and Technology, Dorodna 16, 03-195 Warsaw, Poland; k.skotnicki@ichtj.waw.pl

⁴ ISOF, Consiglio Nazionale delle Ricerche, Via P. Gobetti 101, 40129 Bologna, Italy

* Correspondence: kris@ichtj.pl (K.B.); chrys@isof.cnr.it (C.C.); marcinia@amu.edu.pl (B.M.); Tel.: +48-22-504-1336 (K.B.); +48-61-829-1885 (B.M.)

Abstract: Within the reactive oxygen species (ROS) generated by cellular metabolisms, hydroxyl radicals (HO^\bullet) play an important role, being the most aggressive towards biomolecules. The reactions of HO^\bullet with methionine residues (Met) in peptides and proteins have been intensively studied, but some fundamental aspects remain unsolved. In the present study we examined the biomimetic model made of Ac-Met-OMe, as the simplest model peptide backbone, and of HO^\bullet generated by ionizing radiation in aqueous solutions under anoxic conditions. We performed the identification and quantification of transient species by pulse radiolysis and of final products by LC-MS and high-resolution MS/MS after γ -radiolysis. By parallel photochemical experiments, using 3-carboxybenzophenone (CB) triplet with the model peptide, we compared the outcomes in terms of short-lived intermediates and stable product identification. The result is a detailed mechanistic scheme of Met oxidation by HO^\bullet , and by CB triplets allowed for assigning transient species to the pathways of products formation.

Keywords: methionine; oxidation; pulse and γ -radiolysis; laser flash and steady-state photolysis; free radicals; high-resolution MS/MS



Citation: Pędzinski, T.; Grzyb, K.; Skotnicki, K.; Filipiak, P.; Bobrowski, K.; Chatgililoglu, C.; Marciniak, B. Radiation- and Photo-Induced Oxidation Pathways of Methionine in Model Peptide Backbone under Anoxic Conditions. *Int. J. Mol. Sci.* **2021**, *22*, 4773. <https://doi.org/10.3390/ijms22094773>

Academic Editor: Marcus S. Cooke

Received: 22 March 2021

Accepted: 27 April 2021

Published: 30 April 2021

Publisher's Note: MDPI stays neutral with regard to jurisdictional claims in published maps and institutional affiliations.

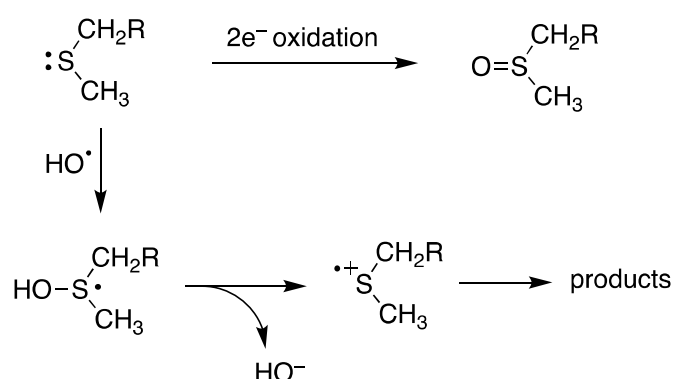


Copyright: © 2021 by the authors. Licensee MDPI, Basel, Switzerland. This article is an open access article distributed under the terms and conditions of the Creative Commons Attribution (CC BY) license (<https://creativecommons.org/licenses/by/4.0/>).

1. Introduction

The oxidation of methionine residues (Met) in peptides and proteins is a crucial reaction in the biological environment [1]. Reactions of both one- and two-electron oxidants with Met have been studied in some details. The reactive oxygen species (ROS) network, initiated from superoxide radical anion ($\text{O}_2^{\bullet-}$) and nitric oxide (NO^\bullet), regulates numerous metabolic processes. The production of two-electron oxidants like H_2O_2 , ONOO^- or HOCl involves the reaction with Met residues in a site-specific manner with formation S and R epimers of methionine sulfoxide, Met(O) [1]. Interestingly, the two epimeric forms of sulfoxide are repaired enzymatically by methionine sulfoxide reductase Msr-A and Msr-B, respectively [2,3]. Met residues in proteins are not only preserved against oxidative stress, but these transformations play an important role in cellular signaling processes [3,4].

Hydroxyl radicals (HO^\bullet) are the most reactive species within the ROS network and have long been regarded as a major source of cellular damage [5]. The main cellular processes that generate HO^\bullet are the Fenton reaction of H_2O_2 , the reduction of HOCl or H_2O_2 by $\text{O}_2^{\bullet-}$ and the spontaneous decomposition of ONOOH [1]. In cells it is estimated that the diffusion distance of HO^\bullet is very small due to its high reactivity with various types of biomolecules with rates close to diffusion-controlled [6,7]. Scheme 1 shows the two-step reaction of HO^\bullet with sulfides like Met to give formally one-electron oxidation, i.e., the formation of sulfuranyl radical followed by heterolytic cleavage [8–10].



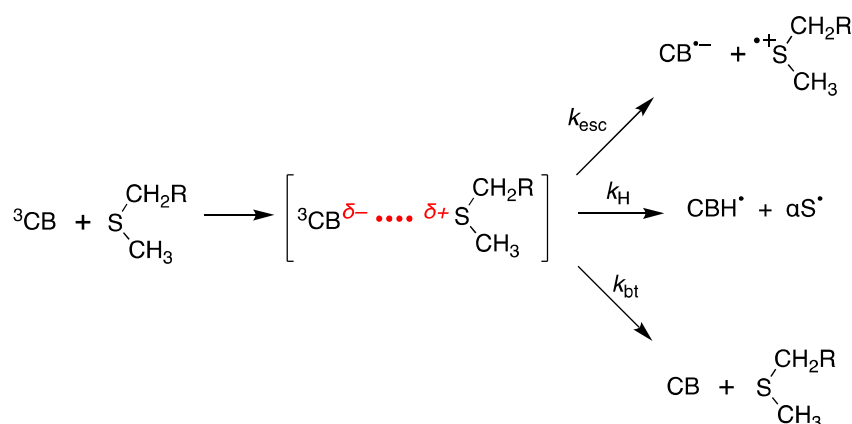
Scheme 1. Methionine ($\text{R} = \text{CH}_2\text{CH}(\text{NH}_3^+)\text{COO}^-$) like thioethers reacts with two-electron oxidants to give the corresponding sulfoxide, while the reaction with HO^\bullet affords other products.

Radiolysis of water provides a very convenient source of hydroxyl radicals HO^\bullet . Time-resolved kinetic studies by pulse radiolysis have expanded our mechanistic understanding of radical reaction pathways of Met at various functionalized environment [11]. Indeed, neighboring group participation of one-electron oxidation of Met ($\text{MetS}^{\bullet+}$) reactivity within particular peptides and/or proteins is of great importance, due to the presence of a manifold of possible participating functionalities (carboxy, amine, hydroxy and amide groups) [12]. For a long time it was believed that the two-centered, three electron (2c-3e) bonds between the oxidized sulfur atom and the lone electron pairs, located on the nitrogen atom in the N-terminal amino group and the oxygen atoms in the C-terminal carboxyl group are responsible for the stabilization of $\text{MetS}^{\bullet+}$ through a five-membered or six-membered ring interaction [13–16]. Subsequent studies showed that heteroatoms present in the peptide bond can be also involved in the formation of similar transient species with 2c-3e bonds with the oxidized sulfur atom [14–18].

There are also a few radiation chemical studies of Met in aqueous solutions, followed by product characterization and quantification. In the reaction of HO^\bullet with free Met in either the absence or the presence of oxygen, the attack at sulfur atom accounts of ~90% affording 3-methylthiopropionaldehyde; the formation of small amounts of the corresponding sulfoxide is due to in situ formation of H_2O_2 rather than to direct oxidation by HO^\bullet [19,20]. Again, studying the reaction of HO^\bullet with tripeptide Gly-Met-Gly provided strong evidence that the corresponding sulfoxide in the tripeptide derives from the in situ formed H_2O_2 . It is relevant to say that the main product of the tripeptide is an unsymmetrical disulfide ($\text{RCH}_2\text{SSCH}_3$) assigned to the chemistry of $\text{MetS}^{\bullet+}$ with parent compound, while the use of aerobic conditions highlighted the formation of other products derived from peroxy radicals of the tripeptide [17].

The present study focuses on the reaction of HO^\bullet with Ac-Met-OMe (1), the simplest model peptide backbone. This reaction was previously studied by pulse radiolysis at the pH range 4–5.7 [14]. Herein we extend the identification and quantification of transient species by pulse radiolysis at pH 7 and of final products of γ -radiolysis by LC-MS and high-resolution MS/MS under anoxic conditions. The purpose of acetylation of the N-terminal amino group is to eliminate the fast intramolecular proton transfer from the amino group to the sulfuranyl moiety, which was suggested earlier as the main decay reaction pathway, while the esterification of the C-terminal carboxyl group eliminates its decarboxylation [8,9,17,21,22]. Therefore, the use of 1 allows to study the reaction of HO^\bullet with Met residue with no contribution of N- and C-terminal functional groups.

Excited triplet states of benzophenones carboxyl derivatives (^3CB) were also shown to be very useful for studying one-electron oxidation reactions of Met-containing molecules of biological significance [21,23,24]. The mechanism of primary photo-induced processes occurring during Met oxidation in aqueous solutions is summarized in Scheme 2.



Scheme 2. Known mechanism of primary photochemical reactions for sensitized photooxidation of methionine derivatives in aqueous solution.

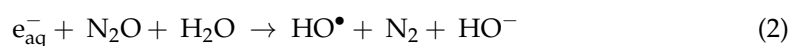
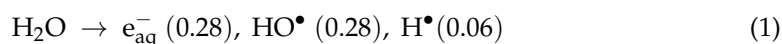
The quenching of ^3CB by Met derivatives leads to formation of a complex that can decay in three primary reactions: charge separation leading to $\text{CB}^{\bullet-}$ and $\text{MetS}^{\bullet+}$; H-atom transfer from alpha carbon atom next to sulfur to form CBH^\bullet and αS^\bullet radicals; and back electron transfer leading to formation of reactants in their ground states. Recently, the reaction of 3-carboxybenzophenone triplet (^3CB) with Ac-Met-NHMe has been studied in some details by some of us [25]. The mechanism of photooxidation of Met moiety showed to involve mainly H-atom abstraction from the two α -positions next to sulfur (see Scheme 2). Herein we included results of CB sensitized photooxidation of Ac-Met-OMe (**1**) in aqueous solutions applying flash photolysis studies for transient detection and continuous photolysis for products identification.

Application at the same time of radiation and photochemical techniques allowed for the first time to have two complementary conditions in order to compare in detail the oxidation mechanisms of Met derivative **1** initiated either by HO^\bullet or ^3CB leading via short-lived intermediates to stable products.

2. Results and Discussion

2.1. Pulse Radiolysis Studies

Pulse irradiation of water leads to the primary reactive species e_{aq}^- , HO^\bullet , and H^\bullet , as shown in Reaction (1). The values in brackets represent the radiation chemical yield (G) in $\mu\text{mol J}^{-1}$. In N_2O -saturated solution ($\sim 0.02\text{ M}$ of N_2O), e_{aq}^- are efficiently transformed into HO^\bullet radicals via Reaction (2) ($k = 9.1 \times 10^9\text{ M}^{-1}\text{s}^{-1}$), affording $G(\text{HO}^\bullet) = 0.56\text{ }\mu\text{mol J}^{-1}$ [7].



The reaction of HO^\bullet with compound **1** was investigated in N_2O -saturated solution of 0.2 mM **1** at natural pH (pH value of 7.0 was recorded). Transient absorption spectra in the range 270–700 nm recorded in the time range of 200 ns to 400 μs were collected in Figure 1.

The transient spectrum obtained 1.1 μs after the electron pulse showed a dominant sharp absorption band with $\lambda_{\text{max}} = 340\text{ nm}$. Based on previous studies on methionine derivatives, this band can be assigned to the HO^\bullet adduct of the sulfur atom HOS^\bullet (cf. Scheme 3 for the structure) [13,14,17]. However, as shown in Figure 1, the transient spectrum profile changes with time, indicating the overlap of various transient species. The transient spectrum profile can be resolved into contributions from the following components: the sulfuranyl radicals (HOS^\bullet), the C_α -centered radicals (αC^\bullet), the α -(alkylthio)alkyl radicals ($\alpha\text{S}(1)^\bullet$ and $\alpha\text{S}(2)^\bullet$), the inter-molecular sulfur–sulfur radical cations ($\text{SS}^{\bullet+}$) and intramolecular sulfur–nitrogen three-electron-bonded radicals (SN^\bullet) (the structures of these intermediates are highlighted in colored boxes in Scheme 3; see also Figures S1 and S2 in

Supplementary Materials for their individual spectra). These intermediates were previously identified during HO[•]-induced oxidation of **1**, but at the pH range 4–5.7 [14].

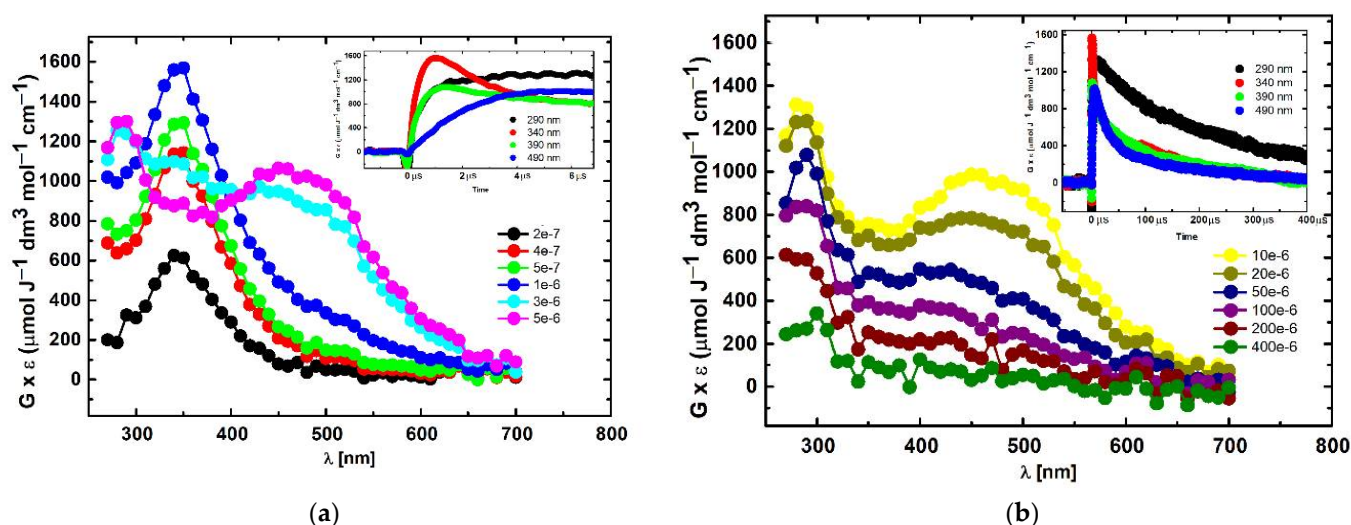


Figure 1. Absorption spectra following HO[•] oxidation of compound **1** (0.2 mM) in N₂O-saturated aqueous solutions at pH 7. Spectra were taken after the following time delays: (a) 200 ns (●), 400 ns (●), 500 ns (●), 1.1 μs (●), 3 μs (●), 5 μs (●) and inset: short-time profiles representing growths at λ = 290 nm (●), 340 nm (●), 390 nm (●) and 490 nm (●); (b) 10 μs (●), 20 μs (●), 50 μs (●), 100 μs (●), 200 μs (●), 400 μs (●) and inset: long-time profiles representing decays at λ = 290 nm (●), 340 nm (●), 390 nm (●) and 490 nm (●) (Dose per pulse = 11 Gy; optical path = 1 cm).

The spectra recorded 1.1, 3 and 6 μs after the electron pulse were resolved into contributions from the same components (HOS[•], αC[•], αS[•], SS^{•+} and SN[•]). Figure 2 shows the spectrum at 6 μs, while Figures S3 and S4 report the spectra at 1.1 and 3 μs, respectively. The sum of all component spectra with their respective radiation chemical yields (*G*-values) resulted in a good fit (⊗ symbols in Figure 2, Figures S3 and S4) to the experimental spectra.

Table 1 reports the radiation chemical yields of each radical and their percentage contribution to the transient spectrum obtained.

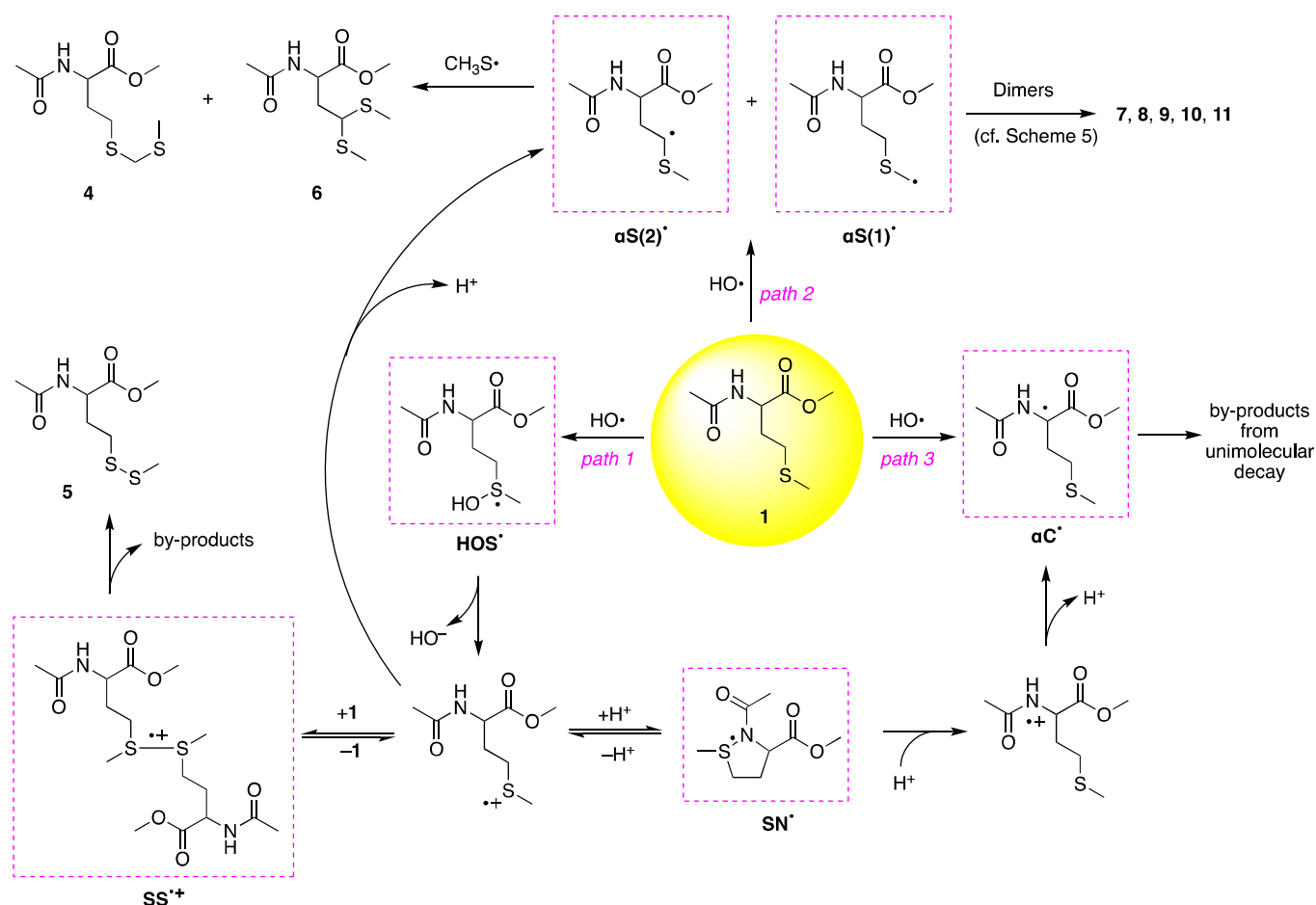
Table 1. The radiation chemical yields (*G*, μmol J^{−1}) of radicals and their percentage contribution (in parenthesis) to the total yield of radicals present in the reaction of HO[•] with compound **1** at different times after electron pulse at pH 7.0 ^a.

Time (μs)	HOS [•]	αC [•]	αS(1) [•] + αS(2) [•]	SS ^{•+}	SN [•]	Total R [•]
1.1	0.39 (73.6%)	0.06 (11.3%)	0.01 (1.9%)	0.04 (7.5%)	0.03 (5.7%)	0.53
3	0.16 (28.6%)	0.02 (3.6%)	0.17 (30.3%)	0.11 (19.6%)	0.10 (17.9%)	0.56
6	0.03 (5.3%)	0.02 (3.5%)	0.26 (45.6%)	0.13 (22.8%)	0.13 (22.8%)	0.57

^a For a procedure of *G* determination see Section 3 and [15].

The calculated total *G*-value of 0.53 μmol J^{−1} for the 1.1 μs spectrum is nearly in agreement with the expected *G*-value of HO[•] (0.56 μmol J^{−1}) available for the reaction of **1** at pH 7 and the concentration (0.2 mM) of **1**. This small difference in *G*-values could be understood, since at this time the reaction of HO[•] radicals with **1** via pathways 2 and 3 (Scheme 3) is about to be completed. The spectrum showed a dominant sharp absorption band at λ_{max} = 340 nm. It is worthy to note that the most abundant radical present at this time is HOS[•], which constitutes more than 70% of all radicals (Table 1). On the other hand, the total *G*-value of 0.56 μmol J^{−1} for 3 μs spectrum is in excellent agreement with

the expected yield of HO^\bullet radicals. The spectrum after 6 μs (Figure 2) was dominated by two distinct absorption bands with the pronounced maxima at $\lambda \approx 290$ and 490 nm. These bands were assigned to αS^\bullet radicals and $\text{SS}^{\bullet+}$ radical cations, respectively. The first one was obtained by hydrogen abstraction (path 2 in Scheme 3), and both of them by a sequence of reactions involving HOS^\bullet radicals and sulfur radical cations ($\text{S}^{\bullet+}$). The spectrum at 6 μs was resolved into contributions from the same components (Table 1). The total G-value of all radical present ($0.57 \mu\text{mol J}^{-1}$) is again in excellent agreement with the expected yield of HO^\bullet radicals. It is worthy to note that the most abundant radicals present at 6 μs are αS^\bullet , $\text{SS}^{\bullet+}$ and SN^\bullet radicals which constitute more than 90% of all radicals. Interestingly, the comparison of the radiation chemical yields of HOS^\bullet radicals and the sum of radiation chemical yields of αS^\bullet , $\text{SS}^{\bullet+}$ and SN^\bullet radicals at 3 μs and 6 μs after the pulse (Table 1) suggested that the increase of $G(\alpha\text{S}^\bullet + \text{SS}^{\bullet+} + \text{SN}^\bullet)$ occurs at the expense of decrease of $G(\text{HOS}^\bullet)$. This observation can be rationalized by the involvement of the $\text{S}^{\bullet+}$ on Met moiety in two equilibria (an acid-base and a concentration) and an irreversible deprotonation channel presented in Scheme 3.



Scheme 3. Proposed mechanism for the reaction of HO^\bullet radicals generated by γ -irradiation of N_2O -saturated aqueous solutions containing 1.0 mM N-acetyl methionine methyl ester (1) at natural pH.

Excellent material balance of all radicals, identified in the system equal to the G-value of HO^\bullet radicals available for the reaction with 1, proved the presence of all radical transients as the precursors of end products. At this point, it has to be stressed that after 6 μs the total G-value of the radicals began to decrease, reaching the value of $0.12 \mu\text{mol J}^{-1}$ at 400 μs which is only slightly higher than the G-value of αS^\bullet radicals ($0.10 \mu\text{mol J}^{-1}$) (Figure S5). This suggests that on this time domain nearly 80% of all radicals formed in the system were consumed in radical-radical processes leading to the final products. Moreover, in

this time domain the rates of these termination processes became dominant compared to the rates of transformation of $SS^{\bullet+}$ and SN^{\bullet} radicals into $\alpha S(1)^{\bullet}$, $\alpha S(2)^{\bullet}$ and αC^{\bullet} radicals, respectively.

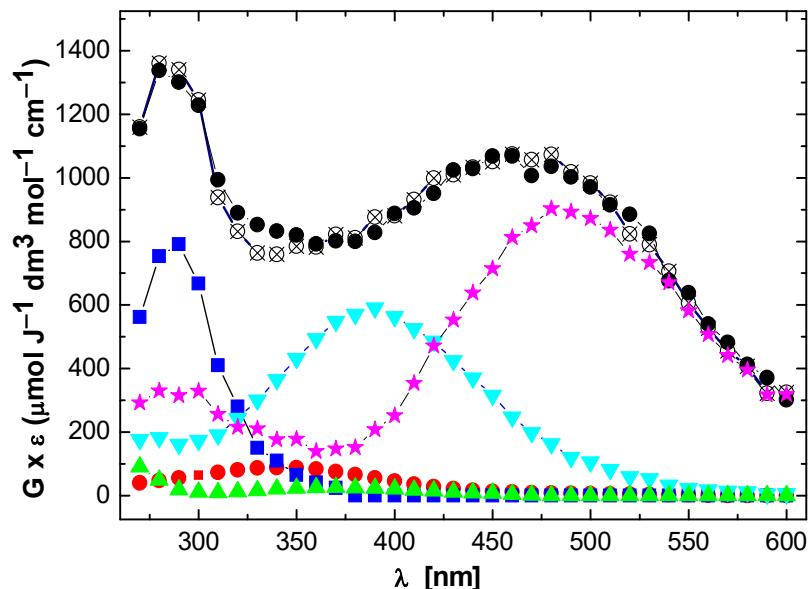


Figure 2. Resolution of the spectral components: HOS^{\bullet} (●), αC^{\bullet} (▲), $\alpha S(1)^{\bullet}$ and $\alpha S(2)^{\bullet}$ (■), $SS^{\bullet+}$ (★), SN^{\bullet} (▼) in the transient absorption spectrum recorded 6 μs (●—experimental; ○—fit) after the electron pulse in N_2O -saturated aqueous solution containing 0.2 mM **1** at pH 7.

Inset in Figure 1a shows kinetic traces recorded at four wavelengths (290, 340, 390 and 490 nm) that correspond to the maxima of absorption bands of the four most abundant radicals present in the irradiated system, i.e., αS^{\bullet} , HOS^{\bullet} , SN^{\bullet} and $SS^{\bullet+}$. These kinetic traces look different, and they reached their maximum signal at various times after the pulse. We assigned the observed buildup at $\lambda = 340$ nm to the formation of HOS^{\bullet} radical. Because HOS^{\bullet} is decaying in a significant way during its formation (see inset in Figure 1a), one has to account for this decay in order to get the proper value for the rate constant of the formation. Furthermore, based on the reference spectra applied in spectral resolutions (Figure S2), one can expect that the optical absorption bands of at least two radicals (αC^{\bullet} and SN^{\bullet}) overlap with the optical absorption band of HOS^{\bullet} , and thus may “contaminate” formation and decay traces observed at $\lambda = 340$ nm. In order to overcome this problem, we extracted the concentration profile of HOS^{\bullet} using spectral resolution of spectra at any desired time delay following the electron pulse ranged from 200 ns to 8 μs (cf. Figure S6A). Similarly, on the basis of the extracted concentration profiles of the other transients ($SS^{\bullet+}$, αS^{\bullet} , αC^{\bullet} and SN^{\bullet}), it was possible to evaluate their kinetic parameters (cf. Figure S6B–E). Otherwise, this would not be possible based just on “raw” time profiles recorded at the wavelengths of their absorption maxima (see insets in Figure 1). Kinetic parameters of all radical transients are collected in Table 2.

The first-order decay of HOS^{\bullet} ($k_d = 5.6 \times 10^5 s^{-1}$) results in radicals with a sulfur radical cationic site ($S^{\bullet+}$). The $S^{\bullet+}$ undergo typical reactions expected for such kind of radicals: deprotonation leading to the αS^{\bullet} radicals, the intermolecular formation of $SS^{\bullet+}$ and intramolecular five-membered cyclic SN^{\bullet} (Scheme 3).

For the equilibrium $S^{\bullet+} + 1 \rightleftharpoons SS^{\bullet+}$, the values of $k_f = 2.2 \times 10^9 M^{-1}s^{-1}$ and $k_r = 3.6 \times 10^4 s^{-1}$ give the equilibrium constant $K = k_f/k_r = 6.1 \times 10^4 M^{-1}$, which is three-fold lower than the previously estimated K for analogous dimeric radical cations derived from $(CH_3)_2S$ [26].

Table 2. Kinetic data for growth and decay of radicals present after the reaction of HO• with compound **1** at pH 7.0 from the pulse radiolysis studies.

k, s^{-1}	HOS•	αC^\bullet	αS^\bullet	SS•+	SN•
k_{growth}	2.1×10^6 $1.1 \times 10^{10} \text{ }^a$	1.5×10^6 $7.5 \times 10^9 \text{ }^a$	$4.1 \times 10^5 \text{ }^b$ $3.6 \times 10^4 \text{ }^c$	4.7×10^5 $2.2 \times 10^9 \text{ }^d$	3.7×10^5
k_{decay}	5.6×10^5	1.4×10^6	4.0×10^3	3.6×10^4	8.2×10^3

^a The second-order rate constants ($M^{-1}s^{-1}$) measured based on 0.2 mM concentration of **1**; ^b the first-order rate constant of the fast growth; ^c the first-order rate constant of the slow growth; ^d the second-order rate constant ($M^{-1}s^{-1}$) measured based on 0.2 mM concentration of **1**, and corrected for the backward reaction of the equilibrium, cf. Scheme 3.

The formation of αS^\bullet radicals occur via two different mono-exponential processes with $k = 4.1 \times 10^5 s^{-1}$ and $k = 3.6 \times 10^4 s^{-1}$ (cf. Figure S6C). The first one is assigned to deprotonation of $S^{\bullet+}$ that is formed directly from HOS•, and the second to deprotonation of $S^{\bullet+}$ that is formed via the reverse reaction involving SS•+. These assignments are strongly supported by the fact that the rate constant of the slow formation of αS^\bullet radicals (cf. Figure S6C) is equal to the rate constant of the SS•+ decay (cf. Figure S6B).

A second-order rate constant of $7.5 \times 10^9 M^{-1}s^{-1}$ was obtained for the reaction of HO• radical with **1**, via path 3 (Scheme 3), by measuring the rate constant of the pseudo-first-order growth $k = 1.5 \times 10^6 s^{-1}$ of the αC^\bullet concentration at 0.2 mM of **1** (cf. Figure S6D), which was assigned to the direct H-atom abstraction from the α -carbon atom by HO• radicals (see path 3 in Scheme 3). This value is reasonable considering in this case a rather low C α -H bond energy [27]. A quite surprising result is the short lifetime of αC^\bullet radicals which decays via a mono-exponential process with the rate constant $k = 1.4 \times 10^6 s^{-1}$ (cf. Figure S6D). We tentatively suggest that by-products are formed by unimolecular decay due to β -fragmentation with formation of the acyl radical, $CH_3C(O)^\bullet$ [28].

The pseudo-first order growth $k = 3.7 \times 10^5 s^{-1}$ of the SN• concentration can be assigned to the overall reaction with the first step leading to $S^{\bullet+}$, followed by the concerted cyclization and deprotonation (see Scheme 3). The decay of the SN• radicals is rather slow and occurs with the pseudo-first order rate constant $k = 8.2 \times 10^3 s^{-1}$. Based on earlier results [14,15], protonation of the SN• radicals provides the most facile mechanistic reaction pathway of their decay. On the basis of the extracted concentration profiles of the SN• radicals in cyclic L-Met-L-Met at various pHs, it was possible to evaluate the rate constant of SN• radicals with protons to be $2.1 \times 10^9 M^{-1}s^{-1}$ [15]. At pH 7, these reactions occur with the pseudo-first order rate constant $2.1 \times 10^2 s^{-1}$, which are much lower than the pseudo-first order rate constant measured for the decay of the SN• radicals formed from compound **1** (vide supra). Therefore, the most probable pathway responsible for the decay of the SN• involves N-protonation (e.g., by water molecules), followed by deprotonation at the α C-carbon leading to αC^\bullet radicals (cf. Scheme 3). These reactions provide an irreversible entry to these C-centered radicals and were previously suggested for linear peptides containing Met residue [14]. Since αC^\bullet radicals are formed in a slow process, this fact, combined with their very short lifetime, rationalizes their absence in the resolved absorption spectra recorded at longer times.

2.2. γ -Radiolysis and Product Analysis

In addition to the reactive species e^-_{aq} , HO•, and H•, radiolysis of neutral water leads also to H^+ (0.28) and H_2O_2 (0.07); in parenthesis the G in $\mu mol J^{-1}$ [7]. In N_2O -saturated solution, the $G(HO^\bullet) = 0.56 \mu mol J^{-1}$, therefore HO• and H• account for 90% and 10%, respectively, of the reactive species (cf. Reactions (1) and (2)).

N_2O -saturated solutions containing compound **1** (1.0 mM) at natural pH were irradiated for 400 and 800 Gy under stationary state conditions with a dose rate of $46.7 Gy min^{-1}$ followed by LC-MS and high-resolution MS/MS analysis. A representative LC-MS analysis of the 800 Gy irradiated sample is shown in Figure 3.

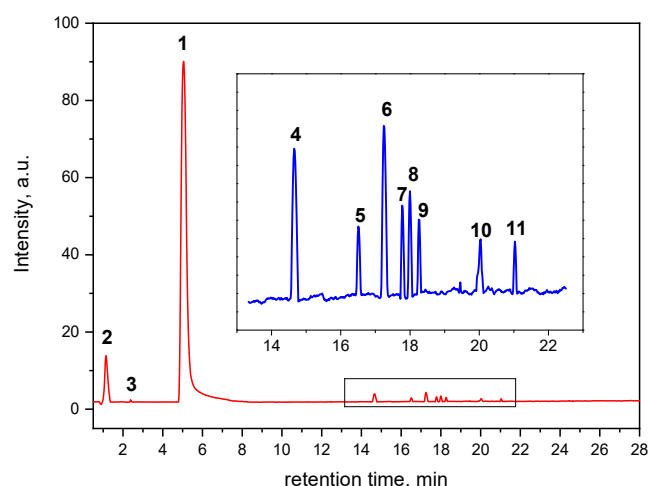
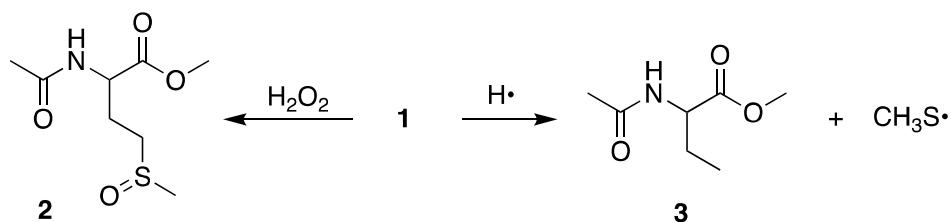


Figure 3. HPLC run of γ -irradiation of N_2O -saturated aqueous solutions of 1.0 mM *N*-acetyl methionine methyl ester (**1**) at natural pH at a dose of 800 Gy (dose rate of 46.7 Gy min^{-1}). The consumption of **1** led to the formation of 10 products. Inset: expansion of the chromatogram between 14 and 22 min.

Eleven compounds were detected in the chromatogram including the starting material **1**. All peaks were identified and their chemical structures assigned by examination of their high-resolution mass data and characteristic fragmentation patterns (see Figures S7 and S8). In Schemes 3 and 4 the structures of all products are reported that will be described in some detail below.



Scheme 4. The reaction of **1** with H_2O_2 and H^\bullet atom affords sulfoxide **2** and α -aminobutyric **3** derivatives, respectively.

Combination of the pulse radiolysis results on reactive intermediates and the structural information obtained from the high-resolution MS/MS allows the depiction the mechanistic proposal of compound **1** transformation by γ -radiolysis (Scheme 3). It is well documented from previous studies on Met derivatives that the sulfoxide **2** is formed due to the in-situ generation of hydrogen peroxide [17,19], while the H^\bullet addition to the sulfur ($k = 1.7 \times 10^9 \text{ M}^{-1}\text{s}^{-1}$) with the formation of a sulfuranyl radical intermediate affords compound **3** and CH_3S^\bullet radical (Scheme 4) [29,30].

From the pulse radiolysis studies described above, the reaction of HO^\bullet with **1** ($k = 1.1 \times 10^{10} \text{ M}^{-1}\text{s}^{-1}$) followed one main and two minor paths. In Scheme 3, the formation of adduct radical (HOS^\bullet) is the main path (path 1), while the two minor ones are: the H-atom abstraction from the CH_2-S-CH_3 moiety to give the intermediate αS^\bullet radicals (path 2) and the H-atom abstraction from the $N-CH-CO$ moiety to give the intermediate αC^\bullet radical (path 3). Table 1 shows that 1.1 μs after the pulse the distribution percentages were 73.6, 1.9 and 11.35% for HOS^\bullet , αS^\bullet and αC^\bullet , but at 6 μs after the pulse the relative contribution changed to 5.3, 45.6 and 3.5%, respectively. The HOS^\bullet follows a first-order decay ($k_d = 5.6 \times 10^5 \text{ s}^{-1}$) by HO^- elimination to give the sulfide radical cation, which is at the crossroad of various possible reactions affording the intermediates $SS^{\bullet+}$, αS^\bullet , SN^\bullet and αC^\bullet . We recall from pulse radiolysis section that the radiation chemical yields of HOS^\bullet and the sum of radiation chemical yields of $SS^{\bullet+}$, αS^\bullet and SN^\bullet species at 3 μs and 6 μs

after the pulse (Table 1) suggest that the formation of $\text{SS}^{\bullet+}$, αS^{\bullet} and SN^{\bullet} species follows the decay of HOS^{\bullet} , as discussed in the previous section.

We suggest that the disulfide radical cation ($\text{SS}^{\bullet+}$), which is in equilibrium with sulfide radical cation ($\text{S}^{\bullet+}$) and starting material, fragments and affords the observed disulfide **5** [17]. Moreover, the $\text{S}^{\bullet+}$ is prompt to deprotonation. Evidence from the pulse radiolysis experiments indicated that SN^{\bullet} radical is the progenitor of αC^{\bullet} radical and the proposed mechanism is suggested in Scheme 3, including the tentatively suggested unimolecular decay by β -fragmentation with formation of acyl radical [28]. We do not have confirmation of this latter pathway by the present LC-MS data.

Lastly, the αS^{\bullet} radicals, which can be both $\alpha\text{S}(1)^{\bullet}$ and $\alpha\text{S}(2)^{\bullet}$ are shown in Scheme 3. Table 1 reports the percentage contribution as a function of time, i.e., 1.9, 30.3 and 45.6% for 1.1, 3 and 6 μs after the pulse, which means that at longer time scale the αS^{\bullet} radicals are the only remaining reactive species together with $\text{CH}_3\text{S}^{\bullet}$ radical derived from the H^{\bullet} atom reactivity (cf. Scheme 4). The cross-termination of $\alpha\text{S}(1)^{\bullet}$ and $\alpha\text{S}(2)^{\bullet}$ with $\text{CH}_3\text{S}^{\bullet}$ affords compounds **4** and **6**, respectively (see Scheme 3).

The data from the high-resolution MS/MS showed that compounds **7**, **8**, **9**, **10** and **11** are dimers of αS^{\bullet} radicals (Scheme 3). Figure S8 shows the high-resolution MS/MS spectra of the five compounds. The accurate masses of these products, m/z 409.1484, 409.1480, 409.1480, 409.1479, 409.1478, correspond to a molecular weight MH^+ equivalent of two αS^{\bullet} radicals. Although the fragmentation patterns are not diagnostic, some information can be extracted. All of them show that initial fragmentations with a loss of CH_4O , CH_4S , $\text{C}_2\text{H}_4\text{O}$ and/or $\text{C}_2\text{H}_2\text{O}$.

Further structural information may be obtained from the analysis of potential diastereoisomers. What is the ratio of the two αS^{\bullet} radicals? It is expected $\alpha\text{S}(2)^{\bullet}$ radical to be in higher concentration than $\alpha\text{S}(1)^{\bullet}$ and in line with the higher stability of secondary vs. primary alkyl radical due to favorable deprotonation from the precursor sulfide radical cation. Assuming that the concentration of $\alpha\text{S}(2)^{\bullet}$ radical is twice that of the $\alpha\text{S}(1)^{\bullet}$ radical, it is expected to having $\alpha\text{S}(2)$ – $\alpha\text{S}(2)$ and $\alpha\text{S}(2)$ – $\alpha\text{S}(1)$ from a probability point of view of termination steps. Figure 4 shows that $\alpha\text{S}(2)$ – $\alpha\text{S}(2)$ has four stereocenters, two are from the starting material fixed at the *S* configuration whereas two new stereocenters generated from the self-termination can be *R* or *S*. In total four products, two of them are identical, and therefore we expect to have *SSSS*, *SRSS* and *SRRS* diastereoisomers.

Figure 4 shows that $\alpha\text{S}(2)$ – $\alpha\text{S}(1)$ has three stereocenters, two are from the starting material fixed at the *S* configuration and one stereocenter is generated from the cross-termination of the two radicals, producing the diastereoisomers *SSR* and *SRS*. In total, five diastereoisomers that we associated with the five dimeric products detected by LC-MS in γ -radiolysis of the compound **1**.

2.3. Photosensitized Oxidation by ^3CB

Sensitized by triplet CB (^3CB) oxidation of Met derivatives leads to numerous transients, well characterized in our earlier studies [23,25,31]. Laser flash photolysis (LFP) results of the ^3CB with **1** are presented in Figure S9. The main species observed are ^3CB and ketyl radical (CBH^{\bullet}), with a minor contribution of radical anion ($\text{CB}^{\bullet-}$) (Figure 5). As expected, the transient species derived from compound **1** could not be directly observed due to the strong absorption overlap of the transients derived from CB photochemistry. However, it is expected that the radical coupling reactions derived from the two αS^{\bullet} radicals are predominant.

The Ar-saturated solutions containing CB (4 mM) and compound **1** (20 mM) at natural pH were irradiated for 20 min using a CW 355 nm laser (50 mW, see Experimental Section for details). A representative LC-MS analysis of the irradiated solution is shown in Figure 6. A variety of compounds were detected in the chromatogram, including the starting material **1** and CB . The high-resolution mass data and fragmentation patterns of all peaks were analyzed and information on their chemical structures were extracted. In Scheme 5, the

structures of major products are reported that will be described in some detail in the following paragraphs.

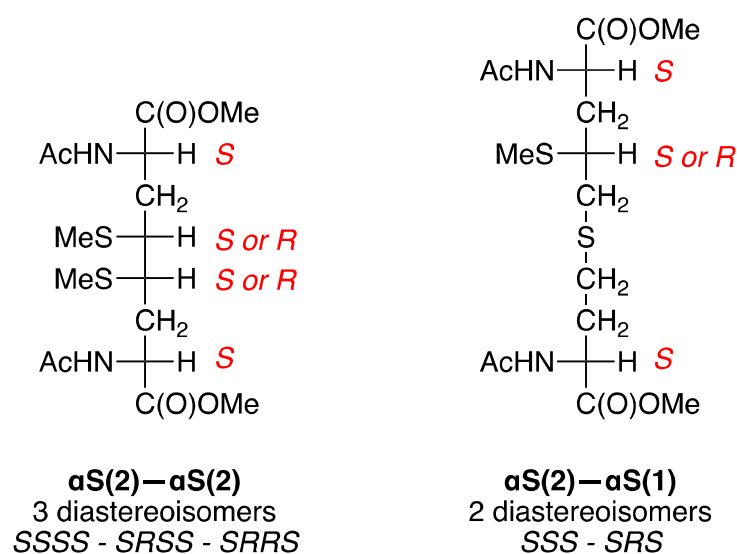


Figure 4. The chemical structures of $\alpha S(2)-\alpha S(2)$ and $\alpha S(2)-\alpha S(1)$ indicating the configuration of stereocenters.

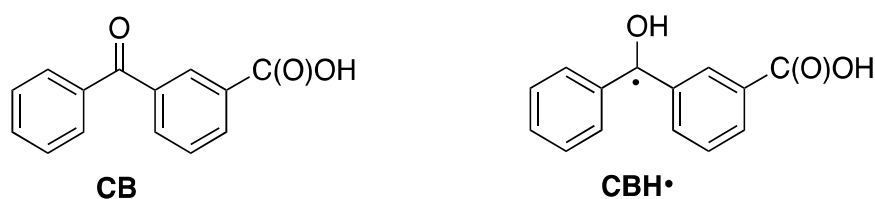


Figure 5. Structures of the sensitizer (3-carboxybenzophenone, CB) and its respective photo-reduction product (ketyl radical, CBH•).

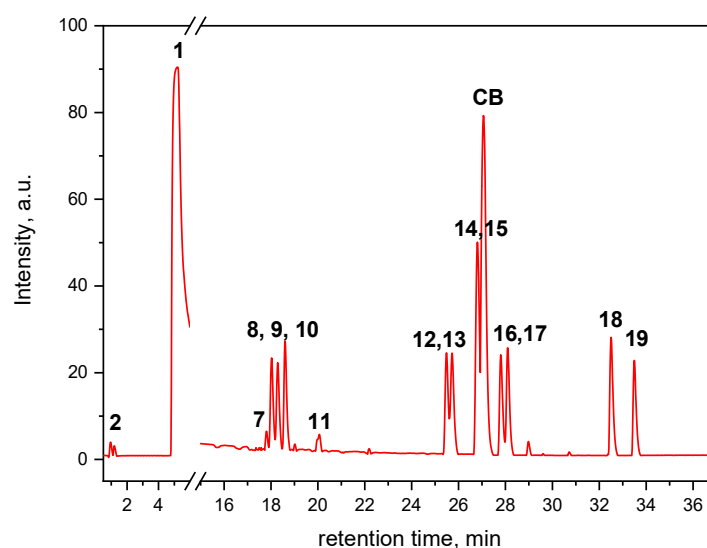


Figure 6. HPLC run of 355 nm irradiated solution containing **CB** (4 mM) and *N*-acetyl methionine methyl ester (**1**) (20 mM). The peaks are labelled with numbers referring to products shown in Scheme 5 and Figure 7.

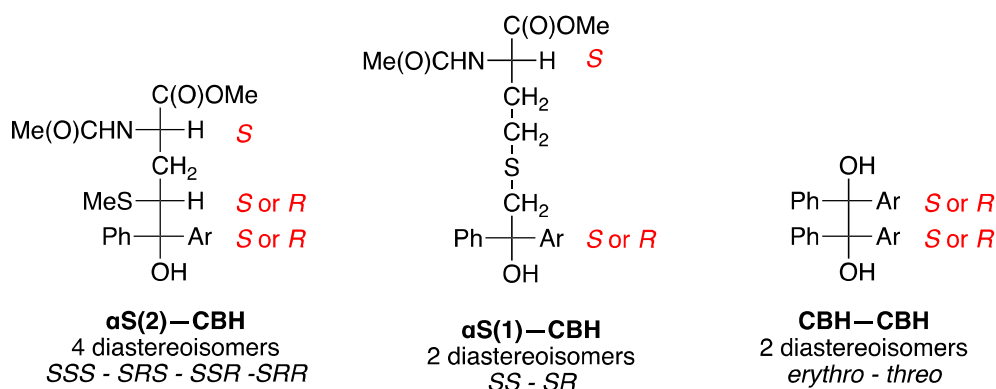
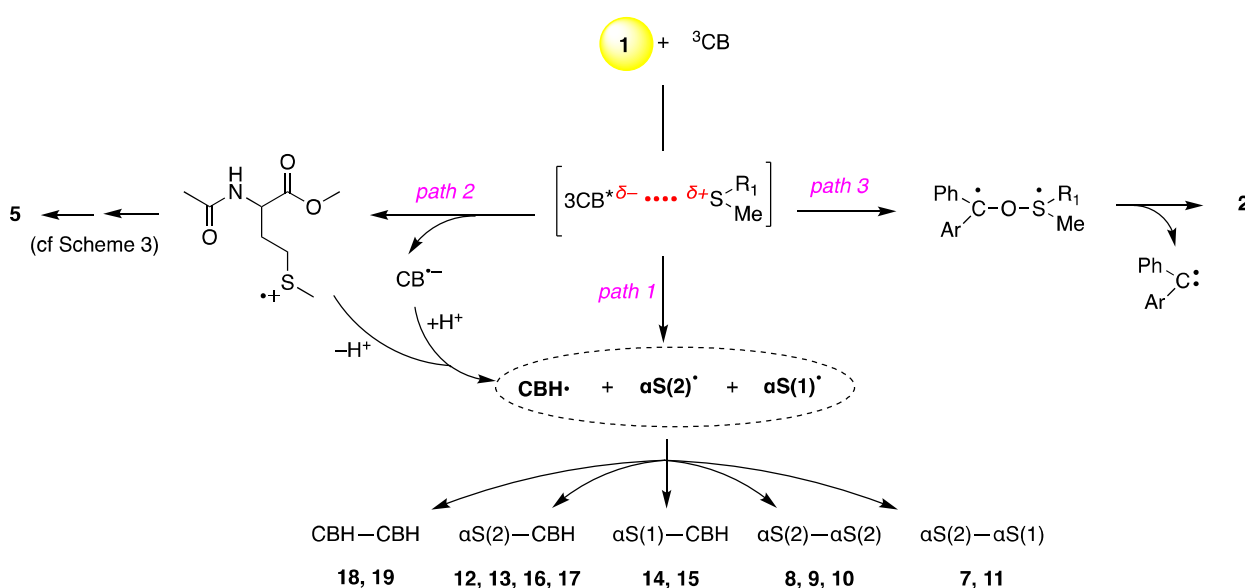


Figure 7. The chemical structures of $\alpha S(2)$ -CBH, $\alpha S(1)$ -CBH and CBH-CBH indicating the configuration of stereocenters.



Scheme 5. Proposed mechanism for the reaction of 3CB triplet with N-acetyl methionine methyl ester (1) at natural pH 7.

Based on LFP results for the reactive intermediates and the structural information obtained from the high-resolution MS/MS, the mechanistic proposal of compound 1 transformation by photolysis can be depicted (Scheme 5). The formation of a complex between ^3CB and 1 through its sulfur atom is well documented followed by the H-atom abstraction as the main pathway, yielding the two $\alpha S(1)^{\bullet}$ and $\alpha S(2)^{\bullet}$ radicals (path 1) [25,31,32]. Evidence that a small portion of the complex undergoes one electron transfer, with the formation of sulfide radical cation ($S^{\bullet+}$), was obtained (path 2). In analogy with the above-described mechanism in the radiolysis section, we detected traces of compound 5 suggesting a small contribution to the formation of $\alpha S(1)^{\bullet}$ and $\alpha S(2)^{\bullet}$ radicals. Moreover, we detected traces of sulfoxide 2. We speculate that the oxidation of sulfur is due the formation of a biradical and its further fragmentation to the corresponding sulfoxide (path 3). The fate of αS^{\bullet} radicals will depend on the relative concentration of $\alpha S(1)^{\bullet}$ and $\alpha S(2)^{\bullet}$ and the presence of a CBH $^{\bullet}$ radical.

The HPLC run in Figure 6 shows compounds in three retention time intervals:

- In the interval of 17.5–19.5 min there are three major peaks that correspond to compounds 8, 9 and 10, and 2 minor peaks that correspond to compounds 7 and 11, which all are the dimers of αS^{\bullet} radicals observed in γ -radiolysis experiments (cf. Scheme 3). It is worth underlining that the accurate masses of these products and the fragmentation patterns are identical in all sets of experiments (Figure S10). We assigned the structures 8, 9 and 10 to the 3 diastereoisomers of the $\alpha S(2)$ - $\alpha S(2)$ dimers

- and **7** and **11** (minor peaks) to the 2 diastereoisomers of $\alpha S(2)$ – $\alpha S(1)$ reported in the previous radiolysis section (see Scheme 5).
- (ii) In the interval of 32–34 min there are two peaks that are individuated as compounds **18** and **19** (Figure 6). Their accurate masses (m/z 455.1527, and 455.1522) correspond to the MH^+ of the dimer CBH–CBH (Figure S11). Figure 7 shows that CBH–CBH has two stereocenters and a plane of symmetry that correspond to *erythro* and *threo* diastereoisomers.
 - (iii) In the interval of 25–29 min there is the major peak that corresponds to **CB**, with two doublets on the right and left sides, respectively, and one singlet in the shoulder of **CB** (Figure 6). In this area of HPLC run there are the cross-coupling products of αS^\bullet and CBH $^\bullet$ radicals. The accurate masses of two couples of compounds named **12**, **13** (m/z 414.1391, 414.1393) and **16**, **17** (m/z 414.1390, 414.1393), as well as their fragmentation patterns, are identical and assigned to $\alpha S(2)$ –CBH (Scheme 5 and Figure S12). Figure 7 shows that $\alpha S(2)$ –CBH has three stereocenters, one is from the starting material fixed at the *S* configuration and two stereocenters are generated from the cross-termination of the two radicals, producing the diastereoisomers *SSS*, *SRS*, *SSR* and *SRR*. Regarding the singlet in the shoulder of **CB**, having also m/z 414.1392, but different fragmentation patterns, it is assigned to $\alpha S(1)$ –CBH (Figure S13). As shown in Figure 7, this compound has two stereocenters, the usual *S* configuration from the starting material and a new one generated from the cross-termination of the two radicals, producing the diastereoisomers *SS* and *SR*. It is likely that, under our HPLC conditions, the two diastereoisomers be under the same peak, or one of them overlap with **CB**.

The above analysis suggests that the concentration of $\alpha S(2)^\bullet$ radical is much higher than $\alpha S(1)^\bullet$, as expected from the competition of the two H-atom abstraction steps with formation of secondary vs. primary alkyl radical, being the difference in BDE energy 2–3 kcal/mol. The LC run (Figure 6) together with the proposed mechanism (Scheme 5) suggests a ratio of 5–5.5 between the two αS^\bullet radicals. In this situation, the intermediates CBH $^\bullet$ and $\alpha S(2)^\bullet$ will be the main players in the self-termination steps with formation of **18**, **19** and **8**, **9**, **10**, respectively, as well as in the cross-termination reaction with formation of **12**, **13**, **16** and **17** diastereoisomers.

3. Materials and Methods

3.1. Pulse Radiolysis

The pulse radiolysis experiments were performed with the LAE-10 linear accelerator at the Institute of Nuclear Chemistry and Technology in Warsaw, Poland with a typical electron pulse length of 10 ns and 10 MeV of energy. A detailed description of the experimental setup has been given elsewhere along with basic details of the equipment and its data collection system [33,34]. The 1 kW UV-enhanced xenon arc lamp (Oriel Instruments, Stratford, CT, USA) was applied as a monitoring light source. The respective wavelengths were selected by MSH 301 monochromator (Lot Oriel Gruppe, Darmstadt, Germany) with a resolution of 2.4 nm. The intensity of analysing light was measured by means of PMT R955 (Hamamatsu, Hamamatsu City, Shizuoka, Japan). A signal from detector was digitised using a Le Croy WaveSurfer 104MXs-B (1 GHz, 10 GS/s) oscilloscope and then send to PC for further processing. A water filter was used to eliminate near IR wavelengths.

Absorbed doses per pulse were on the order of 11 Gy (1 Gy = 1 J kg^{−1}). Experiments were performed with a continuous flow of sample solutions using a standard quartz cell with optical length 1 cm at room temperature (~22 °C). Solutions were purged for at least 20 min per 250 mL sample with N₂O before pulse irradiation. The *G*-values were calculated from the Schuler formula (Equation (3)) [35]

$$G(S^\bullet) = 0.539 + 0.307 \frac{\sqrt{19.6[S]}}{1 + \sqrt{19.6[S]}} \quad (3)$$

where $[S]$ is the HO^\bullet -scavenger concentration and with respect to the current work, concentration of Ac-Met-OMe. This form of the Schuler formula gives $G(\text{S}^\bullet)$ in units of $\mu\text{mol J}^{-1}$, and with respect to the current work, $[S] = 0.2 \text{ mM}$ gives $G(\text{S}^\bullet) = 0.557 \mu\text{mol J}^{-1}$ where (S^\bullet) corresponds to all radicals formed in the system. The dosimetry was based on N_2O -saturated solutions of 10^{-2} M KSCN which following radiolysis, produces $(\text{SCN})_2^{\bullet-}$ radicals that have a molar absorption coefficient of $7580 \text{ M}^{-1}\text{cm}^{-1}$ at $\lambda = 472 \text{ nm}$ and are produced with a yield of $G = 0.635 \mu\text{mol J}^{-1}$ from Equation (3) [36].

3.2. Spectral Resolutions of Transient Absorption Spectra

The observed absorption spectra monitored at various time delays following the electron pulse, were transformed from $A(\lambda_j)$ to $G\varepsilon(\lambda_j)$ by multiplying $A(\lambda_j)$ by the factor (F) from the dosimetry described in Section 3.1. $A(\lambda_j)$ represents the absorbance change of the composite spectrum and $F = \varepsilon_{472} \times G(\text{SCN})_2^{\bullet-} / A_{472}$ where ε_{472} is the molar absorption coefficient of $(\text{SCN})_2^{\bullet-}$ at 472 nm and $G(\text{SCN})_2^{\bullet-}$ is the radiation chemical yield of the $(\text{SCN})_2^{\bullet-}$ (see Section 3.1) and A_{472} represents the observed absorbance change in the thiocyanate dosimeter. The optical spectra thus converted were resolved into specific components (representing individual transients) by linear regression according to the following Equation (4)

$$G\varepsilon(\lambda_i) = \sum_j \varepsilon_j(\lambda_i) G_j \quad (4)$$

where ε_j is the molar absorption coefficient of the j th species and the regression parameters, G_j , are equal to the radiation-chemical yield of the j th species. The sum in Equation (4) is over all radical species present. For any particular time delay of an experiment, the regression analysis included equations such as Equation (4) for each λ_i under consideration. Further details of this method were described elsewhere [15].

The reference spectra of these transients were previously collected and applied in the spectral resolutions (cf. Figure S2 in Supplementary Materials) [15,17]. The molar absorption coefficients of the relevant transients, which will be further identified below, are provided in the following: HOS^\bullet , $\lambda_{\text{max}} = 340 \text{ nm}$ and $\varepsilon_{340} = 3400 \text{ M}^{-1} \text{ cm}^{-1}$; αC^\bullet , $\lambda_{\text{max}} = 270 \text{ nm}$ and $\varepsilon_{270} = 6200 \text{ M}^{-1} \text{ cm}^{-1}$ and $\lambda_{\text{max}} = 370 \text{ nm}$ and $\varepsilon_{370} = 1800 \text{ M}^{-1} \text{ cm}^{-1}$; αS^\bullet , $\lambda_{\text{max}} = 290 \text{ nm}$ and $\varepsilon_{290} = 3000 \text{ M}^{-1} \text{ cm}^{-1}$; $\text{SS}^{\bullet+}$, $\lambda_{\text{max}} = 480 \text{ nm}$ and $\varepsilon_{480} = 6880 \text{ M}^{-1} \text{ cm}^{-1}$; SN^\bullet , $\lambda_{\text{max}} = 390 \text{ nm}$ and $\varepsilon_{390} = 4500 \text{ M}^{-1} \text{ cm}^{-1}$.

For the compound (1) studied in this work, it was not possible to generate these radicals selectively since they undergo fast mutual transformation. Based on our earlier experience, however, we can say with certainty that the changes in molar absorption coefficients within the same type of radicals are not significant and are in the limit of 15% error (5% variation in the experimental data and 10% combined error in the reported molar absorption coefficients for the UV-vis spectra of the intermediates under consideration). The fact that the combined yields of the transient species derived from their respective molar absorption coefficients are at the short time delays equal to the expected initial yield of the scavenged $\bullet\text{OH}$ radicals by 1, i.e., 0.56 mol J^{-1} (based on Schuler's formula (Equation (3) in Section 3.1)), and they also never exceed this value, supports additional validation of the spectral resolutions and eliminates unreasonable fits.

Involvement of the H^\bullet atom reaction is not reflected in the resolved transient spectra since the forming $\text{CH}_3\text{S}^\bullet$ (see Scheme 4) is formed with a very low radiation chemical yield ($<0.06 \text{ mol J}^{-1}$) and is characterised by the very low molar absorption coefficient ($<500 \text{ M}^{-1}\text{cm}^{-1}$). However, the involvement of H^\bullet atoms is reflected in the formation of final products 4 and 6 (see Scheme 3).

3.3. Steady-State γ -Radiolysis

Irradiations were performed at room temperature using a ^{60}Co -Gammacell at different dose rates. The exact absorbed radiation dose was determined with the Fricke chemical dosimeter, by taking $G(\text{Fe}^{3+}) = 1.61 \mu\text{mol J}^{-1}$ [37].

3.4. Laser Flash Photolysis

The laser flash photolysis (LFP) setup used in this work has been described in detail elsewhere [25,31]. Briefly, this setup employs Nd:YAG laser (Spectra Physics, Mountain View, CA, USA, model INDI 40-10) with 355 nm excitation wavelength as light pump and 150 W pulsed xenon (Applied Photophysics, Surrey, UK) to probe the excited sample. A flash photolysis experiment was performed in oxygen-free environment in 1×1 cm rectangular quartz fluorescence cells. Kinetic traces were recorded between 370 and 750 nm at 10 nm intervals. The sample contained the quencher-compound **1** (20 mM) and the sensitizer CB (4 mM) at pH = 7.

3.5. Steady-State Photolysis

Steady-state photochemical irradiation experiments were performed in a 1×1 cm rectangular cell on an optical bench irradiation system using a Genesis CX355STM OPSL laser from Coherent (Santa Clara, CA, USA) with 355 nm emission wavelength (the output power used was set at 50 mW).

3.6. LC-MS/MS Measurements

The LC-MS measurements were carried out using a liquid chromatography Thermo Scientific/ Dionex Ultimate 3000 system equipped with C18 reversed-phase analytical column (2.6 μ m, 2.1 mm \times 100 mm, Thermo-Scientific, Sunnyvale, CA, USA). The LC method employed a binary gradient of acetonitrile and water with 0.1% (*v/v*) formic acid. Separation was achieved with a gradient of 7–60% of acetonitrile at a flow rate of 0.3 mL/min for 42 min. This UHPLC system was coupled to a hybrid QTOF mass spectrometer (Impact HD, Bruker Daltonik, Bremen, Germany). The ions were generated by electrospray ionization (ESI) in positive mode. MS/MS fragmentation mass spectra were produced by collisions (CID, collision-induced dissociation) with nitrogen gas in the Q2 section of the spectrometer.

4. Conclusions

Summarizing the role of various transient species obtained by the two different time-resolved techniques and their connection with the end-product formation (Schemes 3 and 5), the α S(2) \bullet and α S(1) \bullet radicals play an important role in both oxidation processes, although their mode of formation and relative concentration are quite different: (a) in radiolysis, the one-electron oxidation of sulfide (generated by HO \bullet addition followed by HO $^-$ elimination) is followed by α -deprotonation with formation of α S(2) \bullet and α S(1) \bullet radicals, in an approximately 2:1 ratio; (b) in photolysis, the formation of a complex between 3 CB and the sulfur moiety is followed by H-atom abstraction, yielding α S(2) \bullet and α S(1) \bullet radicals in an approximately 5:1 ratio. The final products are formed by radical-radical combination.

The herein described complete and detailed study of the oxidation mechanisms of Met residue, simulating its position in the interior of long oligopeptides and proteins, represents a significant and original contribution to the understanding of oxidation reactions in real biological systems, i.e., proteins, applicable to research in protein therapeutics. This work offers a benchmark for the identification, quantification and mechanistic determination of products derived from oxidation of methionine derivatives.

Supplementary Materials: The following are available online at <https://www.mdpi.com/article/10.3390/ijms22094773/s1>, Figure S1: The structures of six reactive intermediates identified in the pulse radiolysis experiments. Figure S2: Reference spectra used in the resolutions of the transient absorption spectra following \bullet OH-induced oxidation of CH₃C(O)N-Met-OCH₃. Figure S3: Resolution of the spectral components in the transient absorption spectrum recorded 1.1 μ s after the electron pulse in N₂O-saturated aqueous solution containing 0.2 mM AcN-Met-OMe at pH 7.0. Figure S4: Resolution of the spectral components in the transient absorption spectrum recorded 3 μ s after the electron pulse in N₂O-saturated aqueous solution containing 0.2 mM AcN-Met-OMe at pH 7.0. Figure S5: The sum of all radicals (HOS \bullet , α C \bullet , SS \bullet^+ , SN \bullet , α S \bullet) taken in spectral resolutions as a function of time. Figure S6: First-order kinetic fits of the growth and decay of radicals HOS \bullet (panel A), SS \bullet^+

(panel B), αS^\bullet (panel C), αC^\bullet (panel D), and SN^\bullet (panel E). Figure S7: High-resolution MS/MS spectra of the products **4** (m/z 252.0731) and **6** (m/z 252.0732) derived from the cross-termination of $\alpha\text{S}(1)^\bullet$ and $\alpha\text{S}(2)^\bullet$ with $\text{CH}_3\text{S}^\bullet$ and product **5** (m/z 238.0578)—a disulfide. Figure S8: High-resolution MS/MS spectra of the five dimeric products **7** (m/z 409.1484), **8** (m/z 409.1480), **9** (m/z 409.1480), **10** (m/z 409.1479) and **11** (m/z 409.1478) derived from the combination of two αS^\bullet radicals. Figure S9: Transient absorption spectra following LFP of CB (4 mM) and *N*-AcMetOCH₃ (20 mM) for different time delays at pH 7. Figure S10: High-resolution MS/MS spectra of the dimeric products **8** (m/z 409.1481), **9** (m/z 409.1484) and **10** (m/z 409.1480) derived from the combination of two $\alpha\text{S}(2)^\bullet$ radicals. Figure S11: High-resolution MS/MS spectra of the two dimeric products **18** (m/z 455.1527) and **19** (m/z 455.1522) derived from the combination of two CBH^\bullet radicals. Figure S12: High-resolution MS/MS spectra of the products **12** (m/z 414.1391), **13** (m/z 414.1393), **16** (m/z 414.1390) and **17** (m/z 414.1393) derived from the cross-termination of αS^\bullet and CBH^\bullet radicals. Figure S13: High-resolution MS/MS spectra of the product **14** (m/z 414.1392) derived from the cross-termination of αS^\bullet and CBH^\bullet radicals.

Author Contributions: Conceptualization, C.C., T.P., K.B. and B.M.; methodology, K.B., T.P., B.M. and C.C.; radiolysis experiments, K.S. and K.B.; photolysis experiments, K.G. and T.P.; software, P.F.; data analysis, C.C., K.B., T.P., K.G., P.F., K.S. and B.M.; writing—original draft preparation, C.C.; writing—review and editing, C.C., K.B., T.P. and B.M.; and funding acquisition, B.M. All authors have read and agreed to the published version of the manuscript.

Funding: This research was funded by the National Science Centre, Poland, project no. UMO-2017/27/B/ST4/00375 and by statutory funds of the Institute of Nuclear Chemistry and Technology (INCT) (K.B. and K.S.).

Data Availability Statement: All data are displayed in the manuscript.

Acknowledgments: Authors would like to thank G. L. Hug from the Notre Dame Radiation Laboratory (US) for critical comments on the results of time-resolved experiments and Tomasz Szredler (INCT, Poland) for his continuous efforts in implementing improvements to the pulse radiolysis setup in the INCT over the last few years.

Conflicts of Interest: The authors declare no conflict of interest. The funders had no role in the design of the study; in the collection, analyses, or interpretation of data; in the writing of the manuscript, or in the decision to publish the results.

References

- Hawkins, C.L.; Davies, M.J. Detection, identification, and quantification of oxidative protein modifications. *J. Biol. Chem.* **2019**, *294*, 19683–19708. [\[CrossRef\]](#)
- Luo, S.; Levine, R.L. Methionine in proteins defends against oxidative stress. *FASEB J.* **2009**, *23*, 464–472. [\[CrossRef\]](#)
- Lim, J.M.; Kim, G.; Levine, R.L. Methionine in Proteins: It's Not Just for Protein Initiation Anymore. *Neurochem. Res.* **2019**, *44*, 247–257. [\[CrossRef\]](#) [\[PubMed\]](#)
- Javitt, G.; Cao, Z.; Resnick, E.; Gabizon, R.; Bulleid, N.J.; Fass, D. Structure and Electron-Transfer Pathway of the Human Methionine Sulfoxide Reductase MsrB3. *Antioxid. Redox Signal.* **2020**, *33*, 665–678. [\[CrossRef\]](#) [\[PubMed\]](#)
- Halliwell, B.; Gutteridge, J.M.C. *Free Radicals in Biology and Medicine*, 5th ed.; Oxford University Press: Oxford, UK, 2015.
- Winterbourn, C.C. Reconciling the chemistry and biology of reactive oxygen species. *Nat. Chem. Biol.* **2008**, *4*, 278–286. [\[CrossRef\]](#) [\[PubMed\]](#)
- Buxton, G.V.; Greenstock, C.L.; Helman, W.P.; Ross, A.B. Critical review of rate constants for reactions of hydrated electrons, hydrogen atoms and hydroxyl radicals ($\bullet\text{OH}/\bullet\text{O}^-$) in aqueous solution. *J. Phys. Chem. Ref. Data* **1988**, *17*, 513–886. [\[CrossRef\]](#)
- Schöneich, C. Radical-Based Damage of Sulfur-Containing Amino Acid Residues. In *Encyclopedia of Radical in Chemistry, Biology and Materials*; Studer, A.S., Ed.; John Wiley & Sons: Chichester, UK, 2012; Volume 3, pp. 1459–1474.
- Schöneich, C. Sulfur Radical-Induced Redox Modifications in Proteins: Analysis and Mechanistic Aspects. *Antioxid. Redox Signal.* **2017**, *26*, 388–405. [\[CrossRef\]](#) [\[PubMed\]](#)
- Schöneich, C.; Bobrowski, K. Intramolecular hydrogen transfer as the key step in the dissociation of hydroxyl radical adducts of (alkylthio)ethanol derivatives. *J. Am. Chem. Soc.* **1993**, *115*, 6538–6547. [\[CrossRef\]](#)
- Houée-Levin, C.; Bobrowski, K. The use of methods of radiolysis to explore the mechanisms of free radical modifications in proteins. *J. Proteom.* **2013**, *92*, 51–62. [\[CrossRef\]](#) [\[PubMed\]](#)
- Glass, R.S.; Hug, G.L.; Schöneich, C.; Wilson, G.S.; Kuznetsova, L.; Lee, T.; Ammam, M.; Lorange, E.; Nauser, T.; Nichol, G.S.; et al. Neighboring Amide Participation in Thioether Oxidation: Relevance to Biological Oxidation. *J. Am. Chem. Soc.* **2009**, *131*, 13791–13805. [\[CrossRef\]](#)

13. Schöneich, C.; Pogocki, D.; Wisniowski, P.; Hug, G.L.; Bobrowski, K. Intramolecular Sulfur-Oxygen Bond Formation in Radical Cations of N-Acetylmethionine Amide. *J. Am. Chem. Soc.* **2000**, *122*, 10224–10225. [\[CrossRef\]](#)
14. Schöneich, C.; Pogocki, D.; Hug, G.L.; Bobrowski, K. Free radical reactions of methionine in peptides: Mechanisms relevant to β -amyloid oxidation and Alzheimer's disease. *J. Am. Chem. Soc.* **2003**, *125*, 13700–13713. [\[CrossRef\]](#) [\[PubMed\]](#)
15. Bobrowski, K.; Hug, G.L.; Pogocki, D.; Marciniak, B.; Schöneich, C. Stabilization of sulfide radical cations through complexation with the peptide bond: Mechanisms relevant to oxidation of proteins containing multiple methionine residues. *J. Phys. Chem. B* **2007**, *111*, 9608–9620. [\[CrossRef\]](#) [\[PubMed\]](#)
16. Hug, G.L.; Bobrowski, K.; Pogocki, D.; Hörner, G.; Marciniak, B. Conformational influence on the type of stabilization of sulfur radical cations in cyclic peptides. *ChemPhysChem* **2007**, *8*, 2202–2210. [\[CrossRef\]](#) [\[PubMed\]](#)
17. Barata-Vallejo, S.; Ferreri, C.; Zhang, T.; Permentier, H.; Bischoff, R.; Bobrowski, K.; Chatgililoglu, C. Radiation chemical studies of Gly-Met-Gly in aqueous solution. *Free Radic. Res.* **2016**, *50*, S24–S39. [\[CrossRef\]](#) [\[PubMed\]](#)
18. Bobrowski, K.; Hug, G.L.; Pogocki, D.; Marciniak, B.; Schöneich, C. Sulfur radical cation peptide bond complex in the one-electron oxidation of S-methylglutathione. *J. Am. Chem. Soc.* **2007**, *129*, 9236–9245. [\[CrossRef\]](#) [\[PubMed\]](#)
19. Barata-Vallejo, S.; Ferreri, C.; Chatgililoglu, C. Radiation chemical studies of methionine in aqueous solution: Understanding the role of molecular oxygen. *Chem. Res. Toxicol.* **2010**, *23*, 258–263. [\[CrossRef\]](#)
20. Torreggiani, A.; Barata-Vallejo, S.; Chatgililoglu, C. Combined Raman and IR spectroscopic studies on the radical-based modifications of methionine. *Anal. Bioanal. Chem.* **2011**, *401*, 1231–1239. [\[CrossRef\]](#) [\[PubMed\]](#)
21. Bobrowski, K.; Houée-Levin, C.; Marciniak, B. Stabilization and Reactions of Sulfur Radical Cations: Relevance to One-Electron Oxidation of Methionine in Peptides and Proteins. *Chimia* **2008**, *62*, 728–734. [\[CrossRef\]](#)
22. Filipiak, P.; Bobrowski, K.; Hug, G.L.; Schöneich, C.; Marciniak, B. N-Terminal Decarboxylation as a Probe for Intramolecular Contact Formation in γ -Glu-(Pro)_n-Met Peptides. *J. Phys. Chem. B* **2020**, *124*, 8082–8098. [\[CrossRef\]](#)
23. Hug, G.L.; Bobrowski, K.; Kozubek, H.; Marciniak, B. Photo-oxidation of Methionine-containing Peptides by the 4-Carboxybenzophenone Triplet State in Aqueous Solution. Competition between Intramolecular Two-centered Three-electron Bonded (S\S)⁺ and (S\N)⁺ Formation. *Photochem. Photobiol.* **2000**, *72*, 1–9. [\[CrossRef\]](#)
24. Ignasiak, M.T.; Marciniak, B.; Houée-Levin, C. A Long Story of Sensitized One-Electron Photo-oxidation of Methionine. *Isr. J. Chem.* **2014**, *54*, 248–253. [\[CrossRef\]](#)
25. Pędzinski, T.; Grzyb, K.; Kaźmierczak, F.; Frański, R.; Filipiak, P.; Marciniak, B. Early Events of Photosensitized Oxidation of Sulfur-Containing Amino Acids Studied by Laser Flash Photolysis and Mass Spectrometry. *J. Phys. Chem. B* **2020**, *124*, 7564–7573. [\[CrossRef\]](#)
26. Mönig, J.; Goslich, R.; Asmus, K.-D. Thermodynamics of S\S 2 σ /1 σ^* three-electron bonds and deprotonation kinetics of thioether radical cations in aqueous solution. *Ber. Bunsenges. Phys. Chem.* **1986**, *90*, 115–121. [\[CrossRef\]](#)
27. Rauk, A.; Yu, D.; Taylor, J.; Shustov, G.V.; Block, D.A.; Armstrong, D.A. Effects of Structure on aC-H Bond Enthalpies of Amino Acid residues: Relevance to H-Transfers in Enzyme mechanisms and in Protein Oxidation. *Biochemistry* **1999**, *38*, 9089–9096. [\[CrossRef\]](#) [\[PubMed\]](#)
28. Chatgililoglu, C.; Crich, D.; Komatsu, M.; Ryu, I. Chemistry of Acyl Radicals. *Chem. Rev.* **1999**, *114*, 1991–2069. [\[CrossRef\]](#)
29. Chatgililoglu, C.; Ferreri, C.; Melchiorre, M.; Sansone, A.; Torreggiani, A. Lipid geometrical isomerism: From chemistry to biology and diagnostics. *Chem. Rev.* **2014**, *114*, 255–284. [\[CrossRef\]](#) [\[PubMed\]](#)
30. Chatgililoglu, C.; Ferreri, C.; Torreggiani, A.; Salzano, A.M.; Renzone, G.; Scaloni, A. Radiation-induced reductive modifications of sulfur-containing amino acids within peptides and proteins. *J. Proteom.* **2011**, *74*, 2263–2273. [\[CrossRef\]](#) [\[PubMed\]](#)
31. Pędzinski, T.; Markiewicz, A.; Marciniak, B. Photosensitized oxidation of methionine derivatives. Laser flash photolysis studies. *Res. Chem. Intermed.* **2009**, *35*, 497–506. [\[CrossRef\]](#)
32. Ignasiak, M.T.; Pędzinski, T.; Rusconi, F.; Filipiak, P.; Bobrowski, K.; Houée-Levin, C.; Marciniak, B. Photosensitized Oxidation of Methionine-Containing Dipeptides. From the Transients to the Final Products. *J. Phys. Chem. B* **2014**, *118*, 8549–8558. [\[CrossRef\]](#)
33. Bobrowski, K. Free radicals in chemistry, biology and medicine: Contribution of radiation chemistry. *Nukleonika* **2005**, *50* (Suppl. 3), S67–S76.
34. Mirkowski, J.; Wiśniowski, P.; Bobrowski, K. *INCT Annual Report 2000*; INCT: Warsaw, Poland, 2001.
35. Schuler, R.H.; Hartzell, A.L.; Behar, B. Track effects in radiation chemistry. Concentration dependence for the scavenging of OH by ferrocyanide in N₂O-saturated aqueous solutions. *J. Phys. Chem.* **1981**, *85*, 192–199. [\[CrossRef\]](#)
36. Janata, E.; Schuler, R.H. Rate constant for scavenging e[−]_{aq} in N₂O-saturated solutions. *J. Phys. Chem.* **1982**, *86*, 2078–2084. [\[CrossRef\]](#)
37. Klassen, N.V.; Shortt, K.R.; Seuntjens, J.; Ross, C.K. Fricke dosimetry: The difference between G(Fe³⁺) for ⁶⁰Co gamma-rays and high-energy X-rays. *Phys. Med. Biol.* **1999**, *44*, 1609–1624. [\[CrossRef\]](#)

Supporting Information

Radiation- and Photo-induced Oxidation Pathways of Methionine in Model Peptide Backbone Under Anoxic Conditions

Tomasz Pedzinski, Katarzyna Grzyb, Konrad Skotnicki, Piotr Filipiak, Krzysztof Bobrowski*, Chrysostomos Chatgililoglu,* Bronisław Marciniak,*

*Corresponding Authors: chrys@isof.cnr.it (C.C.), marcinia@amu.edu.pl (B.M.), kris@ichtj.pl (K.B.)

Contents:

Figures S1, S2 and S3	Page S2
Figures S4 and S5	S3
Figure S6	S4
Figure S7	S5
Figure S8	S6
Figure S9	S7
Figure S10	S8
Figure S11	S9
Figure S12	S10
Figure S13	S11

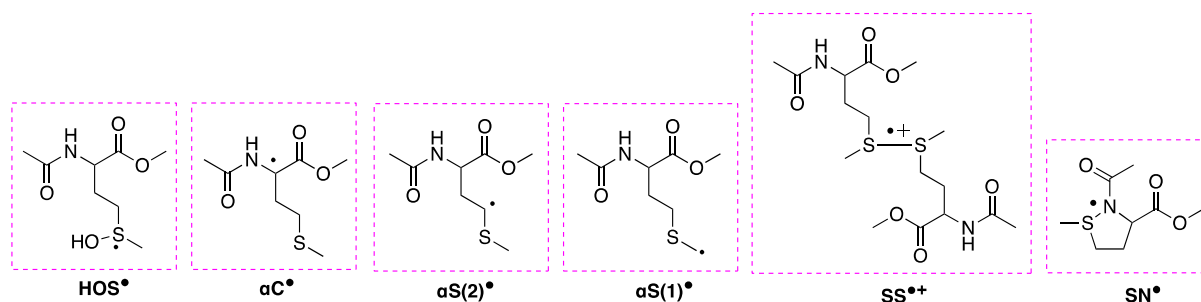


Figure S1. The structures of six reactive intermediates identified in the pulse radiolysis experiments.

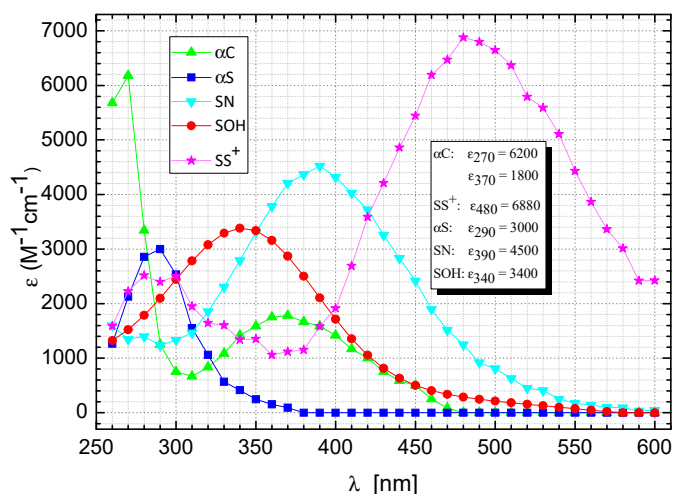


Figure S2. Reference spectra used in the resolutions of the transient absorption spectra following $^\bullet\text{OH}$ -induced oxidation of $\text{CH}_3\text{C}(\text{O})\text{N-Met-OCH}_3$.

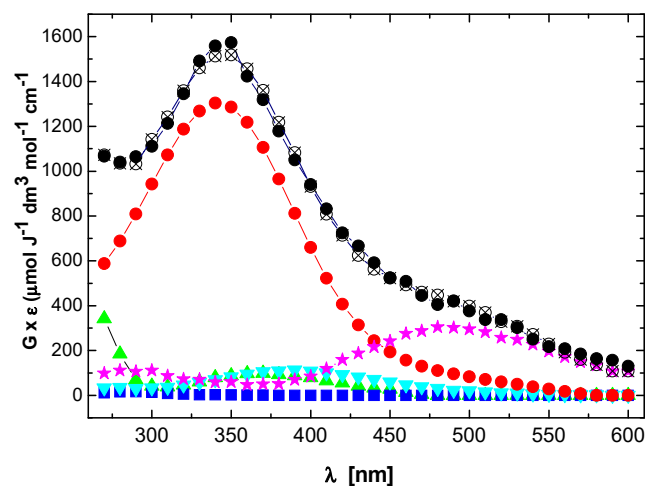


Figure S3. Resolution of the spectral components: HOS^\bullet (●), αC^\bullet (▲), $\alpha\text{S}(1)^\bullet$ and $\alpha\text{S}(2)^\bullet$ (■), $\text{SS}^{\bullet+}$ (★), SN^\bullet (▼) in the transient absorption spectrum recorded 1.1 μs (●— experimental; ⊗— fit) after the electron pulse in N_2O -saturated aqueous solution containing 0.2 mM AcN-Met-OMe at pH 7.0.

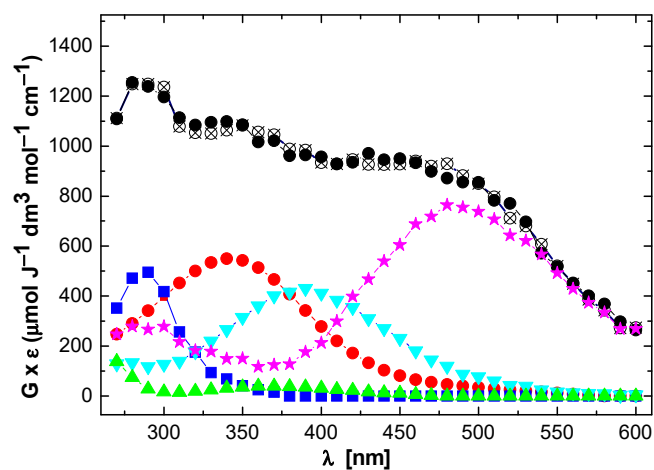


Figure S4. Resolution of the spectral components: HOS^\bullet (●), αC^\bullet (▲), $\alpha\text{S}(1)^\bullet$ and $\alpha\text{S}(2)^\bullet$ (■), $\text{SS}^{\bullet+}$ (★), SN^\bullet (▼) in the transient absorption spectrum recorded 3 μs (●— experimental; ⊗— fit) after the electron pulse in N_2O -saturated aqueous solution containing 0.2 mM AcN-Met-OMe at pH 7.0

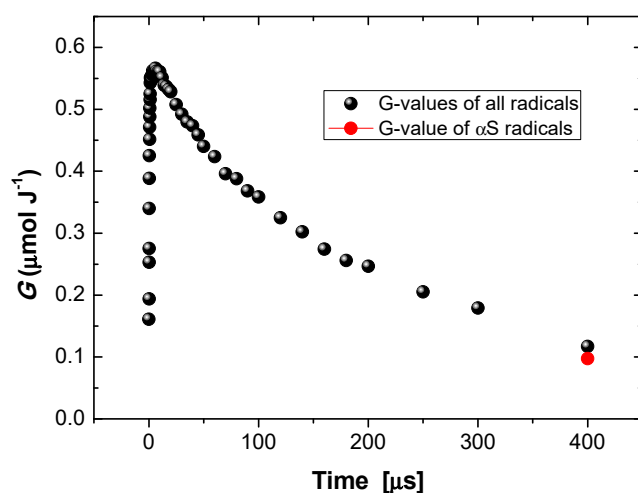


Figure S5. The sum of all radicals (HOS^\bullet , αC^\bullet , $\text{SS}^{\bullet+}$, SN^\bullet , αS^\bullet) taken in spectral resolution as a function of time.

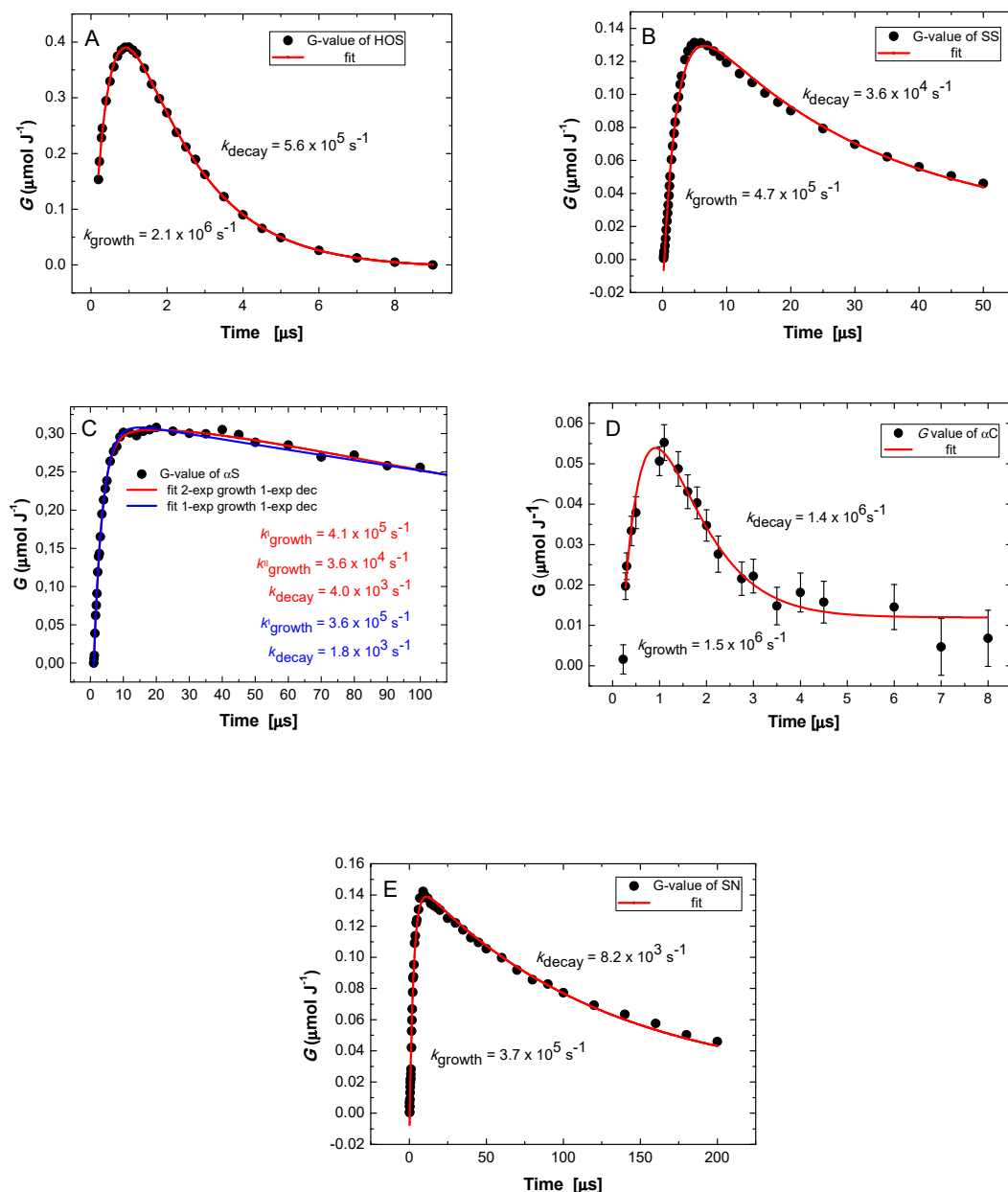
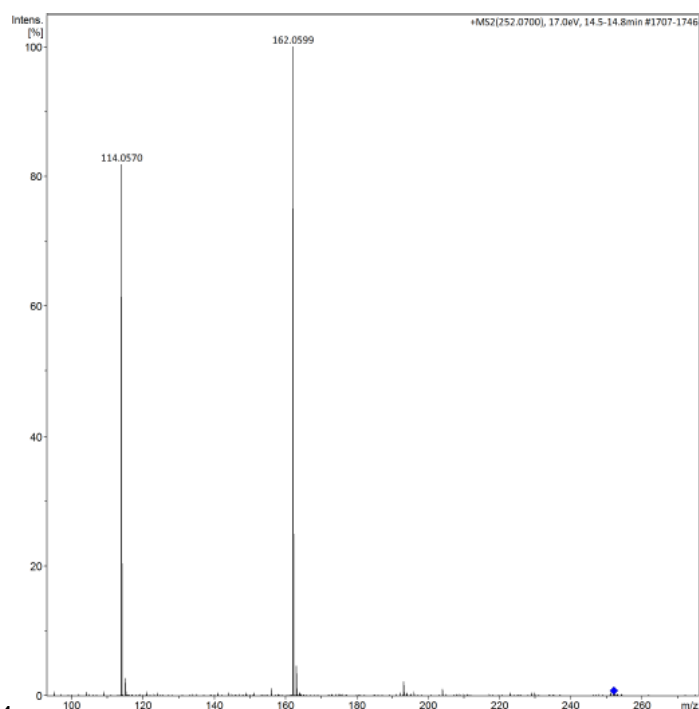
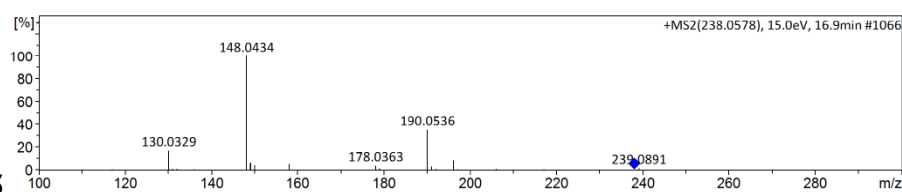


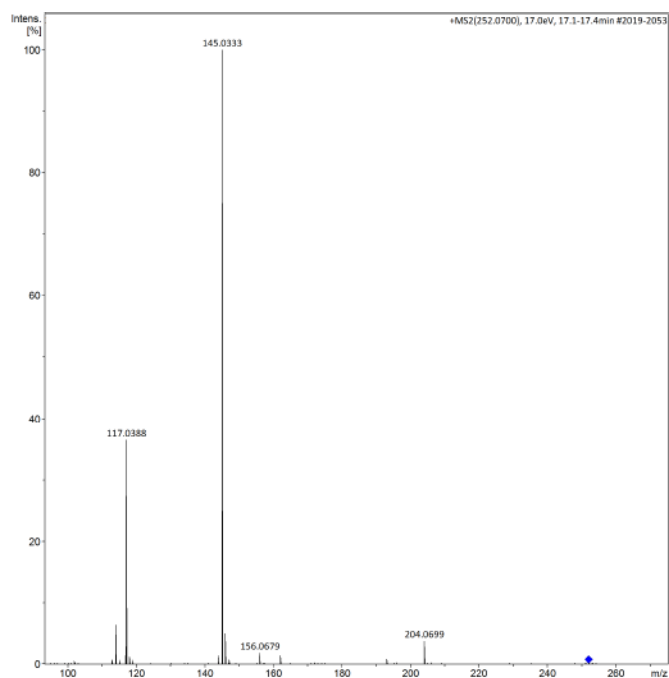
Figure S6. First-order kinetic fits of the growth and decay of radicals HOS• (panel A), SS•⁺ (panel B), αS• (panel C), αC• (panel D), and SN• (panel E).



Compound 4



Compound 5



Compound 6

Figure S7. High-resolution MS/MS spectra of the products **4** (m/z 252.0731) and **6** (m/z 252.0732) derived from the cross-termination of αS (**1**) \cdot and αS (**2**) \cdot with $\text{CH}_3\text{S}\cdot$ and product **5** (m/z 238.0578) – a disulfide.

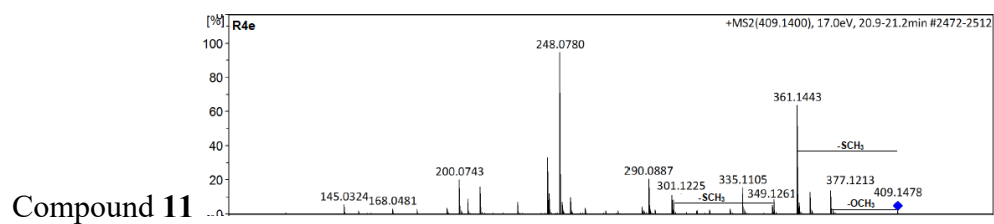
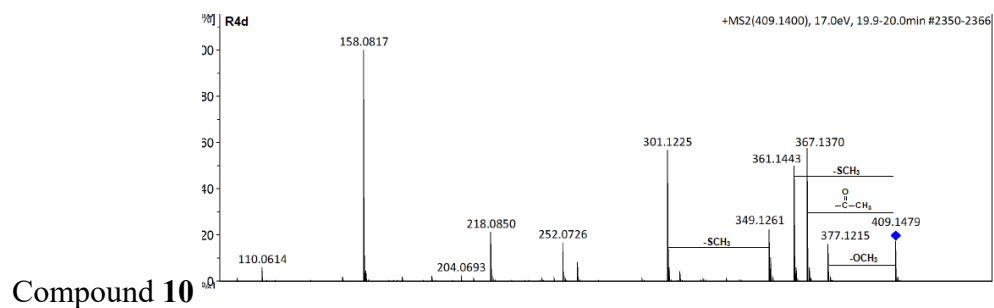
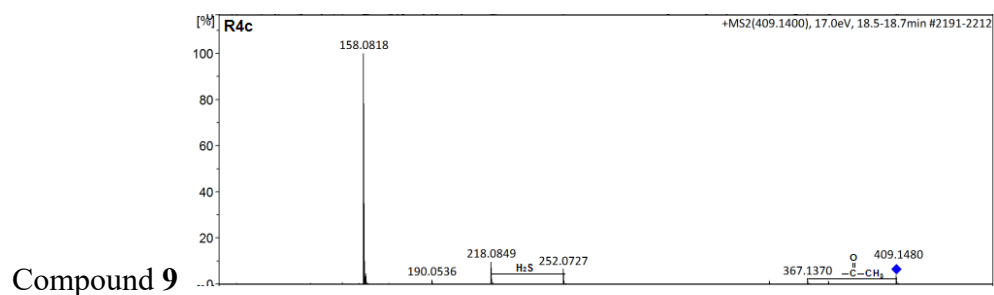
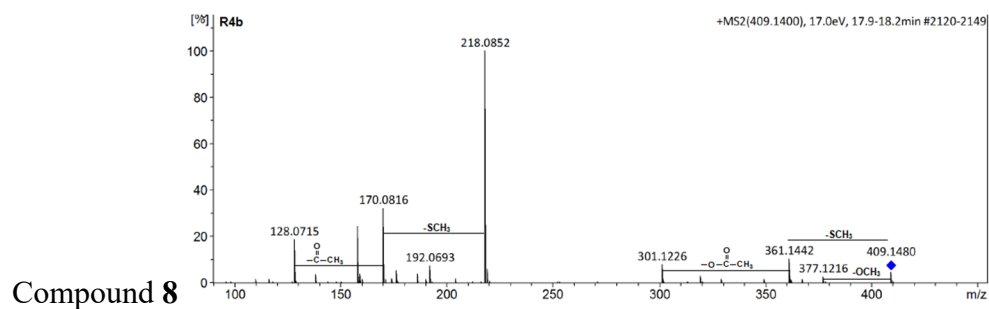
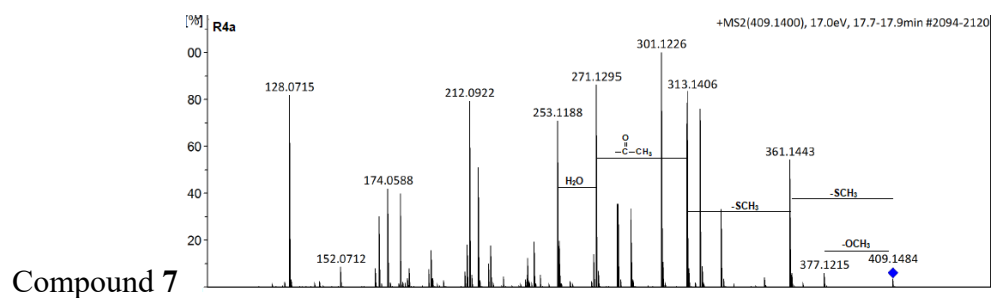


Figure S8. High-resolution MS/MS spectra of the five dimeric products **7** (m/z 409.1484), **8** (m/z 409.1480), **9** (m/z 409.1480), **10** (m/z 409.1479) and **11** (m/z 409.1478) derived from the combination of two αS^\bullet radicals.

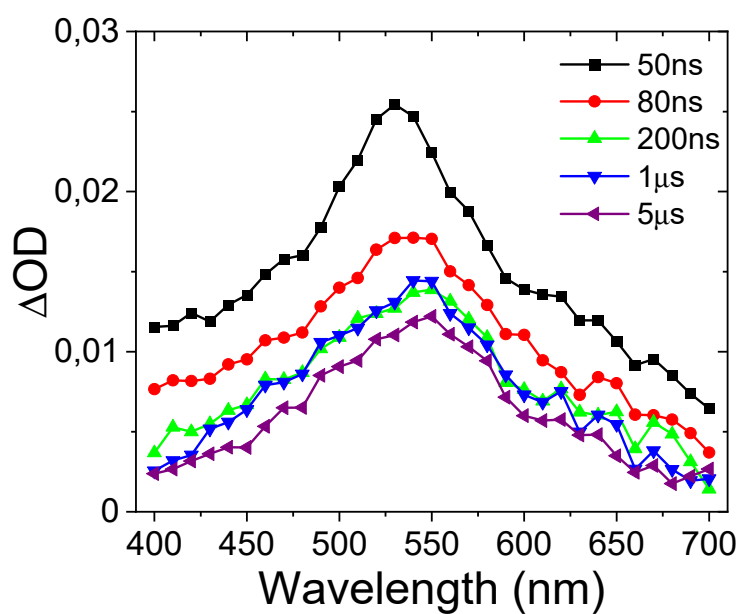
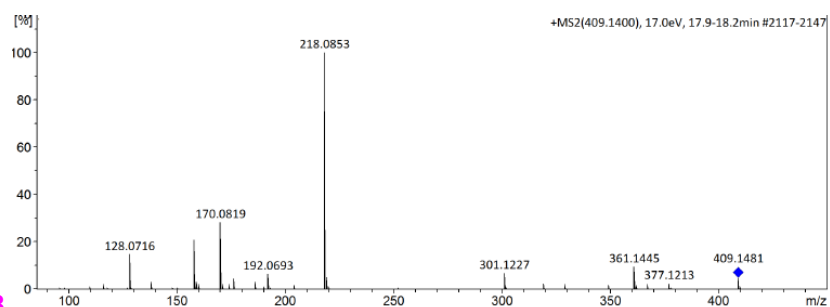
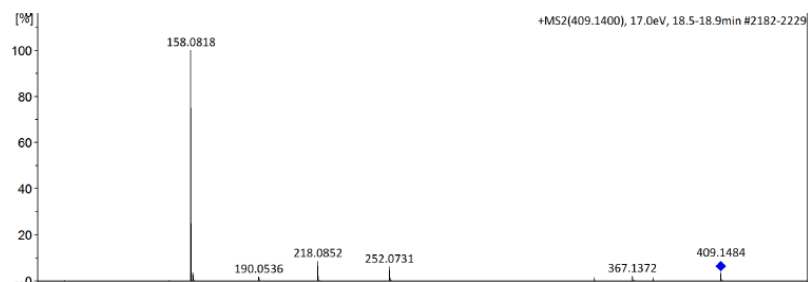


Figure S9. Transient absorption spectra following LFP of CB (4mM) and *N*-AcMetOCH₃ (20mM) for different delay times at pH 7. The initially formed CB excited triplet with a transient absorption maximum at 520 nm (50 ns delay time) yields ketyl radical CBH[•] with a maximum at 550 nm (observed at 1-5 μs timescale).

Photolysis 8



Photolysis 9



Photolysis 10

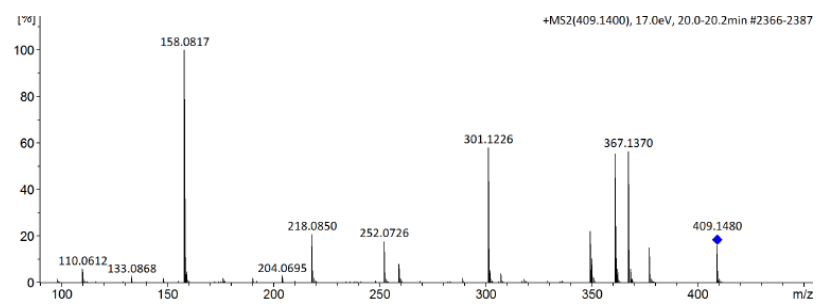
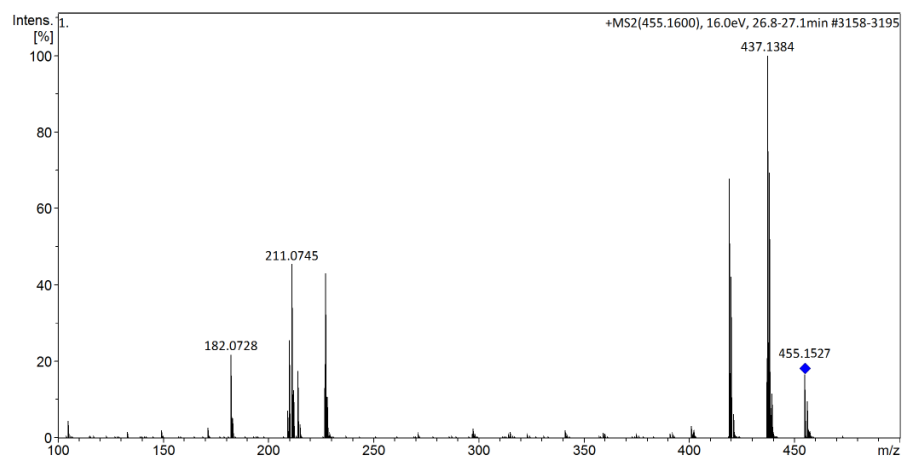


Figure S10. High-resolution MS/MS spectra of the dimeric products **8** (m/z 409.1481), **9** (m/z 409.1484) and **10** (m/z 409.1480) derived from the combination of two $\alpha\text{S}(2)^\bullet$ radicals.

Photolysis 18



Photolysis 19

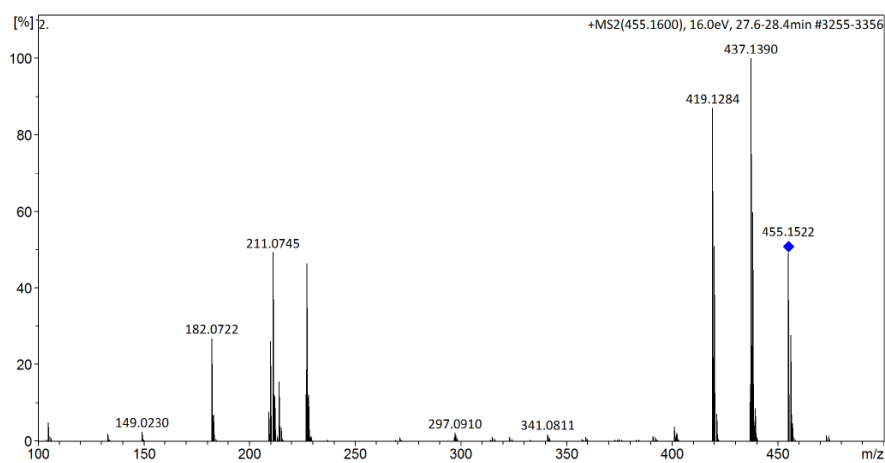
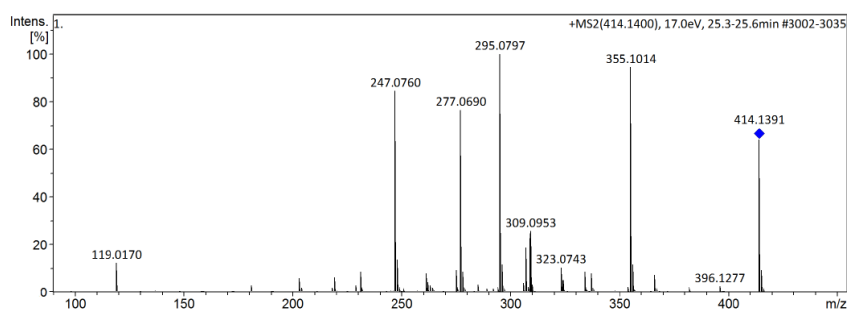
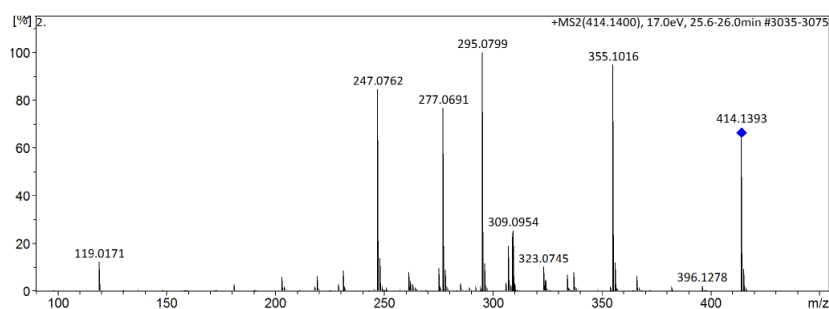


Figure S11. High-resolution MS/MS spectra of the two dimeric products **18** (m/z 455.1527) and **19** (m/z 455.1522) derived from the combination of two **CBH**[•] radicals.

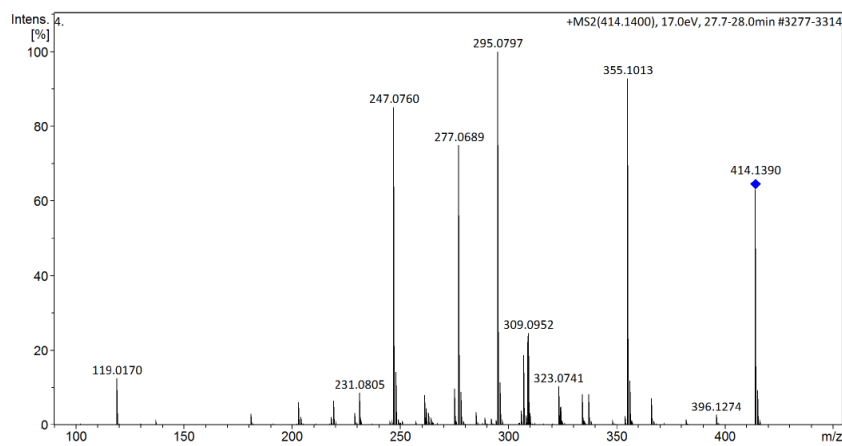
Photolysis 12



Photolysis 13



Photolysis 16



Photolysis 17

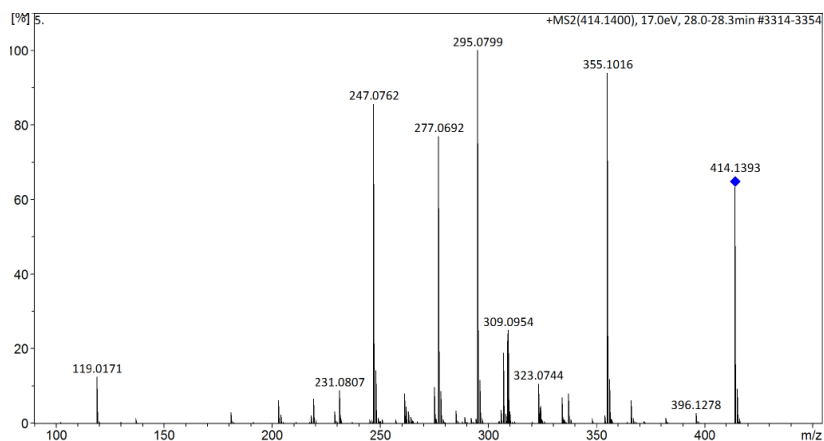


Figure S12. High-resolution MS/MS spectra of the products **12** (m/z 414.1391, **13** (m/z 414.1393), **16** (m/z 414.1390) and **17** (m/z 414.1393) derived from the cross-termination of αS^\bullet and CBH^\bullet radicals.

Photolysis 14

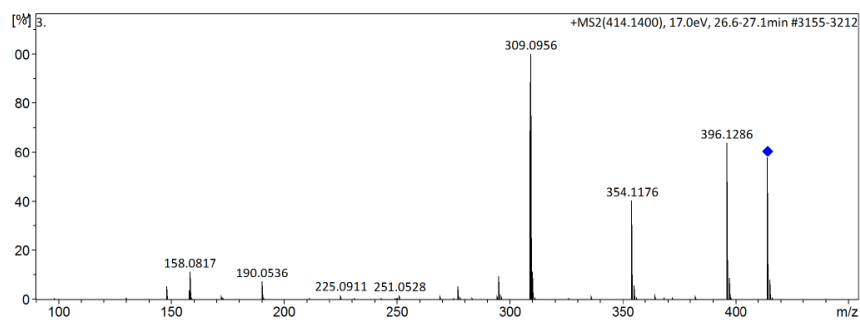


Figure S13. High-resolution MS/MS spectra of the product **14** (m/z 414.1392) derived from the cross-termination of αS^\bullet and CBH^\bullet radicals.

Article

The Fate of Sulfur Radical Cation of N-Acetyl-Methionine: Deprotonation vs. Decarboxylation

Katarzyna Grzyb ¹ , Vidhi Sehrawat ¹  and Tomasz Pedzinski ^{1,2,*} 
¹ Faculty of Chemistry, Adam Mickiewicz University, 61-614 Poznan, Poland

² Center for Advanced Technology, Adam Mickiewicz University, 61-614 Poznan, Poland

* Correspondence: tomekp@amu.edu.pl

Abstract: In the present study, we investigated the photooxidation of the biomimetic model of C-terminal methionine, N-Acetyl-Methionine (N-Ac-Met), sensitized by a 3-Carboxybenzophenone (3CB) excited triplet in neutral and basic aqueous solutions. The short-lived transient species that formed in the reaction were identified and quantified by laser flash photolysis and the final stable products were analyzed using liquid chromatography coupled with high-resolution mass spectrometry (LC-MS) and tandem mass spectrometry (MSMS). Based on these complementary methods, it was possible to calculate the quantum yields of both competing reactions, and the deprotonation was found to be favored over decarboxylation (for neutral pH: $\phi_{-H} = 0.23$ vs. $\phi_{-CO_2} = 0.09$, for basic pH: $\phi_{-H} = 0.23$ vs. $\phi_{-CO_2} = 0.05$). Findings on such a model system, which can possibly mimic the complex protein environment, are important in understanding complicated biological systems, for example, the studied compound, N-Ac-Met, can, to some extent, mimic the methionine in the C-terminal domain of β -amyloid, which is thought to be connected with the pathogenesis of Alzheimer's disease.

Keywords: methionine oxidation; radical coupling; decarboxylation



Citation: Grzyb, K.; Sehrawat, V.; Pedzinski, T. The Fate of Sulfur Radical Cation of N-Acetyl-Methionine: Deprotonation vs. Decarboxylation. *Photochem* **2023**, *3*, 98–108. <https://doi.org/10.3390/photochem3010007>

Academic Editor: Myong Yong Choi

Received: 5 January 2023

Revised: 2 February 2023

Accepted: 3 February 2023

Published: 5 February 2023



Copyright: © 2023 by the authors. Licensee MDPI, Basel, Switzerland. This article is an open access article distributed under the terms and conditions of the Creative Commons Attribution (CC BY) license (<https://creativecommons.org/licenses/by/4.0/>).

1. Introduction

Methionine (Met) is a hydrophobic amino acid with an oxidatively labile thioether group. The oxidative modifications of methionine residue (resulting from the free radical reactions involving neighboring groups) acids are partially reversible via a complex process of enzymatic reduction, playing an important role in the maintenance and protection of the redox status [1].

Methionine in proteins is easily oxidizable, leading to an increase in the side-chain polarity of the residue [2]. As a result, its oxidation has long been regarded as a form of protein damage that occurs randomly in response to oxidative stress. For example, sulfur radical cation sites can interact with tertiary structures of the biosystems [1]. The oxidation also leads to the biological inactivation of hormones, changes in Met-containing proteins, and cataract formation in the eye lens [3]. The one-electron oxidation of methionine-containing compounds has also been closely linked to biological aging and the pathogenesis of neurodegenerative diseases, such as Alzheimer's disease, which are thought to be caused by oxidative stress and characterized by the pathological deposition of amyloid plaques in and around the brain tissue [4–6]. The primary component of the amyloid plaque is a β -amyloid (A β), which is a peptide generally composed of 40 or 42 amino acids containing methionine residue in position 35 (Met35) in its C-terminal domain. The presence of easily oxidized methionine plays a critical role in aggregation, the neurotoxicity of the A β , and secondary radical generation [6,7]. The exact role of Met in proteins is, however, still not fully understood [7]. There is also limited information regarding the possible photoproducts in hypoxic or anaerobic conditions, despite their occurrence in tumors and their destruction using cancer photodynamic therapies [8].

The strongly oxidating hydroxyl radicals ($\bullet\text{OH}$) and excited triplet states of benzophenones as one-electron oxidants have been widely used to study the primary steps of the oxidation of Met-containing peptides [9–15]. In the sensitized photooxidation of methionine-containing compounds, the excited triplet of a sensitizer (for example 3-Carboxybenzophenone, 3CB) accepts an electron from the sulfur moiety, resulting in a charge-transfer (CT) complex that can undergo the following processes: (i) back electron transfer (k_{bet}) yielding reagents in their ground states; (ii) charge separation (k_{sep}) yielding $3\text{CB}^{\bullet-}$ and sulfur radical cation ($>\text{S}^{\bullet+}$); (iii) in-cage proton transfer (k_{H}) from sulfur moiety to $3\text{CB}^{\bullet-}$ yielding relatively stable carbon-centered α -thioalkyl radical (αS). The sulfur radical cation as a primary oxidation product ($>\text{S}^{\bullet+}$) can, furthermore, be stabilized by the interaction with electron-rich atoms (S, N, O) resulting in the formation of inter- and intramolecular three-electron bonded species [16–18].

The fate of the sulfur radical cation is affected by the neighboring groups, for example, the presence of an amide bond eliminates the possibility of proton transfer from the protonated N-terminal group [19–21], and blocking the carboxyl group (for example by esterification) eliminates the possibility of decarboxylation [22,23]. The presence of neighboring amino acid residues with lone pairs from the carboxyl (Asp, Glu), amine (Lys), and hydroxyl groups (Thr, Ser) also impacts the reactions of the sulfur radical cation [24].

In this study, we investigated the one-electron 3CB-sensitized oxidation of the simplest model of C-terminal methionine—N-Acetyl-Methionine (N-Ac-Met, Figure 1). We focused on the competing reactions of sulfur radical cation: decarboxylation and deprotonation that could potentially occur in the methionine residue in the C-terminal domain of β -amyloid.

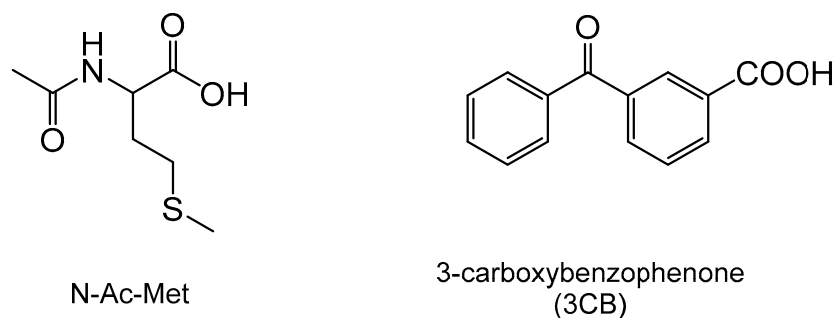


Figure 1. Structure of N-Acetyl-Methionine (N-Ac-Met) and the sensitizer 3-Carboxybenzophenone (3CB).

The stable products of the 3CB-sensitized oxidation of N-Ac-Met have been reported before. In this report, the oxidation products are studied by means of high-resolution mass spectrometry, coupled with high-performance liquid chromatography, steady-state photolysis, and time-resolved flash photolysis.

2. Experimental Section

2.1. Laser Flash Photolysis (LFP)

Nanosecond laser flash photolysis experiments were performed using 3-Carboxybenzophenone (3CB) as a photosensitizer. Samples containing 3CB and N-Ac-Met were excited using 355 nm, the third harmonic of an Nd: YAG laser (Spectral Physics Mountain View, CA, USA, model INDI 40-10) with pulses of 6–8 ns duration. The monitoring system consisted of a 150 W pulsed Xe lamp with a lamp Pulser (Applied Photophysics, Surrey, UK), a monochromator (Princeton Instruments, model Spectra Pro SP-2357, Acton, MA, USA), and an R955 model photomultiplier (Hamamatsu, Japan), powered by a PS-310 power supply (Stanford Research Systems, Sunnyvale, CA, USA). Nd: YAG laser acted as a pump and pulsed Xenon lamp acted as a probe of the exciting sample. A self-constructed flow system was used to avoid the depletion of the starting materials and the accumulation of possible photolysis products. The continuous circulation of aqueous solutions was achieved using a peristaltic pump, followed by simultaneous bubbling with a high purity Argon

for about an hour. All of the flash photolysis experiments were carried out in 1×1 cm rectangular quartz fluorescence cells. Kinetic traces were taken between 370 and 700, at 10 nm intervals. The time-resolved absorption spectra were constructed from the kinetic traces. For the determination of the quantum yields of the transients, relative actinometry was used, taking 3CB in an aqueous solution as the actinometer and $\epsilon_{520} = 5400 \text{ M}^{-1} \text{ cm}^{-1}$ for its triplet-triplet absorption. The concentration profiles were obtained via a multiple linear regression-based software (Decom) using the reference spectra data from the pulse radiolysis studies.

2.2. Steady-State Photolysis

Steady-state photolysis experiments were performed in a 1×1 cm rectangular cell on an optical bench irradiation system using a Genesis CX355STM OPAL laser from Coherent (Santa Clara, CA, USA), with 355 nm emission wavelength (the output power used was set at 50 mW). The concentrations of 3CB and N-Ac-Met were 4.5 mM and 20 mM, respectively.

2.3. Chemicals and Sample Preparation

3CB and N-Ac-Met were purchased from Sigma-Aldrich (St. Louis, MO, USA) and used as received. Water was purified through a Millipore (Merck Milli-Q) system. The pH of the solutions was adjusted by adding potassium hydroxide and/or hydrochloric acid, using a Mettler Toledo Five Easy FE20 pH-meter equipped with a semimicro InLab electrode from Mettler Toledo (Columbus, OH, USA). High purity argon (Linde) was used to purge the freshly prepared solutions of the reagents for photolysis experiments.

2.4. High Performance Liquid Chromatography (HPLC)

The HPLC system (Ultimate 3000, Thermo/Dionex) was equipped with an autosampler, a vacuum degasser, and a diode array detector. Solutions were injected without separation using Chromeleon 7.2. Two eluents were used for the separation and isolation of substrates and stable products after irradiation at 10 and 30 min: eluent A (H_2O) and eluent B (CH_3CN) with 0.1% (*v/v*) formic acid. The separation was achieved with a gradient from 7% to 60% of acetonitrile and water (with 0.1% formic acid), at a flow rate of 0.3 mL/min for 30 min, and the column temperature was set to 45 °C using a C18 reversed-phase analytical column (2.6 μm , 2.1 mm \times 100 mm, Thermo-Scientific).

2.5. Liquid Chromatography-Mass Spectrometry (LC-MS)

The mass spectra were recorded using a hybrid time-of-flight mass spectrometer—QTOF (Impact HD, Bruker). Ions were generated by electrospray ionization (ESI) source under the following conditions: a flow rate of 0.3 mL/min, a nebulizer pressure of 1.5 bar, a capillary voltage of 4000 V, and a drying gas temperature of 200 °C.

3. Results

3.1. Laser Flash Photolysis

The transient absorption spectra obtained from the photosensitized oxidation of **1** (N-Ac-Met) were recorded after different times, after 355 nm laser pulse, and then deconvoluted into individual components (example of the spectral resolution for the time delay of 800 ns for pH 6.7 and 10.7 are presented in Figure 2, panels A and C). The resulting concentrations of each transient species were plotted as a function of time giving the concentration profiles (see Figure 2, panels B and D).

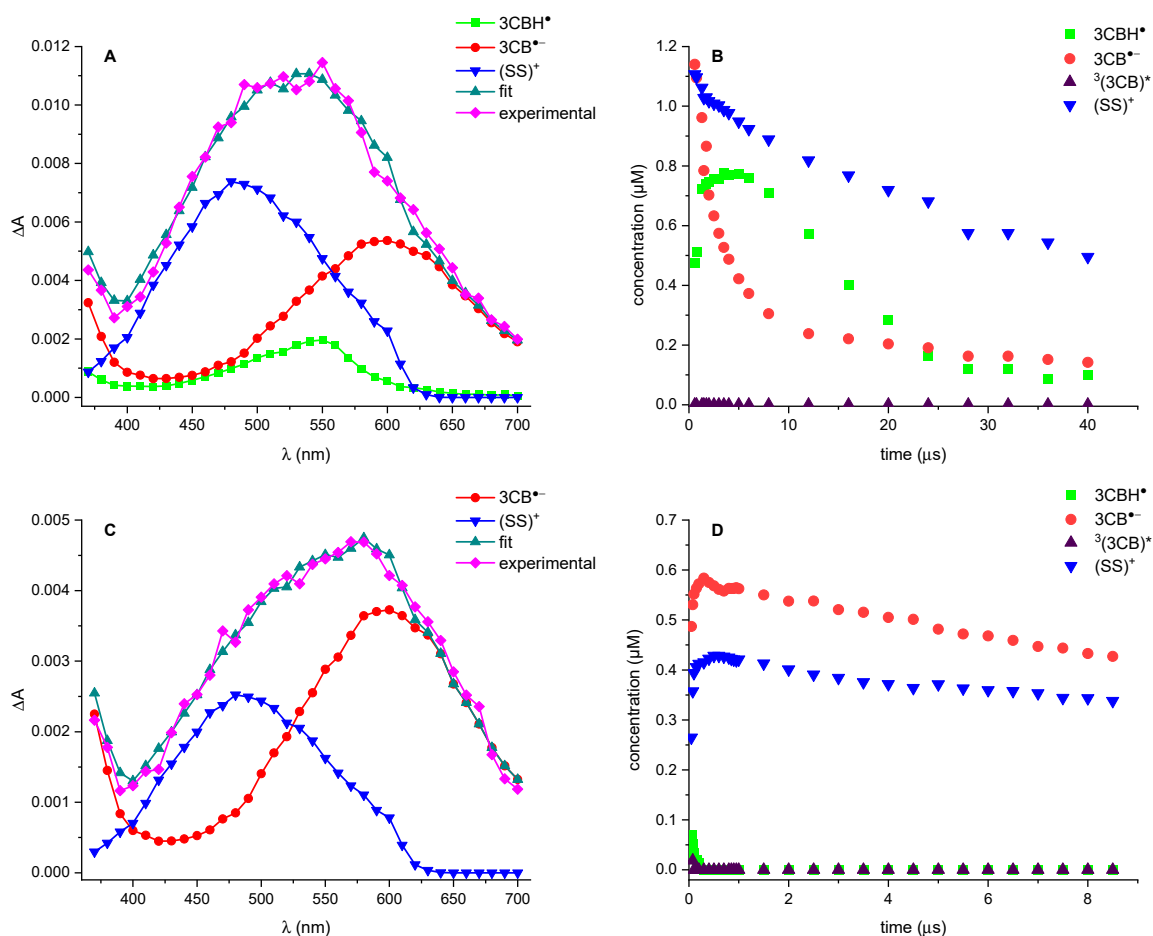


Figure 2. (A) Resolution of the spectral components in the transient absorption spectra 800 ns after laser pulse following quenching of the 3CB (4.5 mM) triplet state by N-Ac-Met (20 mM) at pH 6.7; (B) Concentration profiles calculated at different delay times with respect to the laser pulse for the reaction of 3CB (4.5 mM) excited triplet quenched by N-Ac-Met (20 mM) in aqueous solution at pH = 6.7; (C) Resolution of the spectral components in the transient absorption spectra 800 ns after laser pulse following quenching of the 3CB (4.5 mM) triplet state by N-Ac-Met (20 mM) at pH 10.7; (D) Concentration profiles calculated at different delay times with respect to the laser pulse for the reaction of 3CB (4.5 mM) excited triplet quenched by N-Ac-Met (20 mM) in aqueous solution at pH 10.7.

The same transient species are present at both pHs: ketyl radical 3CBH^\bullet , radical anion $3\text{CB}^{\bullet-}$ and $(\text{S}\cdot\cdot\text{S})^+$. The absence of the triplet excited state (${}^3(3\text{CB})^*$), even at a shorter time, and the high concentration of $(\text{S}\cdot\cdot\text{S})^+$ can be explained by the high concentration of the quencher (20 mM).

At pH 6.7, the initially formed $3\text{CB}^{\bullet-}$ decays, while the concentration of 3CBH^\bullet grows and then decreases, moving toward the equilibrium. On the other hand, in the basic solution, the dominant intermediate is $3\text{CB}^{\bullet-}$; 3CBH^\bullet is present only in small concentrations and for a very short time, and quickly decays.

No stabilization of N-Ac-Met through the formation of $(\text{S}\cdot\cdot\text{N})^+$ was observed ($\lambda_{\text{max}} = 390$ nm, $\epsilon_{390\text{nm}} = 4520$ $\text{M}^{-1} \text{cm}^{-1}$) and no αN (α -amidoalkyl radical) was detected ($\lambda_{\text{max}} = 370$ nm, $\epsilon_{370\text{nm}} = 2000$ $\text{M}^{-1} \text{cm}^{-1}$ [25]). αS ($(\alpha$ -(alkylthio)alkyl radical) was not observed due to its absorption in the UV region $\lambda_{\text{max}} = 290$ nm ($\epsilon_{290\text{nm}} = 3000$ $\text{M}^{-1} \text{cm}^{-1}$) [17], below the experimentally available spectral region (overwhelmed by ground state absorption of 3CB).

The quantum yields, shown in Table 1, were calculated from the initial concentration of the intermediates, which are shown on the concentration profiles in Figure 2. 3CB in an

aqueous solution was used as an internal actinometer. The initial concentration of 3CB* was calculated to be 3.46 μM (pH 6.7) and 1.70 μM (pH 10.7).

Table 1. Quantum Yields of Radical Species Generation from LFP Experiments.

Radical Species	Φ (pH = 6.7)	Φ (pH = 10.7)
3CB $^{\bullet-}$	0.32	0.28
3CBH $^{\bullet}$	0.20	0.10

3.2. LC-MS/MS

The Ar-saturated aqueous solutions containing sensitizer 3CB and N-Ac-Met at a neutral pH were irradiated using a 355 nm continuous-wave laser. Before irradiation, only the starting materials (3CB and N-Ac-Met) were detected using the LC-MS technique. The irradiated samples at pH 6.7 and 10.7 were subjected to further LC-MS analysis.

The irradiation of the samples at both pHs yielded the same products. A representative LC-MS analysis of the solution after 10 min irradiation at pH 6.4 is shown in Figure 3 (LC-MS analysis of the sample before irradiation and irradiated for 30 min as well as the chromatograms of the sample at pH 10.7 can be found in SI in Figure S1 and S2, see Supplementary Materials).

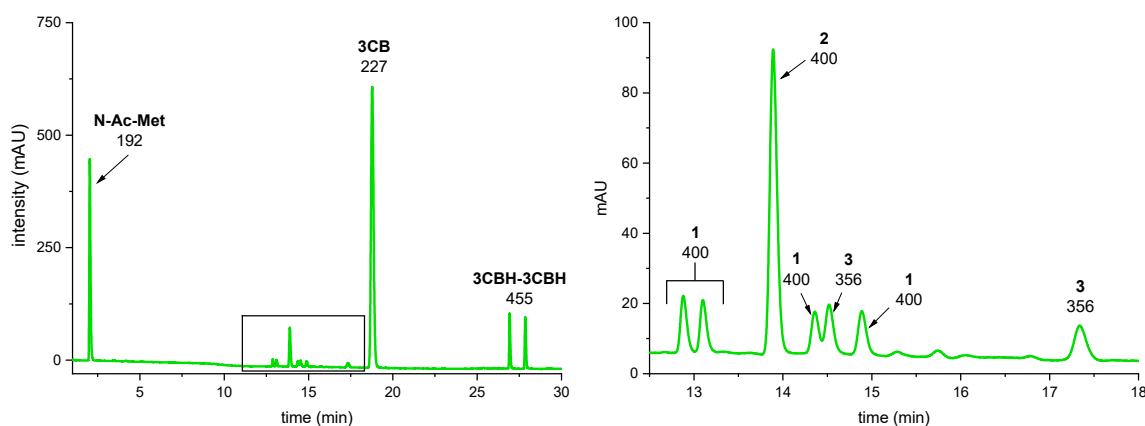


Figure 3. HPLC chromatogram of aqueous solutions containing: N-Ac-Met (20 mM) and 3CB (4.5 mM) at pH 6.4 after 10-min irradiation. The expansion of the chromatograms between 12 and 18 min is shown next to the chromatogram. Peaks are labelled with m/z of the $[M + H]^+$ or $[M + H_2O]^+$ ions of the acquired MS spectrum.

The peaks with m/z 192.0695 and 227.0705 were assigned to the substrates, N-Ac-Met, and 3CB, respectively. The peaks with m/z 455.1501 and 455.1498 were assigned to the products derived from the photosensitizer 3CB: dimers of 3CBH $^{\bullet}$ radicals [26]. Products 1, 2, and 3 were formed in the photooxidation of N-Ac-Met and will be described more closely.

The accurate masses of products 1 and 2 are the same: m/z 400.1240, but their MSMS fragmentations differ significantly, clearly suggesting their isomeric nature. Based on the accurate masses and MSMS fragmentation pattern, it can be deduced that 1 and 2 are the radical cross-coupling product of the αS radical and ketyl radical 3CBH $^{\bullet}$ after the dehydration reaction occurring in the MS source [27–32]. We previously published a detailed explanation of the presence of multiple isomeric αS -3CBH photoproducts in the methionine-containing peptides and a thorough description of the diagnostic ions (circled in red in Figure 4) [22,23]. The MSMS spectra of photoproducts 1 and 2 are shown in Figure 4.

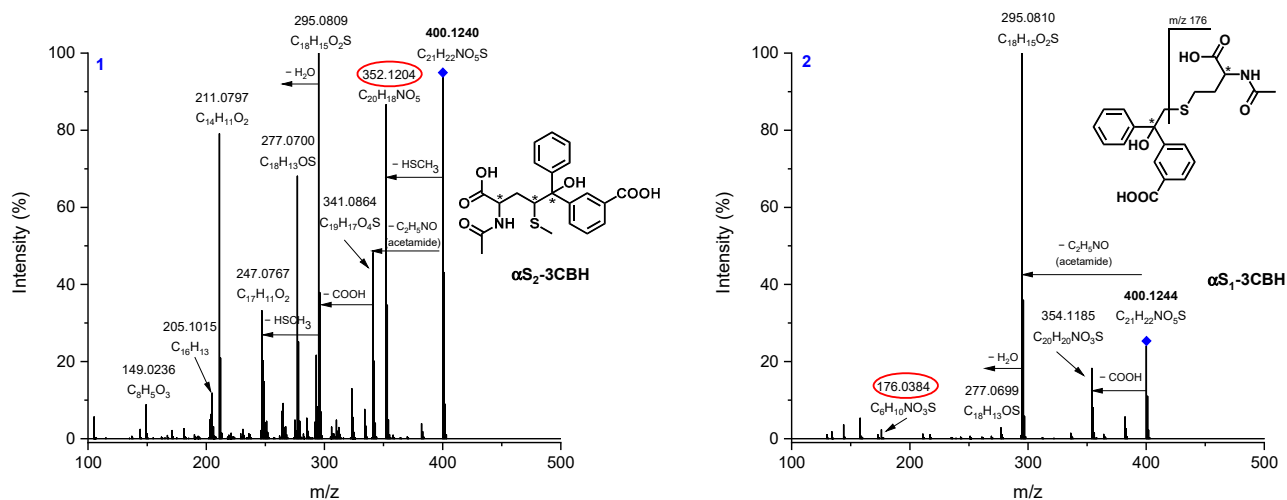


Figure 4. MSMS spectra of photoproducts **1a** and **1b** (fragmentation of m/z 400 ion).

The chromatogram, presented in Figure 3, also shows two peaks, marked 3. Their retention times differ significantly but the accurate masses (m/z 356.1326), as well as the fragmentation patterns, are identical. This m/z corresponds to the molecular formula of $C_{20}H_{22}NO_3$, which can be assigned to the product of the cross-coupling reaction of the αN radical (α -amidoalkyl radical) and the $3CBH^\bullet$ product loss of water molecule (typical reaction occurring in MS ion source [27–32]).

αN radical is formed in the decarboxylation reaction (via pseudo-Kolbe mechanism) from sulfur-centered radical cation $>S^{\bullet+}$ [25] (Figure S3). αN -3CBH has two stereocenters: one is fixed (S) and the other one can have either a R or S configuration, giving two possible diastereoisomers (SS and SR); consequently, there are two peaks on the chromatogram corresponding to these stereoisomers.

The main fragmentation patterns of photoproducts 3 (Figures 5 and S4) correspond to the loss of the $-HSCH_3$ group and the amide bond cleavage (loss of the acetyl group). Other fragment ions were formed after the neutral losses of water molecules and ammonia.

The exact masses of the diagnostic ions from the MSMS experiments that allowed us to suggest the structures of photoproducts are collected in Table 2.

It is noteworthy that no products of αS - αS , αN - αN , or αS - αN radical-coupling were detected, suggesting that virtually all of the αS and αN radicals were ultimately trapped by $3CBH^\bullet$.

Table 2. High-resolution MSMS data for the products of N-Ac-Met oxidation.

Photoproduct	Accurate Mass (Measured)	Exact Mass (Calculated)	Mass Accuracy (ppm)	Molecular Composition
1 (αS_2 -3CBH)	400.1240	400.1219	5.33	$C_{21}H_{22}NO_5S$
2 (αS_1 -3CBH)	400.1244	400.1219	6.33	$C_{21}H_{22}NO_5S$
3 (αN -3CBH)	356.1326	356.1320	1.57	$C_{20}H_{22}NO_3S$

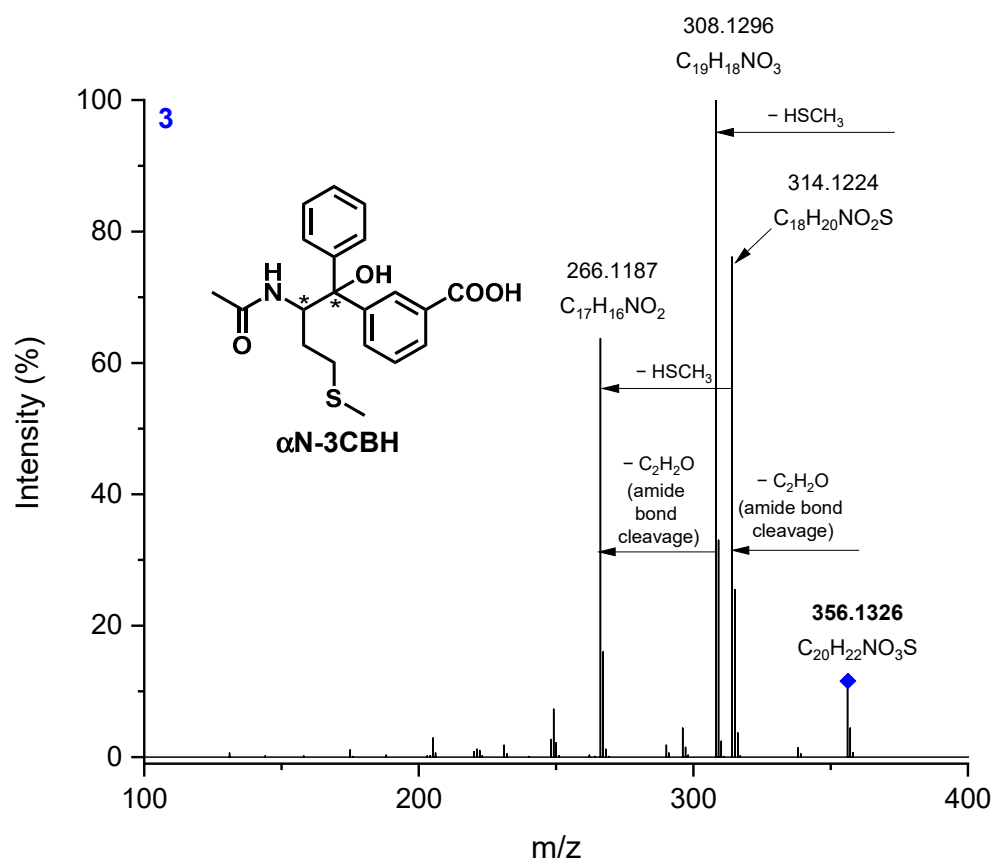


Figure 5. MSMS spectrum of photoproduct 3 (fragmentation of m/z 356 ion).

The quantum yields of the two competing reactions, the deprotonation (formation of α S-3CBH products) and decarboxylation (formation of α N-3CBH products) of N-Ac-Met, are summarized in Table 3. The calculations were based on the quantum yield of the charge separation reaction (k_{sep}) and the ratio of the area under the peaks of the formed photoproducts observed on the chromatogram (Figures 3 and S1), assuming that the α S-3CBH and α N-3CBH photoproducts have the same molar absorption coefficient. The ratio of the photoproducts was the same after 10 and 30 min of irradiation.

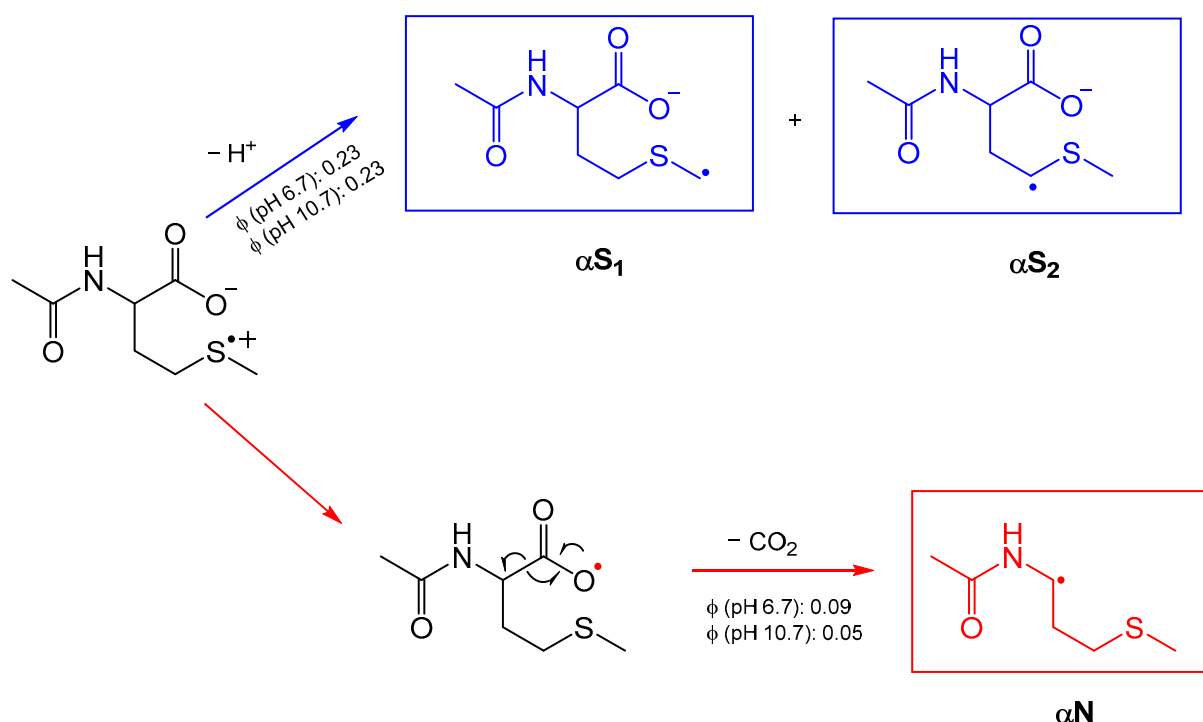
Table 3. Quantum yields of two competing reactions of sulfur radical cation of N-Ac-Met (1)^a.

Reaction Pathway	Φ at pH = 6.4	Φ at pH = 10.7
Deprotonation (α S)	0.23	0.23
Decarboxylation (α N)	0.09	0.05

^a $\pm 15\%$ experimental error.

4. Discussion

The suggested fate of the sulfur radical cation $>S^{\bullet+}$ is presented in Scheme 1. This cation can undergo two competing reactions: deprotonation, yielding α -thioalkyl radical (α S); or decarboxylation via a pseudo-Kolbe reaction, which involves the intramolecular electron transfer from the carboxylate group to the sulfur radical cation, leading to the decarboxylation and formation of α -amidoalkyl radical (α N).



Scheme 1. Two pathways of N-Ac-Met sulfur radical cation: deprotonation yielding two isomeric αS radicals, and decarboxylation yielding αN radical.

Neither αS nor αN radicals could be detected in the LFP experiments; therefore, the reaction paths of the sulfur radical cation were deduced from the analysis of the stable products, carried out using high-resolution mass spectrometry. The stable products formed in the radical cross-coupling reaction of αS and αN with 3CB ketyl are unique and sensitive markers for deprotonation and decarboxylation processes. The αN -3CBH photoproducts were formed at both pH = 6.7 and 10.7; as the carboxylic group is deprotonated (pK_a of the carboxylic group of methionine is 2.16 [33]), the decarboxylation via pseudo-Kolbe mechanism is possible.

One may expect that the decarboxylation of N-Ac-Met with its free carboxylic group should be a common reaction but, contrary to our results, the previously reported quantum yields of decarboxylation in sensitized oxidation was found to be negligible [10,19,34,35]. The earlier results were based on the less sensitive techniques, e.g., laser flash photolysis, pulse radiolysis studies, and CO_2 detection using gas chromatography [24,36,37].

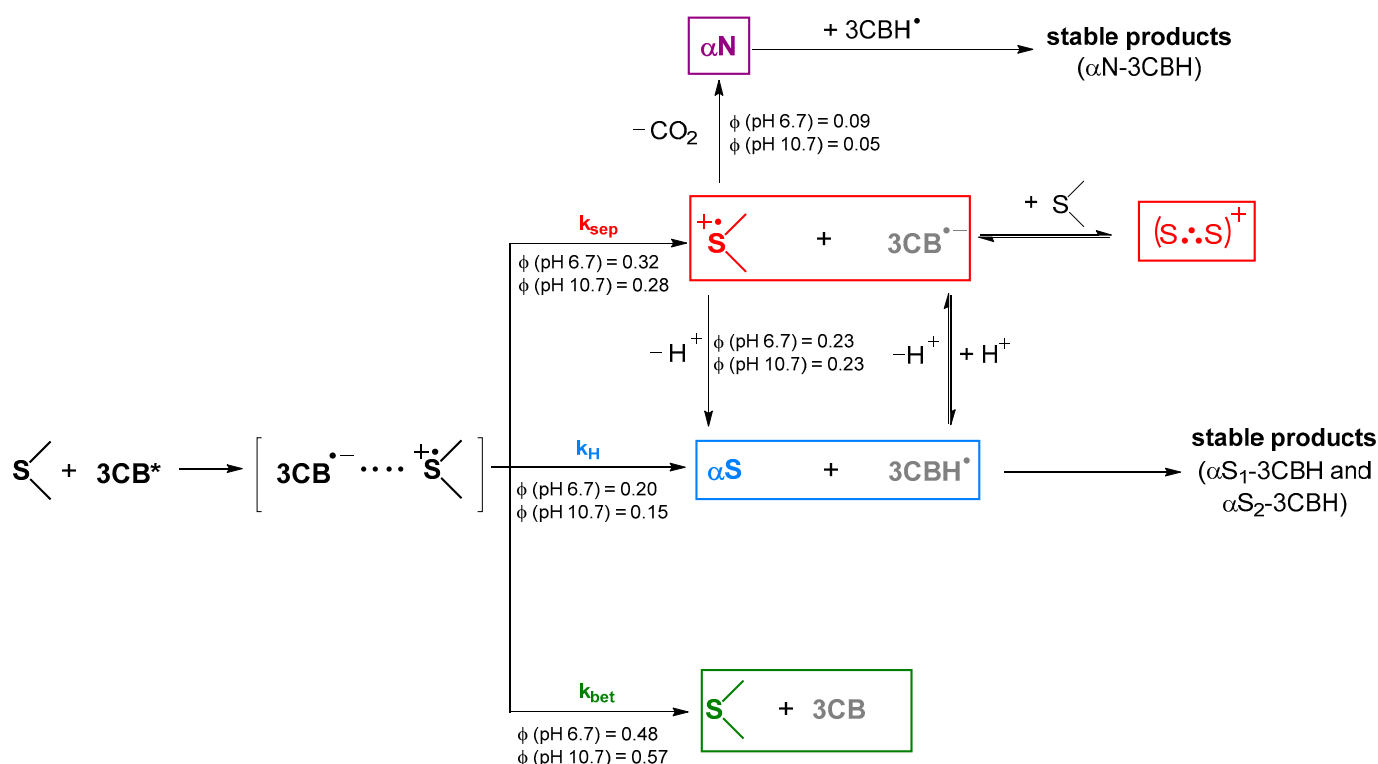
5. Conclusions

In the current paper, we investigated the competition between the deprotonation and decarboxylation of the sulfur radical cation $>\text{S}^{\bullet+}$ of N-Acetyl-Methionine (N-Ac-Met). All of the stable products of 3CB-sensitized oxidation of N-Ac-Met were characterized using LC-MS and MSMS. The accurate masses of the products and the MSMS fragmentation patterns provided the molecular formula and structural information of the photoproducts and, based on that information, their precursor radicals.

The α -thioalkyl radicals (αS) are formed as a result of the deprotonation of $>\text{S}^{\bullet+}$, and eventually lead to the radical cross-coupling isomeric products 1 and 2. The α -amidoalkyl radicals (αN), resulting from the decarboxylation of $>\text{S}^{\bullet+}$, formed photoproducts 3. We provided experimental proof for the decarboxylation of N-Ac-Met, which was previously neglected. Based on the LC-MSMS technique, we found the marker of decarboxylation with a much higher sensitivity than the previously utilized methods: the formation of the stable photoproducts αN -3CBH could act as a probe for decarboxylation as αN radicals are formed only after the loss of CO_2 .

The calculated free-radical reaction yields showed that the preferred reaction pathway of $>\text{S}^{\bullet+}$ is deprotonation ($\phi = 0.23$ for both pH for deprotonation vs. $\phi = 0.09$ at pH 6.7 and $\phi = 0.09$ at pH 10.7 for decarboxylation).

Based on the results from the time-resolved experiments (laser flash photolysis) and stable product analysis (LC-MS and MSMS), the complete mechanism, including the quantum yields of the reactions, of the photosensitized oxidation of N-Acetyl-Methionine is proposed in Scheme 2.



Scheme 2. Mechanism of 3CB* photosensitized oxidation of N-Ac-Met.

In summary, we have presented key insights into the free radical reaction pathways of the biologically relevant methionine residue, which mimics the Met35 in the C-terminal domain of β amyloid. The results of this research offer the first step in the long journey of explaining the pathway leading to the irreversible modifications and damages in protein that cause Alzheimer's disease.

Supplementary Materials: The following supporting information can be downloaded at: <https://www.mdpi.com/article/10.3390/photochem3010007/s1>, Figure S1: HPLC chromatograms of aqueous solutions containing: N-Ac-Met (20 mM) and 3CB (4.5 mM) at pH 6.7 before irradiation (top panel, red), after 10-minute irradiation (middle panel, green) and after 30-minute irradiation (bottom panel, blue). The expansion of the chromatograms after irradiation between 12 and 18 minutes is shown next to the chromatograms. Peaks are labelled with m/z of the $[\text{M} + \text{H}]^+$ or $[\text{M} + \text{H}_2\text{O}]^+$ ions of the acquired MS spectrum.; Figure S2: HPLC chromatograms of aqueous solutions containing: N-Ac-Met (20 mM) and 3CB (4.5 mM) at pH 10.7 before irradiation (top panel, orange), after 10-minute irradiation (middle panel, dark green) and after 30-minute irradiation (bottom panel, purple). The expansion of the chromatograms after irradiation between 12 and 18 minutes is shown next to the chromatograms. Peaks are labelled with m/z of the $[\text{M} + \text{H}]^+$ or $[\text{M} + \text{H}_2\text{O}]^+$ ions of the acquired MS spectrum.; Figure S3: The mechanism of the pseudo-Kolbe reaction.; Figure S4: MSMS spectra of photoproducts 3 at retention time 14.5 and 17.3 min.

Author Contributions: Conceptualization, T.P.; methodology, T.P., V.S. and K.G.; validation, T.P.; investigation, K.G. and V.S.; writing—original draft preparation, V.S., K.G.; writing—review and editing, T.P. and K.G.; visualization, V.S., K.G.; supervision, T.P.; funding acquisition, T.P., K.G. All authors have read and agreed to the published version of the manuscript.

Funding: This research was supported by the Initiative of Excellence—Research University at Adam Mickiewicz University, project no. 006/07/POB3/0004 and project no. 017/02/SNŚ/0008.

Data Availability Statement: Not applicable.

Acknowledgments: Not applicable.

Conflicts of Interest: The authors declare no conflict of interest.

References

- Berges, J.; Trouillas, P.; Houée-Levin, C. Oxidation of protein tyrosine or methionine residues: From the amino acid to the peptide. *J. Phys. Conf. Ser.* **2011**, *261*, 012003. [\[CrossRef\]](#)
- Wang, Z.-Y.; Shimonaga, M.; Muraoka, Y.; Kobayashi, M.; Nozawa, T. Nozawa, Methionine oxidation and its effect on the stability of a reconstituted subunit of the light-harvesting complex from *Rhodospirillum rubrum*: Methionine oxidation and its effect on LH1 subunit. *JBIC J. Biol. Inorg. Chem.* **2001**, *268*, 3375–3382. [\[CrossRef\]](#)
- Schöneich, C.; Bobrowski, K.; Holcman, J.; Asmus, K.-D. Oxidation mechanisms of methionine containing peptides by hydroxyl and peroxy radicals. In *Oxidative Damage Repair*; Elsevier: Amsterdam, The Netherlands, 1991; pp. 380–385. [\[CrossRef\]](#)
- Chen, G.F.; Xu, T.H.; Yan, Y.; Zhou, Y.R.; Jiang, Y.; Melcher, K.; Xu, H.E. Amyloid beta: Structure, biology and structure-based therapeutic development. *Acta Pharmacol. Sin.* **2017**, *38*, 1205–1235. [\[CrossRef\]](#) [\[PubMed\]](#)
- Thal, D.R.; Fändrich, M. Protein aggregation in Alzheimer's disease: A β and τ and their potential roles in the pathogenesis of AD. *Acta Neuropathol.* **2015**, *129*, 163–165. [\[CrossRef\]](#)
- Butterfield, D.A.; Sultana, R. Methionine-35 of A β (1–42): Importance for Oxidative Stress in Alzheimer Disease. *J. Amino Acids* **2011**, *2011*, 198430. [\[CrossRef\]](#)
- Schöneich, C. Redox Processes of Methionine Relevant to β -Amyloid Oxidation and Alzheimer's Disease. *Arch. Biochem. Biophys.* **2002**, *397*, 370–376. [\[CrossRef\]](#)
- Ignasiak, M.T.; Marciniak, B.; Houée-Levin, C. A Long Story of Sensitized One-Electron Photo-oxidation of Methionine. *Isr. J. Chem.* **2014**, *54*, 248–253. [\[CrossRef\]](#)
- Bobrowski, K.; Marciniak, B.; Hug, G.L. 4-Carboxybenzophenone-sensitized photooxidation of sulfur-containing amino acids. Nanosecond laser flash photolysis and pulse radiolysis studies. *J. Am. Chem. Soc.* **1992**, *114*, 10279–10288. [\[CrossRef\]](#)
- Bobrowski, K.; Houée-Levin, C.; Marciniak, B. Stabilization and Reactions of Sulfur Radical Cations: Relevance to One-Electron Oxidation of Methionine in Peptides and Proteins. *Chimia* **2008**, *62*, 728. [\[CrossRef\]](#)
- Pedzinski, T.; Bobrowski, K.; Ignasiak, M.; Kciuk, G.; Hug, G.L.; Lewandowska-Andralojc, A.; Marciniak, B. 3-Carboxybenzophenone (3-CB) as an efficient sensitizer in the photooxidation of methionyl-leucine in aqueous solutions: Spectral, kinetic and acid–base properties of 3-CB derived transients. *J. Photochem. Photobiol. A Chem.* **2014**, *287*, 1–7. [\[CrossRef\]](#)
- Bobrowski, K.; Hug, G.L.; Pogocki, D.; Marciniak, B.; Schöneich, C. Stabilization of Sulfide Radical Cations through Complexation with the Peptide Bond: Mechanisms Relevant to Oxidation of Proteins Containing Multiple Methionine Residues. *J. Phys. Chem. B* **2007**, *111*, 9608–9620. [\[CrossRef\]](#) [\[PubMed\]](#)
- Pedzinski, T.; Markiewicz, A.; Marciniak, B. Photosensitized oxidation of methionine derivatives. Laser flash photolysis studies. *Res. Chem. Intermed.* **2009**, *35*, 497–506. [\[CrossRef\]](#)
- Bobrowski, K.; Hug, G.L.; Pogocki, D.; Marciniak, B.; Schöneich, C. Sulfur Radical Cation–Peptide Bond Complex in the One-Electron Oxidation of S-Methylglutathione. *J. Am. Chem. Soc.* **2007**, *129*, 9236–9245. [\[CrossRef\]](#)
- Goez, M.; Rozwadowski, J.; Marciniak, B. CIDNP Spectroscopic Observation of (S:•+N) Radical Cations with a Two-Center Three-Electron Bond During the Photooxidation of Methionine. *Angew. Chem. Int. Ed.* **1998**, *37*, 628–630. [\[CrossRef\]](#)
- Glass, R.S. Neighboring Group Participation: General Principles and Application to Sulfur-Centered Reactive Species. In *Sulfur-Centered Reactive Intermediates in Chemistry and Biology*; Chatgililoglu, C., Asmus, K.-D., Eds.; Springer: Boston, MA, USA, 1990; pp. 213–226. [\[CrossRef\]](#)
- Hiller, K.-O.; Asmus, K.-D. Oxidation of Methionine by X in Aqueous Solution and Characterization of Some Three-electron Bonded Intermediates. A Pulse Radiolysis Study. *Int. J. Radiat. Biol. Relat. Stud. Phys. Chem. Med.* **1981**, *40*, 583–595. [\[CrossRef\]](#) [\[PubMed\]](#)
- Asmus, K.-D. Sulfur-Centered Three-Electron Bonded Radical Species. In *Sulfur-Centered Reactive Intermediates in Chemistry and Biology*; Chatgililoglu, C., Asmus, K.-D., Eds.; Springer: Boston, MA, USA, 1990; pp. 155–172. [\[CrossRef\]](#)
- Hug, G.L.; Bobrowski, K.; Kozubek, H.; Marciniak, B. Photooxidation of Methionine Derivatives by the 4-Carboxybenzophenone Triplet State in Aqueous Solution. Intracomplex Proton Transfer Involving the Amino Group. *Photochem. Photobiol.* **1998**, *68*, 785–796. [\[CrossRef\]](#)
- Pedzinski, T.; Kazmierczak, F.; Filipiak, P.; Marciniak, B. Oxidation studies of a novel peptide model N-acetyl-3-(methylthio)propylamine. *J. Photochem. Photobiol. A Chem.* **2017**, *336*, 98–104. [\[CrossRef\]](#)

21. Hashimoto, M.; Eda, Y.; Osanai, Y.; Iwai, T.; Aoki, S. A novel decarboxylation of α -amino acids. a facile method of decarboxylation by the use of 2-cyclohexen-1-one as a catalyst. *Chem. Lett.* **1986**, *15*, 893–896. [[CrossRef](#)]
22. Pedzinski, T.; Grzyb, K.; Kaźmierczak, F.; Frański, R.; Filipiak, P.; Marciniak, B. Early Events of Photosensitized Oxidation of Sulfur-Containing Amino Acids Studied by Laser Flash Photolysis and Mass Spectrometry. *J. Phys. Chem. B* **2020**, *124*, 7564–7573. [[CrossRef](#)]
23. Pedzinski, T.; Grzyb, K.; Skotnicki, K.; Filipiak, P.; Bobrowski, K.; Chatgililoglu, C.; Marciniak, B. Radiation- and Photo-Induced Oxidation Pathways of Methionine in Model Peptide Backbone under Anoxic Conditions. *Int. J. Mol. Sci.* **2021**, *22*, 4773. [[CrossRef](#)]
24. Marciniak, B.; Hug, G.L.; Bobrowski, K.; Kozubek, H. Mechanism of 4-carboxybenzophenone-sensitized photooxidation of methionine-containing dipeptides and tripeptides in aqueous solution. *J. Phys. Chem.* **1995**, *99*, 13560–13568. [[CrossRef](#)]
25. Filipiak, P.; Bobrowski, K.; Hug, G.L.; Schöneich, C.; Marciniak, B. N-Terminal Decarboxylation as a Probe for Intramolecular Contact Formation in γ -Glu-(Pro)n-Met Peptides. *J. Phys. Chem. B* **2020**, *124*, 8082–8098. [[CrossRef](#)] [[PubMed](#)]
26. Grzyb, K.; Frański, R.; Pedzinski, T. Sensitized photoreduction of selected benzophenones. Mass spectrometry studies of radical cross-coupling reactions. *J. Photochem. Photobiol. B Biol.* **2022**, *234*, 112536. [[CrossRef](#)] [[PubMed](#)]
27. Xu, S.; Pavlov, J.; Attygalle, A.B. Collision-induced dissociation processes of protonated benzoic acid and related compounds: Competitive generation of protonated carbon dioxide or protonated benzene: CID spectra of protonated benzoic acids. *J. Mass Spectrom.* **2017**, *52*, 230–238. [[CrossRef](#)]
28. Frański, R.; Zalas, M.; Gierczyk, B.; Schroeder, G. Electro-oxidation of diclofenac in methanol as studied by high-performance liquid chromatography/electrospray ionization mass spectrometry: Letter to the Editor. *Rapid Commun. Mass Spectrom.* **2016**, *30*, 1662–1666. [[CrossRef](#)]
29. Balta, B.; Aviyente, V.; Lifshitz, C. Elimination of water from the carboxyl group of GlyGlyH⁺. *J. Am. Soc. Mass Spectrom.* **2003**, *14*, 1192–1203. [[CrossRef](#)]
30. Ma, Y.-C.; Kim, H.-Y. Determination of steroids by liquid chromatography/mass spectrometry. *J. Am. Soc. Mass Spectrom.* **1997**, *8*, 1010–1020. [[CrossRef](#)]
31. D'Agostino, P.; Provost, L.; Hancock, J. Analysis of mustard hydrolysis products by packed capillary liquid chromatography–electrospray mass spectrometry. *J. Chromatogr. A* **1998**, *808*, 177–184. [[CrossRef](#)]
32. da Silva, L.A.; Sandjo, L.P.; Misturini, A.; Caramori, G.F.; Biavatti, M.W. ESI-QToF-MS characterization of hirsutinolide and glaucolide sesquiterpene lactones: Fragmentation mechanisms and differentiation based on Na⁺/H⁺ adducts interactions in complex mixture. *J. Mass Spectrom.* **2019**, *54*, 915–932. [[CrossRef](#)]
33. Haynes, W.M. *CRC Handbook of Chemistry and Physics*; Taylor & Francis Group: Abingdon, UK, 2014.
34. Hug, G.; Marciniak, B.; Bobrowski, K. Sensitized photo-oxidation of sulfur-containing amino acids and peptides in aqueous solution. *J. Photochem. Photobiol. A Chem.* **1996**, *95*, 81–88. [[CrossRef](#)]
35. Marciniak, B.; Bobrowski, K. Photo- and Radiation-Induced One-Electron Oxidation of Methionine in Various Structural Environments Studied by Time-Resolved Techniques. *Molecules* **2022**, *27*, 1028. [[CrossRef](#)] [[PubMed](#)]
36. Filipiak, P.; Hug, G.L.; Bobrowski, K.; Pedzinski, T.; Kozubek, H.; Marciniak, B. Sensitized Photooxidation of S-Methylglutathione in Aqueous Solution: Intramolecular (S:O) and (S:N) Bonded Species. *J. Phys. Chem. B* **2013**, *117*, 2359–2368. [[CrossRef](#)] [[PubMed](#)]
37. Bobrowski, K.; Hug, G.L.; Marciniak, B.; Kozubek, H. The 4-carboxybenzophenone-sensitized photooxidation of sulfur-containing amino acids in alkaline aqueous solutions. Secondary photoreactions kinetics. *J. Phys. Chem.* **1994**, *98*, 537–544. [[CrossRef](#)]

Disclaimer/Publisher's Note: The statements, opinions and data contained in all publications are solely those of the individual author(s) and contributor(s) and not of MDPI and/or the editor(s). MDPI and/or the editor(s) disclaim responsibility for any injury to people or property resulting from any ideas, methods, instructions or products referred to in the content.

Supplementary Information (SI)

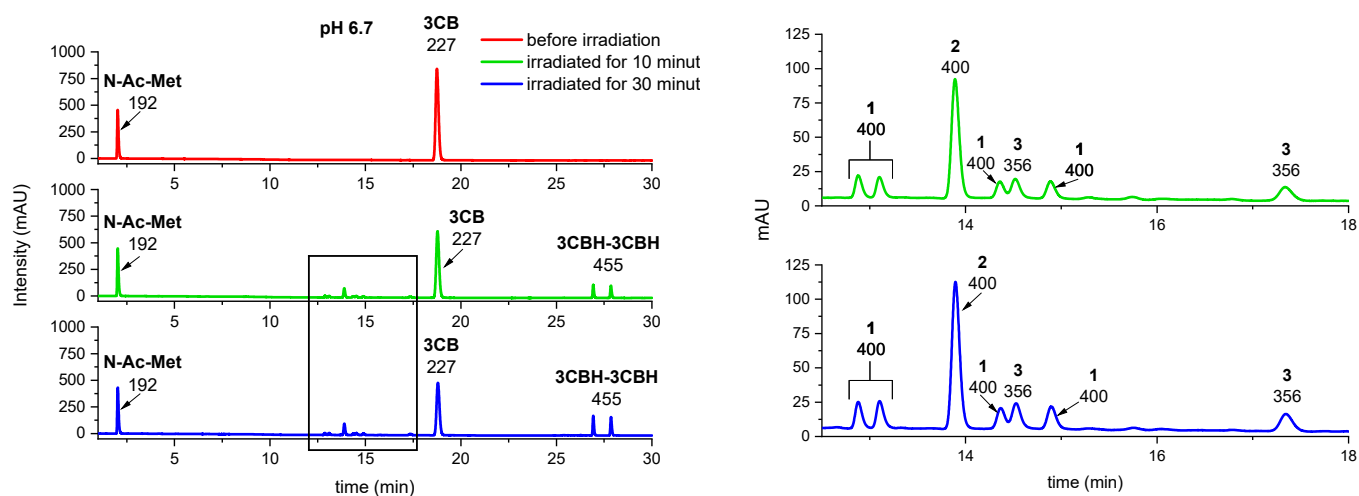


Figure S1. HPLC chromatograms of aqueous solutions containing: N-Ac-Met (20 mM) and 3CB (4.5 mM) at pH 6.7 before irradiation (top panel, red), after 10-minute irradiation (middle panel, green) and after 30-minute irradiation (bottom panel, blue). The expansion of the chromatograms after irradiation between 12 and 18 minutes is shown next to the chromatograms. Peaks are labelled with m/z of the $[M+H]^+$ or $[M+H-H_2O]^+$ ions of the acquired MS spectrum.

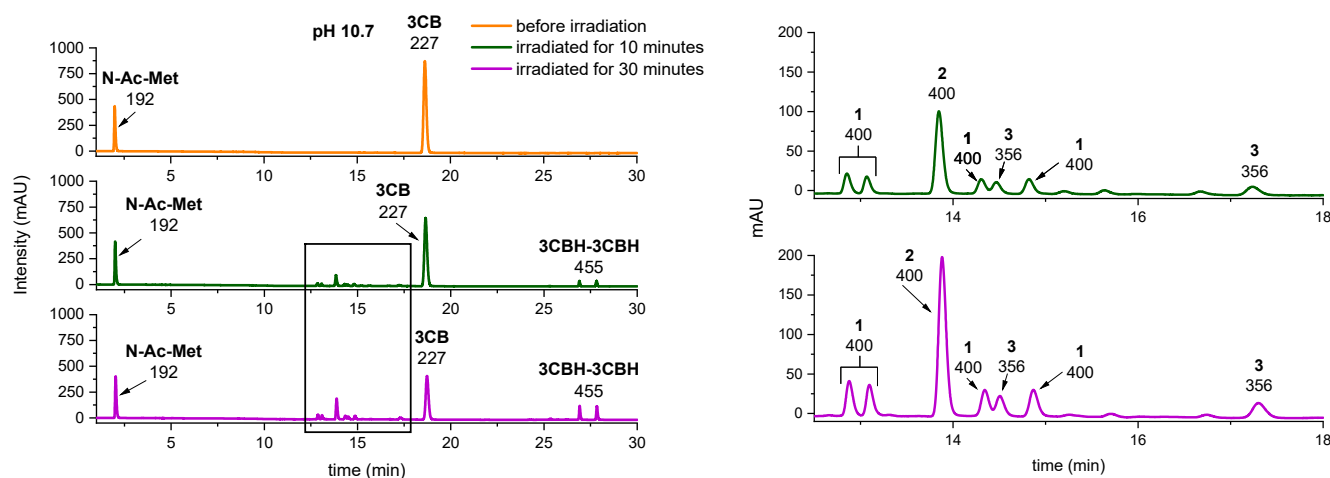


Figure S2. HPLC chromatograms of aqueous solutions containing: N-Ac-Met (20 mM) and 3CB (4.5 mM) at pH 10.7 before irradiation (top panel, orange), after 10-minute irradiation (middle panel, dark green) and after 30-minute irradiation (bottom panel, purple). The expansion of the chromatograms after irradiation between 12 and 18 minutes is shown next to the chromatograms. Peaks are labelled with m/z of the $[M+H]^+$ or $[M+H-H_2O]^+$ ions of the acquired MS spectrum.

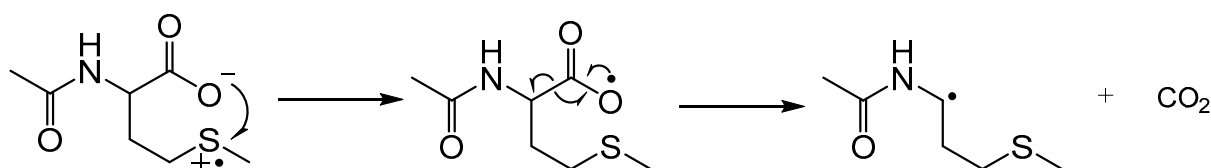


Figure S3. The mechanism of the pseudo-Kolbe reaction.

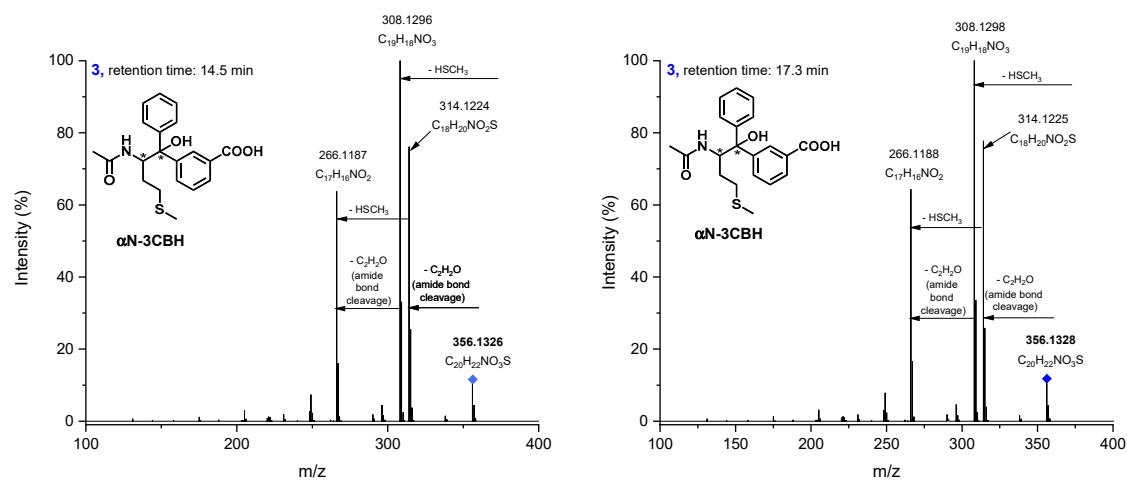
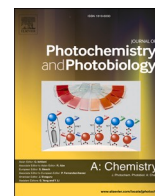


Figure S4. MSMS spectra of photoproducts **3** at retention time 14.5 and 17.3 min.



Efficient decarboxylation of oxidized Cysteine unveils novel Free-Radical reaction pathways

Katarzyna Grzyb^a, Franciszek Kaźmierczak^a, Tomasz Pedzinski^{a,b,c,*}

^a Faculty of Chemistry, Adam Mickiewicz University, 61-614 Poznań Poland

^b Center for Advanced Technology, Adam Mickiewicz University, 61-614 Poznań Poland

^c Radiation Laboratory, Notre Dame University, IN 46556, USA

ABSTRACT

The present study explores the photosensitized oxidation process of Acetyl-Methyl-Cysteine (Ac-MeCys) within a neutral pH aqueous solution. A comprehensive mechanism elucidating this phenomenon is put forth, leveraging outcomes from nanosecond laser flash photolysis (nsLFP) investigations and analysis of resultant stable compounds. The nsLFP findings furnish insights into the transient entities arising from the interaction between the photosensitizer, 3-carboxybenzophenone (3CB), and Ac-MeCys. These insights encompass the quantum yields of these transients. Additionally, the evaluation of enduring products entails the utilization of liquid chromatography and high-resolution mass spectrometry techniques. The principal reaction observed involves the formation of α -amidoalkyl radicals (α N) through decarboxylation, which supersedes the more prevalent α -thioalkyl radicals (α S) reported previously for analogous compounds such as Ac-Methionine. The α N radicals experience two distinct pathways for decay: they either combine with ketyl radicals to yield the α N-3CBH radical coupling product, or undergo beta-scission and hydrolysis, relinquishing CH_3SH and giving rise to a corresponding alcohol.

This investigation highlights how the distance relationship between the thioether group and the peptide backbone influences the oxidation trajectory of Ac-MeCys in comparison to Ac-Met.

1. Introduction

S-Methyl-Cysteine (SMC), a cysteine thioether derivative, is considered an important bioactive compound. It naturally occurs in plants from the *Allium* family such as garlic and onion, *Brassicaceae* family: cauliflower, Chinese cabbage, and legumes [1]. The *Allium* species owes its characteristic aroma and flavor to the presence of S-Alk(en)yl-Cys Sulfoxides (SMCO) [1,2]. Both SMC and the corresponding sulfoxides have not been found to be natural components of mammalian and insect tissues or proteins in higher plants, but they occur relatively often in the form of corresponding γ -glutamyl peptides [3]. Despite the interest that SMC and SMCO have sparked over the years, little is undoubtedly known about the biosynthesis of these compounds. Two main hypotheses have been proposed: transfer of methanethiol to O-acetyl serine (OAS) or direct methylation of free cysteine [4].

It has been found in animal studies that the dietary supplement of SMC and SMCO has therapeutic potential [5]. It could be beneficial for the prevention or treatment of kidney diseases [6], metabolic syndrome [7], and diabetes [8] via its antioxidative, anti-inflammatory, and antifibrogenic activity. Additionally, SMC was reported to be a potent protective agent for neuronal [9] and respiratory systems [10].

Given the potential therapeutic use of SMC, it is important to study the free radical reactions that occur during oxidative stress and the fate of the radicals generated as a result of the oxidation of SMC.

This work is focused on the photosensitized oxidation of Acetyl-Methyl-Cysteine (Ac-MeCys) by the 3-Carboxybenzophenone excited triplet (3CB*) in a neutral aqueous solution (structures of both substrates are shown in Fig. 1).

3-Carboxybenzophenone has been used as a photosensitizer because of its useful, well-described physical and photophysical properties: good water solubility, quantum yield of triplet formation of 1, low extinction coefficient of 3CB-derived radicals in 370–420 nm region where the transient species derived from sulfur-containing compounds exhibit their absorption maxima [11,12].

The Ac-MeCys investigated in this work is a N-acetyl derivative of S-Methyl Cysteine. It contains a thioether moiety that is susceptible to attack by free radical species. The mechanism of photo- and radiation-induced oxidation of a similar compound - Ac-MeCys-NH-CH₃ has already been described in detail [13,14]. Ac-MeCys-NH-CH₃ possesses the peptide-like bond on the C-terminal end, and thus the possibility of decarboxylation is ruled out. On the other hand, in Ac-MeCys the carboxyl group is free so decarboxylation is possible. Ac-MeCys is a

* Corresponding author.

E-mail address: tomekp@amu.edu.pl (T. Pedzinski).

<https://doi.org/10.1016/j.jphotochem.2024.115530>

Received 3 January 2024; Received in revised form 7 February 2024; Accepted 11 February 2024

Available online 15 February 2024

1010-6030/© 2024 Elsevier B.V. All rights reserved.

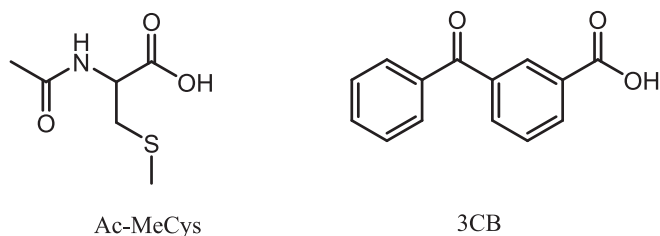


Fig. 1. Structures of Acetyl-MethylCysteine and a photosensitizer – 3-Carboxybenzophenone.

lower homolog of Acetyl Methionine (Ac-Met) that was recently studied by us. It is interesting to see how a small change in the structure of the compounds (a difference of one methylene group) affects the reaction pathways and the quantum yields of the reactions.

2. Materials and methods

The synthetic procedure for Ac-MeCys is described in the [Supporting Information](#).

3-Carboxybenzophenone (3CB) was obtained commercially from Sigma-Aldrich as the best available grade and was used as received. The deionized water for the experiments was purified using a commercial system from Millipore, model Simplicity (Billerica, MA, USA).

The laser flash photolysis (LFP) setup used in this work has been described in detail elsewhere [15]. Samples for LFP experiments were excited using 355 nm, the third harmonic of an Nd: YAG laser (Spectra

Physics Mountain View, CA, USA, model INDI 40–10) with pulses of 6–8 ns duration. The monitoring system consisted of a 150 W pulsed Xe lamp with a lamp pulser (Applied Photophysics, Surrey, U.K.), a monochromator (Princeton Instruments, model Spectra Pro SP-2357, Acton, MA, USA), and an R955 model photomultiplier (Hamamatsu, Japan), powered by a PS-310 power supply (Stanford Research System, Sunnyvale, CA, USA). The data processing system consisted of real-time acquisition using a digital oscilloscope (WaveRunner 6100A, LeCroy, Chestnut Ridge, NY, USA) which was triggered by a fast photodiode (Thorlabs, DET10M, ~1 ns rise time). The data from the oscilloscope were transferred to a computer equipped with software based on Lab-View 8.0 (National Instruments, Austin, TX, USA) which controls the timing and acquisition functions of the system. Kinetic traces were taken between 370 and 700 at 10 nm intervals. The concentration of the quencher (Ac-MeCys) was 3.8 mM.

Steady-state photolysis experiments were performed in a 1 × 1 cm rectangular cell on an optical bench irradiation system using a Genesis CX355STM OPSL laser from Coherent (Santa Clara, CA, USA), with a 355 nm emission wavelength (the output power used was set at 50 mW). The concentrations of 3CB and Ac-MeCys were 2.5 mM and 5 mM, respectively.

The LC-MS measurements were carried out using a liquid chromatography Thermo Scientific/ Dionex Ultimate 3000 system equipped with a C18 reversed-phase analytical column (2.6 μm, 2.1 mm × 100 mm, Thermo-Scientific, Sunnyvale, CA, USA). The column temperature was set to 45 °C. Two eluents were used: water and acetonitrile with 0.1 % (v/v) formic acid. Ac-MeCys oxidation photoproducts were separated using gradient elution from 7 to 60 % of acetonitrile at a flow rate of 0.3

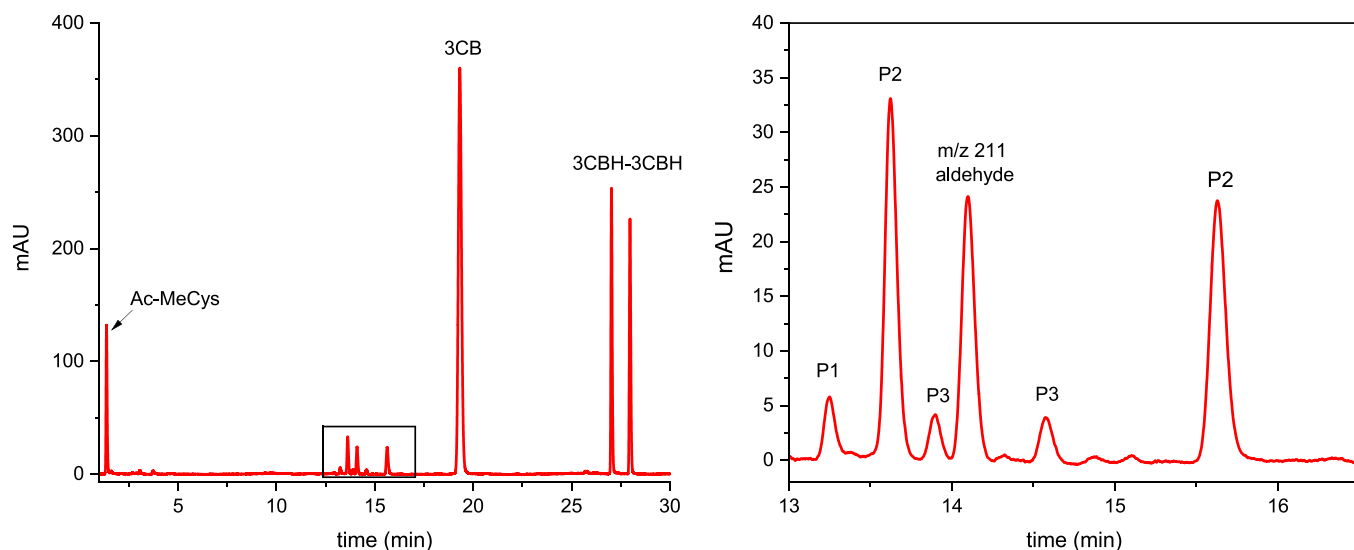


Fig. 2. HPLC chromatogram of aqueous solutions containing: Ac-MeCys (5 mM) and 3CB (2.5 mM) at pH 7.07 after 20-minute irradiation. The expansion of the chromatograms between 13 and 17 min is shown next to the chromatogram.

Table 1

Obtained mass accuracies (errors) for substrates and products yielded in the photooxidation of Ac-MeCys.

Retention time (min)	Accurate mass (measured)	Exact mass (calculated)	Mass accuracy (ppm)	Molecular composition	Compound
1.4	178.0528	178.0538	– 5.56	C ₆ H ₁₂ NO ₃ S	Ac-MeCys
13.3	386.1035	386.1062	– 7.04	C ₂₀ H ₂₀ NO ₅ S	P1
13.6	342.1158	342.1164	–1.72	C ₁₉ H ₂₀ NO ₃ S	P2
13.9	312.1230	312.1236	– 1.87	C ₁₈ H ₁₈ NO ₄	P3
14.1	211.0754	211.0759	– 2.39	C ₁₄ H ₁₁ O ₂	aldehyde (derived from 3CB)
14.6	312.1234	312.1236	– 0.59	C ₁₈ H ₁₈ NO ₄	P3
15.6	342.1155	342.1164	–2.60	C ₁₉ H ₂₀ NO ₃ S	P2
19.3	227.0701	227.0708	– 3.17	C ₁₄ H ₁₁ O ₃	3CB
27.0	455.1479	455.1495	– 3.44	C ₂₈ H ₂₃ O ₆	3CBH-3CBH
28.0	455.1513	455.1513	+ 4.04	C ₂₈ H ₂₃ O ₆	

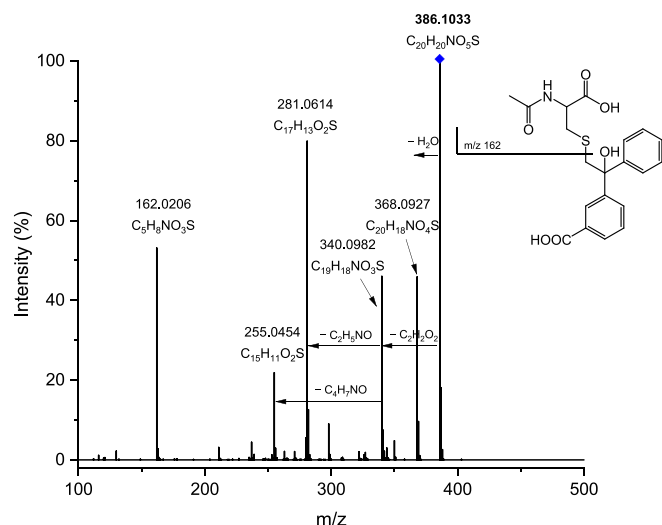


Fig. 3. MSMS spectrum of photoproduct P1 - α S-3CBH (fragmentation of $[M + H - H_2O]^+$ m/z 386 ion).

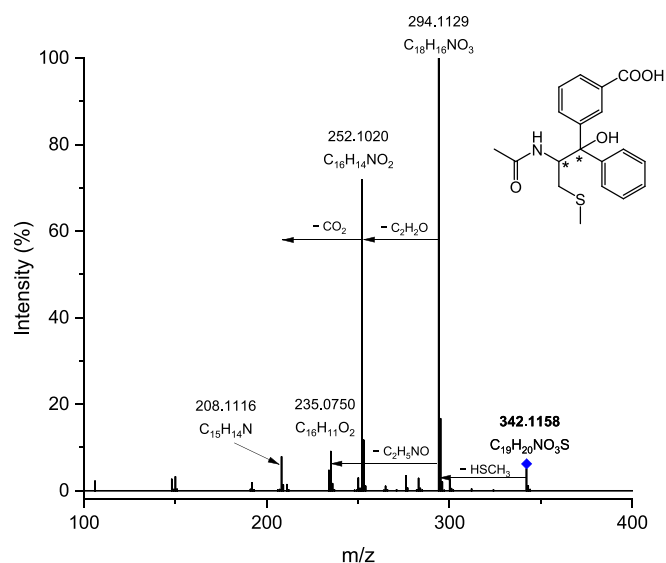


Fig. 4. MSMS spectrum of photoproduct P2 - α N-3CBH (fragmentation of $[M + H - H_2O]^+$ m/z 342 ion).

ml/min for 42 min.

This UHPLC system was coupled to a hybrid QTOF mass spectrometer (Impact HD, Bruker Daltonik, Bremen, Germany). The ions were generated by electrospray ionization (ESI) in the positive mode. MS/MS fragmentation mass spectra were produced by collisions (CID, collision-induced dissociation) with nitrogen gas in the Q2 section of the spectrometer.

$[M + H - H_2O]^+$ ions (ions after dehydration, which is a typical reaction occurring easily in MS ion source [16–21]) of all

photoproducts, were subjected to MSMS analysis.

All of the LFP and stationary irradiation experiments were performed in oxygen-free solutions at neutral pH.

3. Results

3.1. LC-MS/MS

The separation of photoproducts was achieved using high-performance liquid chromatography followed by the analysis of the stable products carried out using high-resolution mass spectrometry.

A representative LC-MS analysis of the solution after 20 min of irradiation (355 nm CW laser, 50 mW) at pH 7.07 is shown in Fig. 2 (LC-MS analysis of the sample before irradiation can be found in the SI in Figures S1).

The peaks with retention times of 1.4 min and 19.3 min were assigned to the substrates: Acetyl MethylCysteine (Ac-MeCys) and 3-Carboxybenzophenone (3CB), respectively, and they were detected both before (see Figure S1) and after (Fig. 2) the laser irradiation. The irradiation caused the appearance of a group of six well-separated peaks between 13 and 16 min and a pair of peaks between 25 and 30 min. The latter peaks are the products of the recombination of the radicals derived from the sensitizer [12].

The high-resolution m/z values as well as the obtained mass accuracies (errors) of the substrates and products can be found in Table 1.

The molecular composition of photoproduct P1 ($C_{20}H_{20}NO_5S$) calculated based on the high-resolution m/z suggests that it is the radical cross-coupling product of α S and 3CBH \bullet (α S-3CBH photoproduct). The formation and structure of this type of photoproduct are well-described in the previous study on the photosensitized oxidation of MeCys and Met derivatives [13].

The MSMS spectrum of the P1 photoproduct can be seen in Fig. 3.

The MSMS spectrum (Fig. 4) and high-resolution MSMS data showed that two products P2 are the products of the radical cross-coupling

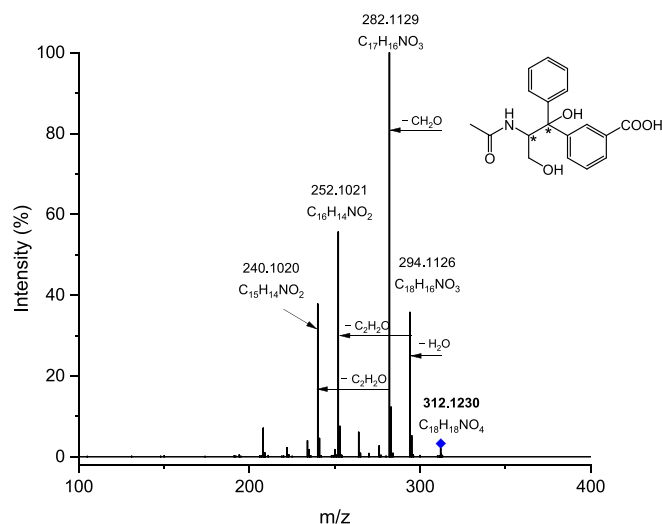
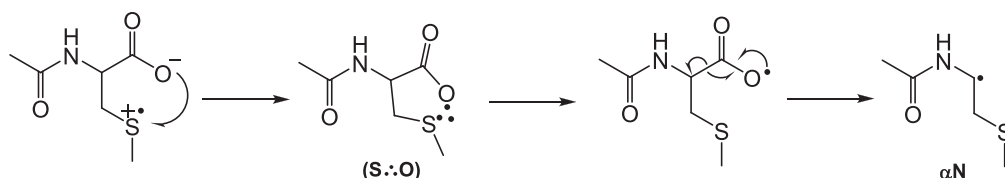
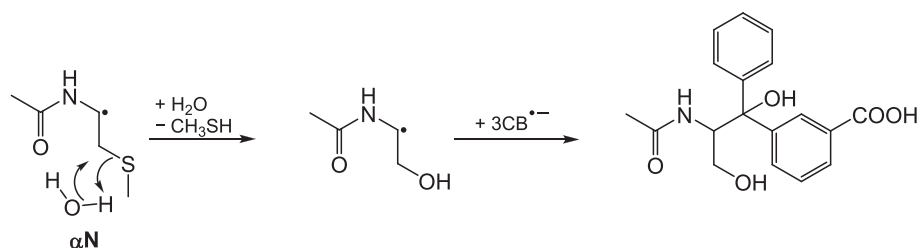


Fig. 5. MSMS spectrum of photoproduct P3 with a retention time of 13.9 min (fragmentation of $[M + H(-H_2O)]^+$ m/z 312 ion).



Scheme 1. Formation of α N via pseudo-Kolbe mechanism.



Scheme 2. Mechanism of formation of P3.

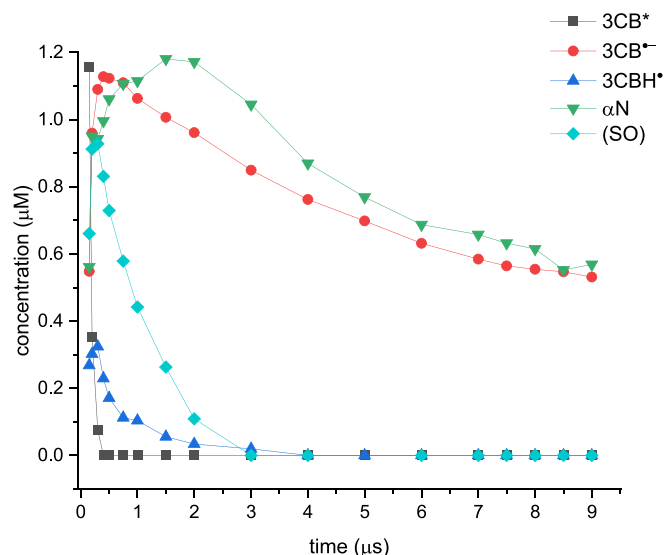


Fig. 6. Concentration profiles calculated at different delay times with respect to the laser pulse for the reaction of 3CB (2.5 mM) excited triplet quenched by Ac-MeCys (5 mM) in aqueous solution at pH = 6.8.

Table 2

Quantum yields of the radical species generated in the LFP experiment.

Radical species	Quantum yields
3CB ^{•-}	0.42
3CBH [•]	0.13
(S:O)	0.35
αN	0.39

reaction of αN (α-amidoalkyl radical) and 3CB^{•-} radicals. Two detected peaks with significantly different retention times (13.6 and 15.6 min) and the same MSMS spectra correspond to the two possible diastereoisomers of αN-3CBH – SS and SR. P2 has two stereocenters: one has a fixed S configuration from the substrate and the other stereocenter is generated from the radical cross-coupling reaction and can have either R or S configuration.

αN radicals are generated in the decarboxylation reaction that occurs via the pseudo-Kolbe mechanism. It involves an electron transfer from the carboxylate group to the sulfur-centered radical (>S^{•+}) and the formation of a five-membered (S:O) ring, stabilized by the two-centered three-electron bond [22]. The mechanism of this reaction is depicted in Scheme 1.

The products P3 with *m/z* 312.1230 and 312.1236 are presented on the chromatogram in Fig. 2 as two peaks with considerably different retention times (13.9 and 14.6 min). Both products exhibit the same MSMS spectrum (Figure 5 and S2), and they were assigned to the molecular composition of C₁₈H₁₈NO₄. The fragmentation spectrum of P3 showed a base peak (a fragmentation ion with 100 % intensity) with *m/z*

282.1129 (C₁₇H₁₆NO₃). This corresponds to the neutral loss of CH₂O. The loss of CH₂O is a common fragmentation pattern for compounds with terminal hydroxyl groups [23–25]. A tentative structure of P3 is shown next to the MSMS spectrum in Fig. 5. Since this product has two stereocenters (similar to the product P2 described above), there are two possible diastereoisomers (SS and SR), and there are two peaks on the chromatogram.

The possible formation pathway of P3 is presented in Scheme 2. The reaction involves beta scission, hydrolysis of αN radical (formed via the pseudo-Kolbe mechanism shown in Scheme 1), and loss of the terminal CH₃SH group. The newly formed radical is trapped by the ketyl radical (3CB^{•-}) ultimately yielding the P3 product.

3.2. Laser flash photolysis

The transient absorption spectra (Figure S3) obtained from photo-sensitized oxidation of aqueous solution of Ac-MeCys at pH = 6.8 were deconvoluted into individual components by using a multilinear regression technique (described in more detail in [26,27]):

$$\Delta A(\lambda_i) = \sum_j \epsilon_j(\lambda_i) a_j$$

where ϵ_j is the extinction coefficient of the *j*th species and the regression parameters, a_j , are equal to the concentration of the *j*th species times the optical path length of the monitoring light. The sum is over all species present.

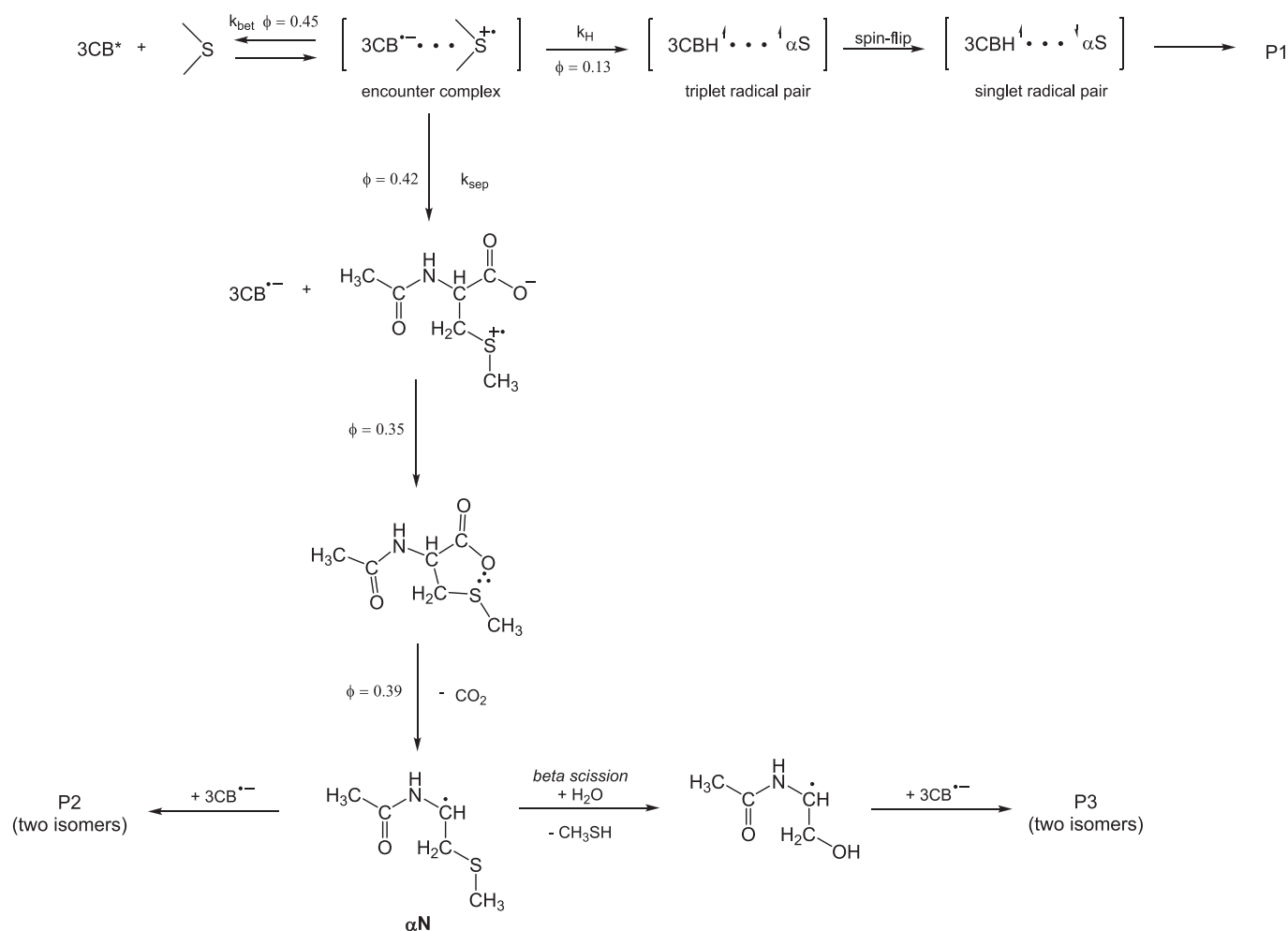
Figure S2 shows the typical spectra following the quenching of 3-carboxybenzophenone: at short times after the laser pulse when the dominating species is the triplet state of 3CB (3CB*) with its absorption maximum at $\lambda_{\max} \approx 520$ nm, then the maximum shifts to longer wavelengths ($\lambda \approx 550$ nm and $\lambda \approx 600$ nm) corresponding to the ketyl radical (3CBH[•]) and 3CB radical anion (3CB^{•-}), respectively.

The efficient intramolecular stabilization of sulfur radical cation (>S^{•+}) through the formation of a two-centered three-electron bond with an oxygen atom (five-membered ring intermediate, (S:O)) was also observed. As shown in the concentration profile in Fig. 6, the decay of (S:O) simultaneously led to the generation of αN. This observation supports the proposed mechanism of the formation of αN via the pseudo-Kolbe mechanism (Scheme 1).

Quantum yields shown below in Table 2 were calculated from the initial concentration of the intermediates shown in the concentration profiles of Fig. 6. Benzophenone dissolved in acetonitrile was used as an external actinometer. The initial concentration of 3CB* was calculated to be 3.1 μM.

4. Discussion

The first step in the 3CB* sensitized oxidation of Ac-MeCys is an electron transfer from the sulfur atom to the carbonyl group of the sensitizer. This radical-ion pair can decay via the following pathways: (i) charge separation (k_{sep}) yielding 3CB^{•-} and >S^{•+}, (ii) back electron transfer (k_{bet}) to regenerate reactants in their ground state, and (iii) proton transfer within the encounter complex leading to the formation of αS and 3CBH[•] (k_{H}). The last pathway leads to the formation of a



triplet radical pair that is non-reactive and cannot undergo the recombination. Therefore to form the stable product (P1) it is essential to produce the reactive singlet radical pair via the spin flip within the encounter complex [28]. The mechanism of Ac-MeCys photooxidation is shown in Scheme 3.

It should be pointed out that the quantum yields of 3CB^{•-} and αN formation calculated from the concentration profiles (Fig. 6 and Table 2) are practically the same within experimental error ($\phi_{3CB^{\bullet-}} = 0.42$ and $\phi_{\alpha N} = 0.39$). This suggests that the only reaction pathway of $>S^{\bullet+}$ is decarboxylation leading to the formation of αN radicals. Deprotonation of $>S^{\bullet+}$ was not observed thus all αS radicals must have resulted from the proton transfer within the encounter complex (k_H). The formation of αN radicals (primary decarboxylation products) was found to be more efficient than the formation of αS. This tendency can be clearly seen from the chromatogram in Fig. 1: the area of the P1 peak (αS-3CBH radical coupling product) is significantly smaller than the combined areas of the peaks of photoproducts P2 and P3 (note that the precursor of both of these products is αN).

Contrary, the sulfur radical cation of a very similar structure of Acetyl-Methionine (Ac-Met) studied by us before [23], decays mostly via deprotonation, yielding αS radicals and subsequently isomeric radical coupling products.

The decarboxylation of Ac-MeCys is definitely more efficient than the decarboxylation of Acetyl-Methionine [29]: $\phi = 0.42$ vs. $\phi = 0.09$, respectively, at neutral pH. Likely the main reason for this substantial difference in quantum yields is the fact that the formation of a five-membered structure of (S:O)-bonded species (which is the precursor

of αN, see Scheme 2) in Ac-MeCys is kinetically preferred over the six-membered ring in Ac-Met (both structures are shown in Figure S4). This preference has been previously observed in other sulfur-containing compounds [22,30–34] and confirmed by the kinetic measurements and rate constant calculations: the formation of a five-membered ring was found to be two orders of magnitude faster than the formation of a six-membered ring [35].

Apart from being scavenged by 3CB^{•-}, αN radicals were found to simultaneously hydrolyze and lose -HSCH₃ group to form the alcohol – photoproduct P3 (see Scheme 2). A similar reaction in which αN undergoes C^β – S bond cleavage and then is hydrolyzed to acetaldehyde has been described before in S-methylcysteine [36,37]. However, the hydrolysis leading to the aldehyde involves the free amino group. In the case of Ac-MeCys, the amino group is blocked (acetylated) and this particular reaction cannot occur. It is also possible that such a P3-type product is formed also in Ac-Met, but, due to the low quantum yield of decarboxylation and a limited sensibility of the detection techniques employed in the study, it was not detected.

5. Conclusions

In this paper, we investigated the mechanism of 3CB-triplet-sensitized oxidation of Acetyl MethylCysteine (Ac-MeCys). The α-amidoalkyl radicals (αN) resulting from decarboxylation, decayed via two pathways: they formed αN-3CBH adducts (photoproducts P2) or underwent beta-scission (loss of CH₃SH) and hydrolysis, ultimately forming respective alcohol – photoproducts P3. αS-3CBH (photoproduct P1)

was formed exclusively within the encounter complex following the spin-flip of the triplet radical pair.

Based on the concentration profiles (Fig. 6) and the areas of the peaks on the chromatogram (Fig. 2), it can be clearly seen that the formation of αN is favored over the formation of αS . This is the opposite tendency than in the Ac-Met which we studied before [29]. This comparison of the reactivity of two similar structures demonstrates how small structural change of the sulfur-containing amino acids leads to significant changes in the mechanism of photooxidation of Ac-MeCys vs. Ac-Met.

CRedit authorship contribution statement

Katarzyna Grzyb: Writing – original draft, Visualization, Investigation, Funding acquisition, Formal analysis. **Franciszek Kaźmierczak:** Visualization, Investigation. **Tomasz Pedzinski:** Writing – review & editing, Supervision, Project administration, Methodology, Investigation, Funding acquisition, Conceptualization.

Declaration of competing interest

The authors declare that they have no known competing financial interests or personal relationships that could have appeared to influence the work reported in this paper.

Data availability

Data will be made available on request.

Acknowledgments

The authors would like to thank Prof. Rafał Frański from Adam Mickiewicz University in Poznań (Poland) for the fruitful discussions about the intricate mass spectra. The authors thank Dr. Gordon L. Hug from Notre Dame University Radiation Laboratory for fruitful discussions of the reaction mechanism. This research was supported by the Initiative of Excellence – Research University at Adam Mickiewicz University, projects 017/02/SNS/0008, 094/07/POB3/0008 and by the U.S. Department of Energy Office of Science, Office of Basic Energy Sciences, under Award Number DE-FC02-04ER1553. K.G. and T.P. would like to acknowledge the Notre Dame Radiation Laboratory (NDRL) staff and personally Professor Sylwia Ptasińska and Professor Ian Carmichael for their hospitality. This is a document number NDRL-5426 from the Notre Dame Radiation Laboratory.

Appendix A. Supplementary data

Supplementary data to this article can be found online at <https://doi.org/10.1016/j.jphotochem.2024.115530>.

References

- [1] M.G. Jones, Biosynthesis of the flavour precursors of onion and garlic, *J. Exp. Bot.* 55 (2004) 1903–1918, <https://doi.org/10.1093/jxb/erh138>.
- [2] A. Shafaei, C.R. Hill, J.M. Hodgson, L.C. Blekkenhorst, M.C. Boyce, Simultaneous extraction and quantitative analysis of S-Methyl-L-Cysteine Sulfoxide, sulforaphane and glucosinolates in cruciferous vegetables by liquid chromatography mass spectrometry, *Food Chemistry: X* 21 (2024) 101065, <https://doi.org/10.1016/j.fochx.2023.101065>.
- [3] G.A. Maw, Biochemistry of S-Methyl-L-Cysteine and its Principal Derivatives, *Sulfur Reports* 2 (1982) 1–26, <https://doi.org/10.1080/01961778208082422>.
- [4] J. Joshi, J.B. Renaud, M.W. Sumarah, F. Marsolais, Deciphering S-methylcysteine biosynthesis in common bean by isotopic tracking with mass spectrometry, *Plant J* 100 (2019) 176–186, <https://doi.org/10.1111/tpj.14438>.
- [5] C.R. Hill, A. Haoci Liu, L. McCahon, L. Zhong, A. Shafaei, L. Balmer, J.R. Lewis, J. M. Hodgson, L.C. Blekkenhorst, S-methyl cysteine sulfoxide and its potential role in human health: a scoping review, *Crit. Rev. Food Sci. Nutr.* (2023) 1–14, <https://doi.org/10.1080/10408398.2023.2267133>.
- [6] M. Yin, C. Hsu, P. Chiang, W. Wu, Antiinflammatory and antifibrogenic effects of s-methyl cysteine and s-methyl cysteine in the kidney of diabetic mice, *Mol. Nutr. Food Res.* 51 (2007) 572–579, <https://doi.org/10.1002/mnfr.200600213>.
- [7] S. Thomas, G.P. Senthilkumar, K. Sivaraman, Z. Bobby, S. Paneerselvam, K. T. Harichandrakumar, Effect of s-methyl-L-cysteine on oxidative stress, inflammation and insulin resistance in male wistar rats fed with high fructose diet, *Iran, J Med Sci* 40 (2015) 45–50.
- [8] G.P. Senthilkumar, Study the effect of s-methyl l-cysteine on lipid metabolism in an experimental model of diet induced obesity, *JCDR* (2013), <https://doi.org/10.7860/JCDR/2013/7304.3571>.
- [9] C. Liu, T. Hsia, M. Yin, s-Methyl cysteine enhanced survival of nerve growth factor differentiated PC12 cells under hypoxic conditions, *Food Funct.* 5 (2014) 1125–1133, <https://doi.org/10.1039/C3FO60689A>.
- [10] T. Hsia, M. Yin, s-Ethyl cysteine and s-methyl cysteine protect human bronchial epithelial cells against hydrogen peroxide induced injury: SEC and SMC protect bronchial epithelia..., *J. Food Sci.* 80 (2014) H2094–H2101, <https://doi.org/10.1111/1750-3841.12973>.
- [11] T. Pedzinski, K. Bobrowski, M. Ignasiak, G. Kciuk, G.L. Hug, A. Lewandowska-Andralojc, B. Marciniak, 3-Carboxybenzophenone (3-CB) as an efficient sensitizer in the photooxidation of methionyl-leucine in aqueous solutions: spectral, kinetic and acid-base properties of 3-CB derived transients, *J. Photochem. Photobiol. A Chem.* 287 (2014) 1–7, <https://doi.org/10.1016/j.jphotochem.2014.04.004>.
- [12] K. Grzyb, R. Frański, T. Pedzinski, Sensitized photoreduction of selected benzophenones mass spectrometry studies of radical cross-coupling reactions, *J. Photochem. Photobiol. b: Bio.* 234 (2022) 112536, <https://doi.org/10.1016/j.jphotochem.2022.112536>.
- [13] T. Pedzinski, K. Grzyb, F. Kaźmierczak, R. Frański, P. Filipiak, B. Marciniak, Early events of photosensitized oxidation of sulfur-containing amino acids studied by laser flash photolysis and mass spectrometry, *J. Phys. Chem. B* 124 (2020) 7564–7573, <https://doi.org/10.1021/acs.jpcc.0c06008>.
- [14] T. Pedzinski, K. Grzyb, K. Skotnicki, P. Filipiak, K. Bobrowski, C. Chatgililoglu, B. Marciniak, Radiation- and photo-induced oxidation pathways of methionine in model peptide backbone under anoxic conditions, *IJMS* 22 (2021) 4773, <https://doi.org/10.3390/ijms22094773>.
- [15] T. Pedzinski, A. Markiewicz, B. Marciniak, Photosensitized oxidation of methionine derivatives, *Laser Flash Photolysis Studies, Res Chem Intermed* 35 (2009) 497–506, <https://doi.org/10.1007/s11164-009-0046-4>.
- [16] S. Xu, J. Pavlov, A.B. Attygalle, Collision-induced dissociation processes of protonated benzoic acid and related compounds: competitive generation of protonated carbon dioxide or protonated benzene: CID spectra of protonated benzoic acids, *J. Mass Spectrom.* 52 (2017) 230–238, <https://doi.org/10.1002/jms.3920>.
- [17] R. Frański, M. Zalas, B. Gierczyk, G. Schroeder, Electro-oxidation of diclofenac in methanol as studied by high-performance liquid chromatography/electrospray ionization mass spectrometry: Letter to the Editor, *Rapid Commun. Mass Spectrom.* 30 (2016) 1662–1666, <https://doi.org/10.1002/rcm.7593>.
- [18] B. Balta, V. Aviyente, C. Lifshitz, Elimination of water from the carboxyl group of GlyGlyH +, *J. Am. Soc. Mass Spectrom.* 14 (2003) 1192–1203, [https://doi.org/10.1016/S1044-0305\(03\)00479-3](https://doi.org/10.1016/S1044-0305(03)00479-3).
- [19] P.A. D'Agostino, L.R. Provost, J.R. Hancock, Analysis of mustard hydrolysis products by packed capillary liquid chromatography–electrospray mass spectrometry, *J. Chromatogr. A* 808 (1998) 177–184, [https://doi.org/10.1016/S0021-9673\(98\)00102-2](https://doi.org/10.1016/S0021-9673(98)00102-2).
- [20] L.A.L. da Silva, L.P. Sandjo, A. Misturini, G.F. Caramori, M.W. Biavatti, ESI-QToF-MS characterization of hirsutinolide and glaucolide sesquiterpene lactones: fragmentation mechanisms and differentiation based on Na + /H + adducts interactions in complex mixture, *J Mass Spectrom* 54 (2019) 915–932, <https://doi.org/10.1002/jms.4433>.
- [21] Y.-C. Ma, H.-Y. Kim, Determination of steroids by liquid chromatography/mass spectrometry, *J. Am. Soc. Mass Spectrom.* 8 (1997) 1010–1020, [https://doi.org/10.1016/S1044-0305\(97\)00122-0](https://doi.org/10.1016/S1044-0305(97)00122-0).
- [22] P. Filipiak, K. Bobrowski, G.L. Hug, C. Schöneich, B. Marciniak, N-Terminal decarboxylation as a probe for intramolecular contact formation in $\gamma\text{-glu-(pro) n-met}$ peptides, *J. Phys. Chem. B* 124 (2020) 8082–8098, <https://doi.org/10.1021/acs.jpcc.0c04371>.
- [23] V. Tak, P.K. Kanaujia, D. Pardasani, A.K. Gupta, M. Palit, R.K. Srivastava, D. K. Dubey, Electrospray ionization tandem mass spectral analysis of oxidation products of precursors of sulfur mustards, *Rapid Commun. Mass Spectrom.* 20 (2006) 2387–2394, <https://doi.org/10.1002/rcm.2605>.
- [24] P. Stefanowicz, K. Kapczynska, M. Jaremko, Ł. Jaremko, Z. Szewczuk, A mechanistic study on the fragmentation of peptide-derived Amadori products, *J. Mass Spectrom.* 44 (2009) 1500–1508, <https://doi.org/10.1002/jms.1639>.
- [25] A.M. Duffield, R.T. Aplin, H. Budzikiewicz, C. Djerassi, C.F. Murphy, W.C. Wildman, Mass Spectrometry in Structural and Stereochemical Problems. LXXXII. 1 A Study of the Fragmentation of Some Amaryllic Acid Alkaloids 2, *J. Am. Chem. Soc.* 87 (1965) 4902–4912, <https://doi.org/10.1021/ja00949a038>.
- [26] P. Filipiak, K. Bobrowski, G.L. Hug, D. Pogocki, C. Schöneich, B. Marciniak, New insights into the reaction paths of 4-carboxybenzophenone triplet with oligopeptides containing n- and c-terminal methionine residues, *J. Phys. Chem. B* 121 (2017) 5247–5258, <https://doi.org/10.1021/acs.jpcc.7b01119>.
- [27] K. Bobrowski, G.L. Hug, B. Marciniak, H. Kozubek, The 4-carboxybenzophenone-sensitized photooxidation of sulfur-containing amino acids in alkaline aqueous solutions. Secondary photoreactions kinetics, *J. Phys. Chem.* 98 (1994) 537–544, <https://doi.org/10.1021/j100053a031>.
- [28] J.R. Woodward, Radical pairs in solution, *Prog. React. Kinet. Mech.* 27 (2002) 165–207, <https://doi.org/10.3184/007967402103165388>.
- [29] K. Grzyb, V. Sehrawat, T. Pedzinski, The Fate of sulfur radical cation of n-acetyl-methionine: deprotonation vs decarboxylation, *Photochem* 3 (2023) 98–108, <https://doi.org/10.3390/photochem3010007>.

- [30] K. Bobrowski, G.L. Hug, B. Marciniak, B. Miller, C. Schöneich, Mechanism of one-electron oxidation of β -, γ -, and δ -hydroxyalkyl sulfides. catalysis through intramolecular proton transfer and sulfur–oxygen bond formation, *J. Am. Chem. Soc.* 119 (1997) 8000–8011, <https://doi.org/10.1021/ja970683r>.
- [31] K. Bobrowski, D. Pogocki, C. Schöneich, Oxidation of (carboxyalkyl)thiopropionic acid derivatives by hydroxyl radicals. mechanisms and kinetics of competitive inter- and intramolecular formation of σ - and σ^* -type sulfuranyl radicals, *J. Phys. Chem. A* 102 (1998) 10512–10521, <https://doi.org/10.1021/jp983136g>.
- [32] G.L. Hug, K. Bobrowski, D. Pogocki, G. Hörner, B. Marciniak, Conformational influence on the type of stabilization of sulfur radical cations in cyclic peptides, *ChemPhysChem* 8 (2007) 2202–2210, <https://doi.org/10.1002/cphc.200700369>.
- [33] K. Bobrowski, C. Houée-Levin, B. Marciniak, Stabilization and reactions of sulfur radical cations: relevance to one-electron oxidation of methionine in peptides and proteins, *Chimia* 62 (2008) 728, <https://doi.org/10.2533/chimia.2008.728>.
- [34] C. Chatgililoglu, M. Grzelak, K. Skotnicki, P. Filipiak, F. Kazmierczak, G.L. Hug, K. Bobrowski, B. Marciniak, Evaluation of hydroxyl radical reactivity by thioether group proximity in model peptide backbone: methionine versus s-methyl-cysteine, *IJMS* 23 (2022) 6550, <https://doi.org/10.3390/ijms23126550>.
- [35] C. Galli, G. Illuminati, L. Mandolini, P. Tamborra, Ring-closure reactions. 7. Kinetics and activation parameters of lactone formation in the range of 3- to 23-membered rings, *J. Am. Chem. Soc.* 99 (1977) 2591–2597, <https://doi.org/10.1021/ja00450a031>.
- [36] M. Goetz, J. Rozwadowski, B. Marciniak, Photoinduced electron transfer, decarboxylation, and radical fragmentation of cysteine derivatives: a chemically induced dynamic nuclear polarization study, *J. Am. Chem. Soc.* 118 (1996) 2882–2891, <https://doi.org/10.1021/ja9536678>.
- [37] O.B. Morozova, M.S. Panov, H.-M. Vieth, A.V. Yurkovskaya, CIDNP study of sensitized photooxidation of S-methylcysteine and S-methylglutathione in aqueous solution, *J. Photochem. Photobiol. A Chem.* 321 (2016) 90–98, <https://doi.org/10.1016/j.jphotochem.2016.01.013>.

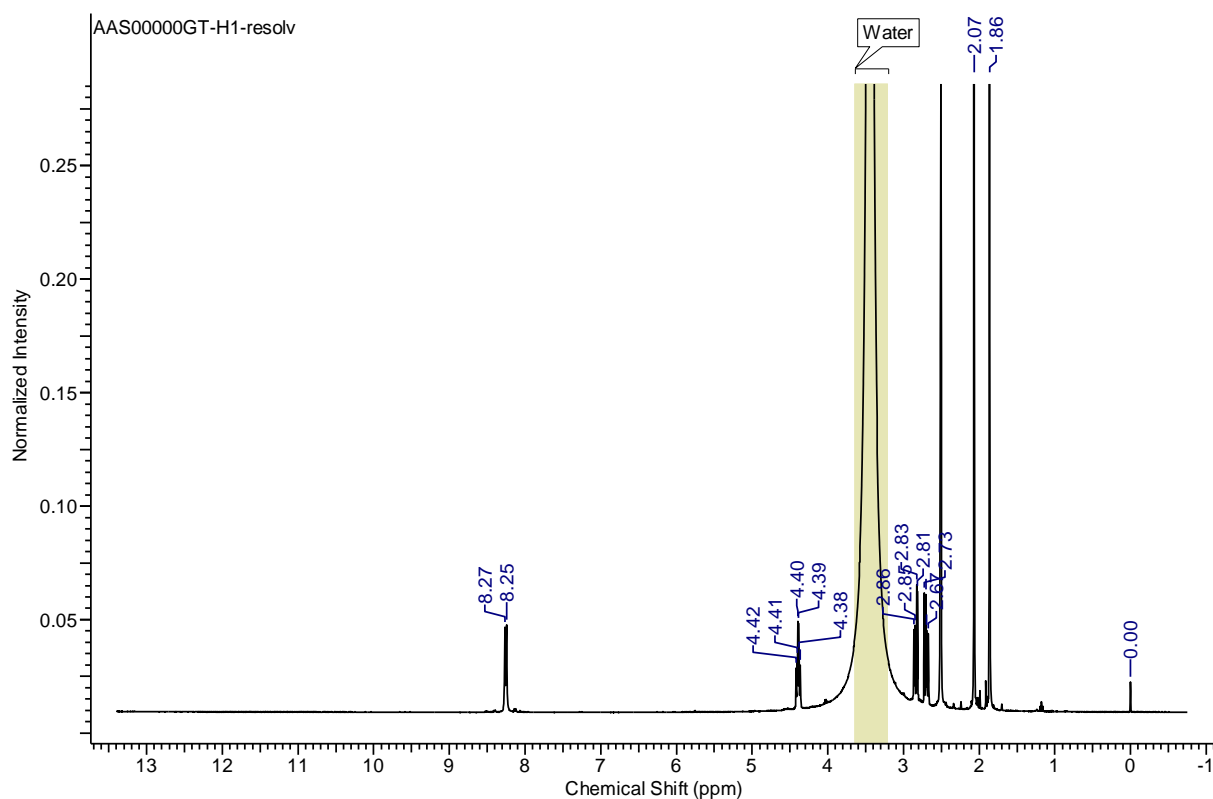
Supplementary Information

The synthetic procedure for Ac-MeCys:

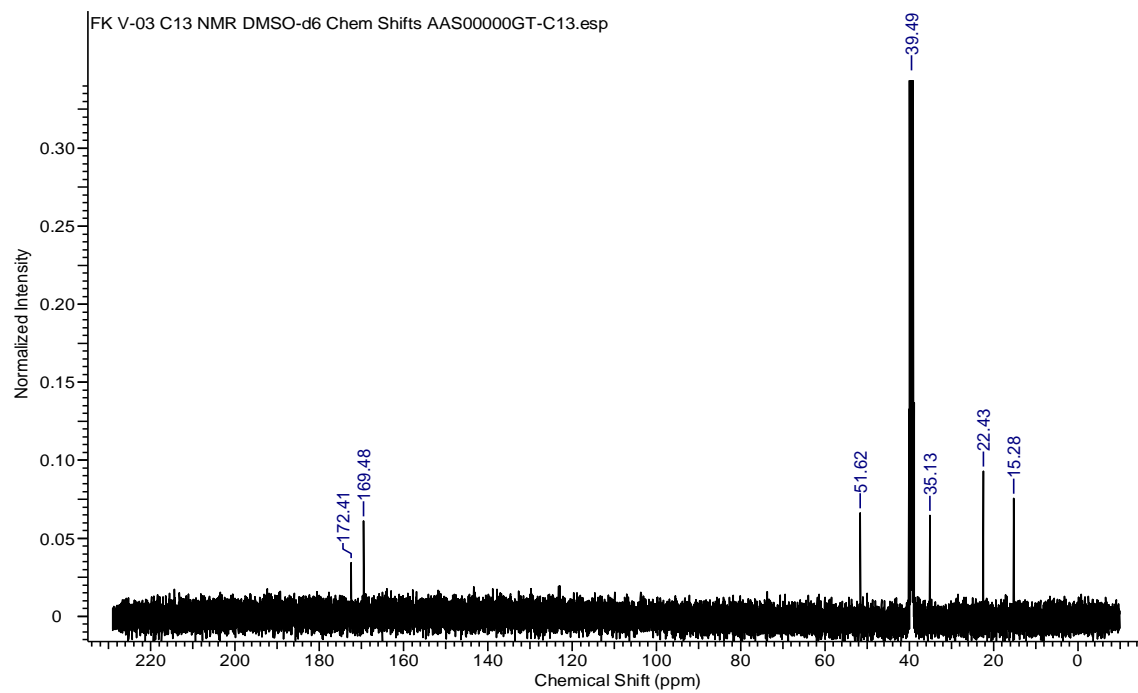
To a stirred suspension of MeCys (0.135 g; 0.001 mM) in anhydrous acetic acid (5 mL) was added dropwise acetic anhydride (0.113 mL, 1.2 eq) and the stirring of the resulted mixture continued overnight. After TLC analysis (methylene chloride-methanol gradient), the volatiles were co-evaporated several times with ethyl acetate and finally the product stored in a vacuum desiccator. Obtained amount was 0.174 g (98% yield) of the final product.

NMR analysis of Ac-MeCys:

¹H NMR (400 MHz, ppm, DMSO-d₆): δ 1.86 (s, 3H); 2.07 (s, 3H), 2.69 (dd, *J*=13.5, 9 Hz, 1H), 2.84 (dd, *J*=13.5, 5 Hz, 1H), 4.39 (m, Hz), 8.22 (d, *J*=7 Hz, 1H), 12.80 (br s, 1H):



¹³C NMR (100 MHz, ppm, DMSO-d₆): δ 15.28, 22.43, 35.13, 51.63, 169.48, 172.41:



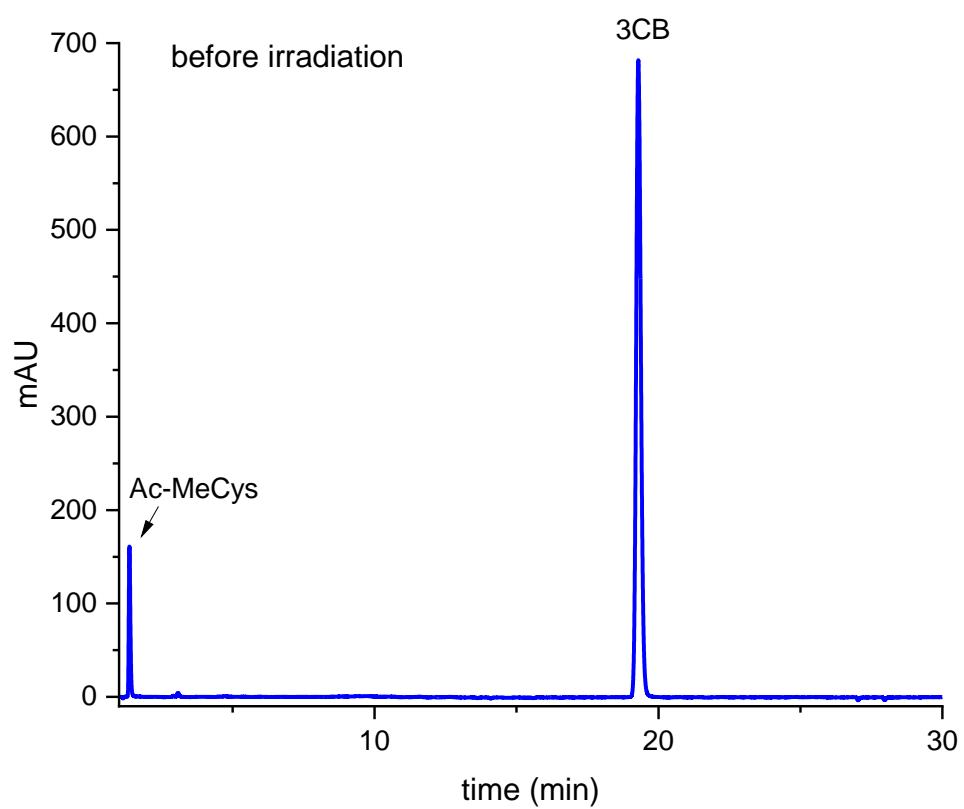


Figure S1. HPLC chromatogram of aqueous solutions containing: Ac-MeCys (5 mM) and 3CB (2.5 mM) at pH 7.07 before irradiation.

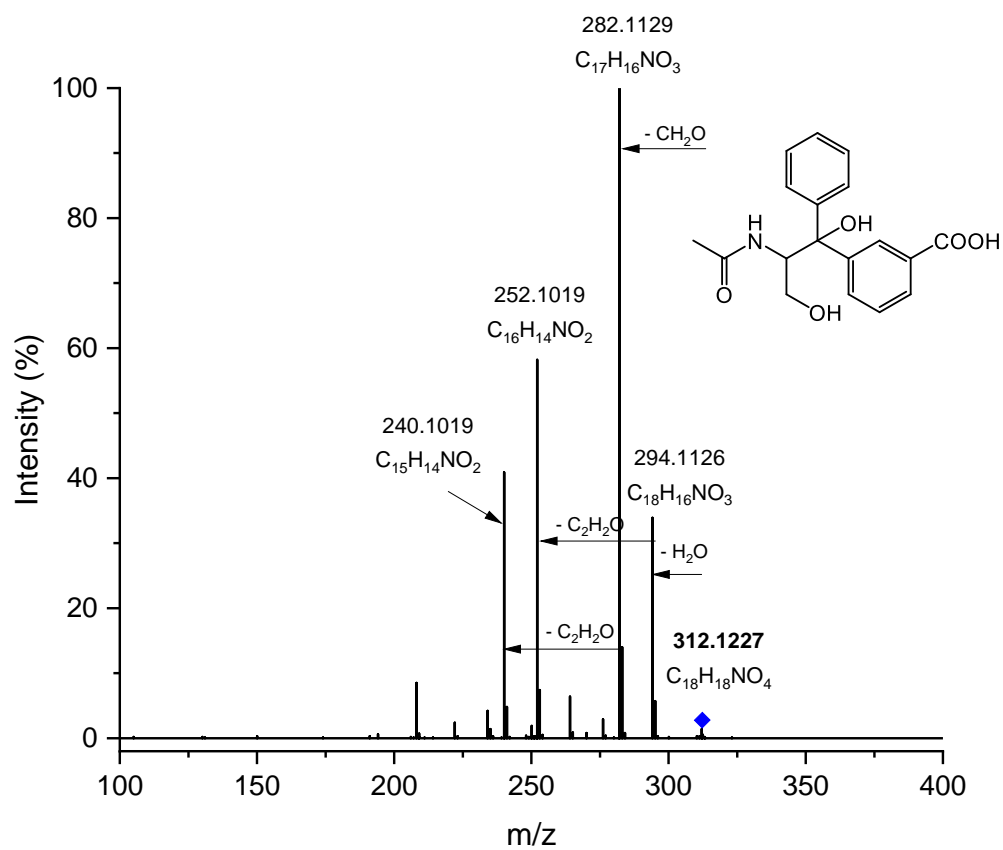


Figure S2. MS/MS spectrum of photoproduct P3 with retention time 14.6 min (fragmentation of $[M+H(-H_2O)]^+$ m/z 312 ion)

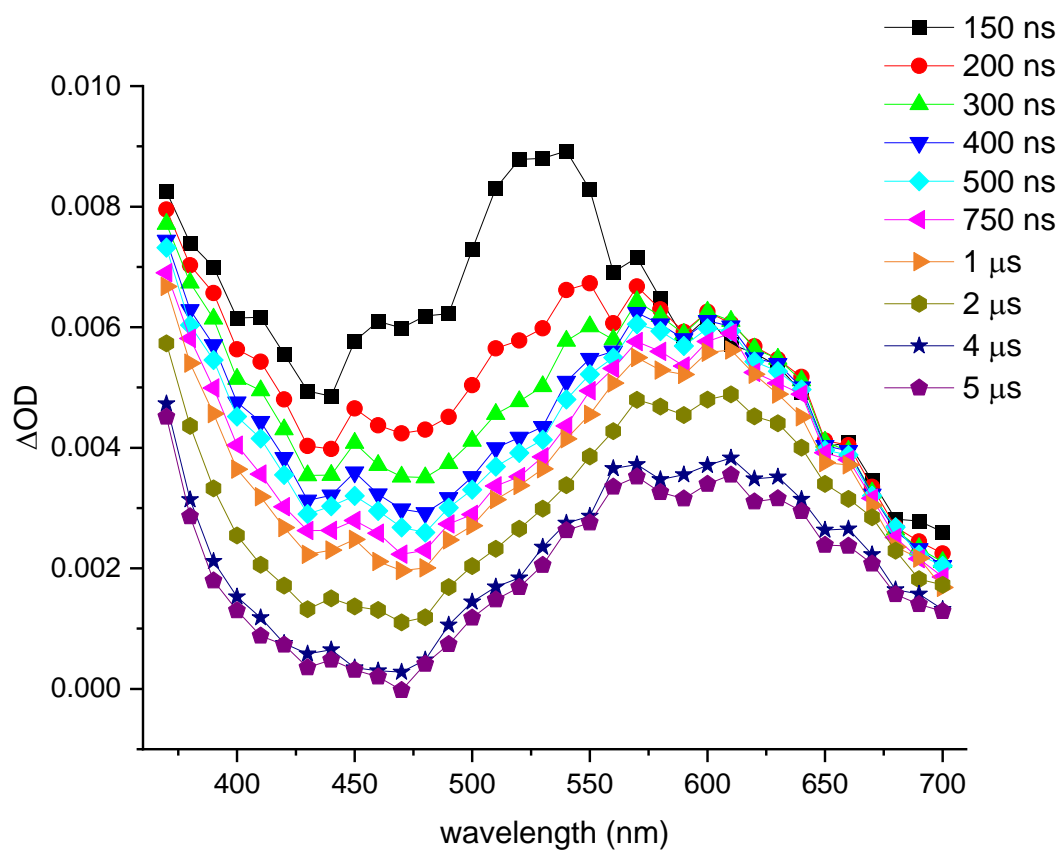


Figure S3. Optical transient absorption spectra recorded after the 355 nm laser pulse at 150, 200, and 300 ns, 400 ns, 500 ns, 750 ns, 1 μ s, 2 μ s, 4 μ s and 5 μ s delays following the 3CB (2.5 mM) triplet state by Ac-MeCys (5 mM) at pH 6.8;

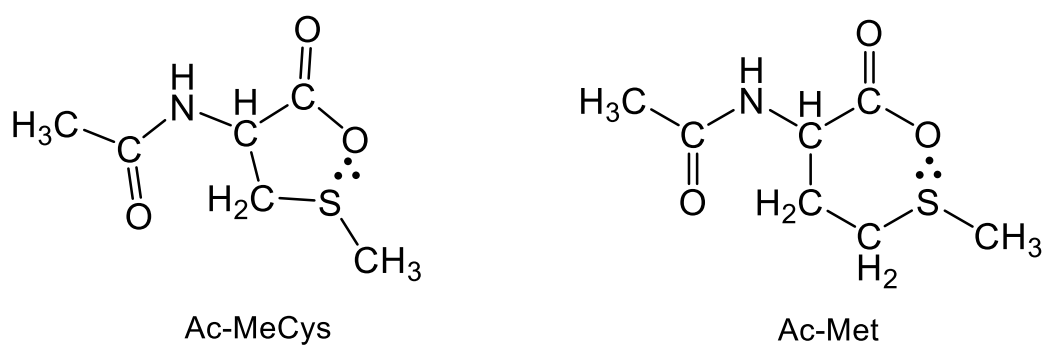


Figure S4. Structures of (S \cdots O) bonded-species of Ac-MeCys and Ac-Met